Development of Melt Polymerization Route for Amino acid Based Functional Polymers and their Self-assembled Nanostructures

A Thesis

**Submitted in Partial Fulfillment of the Requirements
Of the Degree of
Doctor of Philosophy**

By

S. Anantharaj

Reg. No. 20103054

IISER PUNE

Department of Chemistry
**INDIAN INSTITUTE OF SCIENCE EDUCATION AND
RESEARCH, PUNE**
Pune 411008, Maharashtra, India

January 2016

Dedicated to….

My Parents

Dr. M. Jayakannan
Associate Professor
Department of Chemistry

CERTIFICATE

Certified that the work incorporated in the thesis entitled *"Development of Melt Polymerization Route for Amino acid Based Functional Polymers and their Self-assembled Nanostructures"* Submitted by **Mr. S. Anantharaj** was carried out by the candidate under my supervision. The work presented here or any part of it has not been included in any other thesis submitted previously for the award of any degree or diploma from any other University or Institution.

Date: 27th January 2016
Pune (MH) India

Dr. M. Jayakannan
(Thesis Supervisor)

27/01/2016

DECLARATION

I declare that this written submission represents my ideas in my own words and where others' ideas have been included; I have adequately cited and referenced the original sources. I also declare that I have adhered to all principles of scientific honesty and integrity and have not misrepresented or fabricated or falsified any idea/data/fact/source in my submission. I understand that violation of the above will be cause for disciplinary action by the institute and can also evoke penal action from the sources which have thus not been properly cited or from whom proper permission has not been taken when needed.

Date: 27ᵗʰ January 2016

Pune (MH) India

S. Anantharaj

Roll No: 20103054

ACKNOWLEDGEMENTS

I would like to thank all instruments' technicians of IISER Pune for their support: Pooja, Deepali (NMR) Swati (MALDI), Neetha (HRMS), Meghna (AFM), Anil, Yatish (FE-SEM). I thank National Chemical Laboratory (NCL) Pune for HR TEM facilities.

A heartfelt thanks all my friends who made the IISER Pune experience something special, in particular, Tamil Friends Dharmaraja, Suresh, Mani, Mano, Ravi, Sankar, Siva, Bala, Vijayakanth, Alagar, Sivasankar, Madan, Rajasekar and Nanda: Wilbee, Kavita, Kundan, Satheesh (room mate), Arun Tanpure, Santhosh G, Gopal, Kiran, Ganesh M, Sarat D, Rajesh, Madhuri: Naveen, Mahesh, Avdhoot, Meghna, (Theoretical friends), all other friends. I also thank all the staff members in administration, finance, accounts, stores, library, canteen especially, Ms. Naina, Mr. Mayuresh Mr. Nitin and Mr. Mahesh for their immediate help whenever I needed them. Special thanks to Dharamaraja for his useful suggestions but also for being there to listen when I needed an ear.

I am truly grateful to my parents for their immeasurable love and care. They have always encouraged me to explore my potential and pursue my dreams. They helped me a lot to reach this stage in my life. I would also like to thank my brother and sisters for their everlasting encouragement and supports.

Furthermore, I would like to thank all members of the IISER-Pune, for their help and support of my thesis work. Special thanks to Dr. Srivatsan for entertainment during the cricket match. I also apologize to everyone who may not be mentioned personally, here.

.   S. Anantharaj

SYNOPSIS

Amino acids are biological monomers and their peptide sequence and chain length played a crucial role on the size, function and secondary structure of proteins. Synthetic polymers based on amino acids attracted significant interest in chemistry-biology interface due to their potential application in therapeutics, cosmetics, biodegradable and biocompatible engineering thermoplastics. The development of new synthetic strategies for L-amino acid resources would open up new direction of research activities of amino acid based polymeric materials. The thesis work is aimed to develop new eco-friendly melt polycondensation approach for L-amino acid resources under solvent-free conditions. This new process provides opportunity for developing helical poly(ester-urethane)s, side chain hydrogen boned polyesters, water soluble cationic polyesters and redox cleavable polyesters based on simple and multifunctional L-amino acid natural resources. The thesis has been divided into following five chapters:

(i) Chapter 1: The introduction chapter provides complete literature survey on the synthesis of amino acid based polymers, their self-assembly, application in biomedical field and describe the aim of the thesis work.

(ii) Chapter 2: A new ***dual ester-urethane melt polycondensation*** approach was developed for ***novel poly(ester-urethane)s*** based on L-amino acid natural resources. Synthesis of amino acid monomers, development of melt condensation approach, confirmation of the new approach by NMR and MALDI-TOF analysis, molecular weight determination, thermal properties and development of appropriate model reaction for studying the mechanism are described.

(iii) Chapter 3: The role of the melt condensation t***emperature and catalyst selective*** on the reactivity of the L-amino acid monomers were studied in detail. Wide ranges of catalysts were optimized for the above process based on alkali, alkaline earth, transition metal and lanthanide salts and complexes. A-B, A-B-A type species and helical poly(ester-urethane)s were produced. Further, efforts were also taken to study the mechanism and optical purity of the polymers and oligomers.

(iv) Chapter 4: New classes of ***hydrogen-bonded functional polyesters*** were made from multi-functional amino acids such as L-aspartic and L-glutamic acids. The roles of the hydrogen-bonding interaction on the amyliod-like fibrils formation of these new classes of polyesters were investigated in detail. The polymers were converted into cationic polyester nanoparticles in water and subsequently reversibly transformed into fluorescent amyloid-fibrils using dansyl fluorophores. Photophysical and morphological studies were carried out to understand the reversible self-assembly in detail.

(v) Chapter 5: Disulfide containing ***redox degradable polyesters*** are made based on L-cystine monomer. These polyesters were found to exhibit nano-fibrous morphology. The disulfide chemical linkages were found to be completely redox degradable; as a result the long chain polymers were turned into monomeric units. These nanoparticles were found to be highly bio-compatible and non-toxic to cancer cells and open new opportunity for their futuristic drug delivery applications.

The last chapter summarized the thesis work with future perspectives.

In chapter 2, a new *dual ester-urethane* melt polycondensation approach for amino acid monomers. In this new process, amino acids were readily converted into dual ester-urethane monomers and polycondensed with diols under melt conditions to produce high molecular weight polymers. The new synthetic process was tested for more than half-dozen of amino acids and diols. The mechanistic

New Dual Ester-Urethane Condensation Chemistry
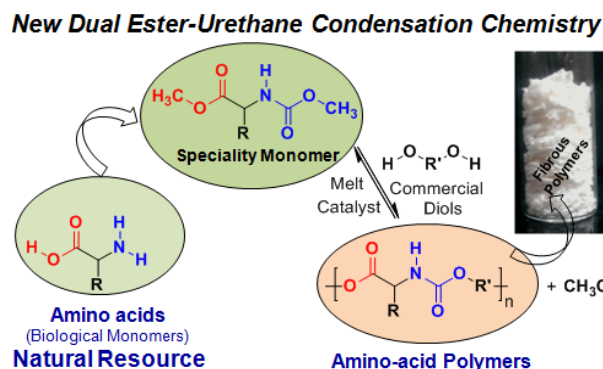
aspects of the new process were studied by NMR and MALDI-TOF-MS and control reactions were carried out to understand the kinetics of the polymerization. The role of the catalyst, polymerization temperature and repeating unit structure on the molecular weight of the polymers and their thermal properties were also investigated. The new polymers were self-organized as β-sheet in aqueous or organic solvents and their thermal

properties such as glass transition temperature and crystallinity could be readily varied using different L-amino acid monomers or diols in the feed.

In chapter 3, temperature and catalyst driven chemoselective polymerization route was developed for amino acid monomers to produce diverse macromolecular structures such as linear poly(ester-urethane)s, functional polyesters, A-B diblocks and A-B-A triblocks. Amino acids were converted into carboxylic ester and urethane dual functional monomers in which the ester part acted as low temperature site for chemoselective reaction towards alcohols. Under this reaction condition; the urethane (or carbamate) part of the monomer unit was completley inert towards alcohol. The influence of catalyst on the process was investigated by choosing wide ranges of catalysts from alkali, alkali earth metal,
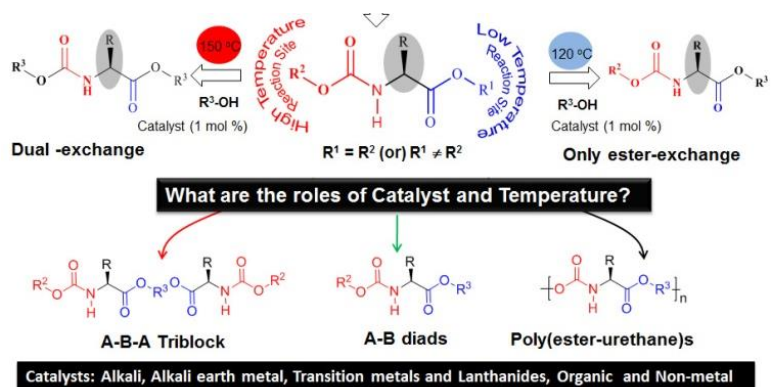
transition metal and lanthanide series belonging to oxides, nitrates, chloride, acetates, acetylacetonate and alkoxides. The temperature and catalysts selectivity in amono acids were further expanded to make A-B and A-B-A blocks by carefully choosing the mono- or diols. More than two dozen were identified for producing poly(ester-urethane)s based on simple amino acid monomers. Theoretical studies revealed that the carbonyl carbon in ester possessed low electron density compared to the carbonyl carbon in urethane groups which facilitated chemoselective process. Electron and atomic force microscopic analysis of the polymers revealed the formation of helical nano-fibrous morphology.

The chapter 4 reports the development of new non-peptide functional polyesters based on natural L-amino acids that underwent reversible self-organization from amyloid-like fibrils to collapsed coil-like spherical structures. The newly designed synthetic polyester self-assembled through β-sheet hydrogen bonding interactions to produce amyloid-like fibrils consisting of hierarchical double helical structures. Upon de-protection, the amyloid fibrils underwent coil-like conformational change to produce cationic spherical nano-particles in aqueous medium. Reversible conformational change

from the spherical species to expanded fibril structures was achieved via fluorophore substitution. Two multi-functional amino acids: L-glutamic and L-aspartic acids were
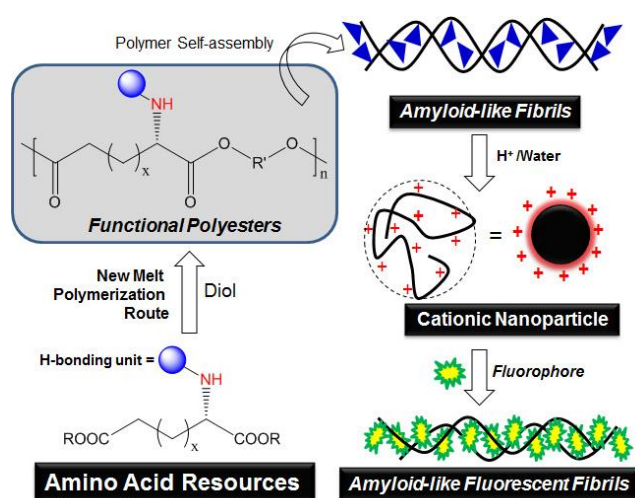
chosen for the above purpose and polymerized with diols under melt conditions to produce high molecular weight functional polyesters. The size and shape of the amyloid fibrils and spherical assemblies were studied by dynamic light scattering, water contact angle measurements, Zeta potential, electron and atomic force

microscopes, etc. The newly developed amino acid based polymers and their self-assembled amyloid-fibrils, spherical charge nano-particles and fluorescent amyloid-fibrils are potential candidates in biomedical applications.

The chapter 5 describes the development of solvent free melt process to disulfide linkage containing redox degradable polymeric materials. For this purpose, L-cystine was chosen and it was suitably converted into multi-purpose monomer. The amine functionality in L-cystine was converted into Boc urethane which act as β-sheet hydrogen bonding vector for seeding amyloid-fibril and also as cationic resources upon de-protection into -NH$_3^+$X$^-$ polymeric salts. The dicarboxylic acids were converted into methyl esters which have capabilities to undergo thermo-selective melt

polymerization to produce disulfide linkage containing linear polyesters. The disulfide linkage in the polyester backbone is redox degradable; thus, the polymers can be degraded into their monomer species. Upon Boc de-protection; the disulfide polyester turned into water dispersible cationic polyester and it was found to self-assemble as
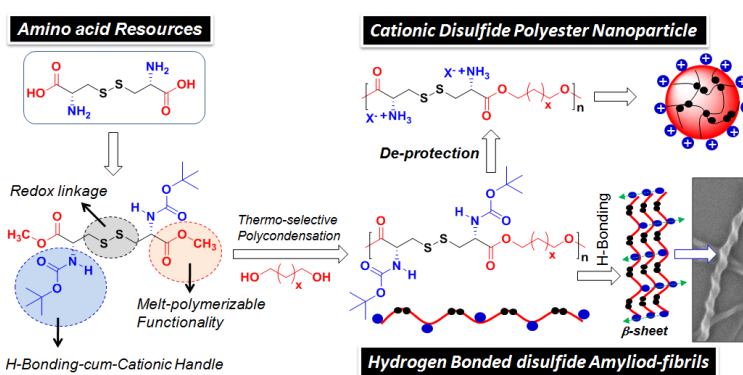
stable nanoparticles. The redox degradation behaviors of nascent disulfide polyester were studied using DTT and the process was monitored by ^{1}H-NMR and GPC techniques. The cytotoxicity studies in normal and cancer cell lines revealed that these cationic disulfide polymers and neutral polymers are highly biocompatible and non-toxic to cells.

The last chapter summarizes the outcome and future direction of research work carried out in the Ph.D. thesis.

TABLE OF CONTENTS

Chapter 1

Introduction

1.1. Introduction to Amino acids

Amino acids are biologically important organic compounds that play central roles both as building blocks of proteins and as intermediates in metabolism.[1] A large proportion of our cells, muscles and tissue are made up of amino acids in the form of protein, meaning they carry out many important biological functions.[2-5] There are twenty α-amino acids that are commonly found in naturally occurring polypeptides. Amino acids are made up of amine ($-NH_2$) and carboxylic acid ($-COOH$) functional groups, along with various side chain functional and non-functional groups such as hydroxyl, carboxylic acid, amine and alkyl groups respectively. Depending on the pH, the amino acids either exhibit zwitterion characters or dipolar ion. All the amino acids are chiral compounds except glycine; thus, they exit as enantiomers and they have L-configuration. Amino acids are classified into various categories depending upon the side chain functional group of the amino acids such as, acidic, basic, aliphatic, aromatic, thiol, alcohol and amidic (in figure 1.1). The current production of amino acids is more than two million tons per year. Amino acids are widely used in various daily life applications that include food additives, cosmetics, polymeric materials, pharmaceuticals etc.[6]
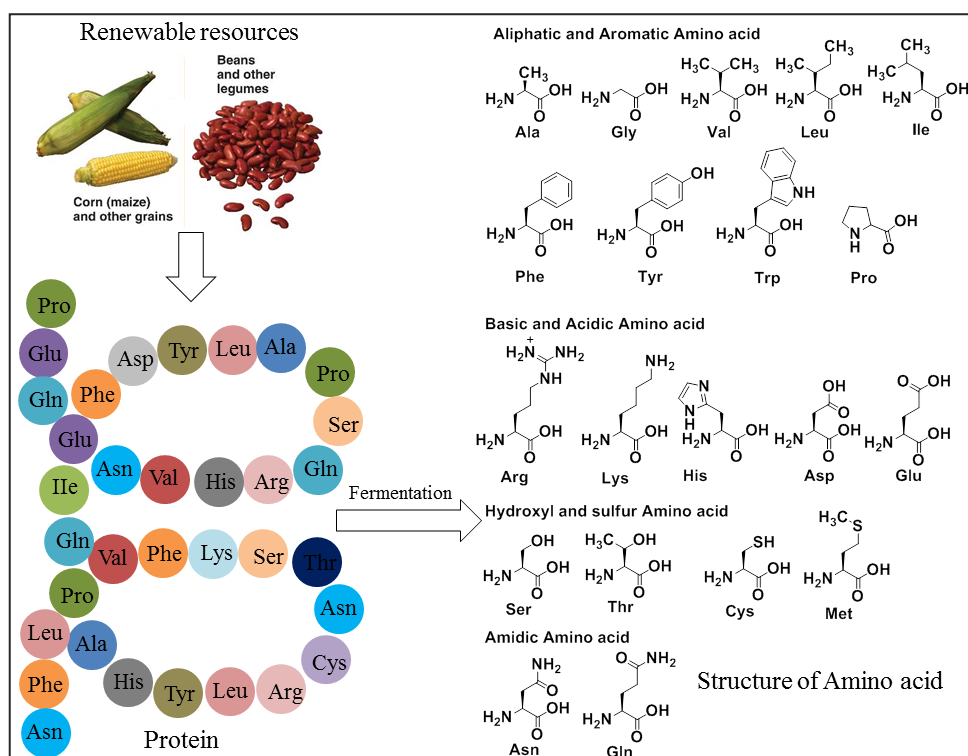
Figure 1.1. *Natural α-amino acid from renewable resources and their chemical structures*

Amino acids are produced by four different methodology namely extraction, chemical synthesis, fermentation and enzymatic catalysis. In extraction method, protein rich materials such as hair, meat extracts and plant hydrolysates are used as raw materials. Strecker amino acid synthesis is one of the well-known methods for chemical synthesis of α-amino acid.[7-9] In this method α-amino nitrile is obtained from ammonia, an aldehyde / ketone and hydrogen cyanide; the nitrile group is then hydrolyzed to yield the α-amino acid. An alternative method for α-amino acid synthesis is amidocarbonylation reaction using transition metal catalyst.[10-11] In this method N-acyl amino acid is synthesized from three components, i.e. an aldehyde, amide and CO. Enzymatic biocatalysts process is living organisms are used as catalyst for the production of amino acids.[12] Based on these approaches, L-aspartic acid was synthesised from fumaric acid and ammonia using L-aspartate ammonia lyase enzyme as catalyst. Similarly L-phenyl alanine was synthesised from (*E*)-cinnamic acid by employing phenylalanine ammonia lyase enzyme as the catalyst.[13]
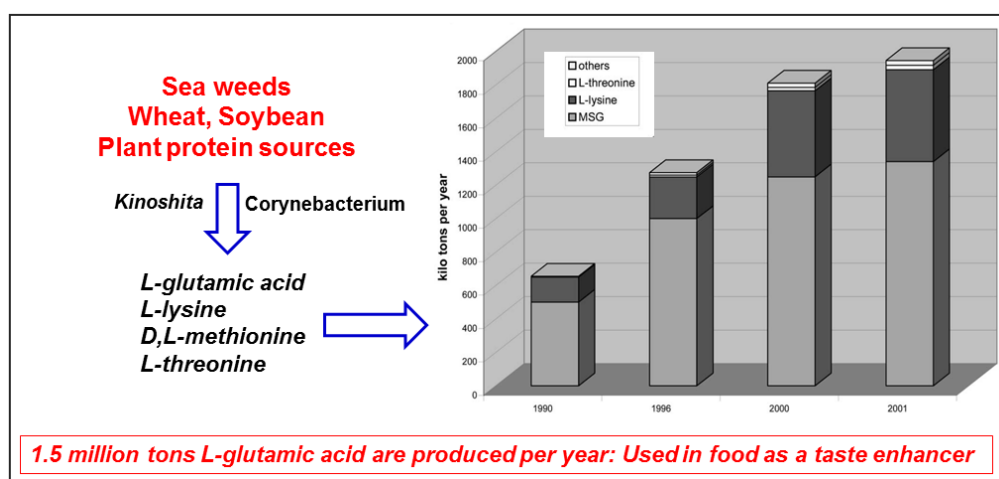
Figure 1.2.*Fermentation route for amino acid and their production in kilotons/year (adopted from Hermann T. J. Biotechnol.* **2003***, 104,* 155-172*).*

Fermentation is another important method for synthesis of α-amino acid. In fermentation method,[12] living microorganisms are used for synthesis of amino acid from simple and cheap raw materials. In this method α-amino acid can be synthesized on industrial scale as an optically pure compound. Hermann et al developed synthetic methodology for bulk scale synthesis of L-glutamic and other amino acid using Corynebacterium glutamicum as bacterium.[14] L-glutamic acid is one of the most extensively synthesized amino acid using this method and its mono sodium glutamate salt is used as a taste enhancer in foodstuffs (in figure 1.2). This process is widely

employed to isolate α-amino acid by environmental friendly fermentation methods with high optical purity, large scale synthesis and low price.[14]

1.2. Oligopeptides and their secondary structures

The condensation reaction between amine protected free carboxylic acid and carboxylic acid protected free amine group of amino acids in presence of coupling reagent (DCC) yield an amide bond.[15] Typically oligopeptides are synthesized by two different synthetic methodologies such as (i) liquid phase and (ii) solid phase synthesis (in scheme 1.1).[16-17] Liquid phase synthesis is the classical method; it can be used for large scale synthesis of peptides. However this process is slow and time consuming since each and every step of the reaction requires purification of the product. In addition, this approach requires protection of C-terminus (free carboxylic acid) of first amino acid with some protecting group (e.g. Boc or Fmoc).
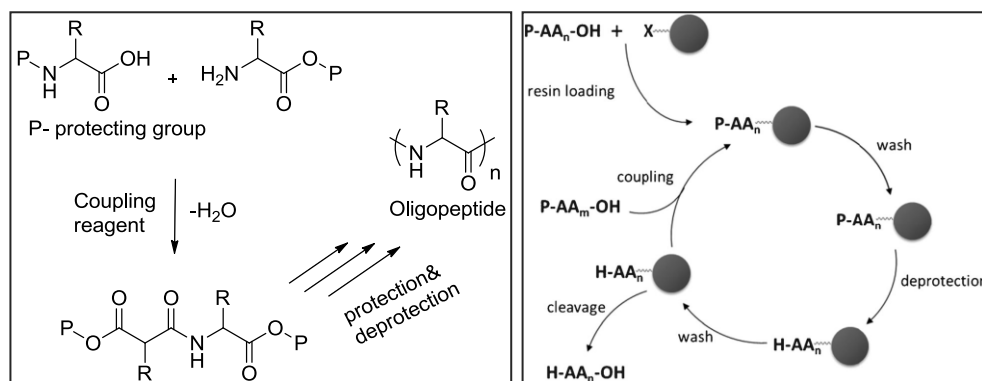
Scheme 1.1. *(a) Synthesis of oligopeptides by solution phase (a) and solid phase (b) approaches (adopted from Ramakers et al. Chem. Soc. Rev., 2014, 43, 2743-2756)*

Solid phase peptide syntheses (SPPS) are used as common technique for synthesis of polypeptide because C-terminus of the first amino acid is protected by an activated solid support such as polystyrene and polyacrylamide and also every step of the reaction mixture does not need purification. In SPPS, the repetitive cycles of deprotection of the N-terminus and insertion of C-terminus amino acid was followed by washing the unreacted residue to yield the required oligopeptides. At the end of the reaction the resin was deprotected to produce the desired peptide. The resin plays the two important roles in peptide synthesis (i) protecting group of C-terminus amino acid and (ii) it helps to separate the peptide product from the reaction mixture. However, these two methods require protection and deprotection reactions in each step of peptide synthesis which leads to a decrease in the yield.[18]

Amphiphilic oligopeptides are known for forming stable and ordered morphologies when subjected to optimal environment at nano domains such as micelles, vesicles, nanorods, fibres etc. These structures are interesting to study to better understand their assembly and, concomitantly apply to fields as potential drug/, gene carriers, and for cell adhesion, skin care technology, as antimicrobial agents, regenerative medicines etc.[19-21] Amino acids are one of the major natural resources that have been frequently instilled into these polymers in order to improvise the functions of nanoscaffolds on a whole. The amide bond of peptide chain plays important role in self-assembly due to their hydrogen bonding interaction. Polypeptides and oligopeptides are known to form high order complex quaternary structures that are composed of subunits with characteristic secondary structures such as α-helix, β-sheet etc,. The non-covalent interactions (hydrogen bonding, π-π stacking etc.,) within the peptide repeating units are known to facilitate the ordered self-assemblies.[22] In order to draw application and well defined structure, along with functionality (conferred by amino acid residues), peptides are generally conjugated with lipids or alkyl chains of various lengths.
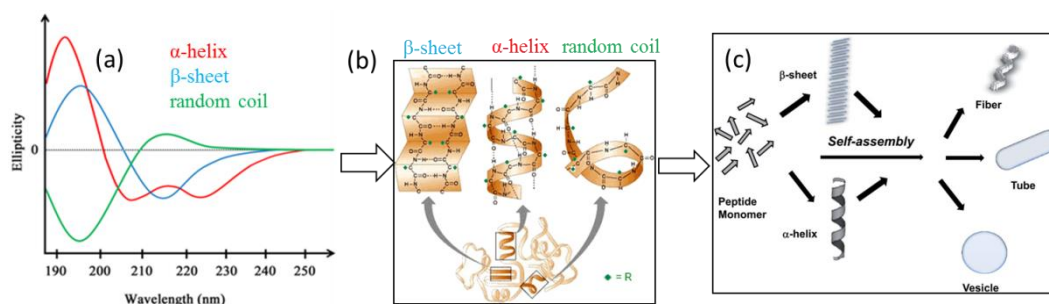
Figure 1.3. *The self-assembly of oligopeptides using CD analysis (a), secondary structure (b) and their morphology (c) (adopted from Panda al. Polym. Chem.,* **2014***, 5, 4418-4436)*

Peptide amphiphiles (PA) are class of amphiphiles that can be tuned into a range of nanostructures.[23-25] Due to the presence of amino acid residues, these nanostructures are self assembled for biological functions such as cell signaling transduction and cell adhesion etc. Intrinsic design of these amphiphiles contains a hydrophobic tail that drives the self-assembly in aqueous environment, simultaneously exposing functional groups onto the surface of the nanoscaffolds. The peptide a βAβAKLVFF has been studied over a period of time and it has been observed to form protofilaments which with time form short fibres. They were gradually transform to helical twisted ribbon in 24 h and over a month further evolve

into nanotubes. This peptide shows a variety of structures present in a single system with a low kinetic transformation. Lipopeptide C_{16}-KKFFVLK is another unique example of reversible morphology between helical ribbons and nanotapes. This peptide shows temperature dependent morphology from twisted nanotapes upon heating to gradually winding into helical ribbons upon cooling. Lipopeptides with strong hydrogen bonding have been observed to form cylindrical fibres where in the peptides lie perpendicular to the axis of fiber. One such example is the pentapeptide IKVAV headgroup containing PA which upon aggregation forms cylindrical nanofibre above its critical aggregation concentration (CAC), this has been shown in figure 1.4a.[20] Intermolecular strong hydrogen bonding is considered to be the driving force behind self-assembly and mechanical stability of these nanostructures. Using alternating hydrophobic and negatively charged amino acid residues in PA 1-D nanobelts were observed (figure 1.4b).[26]
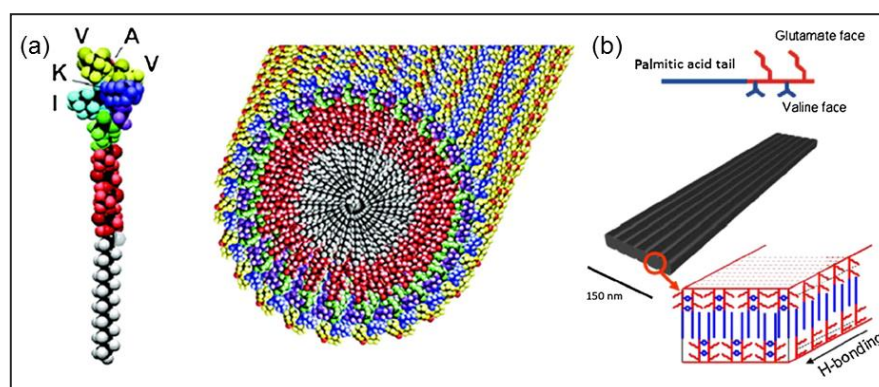
Figure 1.4. *Peptide IKVAV head group containing PA forming cylindrical fiber above CAC (a) and Glutamate (negative) and Valine (hydrophobic), conjugated with Palmitic acid tail giving rise to nanobelts of width 150nm (b). (adopted from Dehsorkhi et al. J. Pept. Sci.* **2014***, 20, 453–467).*

Collagen based PA show the role of alkyl chains that are conjugated with peptides in their self-assembly into polyproline II triple helix structure. It has been observed that lipid alkyl chains induce α-helix conformation to PAs. The influence of C_{12} alkyl chain on amyloid peptide core Lys-Aβ (11-17) has been studied. A single substitution alkyl chain (C_{12} Aβ (11-17)) gave short twisted fibres, however double substitution ($2C_{12}$ Aβ (11-17)) gave rise to long fibrils. Apart from structural morphologies, the applications of these peptide amphiphile have attracted a lot of attention recently. This includes responsiveness to stimuli such as light, temperature, pH, enzymes etc. An amyloid forming Ac-Lys-Thr-Val-ILe-ILe-Glu-NH_2 attached to

nitrobenzyl group was responsive to UV light. The structure transforms from β-sheet to random coil upon exposure to UV light due to cleavage of nitrobenzyl group (figure 1.5a).[27] Another interesting amyloid peptide based sequence KLVFF (C$_{16}$-KKFFVLK) was shown to possess reversible transformation from helical ribbons (coexisting with nanotubes) to nantapes upon heating as shown in figure 1.5b.[25] The change could be attributed to aromatic residue interactions upon subjecting to heat.
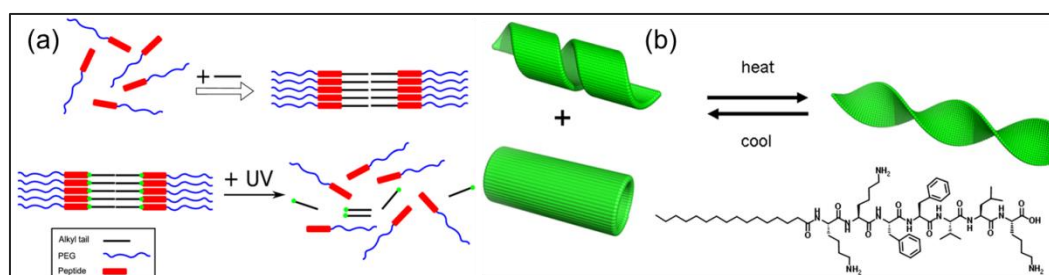
Figure 1.5. *Disassembly of photocleavable PA (a) and Transformtion in PA induced by temperature change (b) (adopted from Dehsorkhi et al. J. Pept. Sci.* **2014***, 20, 453–467).*

The use of UV cleavable nitrobenzyl group and its effect on self-assembly of PA has been exploited by other groups too. For example Stupp group has shown formation of hydrogel upon UV radiation of a PA comprising of an alkyl chain and nitrobenzyl moiety to Arg-Gly-Asp-Ser peptide unit.
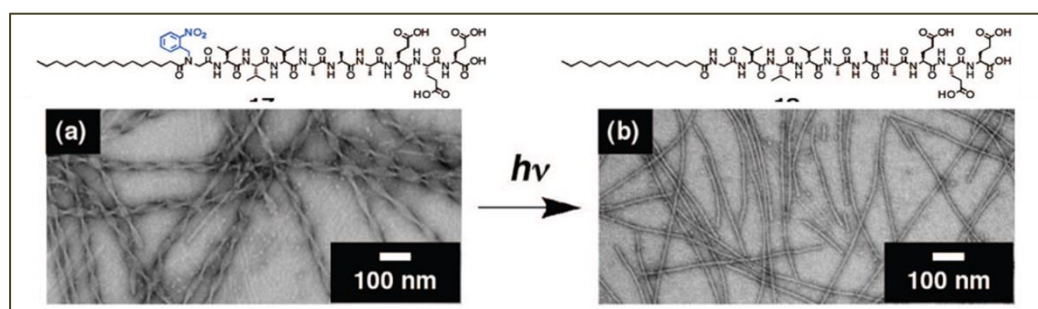
Figure 1.6.*The PA having GV$_3$A$_3$E$_3$ having helical morphology (a) as seen in TEM, cleaved in under UV light to produce nanotapes (b). (adopted from Palmer et al. Acc. Chem. Res.* **2008***, 41, 1674-1684).*

The same group also reported another PA having lipid chain conjugated to peptide sequence with nitrobenzyl group which assembled into quadruple helices and upon UV irradiation transformed into single fibers. PAs have also been synthesized based on their responsiveness towards temperature change. Collagen stimulating PA C$_{18}$-KTTKS were observed to have β-sheet structure at room temperature by CD analysis, and upon heating this PA above 55ºC (lipid layer melting point) turned into random coil. This change in morphology of the nanostructure was found to be

reversible in nature. PAs containing Palmitoyl tail and oligopeptide sequence $GV_3A_3E_3$ were attached to 2-nitrobenzyl groups. These UV cleavable PA self assemble in helical architectures with width 33 ± 2 nm and pitch $92\pm 4nm$. Upon exposing to UV light at 350 nm the helical nature of the fibers formed by the PA was lost into cylindrical fibrils with 11nm as shown in figure 1.6.[28]

1.3. Polypeptides

Polypeptides are made up of amide repeating unit of amino acids. Polypeptides are synthesized by polycondensation (chemical synthesis) reaction, in which the amino acid carboxylic group converted into active ester such as acid chloride, p-nitrophenyl ester etc. (in scheme 1.2).[29] The esters were self-condensed with amine group in presence of base to yield polypeptide. Alternatively self-condensation of amino acid using coupling reagent with removal of water produced polypeptide. Unfortunately these methods produced only low molecular weight polymers and they are not useful for making high molecular weight polypeptides for commercial application.
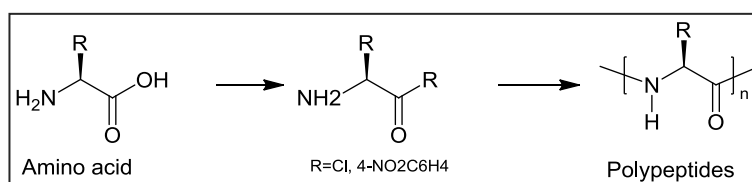
Scheme 1.2. *Synthesis of polypeptides by polycondensation approach*

Endo and coworkers developed synthesis of polypeptide using polycondensation approach; (in scheme 1.3) in this method the amine functional group was converted into phenyl carbamate using diphenyl carbonate which produced in situ N-carboxy anhydride monomer.[30] The self-condensation of this monomer followed by the removal of carbon dioxide and phenol produced polypeptides. This approach also afforded only low molecular weight polypeptide.
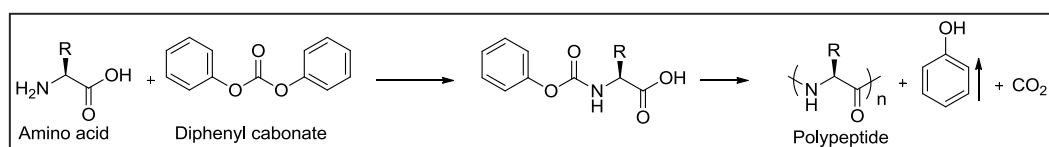
Scheme 1.3. *Synthesis of polypeptide by phenyl carbamate monomer based polycondensation approach.*

ROP approach for Polypeptides

The ring opening polymerization of NCA monomer by initiator (alcohol or amine) in presence of catalyst yielded polypeptides.[31] The ring opening polymerization (ROP) approach has various advantages such as: (i) polymers molecular weight can be controlled based on monomer to initiator ratio, ($X_n=(M)/(I)$), (ii) narrow polydispersity of the polymers and (iii) the living nature of ROP process can be used for making diverse polymer architecture such as block, graft, etc. Various catalysts have been studied for ROP approach to provide controlled molecular weight polymer.[32-33] NCA monomers were typically synthesized using Fuchs-Farthing method, in which α-amino acid reacted with triphosgene and ended up with a racemization free NCA product. (in scheme 1.4) [34-35]
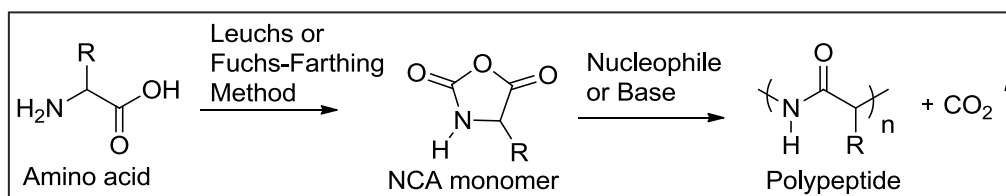
Scheme 1.4. *Synthesis of polypeptide by rop of NCA monomer*

The living or controlled polymerization of NCA was achieved using various initiators; usually primary amine[36-37] and alkoxide anions[38-39] were used as initiators. The ROP of NCA method commonly follows two mechanistic pathways namely (i) normal amine (NAM) and (ii) activated monomer (AMM) mechanism to provide the polypeptide (in scheme 1.5).[40-41] In AMM mechanism, tertiary amine and metal alkoxide (non-nucleophilic base) are used as the initiators. In the first step of the mechanism, initiator abstracts the proton from –NH of NCA monomer yielding NCA anion. In the subsequent step deprotonated NCA anion can initiate the polymerization by attacking ester carbonyl carbon of another monomer to provide unstable carbamic acid intermediate; which decomposes to generate the amine functional group by the release of CO_2. The repetitive cycle of second step of the polymerization process yielded polypeptide. The NCA polymerization using AMM mechanism tends to yield uncontrolled polymer with high polydispersity index. NCA polymerizations by NAM mechanism are generally initiated by a molecule containing at least one proton such as primary amine, secondary amine, alcohol and water as the initiator. The initiation step depends upon the nucleophilic substitution of primary amine at the ester carbonyl carbon of NCA monomer to yield the unstable carbamic acid intermediate. This

subsequently decomposes by release of CO_2 and generates the new amine group. The repetitive cycle of nucleophilic substitution followed by removal of CO_2 delivers the polypeptide. The NCA polymerization by NAM approach offers controlled molecular weight polymers; however this method is associated with some side reactions such as formation of cyclic structures which leads to formation of low molecular weight polymers.
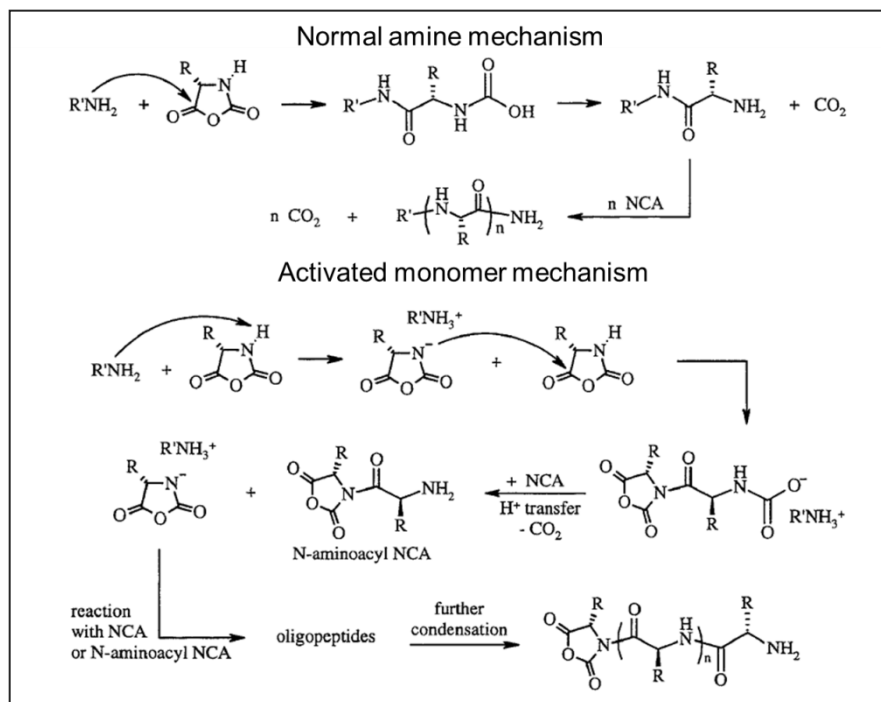
Scheme 1.5. *The rop of NCA monomer via normal amine mechanism and activated monomer mechanism (adopted from Deming J. Polym. Sci. Polym. Chem.* **2000**, *38,* 3011-3018)

Deming was the first to demonstrate the living polymerization of NCA using Ni (COD)bpy metal catalyst via eight member cyclic transition state mechanism to deliver the polypeptide with controlled molecular weight and low polydispersity index (in scheme 1.6).[42] In this process, the NCA monomer reacted with metal catalyst to yield the metallocyclic complex as the covalent propagating species. In addition, this cyclic intermediate was reacted with new NCA monomer followed by removal of CO_2 and proton transfer reaction to yield controlled molecular weight of polypeptide. These polypeptides are purified from metal complex residue by dialysis or precipitation method.
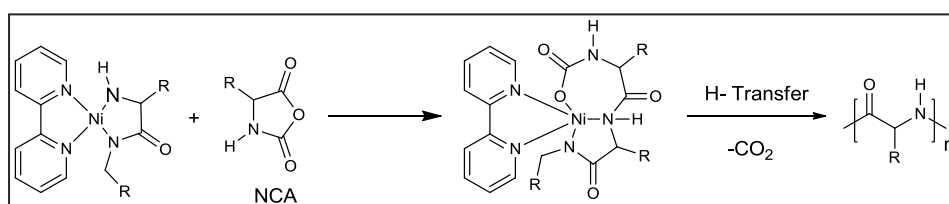
Scheme 1.6.*Synthesis of living polypeptide achieved via Ni transition metal catalyst*

Functional polypeptides were synthesized via NCA route using protection and deprotection methodology. (in figure 1.7)[31] The functional group could be carboxylic acid, amine, hydroxyl, thiol, imidazole, guanidine etc. in side chain of polypeptides depending upon the amino acids. Hernandez et al. reported the amine functional poly peptides using ROP polymerization approach.[43] In this process the side chain protected lysine NCA monomer was polymerized using ROP followed by deprotection reaction that delivered the amine functional polymer. Similarly the carboxylic functional polypeptides are also reported in the literature. The side chain protected aspartic and glutamic acid NCA monomer were polymerized and then subsequently deprotected to produce the carboxylic functional polypeptides.[44]
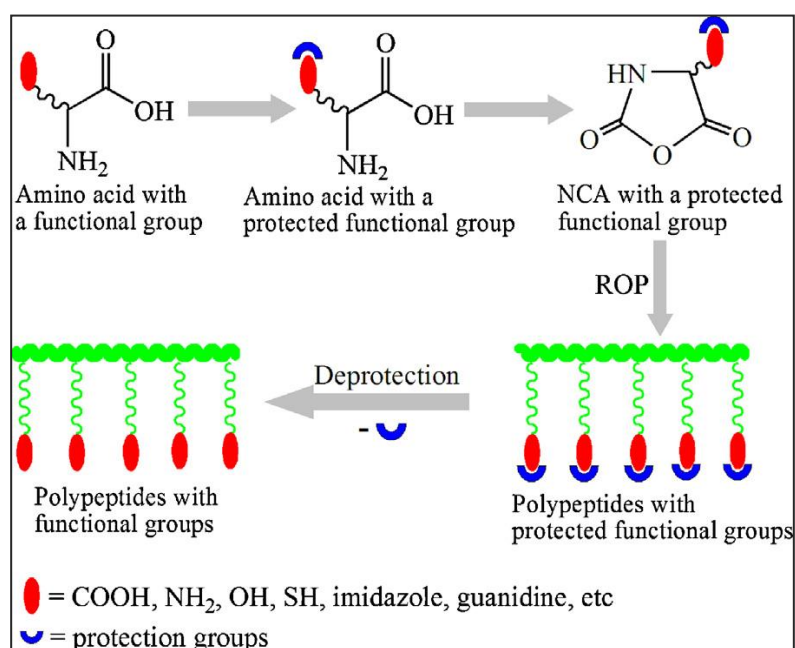
Figure 1.7. *Synthetic scheme for side chain containing functional polypeptide* (*adopted from Deng et al. Prog Polym Sci.* **2014***, 39,* 330-364*)*

Lee et al. prepared imidazole functional polypeptide using dinitro phenyl protected histidine monomer.[45] The protected histidine polymer was deprotected using 2-mercaptoethanol at room temperature to provide the histidine functional polypeptide. Heise et al. developed thiol functional polypeptide from S-tert-butylmercapto-L-cysteine NCA monomer.[46] The side chain disulfide protected NCA monomer was polymerized; then deprotected using dithiothreitol (DTT) to yield the thiol functional polypeptide. Xing et al. synthesized cystine NCA monomer from cystine amino acid using PBr_3 in dichloromethane.[47] The cystine NCA monomer was copolymerized with benzyl protected glutamic acid and PEG-NH$_2$ as the initiator to generate disulfide based core cross-linked polymer. Hayakawa et al. fabricated guanidine functional polypeptide from L-arginine amino acid.[48] Tooney et al. and Yamamoto et al reported hydroxyl functional polypeptide from L-serine and L-Dihydroxy phenylalanine (DOPA) amino acid.[49] In this process O-protected L-serine and L- DOPA NCA monomer was polymerized followed by deprotection that provided the hydroxyl functional polypeptide.
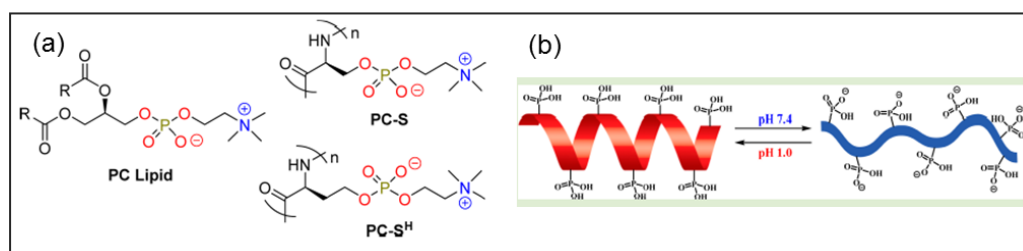
Figure 1.8. *Synthesis of functional polypeptide by rop of NCA monomer for phoshorylchloline (a) and phosphonate (b). (adopted from Yakovlev et al. ACS Macro Lett.* **2014***, 3,* 378-381. *(b) J. Am. Chem. Soc.* **2015***, 137,* 4078-4081*).*

Yakovlev et al. prepared phosphonate containing polypeptide and block copolypeptides by ring opening polymerisation of L-serine based NCA monomer.[50] In this approach, the hydroxyl group of L-serine amino acid was protected via the phosphonate functional group, which was polymerised by ROP in presence of Co(PMe$_3$)$_4$ as the catalyst and then deprotected to yield the phosphonate containing polypeptides. (in figure 1.8b) The living nature of the NCA polymerisation approach was used for the synthesis of block copolypeptide based on L-phenyl alanine and L-lysine containing phosphonate polypeptides. Same author reported polypeptides containing phosphorylcholine using serine and homoserine amino acids. The side chain protected serine and homoserine amino acid NCA monomer was derivatized to

contain a halogen and then polymerised to yield the halide functional poly(peptides). This was post polymerised using N-alkylation reaction followed by deprotection to produce the phosphorylchloline containing polypeptide.[51] (in figure 1.8a). The second method of synthesis of functional polypeptides did not involve protection and deprotection of the side chain functional groups. This method was developed for numerous functional group including oligoethylene glycol, alkene, alkyne, azide, chloride, vinyl benzyl, vinyl sulfone, peptide and sugar.[31] The alkene functional polymer was post functionalized by Michael addition reaction with various thiol derivatives. Further alkyne functional group was post functionalized using click chemistry that yielded various structures.
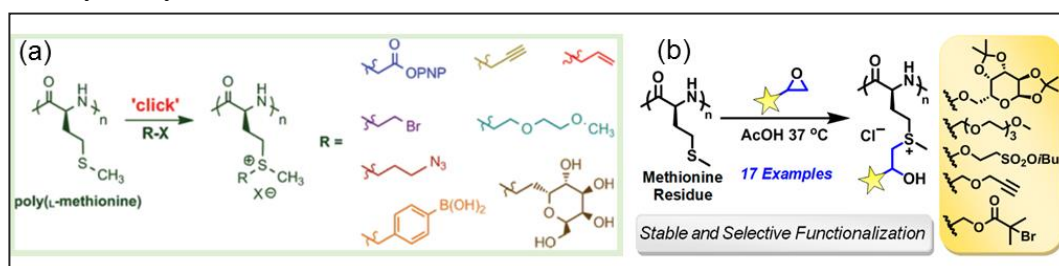
Figure 1.9. *Synthesis of functional polypeptide based on methionine amino acids and their post functionalization. (adopted from Deming and coworkers (a) Biomacromolecules* **2012***, 13,* 1719-1723 *and (b) Biomacromolecules* **2015***, 16,* 1802-1806*).*

Recently Deming and co-workers developed post polymerisation approach for polypeptide based on L-methionine amino acid; in this method thioether of poly (L-methionine) was alkylated by various functional groups containing alkyl halides and triflates to yield stable sulfonium ion derivatives.[52] The controlled molecular weight of poly (L-methionine) was synthesised by ROP of L-methionine NCA monomer and Co(PMe_3)_4 as the catalyst (in figure 1.9a). Same author reported the post polymerisation of poly (L-methionine) by alkylation of various functional epoxides to yield the hydroxyl functional sulfonium salt. In this method thioether of poly (L-methionine) was treated with multi-functional epoxide derivative where acetic acid solvent acts as the proton source to generate stable sulfonium salt. The benefit of these two methods is that multiple functional polypeptides can be synthesised without additional protection and deprotection reaction.[53] (in figure 1.9b)
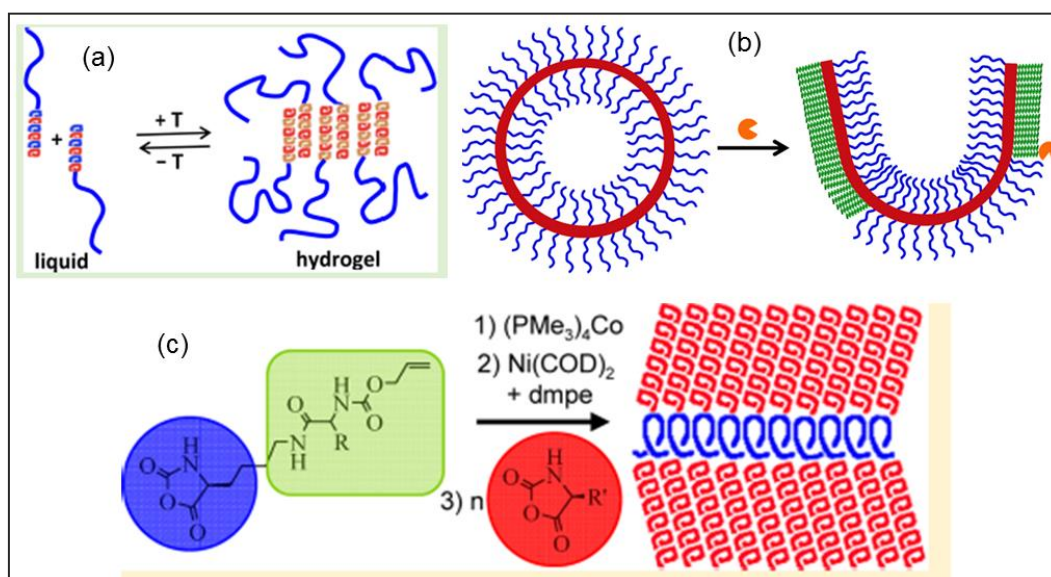
Figure 1.10. *Self-assembly of block copolypeptides based on amino acids (adopted from Deming and coworkers. Biomacromolecules* **2015***, 16,* 1331-1340. *(b) Biomacromolecules* **2013***, 14,* 3610-3614*) and (c) J. Am. Chem. Soc.* **2012***, 134,* 19463-19467*).*

The advantage of NCA polymerization approach is that polypeptide containing various functional groups can be synthesized with precise control over molecular weights.[54] The living nature of NCA polymerization technique can extend to various other structures such as di-block, tri-block, graft etc. copolymers via sequential addition of the monomers. The block copolymers are an ideal candidate for self-assembling materials where the self-assembly, chemical and mechanical properties of the polymer can be altered depending upon the composition of block copolymers. Zhang et al. developed reversible self-assembly of copolypeptides from liquid to gel and vice versa using temperature as a variable (in figure 1.10a).[55] The authors prepared non-ionic diblock copolypeptides containing hydrophilic poly (γ-[2-(2-methoxyethoxy)ethyl]-rac-glutamate) and hydrophobic poly(L-leucine) segments. This approach demonstrated the loading of guest molecule in liquid state and their release upon increasing the temperature due to its gel formation. Deming and coworkers developed the diblock copolypeptide, poly (L-methionine)$_{65}$-b-poly(L-leucine$_{0.5}$-stat-L-phenylalanine$_{0.5}$)$_{20,}$ and they self-assembled into vesicles upon oxidation reaction (in figure 1.10b).[56] In this study, enzyme is used as a tool to alter self-assembly of vesicle, which leads to release of cargo from self-assembled vesicle.

Changes in the self-assembly of copolypeptides was further supported by CD spectroscopic analysis, which shows the transition of secondary structure from α-helix to random coil conformation. Rhodes et al. prepared high density brush copolypeptides via tandem catalyst method;[57] in this study alloc-α-aminoamide containing NCA monomers were polymerised using (Co(PMe$_3$)$_4$) as catalyst to produce the allyl functional polypeptides. Subsequently Ni(COD)$_2$ catalyst was added to activate the side chain double bond and then addition of new NCA monomer produce the graft polypeptides (in figure 1.10c). Since these polypeptides are composed of amino acid residues, these polymers are biocompatible as well as bioactive in nature.

1.4. Amino acid based poly(ester-amide)s

Poly depsipeptides are made up of alternating copolymers of α-amino acid and α-hydroxy acid containing degradable aliphatic ester linkage. The ROP of morpholine 2, 5-dione is the one of the major synthetic approach to prepare the polydepsipeptide polymer. (in scheme 1.7)[58]
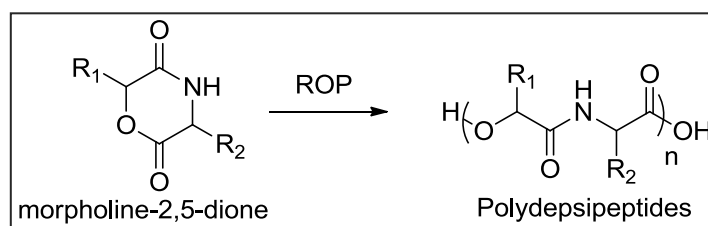
Scheme 1.7. *Synthesis of poly (ester-amide) by ROP of depsipeptides*

The 6-membered ring of morpholine-2,5-dione derivatives were prepared using α-amino acid and α-hydroxy acid as the starting material. The morpholine-2,5-dione derivatives were subjected to ring opening polymerization using tin octanoate as the catalyst and alcohol as the initiator to afford the poly depsipeptides. Due to controlled or living nature of ROP depsipeptides provided various polymer structures such as random, alternating, diblock, triblock and graft copolymers. The advantages of this approach are that (i) it can be used for nonfunctional or different functional polymer including carboxyl, hydroxyl, amine and thiol functional group depending upon the type of α-amino acid used in the polymerization process and (ii) the degradation of these polymers can be tuned based on the type of α-amino acid and α-hydroxy acid. Feijen et al. developed first synthetic methodology for ROP of

depsipeptides, in which Glycine and D,L-lactic acid based morpholine-2,5-dione derivative were polymerized using Sn(Oct)₂ as a catalyst.[59] The same polymerization approach has been expanded to polymerize morpholine-2,5-dione derivative with various amino acids (glycine, alanine or valine) and α-hydroxy acids (glycolic acid, lactic acid). Feijen et al. prepared the functional polymers based on various protected amino acids including aspartic acid, glutamic acid and lysine using ROP of morpholine-2, 5-dione derivatives.[60] Further deprotection of polymers provided the various functional polymers including carboxylic acid and amine.
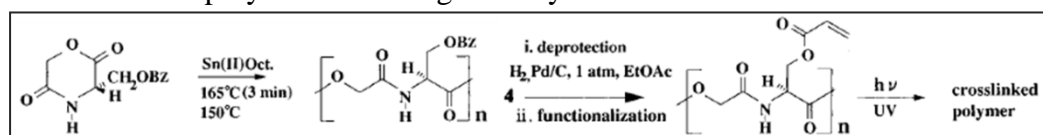
Scheme 1.8. *Synthesis of hydroxyl functional poly (ester-amide) by ROP of depsipeptides and their post functionalization*

John et al. carried out the ROP of depsipeptide with glycolic acid and O-benzyl-L-serine that produced benzyl protected polydepsidpeptides, and then deprotection of benzyl group produced hydroxyl functional group.[61] The hydroxyl functional polymers reacted with acryl chloride resulting in acrylate polymer; further acrylate polymer was photopolymerized to form crosslinked gel (in scheme 1.8).
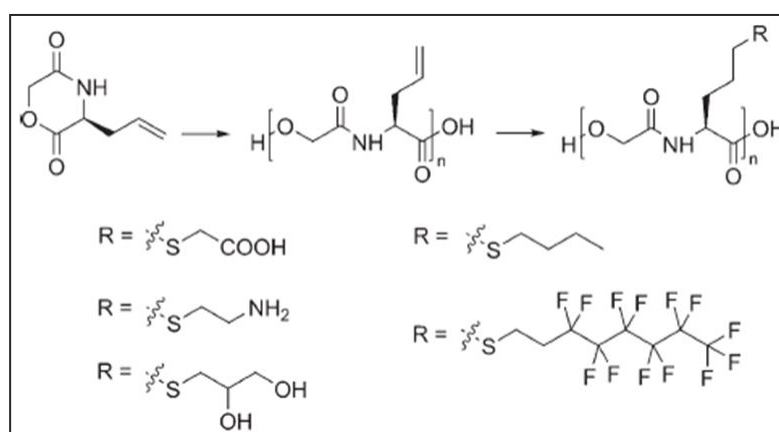
Scheme 1.9. *Synthesis of allyl functional poly (ester-amide) by ROP of depsipeptides and their postfunctionalisation with various thiol derivatives*

Recently Kolk et al. revisited and optimized reaction condition for the ROP of morpholine-2,5-dione using protected L-lysine or L-2-allyl glycine to develop high molecular weight polymer.[62] In addition the allyl group was post polymerized using various thiol group including thioglycolic acid, cysteamine hydrochloride, 1-thioglycerol, 1-butanethiol etc., to produce the functional polymer. Though the

reactivity of depsipeptide monomer was low for homo polymerization reaction, the copolymerization of depsipetide monomers with lactide and caprolactone could yield high molecular weight polymers (in scheme 1.9). Ouchi, Morita and Feng authors synthesized various random copolymers based on functional depsipeptide monomer. The polymer backbone contains degradable aliphatic ester as the functional group; hence these polymers were used in various biomedical and biomaterial applications.
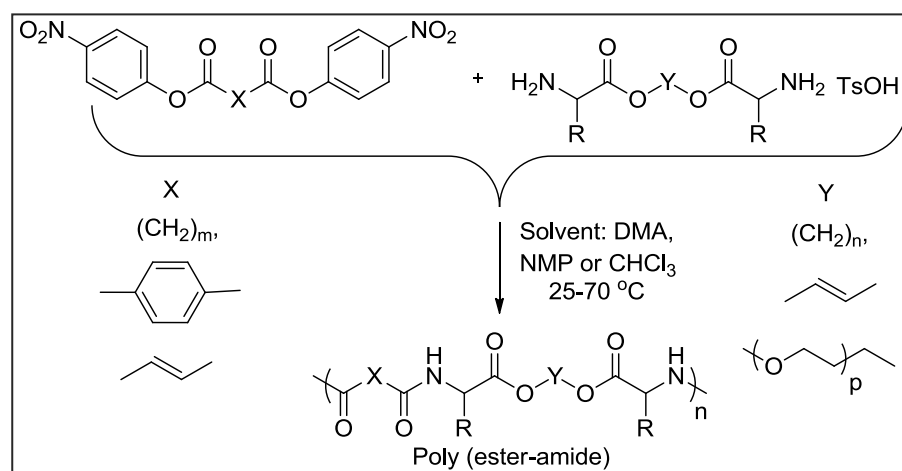
Scheme 1.10. *Amino acid based saturated and unsaturated poly (ester-amide) by solution polycondensation approach.*

Solution polycondensation methodologies have been intensively investigated for L-phenyl alanine based poly (ester-amide) because the starting material and polymer are easy to synthesize and purify, and most of these polymers are enzymatically degradable in nature (in scheme 1.10). Arabuli et al. prepared a family of novel biodegradable poly (ester-amide) based on L-phenyl alanine by reacting bis (p-nitrophenyl) adipate with di-p-toluenesulfonic acid salts of 1,2-ethanediol, 1,3-propanediol, or 1,4-butanediol bis L-phenyl alanine diesters.[63] The polymerization reactions are carried out in either N-methyl-2-pyrrolidone (NMP) or $CHCl_3$ as the solvent at 25 °C for 48 h and triethyl amine is incorporated as an acid acceptor. The poly (ester-amide)s degraded in presence of α-chymotrypsin at 37 °C under pH=8.0 conditions, the results revealed that increasing the aliphatic diol chain length in the polymers increases the rate of degradation. Katsarava and coworkers optimized the polycondensation reaction conditions with dimethyl acetamide as the solvent at 65 °C for 48 h and triethyl amine used as a proton acceptor to afford high molecular weight polymers.[64] The aliphatic diol was replaced with an oligoethylene glycol to produce poly (ether ester amide). Gillies et al. prepared a set of amine functional poly (ester-

amide) by varying the mole ratio of L-lysine Boc and L-phenylanine amino acids (from 0:100 to 20:80) in the feed (in scheme 1.11).[65-66] The L-lysine Boc group could be completely deprotected without disturbing the polymer backbone. The hydrolytic and enzymatic degradation of these poly (ester-amide)s increases on increasing the L-lysine content in the polymer. The functional poly (ester-amide) could be used to conjugate the drug molecule and other bio-active compounds for biomedical and biomaterial applications.
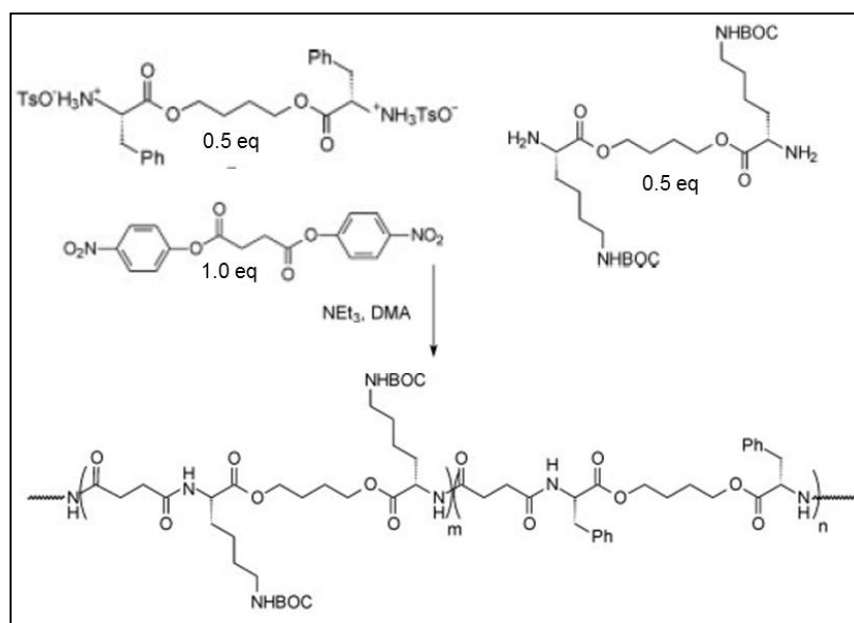
Scheme 1.11. *Synthesis of amine functional poly (ester-amide) copolymers based on amino acids using polycondensation approach*

Recently a sets of novel PE(E)A was prepared from L-phenylalanine or L-arginine and D,L-allyl glycine amino acids, which contained carbon-carbon double bond in the pendent chain of polymer (in scheme 1.12).[67-68] Upon increasing the D, L-allyl glycine amino acid content in the polymer chain the enzymatic degradation decreases. Further the allyl functional groups were post polymerized to provide various functional groups such as carboxyl, amine, hydroxyl, sulfonate etc. for biomedical application. The poly(ester-amide) were also synthesized by various other amino acids including L-phenyl alanine, L-alanine, L-leucine, L-isoleucine, L-norleucine, D,L-methionine and L-arginine. In addition, the poly(ester-amide) with higher hydrophobic content tend to degrade faster with α-chymotrypsin, possibly due to their better affinity towards α-chymotrypsin.
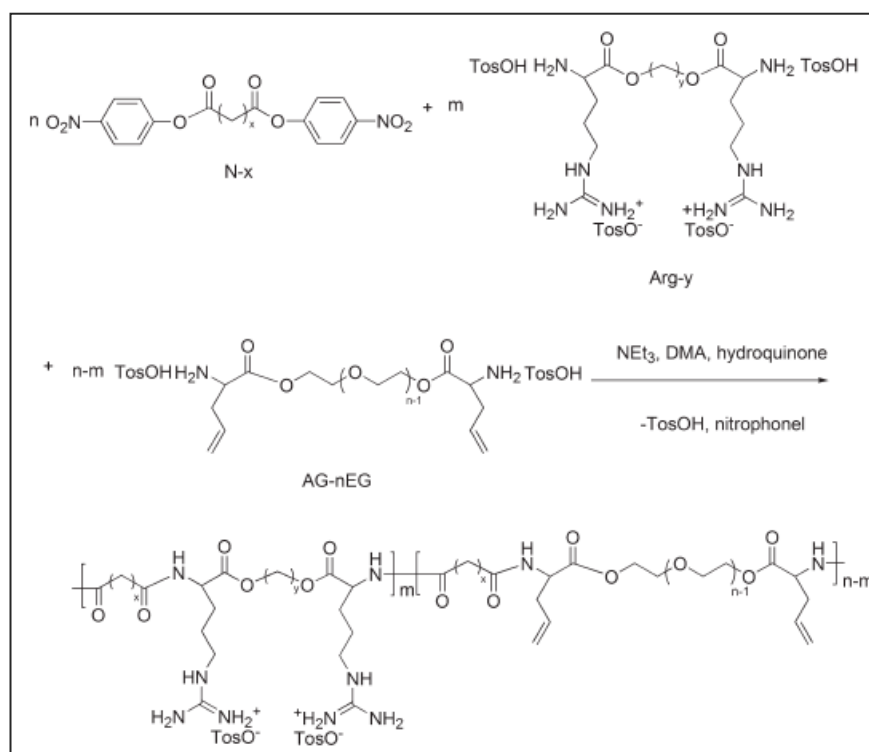
Scheme 1.12. *Arginine based poly (ester-amide) by solution polycondensation technique.*

The unsaturated poly (ester-amide)s were synthesized using either unsaturated diols diacids or diacid chlorides. Guo et al. prepared a set of unsaturated poly (ester-amide) by solution polycondensation approach.[69] In this process two unsaturated monomers, di-p-nitrophenyl fumarate and L-phenyl alanine 2-butene-1,4-diol diester p-toluene sulfonate and four other saturated monomers (based on 1,4-butanediol, 1,6-hexanediol, adipoyl chloride and sebacocyl chloride) were used in different mole ratio for polymerization. The advantage of unsaturated poly (ester-amide) is that it can be attached with bioactive molecule for biomedical and non-biomedical applications. The enzymatic degradation of unsaturated poly (ester-amide) using α-chymotrypsin showed slower degradation compared to saturated poly (ester-amide). The mixture of saturated and unsaturated monomers reacted to provide partially unsaturated poly (ester-amide). For example Chu and Guo coworkers synthesized the partially unsaturated poly (ester-amide) using L-phenyl alanine, aliphatic diacid chlorides (succinyl chloride, adipoyl chloride, sebacoyl chloride and fumaryl chloride), and 1,4-butanediol (in scheme 1.13).[70] The T_g and biodegradability of the polymer could be tuned based on the ratio of saturated and unsaturated monomer in the feed.
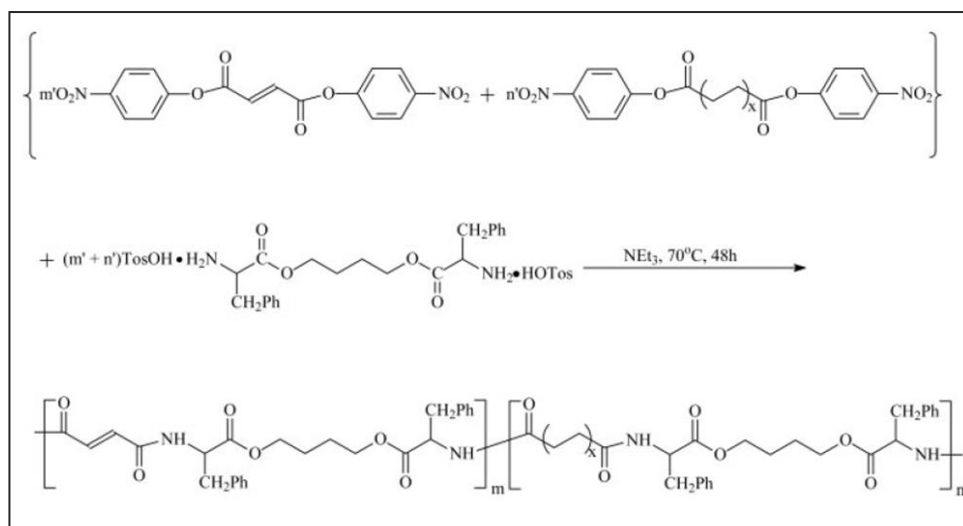
Scheme 1.13. *Synthesis of phenyl alanine amino acid based poly (ester-amide) by solution polycondensation method*

Amino acid based melt polycondensation approaches are particularly interesting due to the natural availability of the monomer in bulk scale: also the polymers can be used in biomedical and biomaterial applications. Asin et al. prepared poly (ester-amide) based on glycine, different diol and dicarboxylic acids by melt polycondensation method (in scheme 1.14).[71]
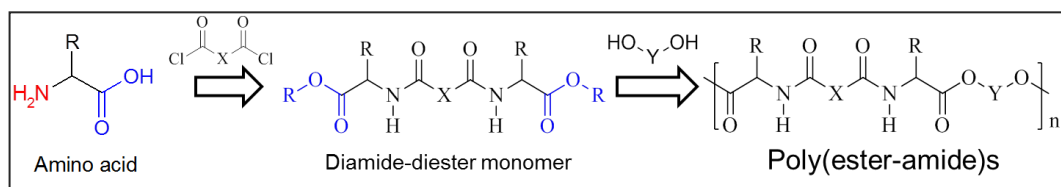
Scheme 1.14. *Synthesis of poly (ester-amide) by transesterification method*

The amino acid monomer diamide-diester was synthesized by reaction between diacyl chloride and amino acid ester in the presence of base. The diamide-diester monomer was polymerized at 160 °-190 °C with nitrogen purge and then at 200 - 220 °C in vacuum (0.3 mmHg) to produce the poly (ester-amide). The disadvantages of the polymerization process were that (i) the polymer produced was a racemic product and (ii) due to amide functionality the reactions were carried out at higher temperature, which leads to the undesirable side reactions.

1.5. Poly (α-hydroxy acids)

The α-hydroxy acids are synthesized from α-amino acid via diazotization reaction using sodium nitrite in acidic condition (in scheme 1.15).[72-73] In this reaction α-amino acid amine functional group was converted into hydroxyl group to give α-hydroxy acid. α-Amino acid based α-hydroxy acid has various advantages: (i) α-hydroxy acid has the similar structure like lactic acid and depending upon the amino acid starting material, the functional lactic acid monomer can be synthesized, and (ii) stereochemistry of the α-amino acid is retained after the diazotization reaction. α-hydroxy acid underwent self-condensation reaction in presence of p-toluene sulfonic acid as catalyst to produce dilactide monomer. Another synthetic approach for dilactide monomer is where α-hydroxy acid is made to react with α-halo carboxylic acid or α-halo acylhalide to result in the dilactide monomer. By these methods, various functional dilactide monomers have been synthesized including carboxyl, amine, alkene, alkyne etc. The dilactide monomers were polymerized using ring opening polymerization technique in the presence of Sn(Oct)₂ as the catalyst to produce polyester with desired molecular weight.
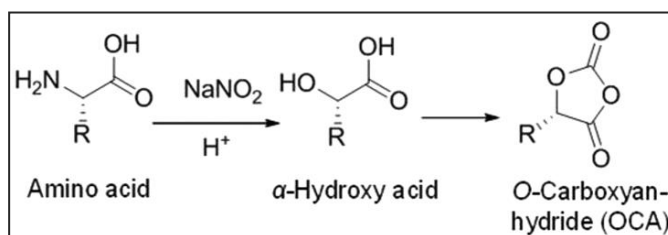
Scheme 1.15. *Synthesis of O-carboxyanhdride from α-amino acids*

These approaches have been widely used for various functional α-hydroxy acids such as carboxylic acid, amine, alkene, alkyne and oligoethylene glycol (OEG) (in scheme 1.16).[72] The carboxylic acid functional polyesters based on α-hydroxy acid have been prepared from the ROP of benzyl protected dilactide, which is subsequently deprotected using catalytic hydrogenation.[74-75] The ROP of hydroxyl protected dilactide monomers was carried out in presence of Sn(Oct)₂ as catalyst followed by deprotection reaction to give the hydroxyl functional polyester containing α-hydroxy acid.[76-78] Weck and co-workers reported the amine functionalized polyester based on α-hydroxy acids. In this process, the amine protected dilactide monomer was polymerized using ROP followed by deprotection to provide the amine functional polyester.[79]
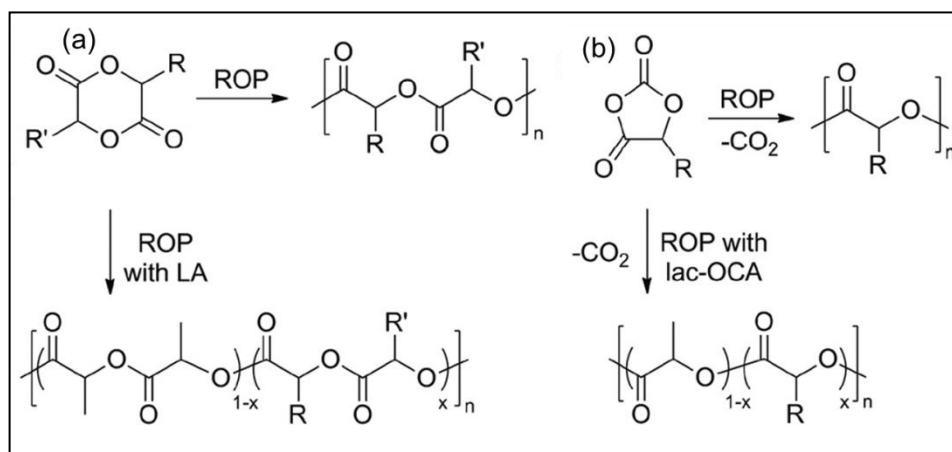
Scheme 1.16. *Synthesis of functional poly ester via ROP of dilactide monomer (a) and O-carboxyanhydride monomer*

Jiang et al. synthesized OEG/PEG functionalized polymers using ROP of dilactide to provide water soluble polyester (in scheme 1.17).[80-81] In addition the alkene and alkyne containing functional polyester was post polymerized by thiol-ene and thiol-yne respectively. These functional polyesters have been widely applied in biomaterial and biomedical fields because of their biodegradable nature.
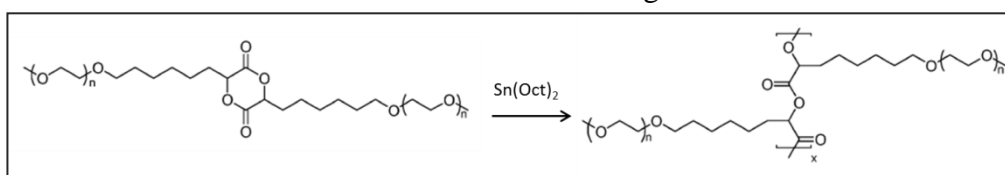
Scheme 1.17. *Synthesis of oligoethylene glycol functional poly ester by rop dilactide monomer*

Farokhzad, Langer and co-workers demonstrated solvent free polycondensation reaction for α-hydroxy acid using p-toluene sulfonic acid as a catalyst to afford the polyester via removal of water as by product (in scheme 1.18).[82-83]
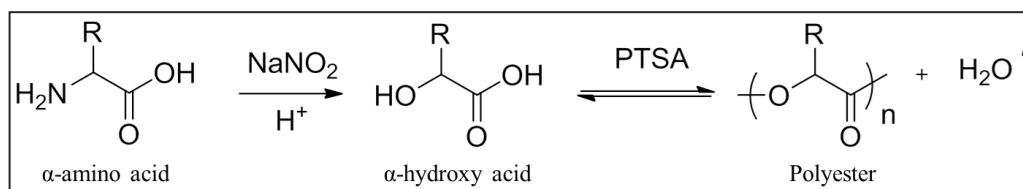
Scheme 1.18. *Synthesis of polyester from α-hydroxy acid by melt polycondensation approach*

In addition the condensation approaches have been expanded to include various functional amino acids based polyesters such as hydroxyl and amine group. In the A-B condensation approach there is no need to maintain the stoichiometric ratio due to its in built monomer. The drawback of this approach is that A-B (A-carboxylic acid, B-alcohol) polycondensation method tends to produce more cyclic product compared to linear polymer; which hampers the development of high molecular weight polyesters. The overall conclusion is that there is no synthetic methodology known in the literature for amino acid based melt polycondensation approach to develop high molecular weight polymer.

1.6. Amino acid based polyurethane and poly (urea)

Polyurethanes are typically synthesized by the reaction of diisocyanide with diol in presence of catalyst. Urethane functional group (-NHCOO) is made up of hydrogen bonded NH groups, which increase the mechanical and thermal stability of the polymers. Endo and coworkers treated sodium salt of L-phenyl alanine with five membered carbonate in presence of ethylene glycol to produce the A-B type urethane monomer (in scheme 1.19).[84] Further this A-B monomer underwent self-condensation in the presence of coupling reagent dicyclohexylcarbodiimide (DCC) resulting in only low molecular weight polyurethane.
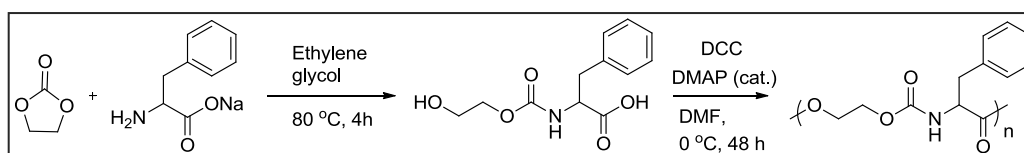
Scheme 1.19. *Synthesis of polyurethane by AB polycondensation approach*

Endo and coworkers reported synthesis of polyurethane based on L-tyrosine amino acid; in this process the L-tyrosine amino acid carboxylic acid was converted into L-tyrosine methyl ester amine salt, further amine salt was treated with ditertbutyltricarbonate in presence of base to produce L-tyrosine isocyanide monomer. This L-tyrosine isocyanide monomer was self-condensed in presence of base yielding L-tyrosine based polyurethane (in scheme 1.20).[85-86]
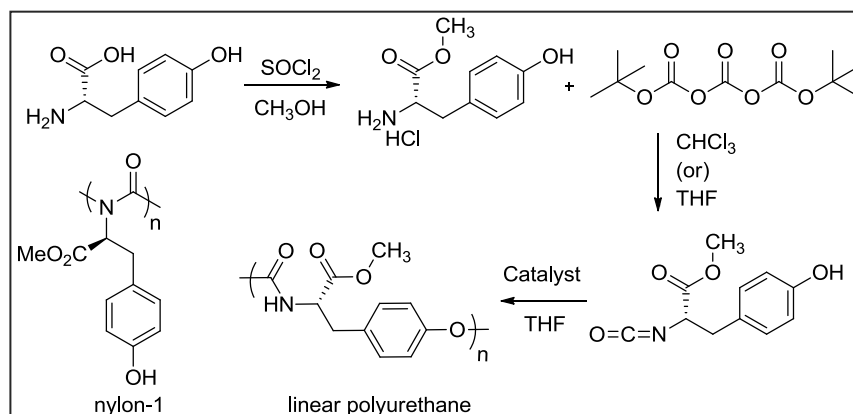
Scheme 1.20. *Synthesis of polyurethane based on L-tyrosine amino acid*

Same author reported L-lysine hydrochloride amino acid reacted with bifunctional cyclic carbonate in presence of base and dimethyl acetamide as solvent to give the hydroxyl functional polyurethane (in scheme 1.21).[87]
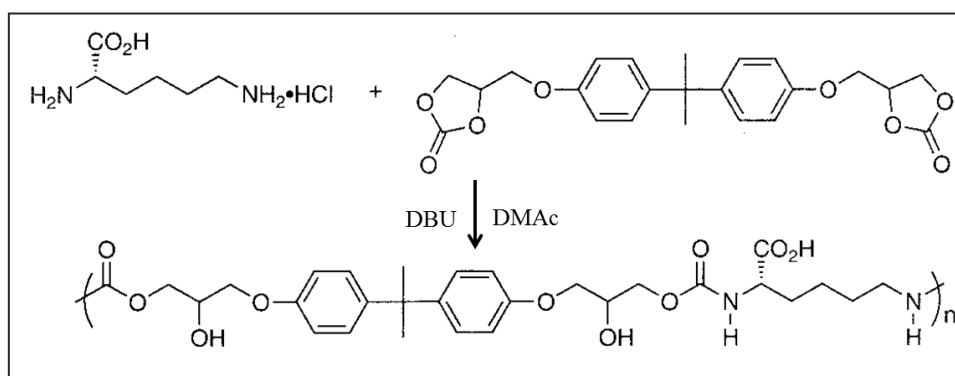
Scheme.1.21. *Synthesis of poly hydroxyl urethane based on L-lysine hydrochloride using rop of five membered cyclic carbonate*

The poly (ester-urea)s are made up of half ester and half urea functional group. These polymers were synthesized by both solution polycondensation and interfacial polycondensation process.
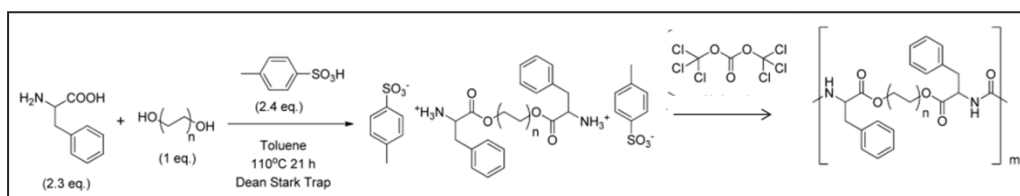
Scheme 1.22. *Phenyl alanine based poly (ester-urea) by solution polycondensation method.*

The α-amino acid reacted with diol group in presence of PTSA to produce di-p-toluenesulfonic acid salts of bis- (α-amino acid) α,ω-alkylene diesters (BAAD). Becker and coworkers synthesized poly (ester-urea)s by BAAD p-toluene sulfonic acid salt of phenyl alanine or tyrosine reacting with triphosgene via interfacial polycondensation reaction in presence of sodium carbonate as base (in scheme 1.22).[88-93] Due to aliphatic ester functional group these polymers are biodegradable in nature, and the urea functional group provides mechanical stability as well as water solubility for the polymers. The combination of ester and urea functional group in these polymers has been applied for various applications.[94]

1.7. Amino acid based polycarbonate

Bisphenol reacted with phosgene or activated esters in presence of catalyst to afford polycarbonate. Most of the bisphenol compounds used for polycarbonate synthesis are toxic in nature; to overcome these issues naturally available tyrosine amino acid based bisphenol monomer was developed for polycarbonate synthesis. Kohn and coworkers developed synthetic methodology for tyrosine based polycarbonate (in scheme 1.23);[95] in this method 3 (4-hydroxylphenyl) propionic acid was treated with tyrosine alkyl ester in presence of coupling reagent dicyclohexylcarbodiimide (DCC) to produce the tyrosine based bisphenol monomer. This tyrosine based Biphenol monomer reacted with phosgene or triphosgene giving rise to polycarbonate. Tyrosine based polycarbonates were synthesized using various substituents including alkyl, polyethylene glycol etc. [96]
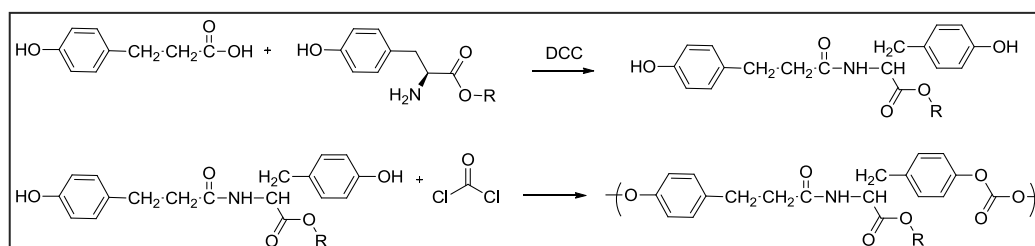
Scheme 1.23. *Synthesis of polycarbonate based on tyrosine bisphenol derivative by polycondensation approach*

1.8. Amino acid based hyperbranched polymer and poly acrylate

Hyper branched polymers are obtained in a one step polymerization of AB_x monomers ($x \geq 2$) or copolymerization of A_2 and B_n monomers ($n \geq 2$), representing an interesting alternative approach for dendrimer. These polymerization processes have various advantages over other approaches, such as bulk scale synthesis of polymers because of one step reaction, three-dimensional globular architecture, low viscosity, high solubility, abundance of functional end groups and internal cavities in the molecule. Amino acid based hyperbranched polymers are highly attractive due to naturally occurring optically pure starting material as the monomer and also the functional hyperbranched polymers can be post functionalised for further applications.
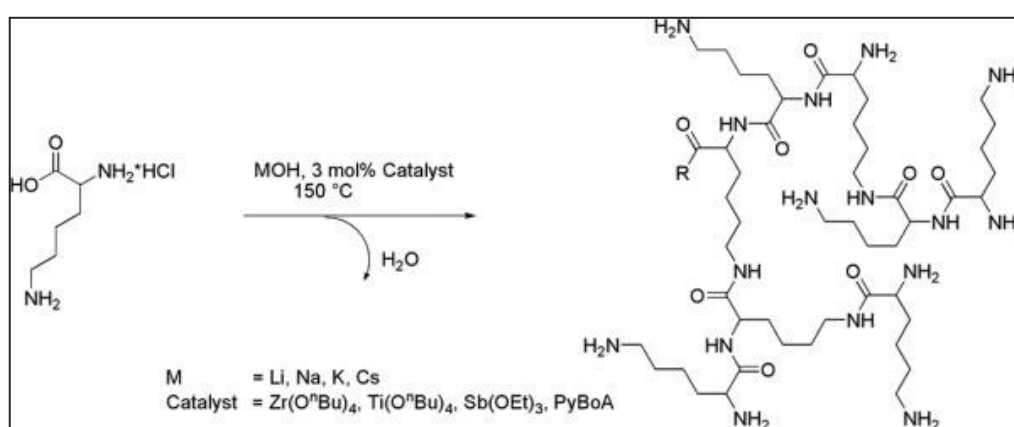
Scheme.1.24. *Synthesis of hyperbranched polymer based L-lysine amino acid by polycondensation approach* (adopted from *Scholl et al. J. Polym. Sci., Part A:Polym. Chem.* **2007***, 45,* 5494*)*

Menz and chapman explored the hyperbranched polymerization approach based on L-lysine amino acid; in this method N-hydroxy succinimide ester of L-lysine hydrochloride was polymerised using AB_2 approach to produce the L-lysine based hyperbranched polymer.[97] Scholl and coworkers reinvestigated the thermal polymerization of L-lysine hydrochloride using various catalysts to yield the hyperbranched polypeptide (in scheme 1.24).[98-99] Recently Li and coworkers developed neutral amino acid based hyperbranched polymers by melt polycondensation approach.[100] In this methods amino acid was reacted with acryl chloride to afford the acrylamide, that further underwent Michael addition of double bond by thiol group containing diol to produce amino acid based AB_2 monomer. The AB_2 monomer self-condensed in presence of Ti(OBu)$_4$ as catalyst to produce the amino acid based hyper branched poly(ester-amide)s (in scheme 1.25). The

disadvantage of this process is that the amino acid monomers are synthesized using multi-step reaction and also thiol compounds are used as the starting material. The above study showed that hyper branched polymers based on amino acids reports are less known in the literature.
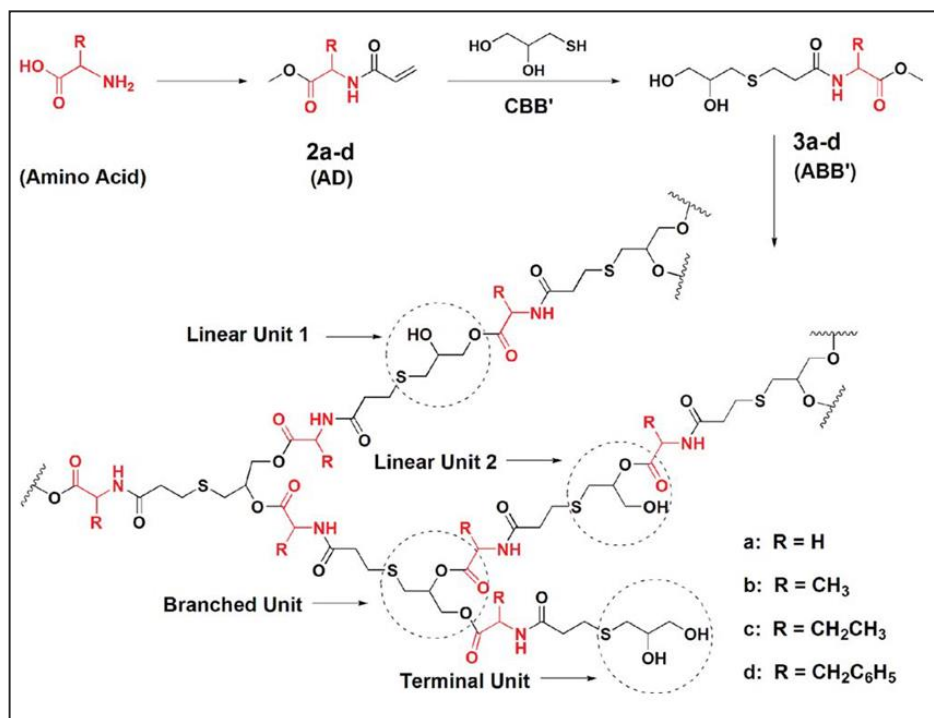
Scheme.1.25. *Synthesis of hyper branched polymer based on amino acid by transesterification approach (adopted from Bao, Y-M. et al. J. Polym. Sci., Part A: Polym. Chem.* **2010***, 48,* 5364*)*

Amino acid pendent polyacrylates

The side chain functionalized amino acid polymers can be prepared by addition polymerization technique. Amino acid reaction with meth (acryl) chloride in presence of base provides a vinyl substituted amino acid monomer. Amino acids have amine and carboxylic acid functional group, and their C-terminal or N-terminal vinyl monomers can be synthesized (in scheme 1.26).
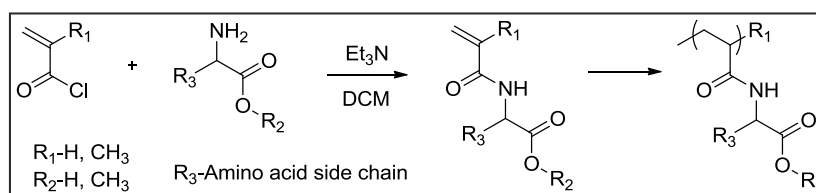
Scheme 1.26. *Synthesis of side chain functionalized amino acid polymers by addition polymerization approach*

The vinyl substituted monomers were polymerized via two different methodologies, i.e. conventional free radical polymerization (FRP) or control radical polymerization (CRP) method. In FRP the vinyl monomer undergoes polymerization reaction to afford the side chain functionalized amino acid polymers.[101-104] The disadvantage of the FRP approach is that there is no control over the molecular weight of the polymer. In CRP three main polymerization techniques used for the addition polymerization such as nitroxide mediated polymerization (NMP), atom transfer radical polymerization (ATRP) and reversible addition fragmentation chain transfer (RAFT) polymerization. In recent years CRP techniques have played an important role in the synthesis of controlled molecular weight polymers using radical polymerization. Due to living or controlled nature of the polymerization process various polymer architecture could be synthesized such as diblock, triblock, branched, graft structure etc. The disadvantage of these polymerization processes is that the backbone of polymers is made up of carbon-carbon covalent bond therefore these polymers are not biodegradable in nature. Various amino acid derivatives have been synthesized using CRP techniques to generate pH responsive materials for biomedical applications (in Figure 1.11). Recently the vinyl substituted dipeptide and higher analogues of the amino acid derivative were polymerized to provide the polymer with polypeptide in the side chain.
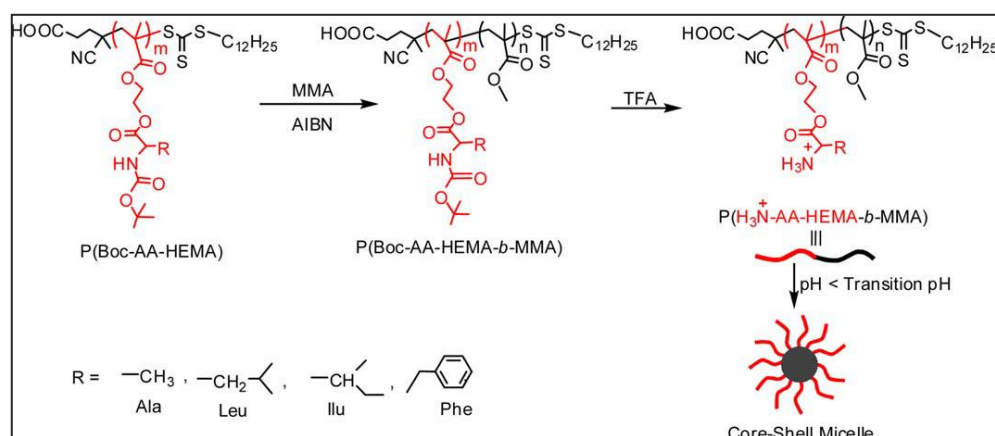
Figure 1.11. *Synthesis of amino acid based cationic amine functional block copolymer by RAFT polymerization approach (adopted from Roy et al. J. Appl. Polym. Sci. 2014, Doi: 10.1002/APP.41084)*

1.9. Application of amino acid based polymers

Amino acid containing polymers are widely used for diverse biomedical application like delivery carriers for drug/, gene and tissue engineering discussed in detail below.

Drug Delivery

Polymer based drug delivery plays an important role in enhancing drug targeting, decreasing systemic drug toxicity and protection of drug against biochemical degradation.[105-106] Various self-assembled polymeric architectures have been used as polymeric drug carriers, including microspheres, nanoparticles, micelles, hydrogels, etc. Many of the pharmaceutical agents are hydrophobic in nature; therefore the drug can be attached with polymer carrier by two different approaches, (i) physical incorporation and (ii) chemical conjugation to improve the controlled release of drug as well as targeted drug delivery. The design and synthesis of polymer scaffolds for drug delivery is a challenging task. Typically the polymer scaffold should be non-toxic, non-immunogenic, biodegradable and biocompatible in nature. Polymer based drug delivery has attracted much attention compared to other small molecule drug carrier due to Enhanced Permeability and Retention (EPR) effect.[107-108] Based on this concept polymer scaffolds are expected to have increased accumulation of drug in tumor tissues compared to normal tissues. Amino acid based polymers can be applied for drug delivery application because amino acids are obtained from natural resources.

Zilinskas et. al synthesized poly(ester-amide) (PEA)-g- polyethylene oxide copolymer by reaction of amine bearing PEA with MeO-PEG-carboxylic acid.[109] These copolymers were self-assembled into micelle structure in aqueous medium which can load hydrophobic Nile red dye. The cytotoxicity tests performed *in vitro* on HeLa cells showed that the polymers are non-toxic in nature. The results revealed that the micelle could be useful as drug delivery system. Guo and chu prepared novel biodegradable poly (ester-amide)s microsphere based on amino acids and they were applied for paclitaxel anti-cancer drug delivery (in figure 1.12). The author suggested that the high drug loading efficiency of the poly (ester-amide)s microsphere shows their potential to load highly hydrophobic anti-cancer drugs. Same author explored polyester-amide based on phenyl alanine hydrogel for paclitaxel drug delivery.[110] Hydrogels were obtained from photo polymerization of unsaturated phenyl alanine poly (ester-amide) and polyethylene glycol diacrylate using photo initiator.

Depending upon the ratio of phenyl alanine unsaturated polymer and PEG diacrylate in the polymerization reaction, the release of the drug could be controlled. In the case of highly crosslinked hydrogel, the initial burst release of the drug was significantly reduced. The release of drug was high in the enzymatic medium compared to aqueous medium. The overall result revealed that this system can be successfully used for long-term and sustained release of hydrophobic drugs.
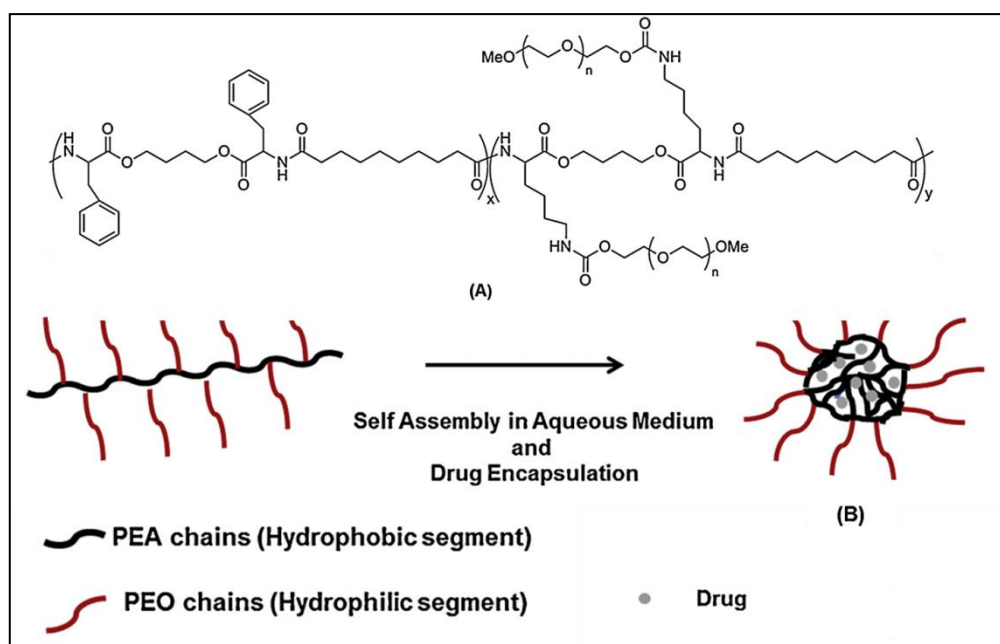
Figure 1.12. *(A) Structure of amphiphilic phenyl alanine graft copolymer with PEG-OMe, (B) this amphiphilic polymer self-assembled micelles could able to load hydrophobic drug molecule (Adopted from Fonseca et al. Prog Polym Sci* **2014***, 39, 1291-1311)*

Ditto et al. explored the biodegradable L-tyrosine phosphate nanosphere as an intracellular delivery system. These nanospheres were found to be nontoxic to human cells and degraded within 7 days.[111] Li and Chu synthesized poly (ester-amide) from L-phenyl alanine, 1,4-butanediol and sebacic acid that resulted in electro spun nanofibers with an average diameter of 640 nm.[112] The nanofibers were pre-loaded with 4-amino-2,2,6,6-tetramethylpiperidine oxide and its release was higher in enzymatic medium compared to physiological conditions (pH=7.4 PBS, 37 °C). The authors revealed that these electro-spun fibers were found to be a potential material for certain therapeutic applications. Ouchi et al. synthesized microspheres based on poly(L-glycolic acid), PEG-b-poly (DL-lactic acid) and polydepsipeptide-b-poly DL-lactic acid with pendent carboxyl or amine groups for controlled release of proteins

(bovine serum albumin, or lysozyme).[113] It was found that in the presence of ionic copolymers, the release of protein was slow due to electrostatic interaction between protein and the ionic block copolymer. The authors also found that proteins denaturation was not observed during the formation of microsphere and during the release of protein.
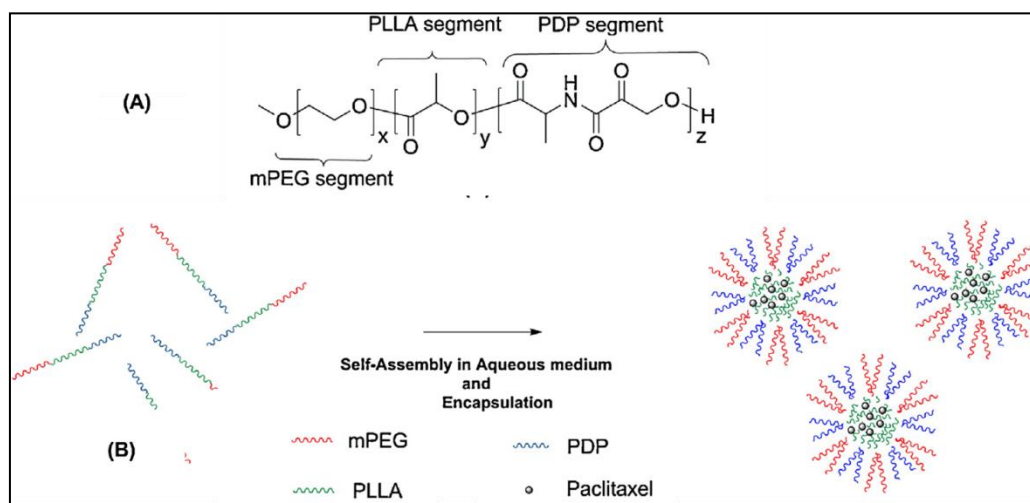
Figure 1.13. *(A) Structure of triblock copolymer containing PEG, PLLA and PDP segment, (B) the self-assembled triblock copolymer micelle could load the paclitaxel drug molecule (adopted from Fonseca et al. Prog Polym Sci* **2014***, 39,* 1291-1311*)*

Zhao et al. developed triblock copolymer containing PEG, poly L-lactic acid and a poly depsipetptide obtained from L-alanine and glycolic acid (in figure 1.13).[114] These polymers were able to self-assemble in aqueous medium into micelle for loading paclitaxel anti-cancer drug. The results revealed that the drug loaded micelle obtained from triblock copolymer showed higher anticancer activity compared to PEG and poly L-lactic acid.

Gene delivery

The development of novel viral or non-viral vectors has attracted much attention due to their growing interest in gene therapy for the treatment of various diseases.[115] Gene delivery can be defined as the transfer of genetic material into specific cell to prevent or treat a disease. In this process cationic charged polymers form nano-complexes with negatively charged genetic material to provide stable polyplex. These polyplex are taken up by endocytosis followed by endosome acidification and endosomal rupture to deliver the genetic material into nucleus. The success of delivery depends upon finding safe and efficient gene delivery systems. The polymeric gene carrier should fulfill the following criteria for efficient gene

delivery system, namely (i) display high specificity for the targeted cell, (ii) protect the genetic material from degradation and undesirable interactions and (iii) enhance the cell binding and intracellular delivery into cytoplasm or nucleus (in figure 1.14). Cationic polymers have attracted much attention in gene delivery due to their potential advantages, including large DNA loading capacity, reduced immunogenicity and ease of large scale production. L-lysine and L-arginine are two important cationic amino acids available naturally. Amino acid based Poly (L-lysine) and Poly (L-arginine) are the widely used polymers for gene delivery application. However these systems have a relatively high toxicity due to their non-degradable nature, low water solubility and low transfection efficiency. In gene delivery hydrolytically degradable and enzymatically biodegradable polymers have more advantage over non degradable polymer. Therefore development of biodegradable cationic polymers have attracted much attention for gene delivery application. Degradable gene carrier polymer may decrease the cytotoxicity and also enhance transfection due to facilitated intercellular unpacking and release of DNA.
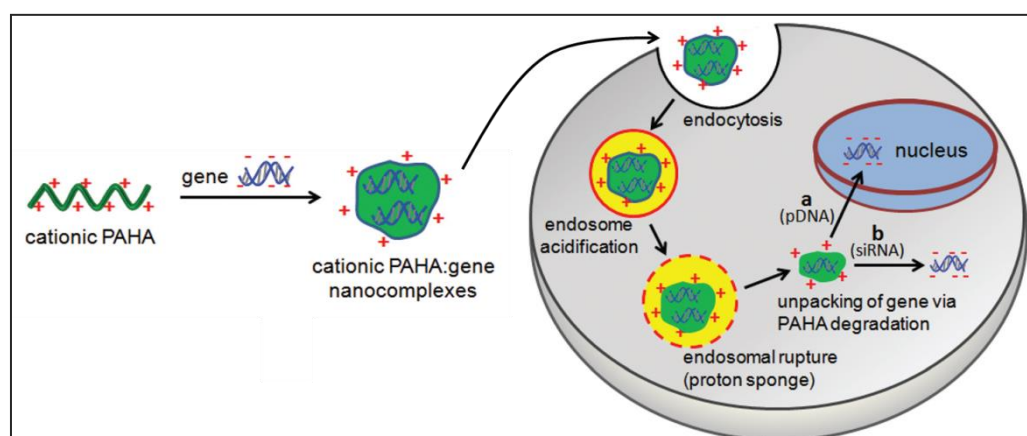
Figure 1.14. *The schematic diagram for the overview of cationic polymer based gene delivery (Adopted from Yu et al. Polym Chem.,* **2014***, 5, 5854-5872)*

Yamanouchi et al. synthesized novel degradable cationic arginine based polyester amide by solution condensation method, and was evaluated for their biosafety and capability to transfect rat vascular smooth muscle cells, a major cell type participating in vascular diseases. These polyester amide showed high binding capacity toward plasmid DNA due to the strong basic guanidine group and can be attractive candidates for non-viral gene delivery because of their high cellular uptake nature and reliable cellular biocompatibility of arginine compared to other cationic polymer (in figure 1.15). Though arginine polyester amide delivered plasmid DNA

into cells, a large amount of DNA was trapped in endocytotic compartment, which led to decrease in transfection efficacy. [116]
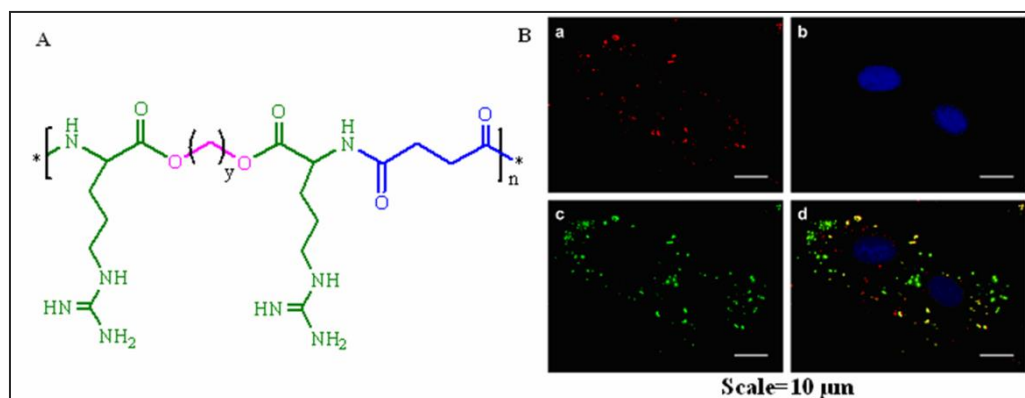
Figure 1.15.*(A) Chemical structure of Arginine poly(ester-amide)(y=3-6); (B) CLSM images of rat A 10 SMCs.(a) Red dots from rhodamine-stained plasmid DNA/Argine-poly(ester-amide) complex, (b) blue staining of nucleus, (c) green staining of acidic components, (d) merged images of a to c.)(adopted from Sun et al. Biomacromolecules **2011**, 12, 1937-1955)*

Li and Huang prepared a non-toxic, poly (D, L-lactide-co-4-hydroxy-L-proline) (PLHP) by ring opening polymerization of D,L-lactide with N-cbz-4-hydroxy-L-proline for sustained gene delivery.[117] These copolymers exhibited less cytotoxicity than poly (ethylene-imine) and poly (L-lysine hydrochloride) in human embryonic kidney 293 cell lines. Gene transfer efficiency of pDNA and copolymer showed high transfection efficiency for more than a week compared to poly (ethylene imine) and poly (L-lysine hydrochloride). These results revealed that PLHP copolymer is a promising candidate for long term gene delivery due to their good biocompatibility and biodegradable nature. Liu et al. reported biodegradable poly (ester-urethane) grafted with short chain poly (ethylene-imine)-800 (PEU-g-PEI$_{800}$) for gene delivery application.[118] The PEU-g-PEI$_{800}$ polymers showed lower cytotoxicity, higher buffer capacity, higher degradation rate and higher transfection efficiency than PEU, PEI800 and PEI 25000 controls. (in figure 1.16). Triblock copolymer poly (L-lysine-g-(lactide-b-ethylene glycol)) was synthesized by Park and Healy as a gene delivery scaffold.[119] These triblock copolymers were able to complex with DNA at very low concentration, which led to improved transfection efficiency and reduced overall cytotoxicity. The variation of polymer composition with DNA complex provided the control over intracellular plasmid dissociation rates.
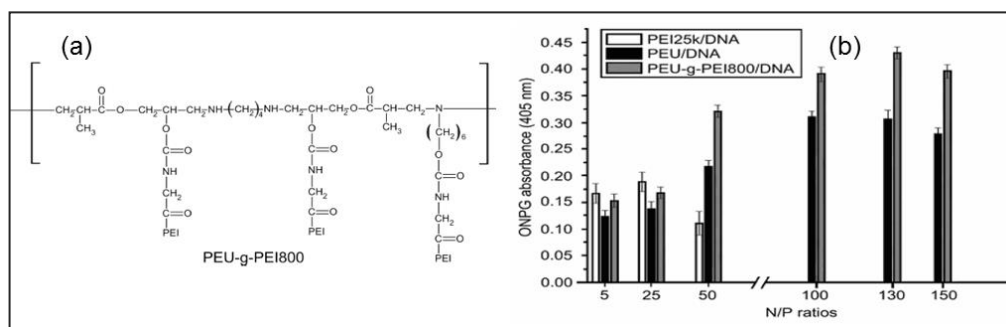
Figure 1.16. *(a) Structure of poly (ester-urethane)-g-PEI800 and Transfection efficiency of PEU-g-PEI800/DNA complexes in COS-7 cells (b)(adopted from Sun et al. Biomacromolecules* **2011***, 12,* 1937-1955)

Li et. al reported the synthesis of novel amphiphilic polycationic dendritic poly (L-lysine)-b-poly (L-lactide)-b-dendritic poly (L-lysine) with different Poly (L-lysine) dendritic generations of two to five as DNA carrier.[120-122] The amphiphilic polycationic polymers showed lower cytotoxicity in human hepatocellular carcinoma cell line compared to linear poly L-lysine 23kDa and 2kDa polyethyleneimine. In vitro gene transfection experiments indicated that transfection efficiency was ten times higher than that of naked DNA. These result revealed that with increase in the lysine dendritic generation unit the DNA binding affinity and transfection activity increases.

Tissue engineering

Tissue engineering is an interdisciplinary field that merges the expertise of life sciences, material sciences and engineering, which aims to replace damaged, injured or worn parts of the human body with new functional tissue and organs.[123] Typically the polymer scaffold for tissue engineering should be selected with respect to: (i) cytotoxicity, (ii) ability to support the cell growth, (iii) inflammatory property and (iv) mechanical properties. The key elements of tissue engineering are cells, three-dimensional scaffolds and growth factors. The polymer scaffolds play a significant role in cell adhesion, migration, proliferation, and so on. In tissue engineering biodegradable polymers have been widely used due to the fact that degradable polymers will disappear once the regeneration of tissue takes place. There are three important synthetic biodegradable polyesters that have been used for tissue engineering application such as polylactic acid, polyglycolic acid and poly carprolactone. However these polymers have some disadvantages in tissue

engineering because of their absence of active chemical and biological functions. The α-amino acid based degradable polymers have attracted much attention in tissue engineering application due to their combining merits of biodegradation and natural amino acid as the building block.
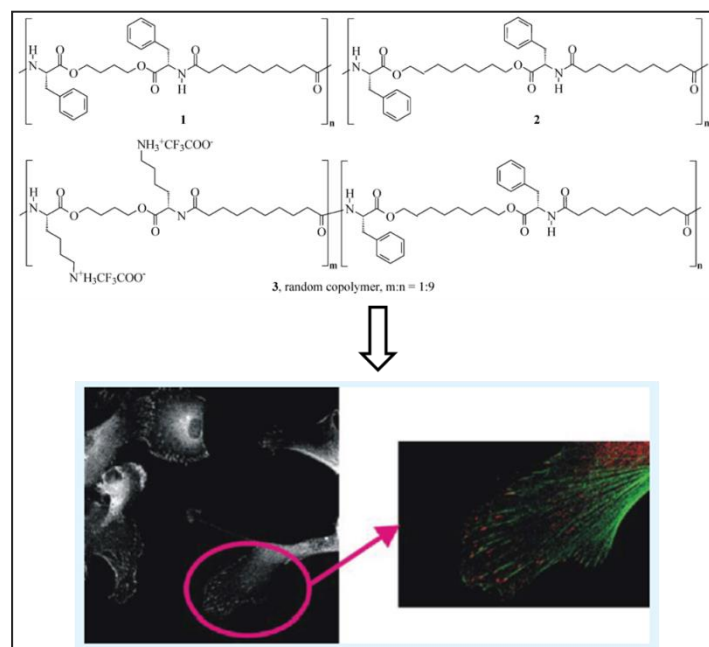
Figure 1.17. (a) structure *of phenyl alanine based poly(ester-amide) homopolymer and phenyl alanine and lysine based copolymer for tissue engineering application, (b) Confocal microscopy images of vinculin immunostained HCASMCs on glass coverslips,Black and white images show vinculin immunostaining only, while fluorescence labelling of HCASMC F-actin (green), vinculin (red), and nuclei (blue) are all shown in the composite images. (adopted from Knight et al. ACS Appl Mater Inter-faces* **2012***, 4,* 1303-1312*).*

Ohya et. al developed poly (depsipeptide-co-lactide) copolymers by ring opening polymerization of L-lysine and L-aspartic acid monomer.[124] These polymers provided 3-D porous sponges by the freeze-drying technique. The results revealed that the porous sponges were able to promote cell adhesion and growth for tissue engineering application. In addition, the polymer scaffolds were found to be biodegradable in nature and also the rate of biodegradation depended on the amount of depsipeptide in the copolymer. Karimi et al. prepared poly(ester-amide)s based on α-amino acids L-phenyl alanine, L-methionine and a diol (1,4-butanediol or 1,6-hexanediol) and sebacic acid by interfacial polymerization.[125] The 3-D scaffolds obtained from the poly (ester-amide)s have shown excellent porosities and found to be interesting for tissue engineering applications. Knight et. al synthesized a family of α-

amino acid based biodegradable poly (ester-amide) by interfacial and solution polycondensation approach, and they are used for vascular tissue engineering application.[126] Results indicated poly (ester-amide)s were able to support cell adhesion, spreading and proliferation, which made them promising materials for vascular tissue engineering scaffolds. Cheng et al. explored a set of biodegradable poly (ester-amide) elastomers based on α-amino acid with excellent elasticity, good *in vivo* biocompatibility and slow biodegradation rate (in scheme 1.17).[127] Poly(gamma-glutamic acid)-graft-chondroitin sulfate-blend-poly(epsilon-caprolactone) composite biomaterial was used as scaffold in cartilage tissue engineering due to their excellent biodegradation and biocompatibility for chondrocytes and it has also been applied as temporary substitutes for articular cartilage regeneration.

Since amino acids are produced in large scale by environmentally friendly fermentation method, developing new synthetic methodology for amino acid based polymer would be quite promising for multiple applications. From the previous discussion, it is understood that amino acid containing polymers are produced by three major polymerisation techniques like condensation, addition and ring opening polymerisation techniques. Based on these synthetic routes amino acids have been widely explored for many polymer syntheses: polypeptide, poly (ester-amide), polyester, polycarbonate, polyurethane and poly (ester-urea). Till date the ROP approach for NCA is one of the major synthetic methodologies used to make amino acid based polymer structure. The other synthetic methodologies available for amino acid polymer synthesis have not been explored widely. Solvent free melt polycondensation approach is an important polymer synthetic methodology that allows the direct utilization of the polymer as raw material and it also facilitates polymer synthesis on a large scale. The above discussion vividly explains that the melt polycondensation approach is not explored for L-amino acid resources to make thermoplastic polymers. Thus, the design and development of L-amino acid based polymers using commercially important melt polycondensation method is a challenging task. The development of melt polycondensation approach will also allow one to access the new polymer structures which are yet to be explored.

1.10. Aim of the thesis work

In general, solvent free melt polymerization processes are highly preferred in the manufacturing of engineering thermoplastics because of the direct processing of the polymers into desired products. In the area of fully aliphatic or aliphatic-aromatic polyesters, solvent free melt methodologies such as transesterification were developed and this process is employed for the manufacturing few million tons of these polymers every year. In the transesterification reaction (in scheme 1.27), a diester monomer reacts with equimolar amount of diol under melt conditions at high temperatures to produce polyester followed by the removal of low boiling alcohol.
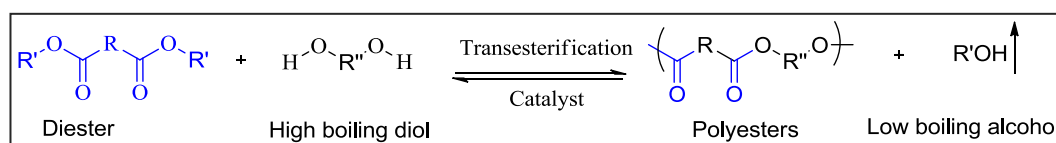
Scheme 1.27. *Transesterification reaction for the synthesis of Polyesters*

Deepa et al. from our laboratory developed melt transurethane polycondensation chemistry for polyurethanes under solvent and isocyanate free conditions.[128] The urethane linkage can be considered as a half-ester-half-amide bond (ROCONHR'); thus, during the transurethane process the ester bond in the di-urethane monomer (or carbamate) is cleaved selectively so as to form the new urethane linkage (in scheme 1.28).
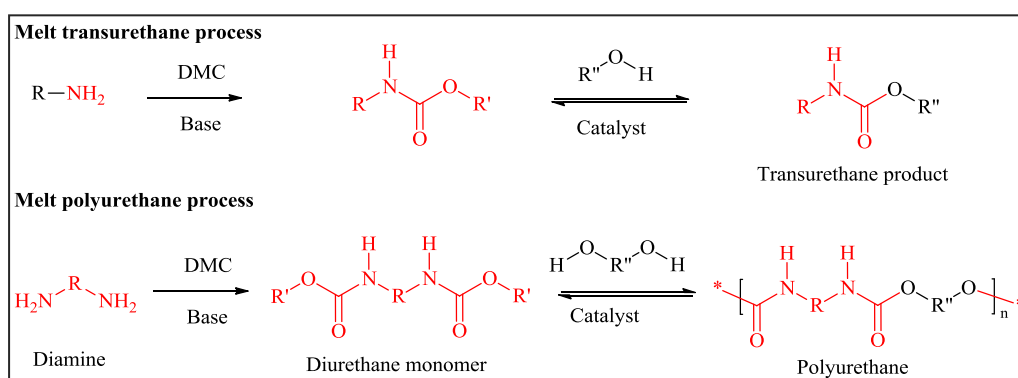
Scheme 1.28. *Melt transurethane reaction for the synthesis of Polyurethane*

In this melt transurethane process, a di-urethane monomer was polycondensed with equimolar amounts of diol in presence of a catalyst at high temperature under melt conditions to produce polyurethanes followed by the removal of low boiling alcohol. One of the significant features of the melt transurethane process is that the di-urethane monomer described in the process is non-toxic and can be easily handled,

purified or stored unlike isocyanates in the laboratory. Further, the di-urethane monomers were also made from commercial diamines; thus, the entire approach became viable for large scale synthesis of polyurethanes under melt condensation approach.

The amino acids are made up of acid and amine functionalities; thus, the development of new methodology combining the melt transurethane process developed in our laboratory (for amines) with the well-known transesterification in the literature (for carboxylic esters), would open up new avenue of research opportunities for new classes of L-amino acids based polymers.
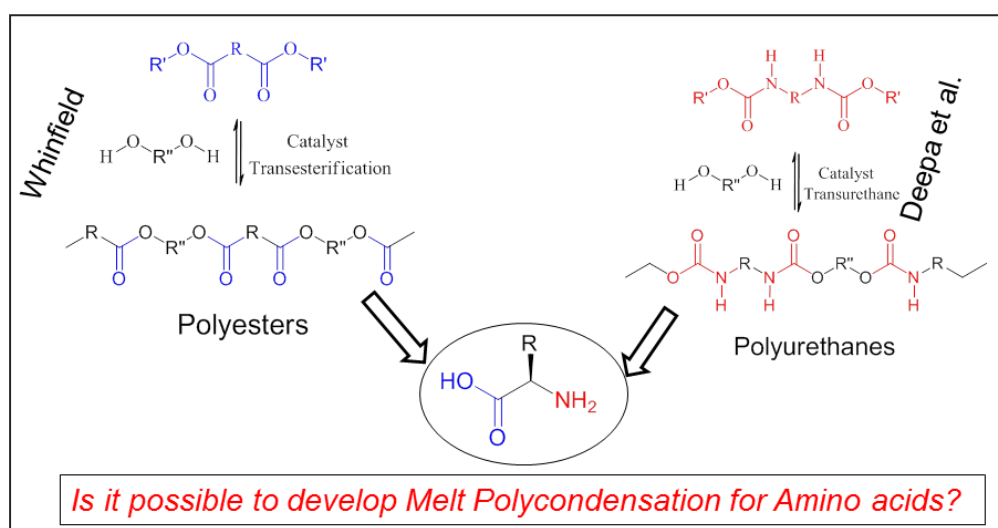
Scheme 1.29. *Proposal for the development of new dual ester-urethane melt polycondensation for L-Amino acids in the thesis work*

The thesis is aimed to develop new *dual ester-urethane polycondensation chemistry* for L-amino acid based monomers under eco-friendly solvent free melt polymerization route. The amine and carboxylic functionalities of the amino acids will be converted into N-carbamate (urethane) and ester monomers for the above purpose *(details are provided in the chapter-2).* Naturally occurring L-amino acids are subjected to tailor made synthetic approaches to make new ester-urethane monomers. The melt condensation process involved the simultaneous condensation of both ester and urethane functionalities with commercial diols to produce a new class of L-amino acid based poly(ester-urethane)s (in scheme 1.29). Further, the new synthetic approach is robust in the sense that one of the functionality in the monomer could be selectively activated depending upon the temperature and catalysts employed for the condensation reaction. This new synthetic approach facilitates the synthesis of new classes of poly(ester-urethanes), hydrophilic-hydrophobic diblock and triblock

species, side chain hydrogen bonded polyesters and cationic polyesters with redox degradability. These structures are produced by the other synthetic methodologies described in the introduction chapter.

The thesis work is focused on the design and development of these diverse L-amino acid based polymers by solvent free melt polycondensation approach study their self-assembled nanostructures. The thesis work is divided into four chapters and reports the following important scientific outcome in detail:

(i) Development of new ***dual ester-urethane melt polycondensation*** approach for the ***novel poly(ester-urethane)s*** based on L-amino acid natural resources. This approach was demonstrated for more than 6 amino acid monomers and 50 different polymer structures.

(ii) ***Temperature and catalyst selective reactivity*** of the L-amino acid monomers was identified to tailor-make A-B and A-B-A type species. Wide ranges of catalysts were optimized for the above process based on alkali, alkaline earth, transition metal and lanthanide salts and complexes. Further, efforts were taken to study the mechanism as well as optical purity of the polymers and oligomers.

(iii) ***Hydrogen-bonded functional polyesters*** were made from multi-functional amino acids such as L-aspartic and L-glutamic acids. The hydrogen-bonding interaction facilitated the polyesters to produce amyliod-like fibrils. The polymers were suitably modified into cationic polyester nanoparticles in water. The self-assembly was reversed form particle to amyloid-fibrils using danyl fluorophores.

(iv) ***Redox degradable polyesters*** are made based on L-cystine monomer. These polyesters were found to self-assemble as nano-fibrous and they also degraded into monomeric species upon reacting with DTT. The deprotected polyester turned into water soluble cationic nanoparticles. These nanoparticles were also found to be highly bio-compatible and non-toxic to cancel cells for futuristic drug delivery applications.

Finally, the thesis has been summarized in the last chapter with future perspectives.

1.11 References:

1. Deming, T. J. *Prog Polym Sci.,* **2007**, *32*, 858–875.

2. Gomes, S.; Leonor, I. B; Mano, J. F.; Reis, R. L.; Kaplan, D. L. *Prog Polym Sci.,* **2012**, *37*, 1-17.

3. Maji, S. K.; Perrin, M. H.; Sawaya, M. R.; Jessberger, S.; Vadodaria, K.; Rissman, R. A.; Singru, P. S.; Nilsson, K. P. R.; Simon. R.; Schubert. D.; Eisenberg, D.; Rivier, J. Sawchenko, P.; Vale, W.; Riek, R. *Science* **2009**, *325*, 328-332.

4. Dobson, C. M. *Nature* **2003**, *426*, 884-890.

5. Lutz, J. F.; Boerner, H. G. *Prog Polym Sci* **2008**, *33*, 1-39.

6. Ikeda, M. *Adv Biochem Eng Biotechnol* **2003**, *79*, 1-35.

7. Strecker, A.; Liebigs, J. *Ann. Chem.* **1850**, *75*, 27

8. Bucherer, H. T.; Fischbeck, H. T. *J. Prakt. Chem.* **1934**, *140*, 69

9. Bucherer, H. T.; Steiner, W. *J. Prakt. Chem.***1934**, *140*, 291

10. Beller, M.; Eckert, M. *Angew. Chem.* **2000**, *112*, 1026

11. Beller, M.; Eckert, M.; *Angew. Chem. Int. Ed.* **2000**, *39*, 1010

12. Breuer, M.; Ditrich, K.; Habicher, T.; Hauer, B.; Kebeler, M.; Sturmer, R.; Zelinski, T. *Angew. Chem. Int. Ed.* **2004**, *43*, 788-824

13. Yamada, S.; Nabe, K.; Izuo, N. *Appl. Environ. Microbiol.* **1981**, *42*, 773-778.

14. Hermann T. *J. Biotechnol.* **2003**, *104*, 155-172.

15. Faham, A-E.; Albericio, F *Chem. Rev.* **2011**, *111*, 6557-6602.

16. Kent, S. B. H. *Chem. Soc. Rev.,* **2009**, *38*, 338-351.

17. Chandrudu, S.; Simerska, P.; Toth, I. *Molecules*, **2013**, *18*, 4373-4378.

18. Bacsa, B.; Horvati, K.; Bosze, S.; Andreae, F.; Kappe, C. O. *J Org Chem.* **2008**, *73*, 7532-7542.

19. Ramakers, B. E. I.; Van Hest, J. C. M.; Lowik, D. W. P. M. *Chem. Soc. Rev.,* **2014**, *43*, 2743-2756.

20. Panda, J. J.; Chauhan, V. S. *Polym. Chem.,* **2014**, *5*, 4418-4436.

21. Cui. H.; Webber. M. J.; Stupp, S. I. *Biopolymers*, **2010**, *94*, 1-18.

22. Paramonov, S. E.; Jun, H. W.; Hartgerink, J. D. *J. Am. Chem. Soc.* **2006**,*128*, 7291-7298.

23. Hamley, I. W.; *Soft Matter.* **2011**, *7*, 4122-4138.

24. Trent, A.; Marullo, R.; Lin, B.; Black, M.; Tirrell, M. *Soft Matter.* **2011**, *7*, 9572-9582.

25. Castelletto, V.; Hamley, I. W.; Perez, J.; Abezgauz, L.; Danino, D. *Chem. Commun*. **2010**, *46*, 9185-9187.

26. Gore, T.; Dori, Y.; Talmon, Y.; Tirrell, M.; Bianco-Peled, H. *Langmuir* **2001**, *17*, 5352-5360.

27. Tang, C.; Qiu, F.; Zhao, X. *J. Nano Mat.* **2013**, *2013*, 1-9.

28. Muraoka, T.; Cui, H.; Stupp, S. I. *J. Am. Chem. Soc.* **2008**, *130*, 2946-2947.

29. Yamada, S.; Koga, K.; Sudo, A.; Goto, M.; Endo, T. *J. Polym. Sci. Polym. Chem.* **2013**, *51*, 3726-3731

30. Kamei, Y.; Sudo, A.; Endo, T. *Macromolecules*, **2008**, *41*, 7913-7919

31. Deng, C.; Wu, J.; Cheng, R.; Meng, F.; Klok, H-A.; Zhong, Z. *Prog Polym Sci.* **2014**, *39*, 330-364.

32. Deming, T. J. *Chem. Rev.* DOI: 10.1021/acs.chemrev.5b00292

33. Kricheldorf, H. R. *Angew. Chem. Int. Ed.* **2006**, *45,* 5752 - 5784

34. Farthing, A. C.; Reynolds, R. J. W.; *Nature* **1950**, *165*, 647-657.

35. Coleman, D.; Farthing, A. C. *J Chem Soc* **1950,** 3218-3222.

36. Aliferis, T.; Iatrou, H.; Hadjichristidis N. *Biomacromolecules*, **2004**, *5*, 1653-1656.

37. Vayaboury, W.; Giani, O.; Cottet, H.; Deratani, A.; Schue, F. *Macromol Rapid Commun.* **2004**, *25*, 1221.

38. Deming, T. J. *Nature* **1997**, *390*, 386-389.

39. Deming, T. J. *Macromolecules* **1999**, *32*, 4500-4502.

40. Hadjichristidis, N.; Iatrou, H.; Pitsikalis, M.; Sakellariou, G. *Chem Rev* **2009**, *109*, 5528-5578.

41. Deming, T. J. *Adv Polym Sci* **2006**, *202*, 1118.

42. Deming, T. J. *J. Polym. Sci. Polym. Chem.* **2000**, *38*, 3011-3018.

43. Hernandez, J. R.; Klok, H. A. *J Polym Sci Part A Polym Chem* **2003**, *41*, 1167-1187.

44. Nguyen, L-Y.T.; Vorenkamp, E.J.; Daumont, C. J. M.; ten Brinke, G.; Schouten, A. J. *Polymer* **2010**, *51*, 1042

45. Lee E. S.; Shin, H. J.; Na, K.; Bae, Y. H.; *J Control Release* **2003**, *90*, 363-374.

46. Habraken, G. J. M.; Koning, C. E.; Heuts, J. P. A.; Heise, A. *Chem Commun* **2009**, 3612.

47. Xing, T.; Lai, B.; Ye, X.; Yan, L. *Macromol Biosci* **2011**, *11*, 962.

48. Hayakawa, T.; Kondo, Y.; Yamamoto, H.; Murakami, Y. *Bull Chem Soc Jpn,* **1969**, *42*, 479-482.

49. Yamamoto, H.; Hayakawa, T. *Macromolecules*, **1976,** *9*, 532.

50. Yakovlev, I.; Deming, T. J. *ACS Macro Lett.* **2014**, *3*, 378-381.

51. Yakovlev, I.; Deming, T. J. *J. Am. Chem. Soc.* **2015**, *137*, 4078-4081.

52. Kramer, J. R.; Deming, T. J. *Biomacromolecules* **2012**, *13*, 1719-1723.

53. Gharakhanian, E. G.; Deming, T. J. *Biomacromolecules* **2015**, *16*, 1802-1806.

54. Habraken, G. J. M.; Heise, A.; Thornton, P. D. *Macromol. Rapid Commun.* **2011**, *33*, 272-286.

55. Zhang, S.; Alvarez, D. J.; Sofroniew, M. V.; Deming, T. J. *Biomacromolecules* **2015**, *16*, 1331-1340.

56. Rodriguez, A. R.; Kramer, J. R.; Deming, T. J. *Biomacromolecules* **2013**, *14*, 3610-3614.

57. Rhodes A. J.; Deming, T.J. *J. Am. Chem. Soc.* **2012**, *134*, 19463-19467.

58. Feng, Y.; Lu, j.; Behl, M.; Lendlein, A. *Macromol. Biosci.* **2010**, *10*, 1008-1021.

59. Helder, J.; Kohn, F. E.; Sato, S.; van den Berg, J. W.; Feijen, *J. Makromol. Chem., Rapid Commum.* **1985**, *6*, 9-14.

60. in 't Veld, P. J. A.; Dijkstra, P. J.; Feijen, *J. Makromol. Chem.* **1992**, *193*, 2713-2730.

61. John, G.; Morita, M. *Macromol. Rapid Comm.* **1999**, *20*, 265-268.

62. Franz, N.; Klok, H. A. *Macromol. Chem. Phys.* **2010**, *211*, 809-820.

63. Arabuli, N.; Tsitlanadze, G.; Edilashvili, L.; Kharadze, D.; Goguadze, T.; Beridze, V.; Gomurashvili, Z.; Katsarava, R. *Macromol. Chem. Phys.* **1994**, *195*, 2279-2289.

64. Katsarava, R.; Beridze, V.; Arabuli, N.; Kharadze, D.; Chu, C. C.; Won, C. Y. *J. Polym. Sci. Pol. Chem.* **1999**, *37*, 391-407.

65. De Wit, M. A.; Wang, Z. X.; Atkins, K. M.; Mequanint, K.; Gillies, E. R. *J. Polym. Sci. Pol. Chem.* **2008**, *46*, 6376-6392.

66. Atkins, K. M.; Lopez, D.; Knight, D. K.; Mequanint, K.; Gillies, E. R. *J. Polym. Sci. Pol. Chem.* **2009**, *47*, 3757-3772.

67. Pang, X.; Chu, C. C. *Biomaterials* **2010**, *31*, 3745-3754.

68. Pang, X.; Wu, J.; Reinhart-King, C.; Chu, C. C. *J. Polym. Sci. Pol. Chem.* **2010**, *48*, 3758-3766.

69. Guo, K.; Chu, C. C.; Chkhaidze, E.; Katsarava, R. *J. Polym. Sci. Pol. Chem.* **2005**, *43*, 1463-1477.

70. Guo, K.; Chu, C. C. *J. Polym. Sci. Pol. Chem.* **2007**, *45*, 1595-1606.

71. Asin, L.; Armelin, E.; Montane, J.; Rodriguez-Galan, A.; Puiggali, J. *J Polym. Sci. A:Polym Chem* **2001**, *39*, 4283.

72. Yu, Y.; Zou, J.; Cheng, C. *Polym. Chem.*, **2014**, *5*, 5854

73. Yin, Q.; Yin, L.; Wang, H.; Cheng, J. *Acc. Chem. Res.* **2015**, *48*, 1777-1787.

74. Kimura, Y.; Shirotani, K.; Yamane, H.; Kitao, T. *Macromolecules*, **1988**, *21*, 3338-3340.

75. Thillaye du Boullay, O.; Saffon, N.; Diehl, J-P.; Martin-Vaca B.; Bourissou, D. *Biomacromolecules*, **2010**, *11*, 1921-1929.

76. Leemhuis, M.; van Nostrum, C. F.; Kruijtzer, J. A. W.; Zhong, Z. Y.; ten Breteler, M. R.; Dijkstra, P. J.; Feijen J.; Hennink, W. E. *Macromolecules*, **2006**, *39*, 3500-3508.

77. Marcincinova-Benabdillah, K.; Boustta, M.; Coudane J.; Vert, M. ***B****iomacromolecules*, **2001**, *2*, 1279-1284.

78. Marcincinova Benabdillah, K.; Coudane, J.; Boustta, M.; Engel R.; Vert, M. *Macromolecules*, **1999**, *32*, 8774-8780.

79. Gerhardt, W. W.; Noga, D. E.; Hardcastle, K. I.; García, A. J.; Collard D. M.; Weck, M. *Biomacromolecules*, **2006**, *7*, 1735-1742.

80. Jiang, X.; Smith III M. R.; Baker, G. L. *Macromolecules*, **2008**, *41*, 318-324.

81. Jiang, X.; Vogel, E. B.; Smith III M. R.; Baker, G. L. *J. Polym. Sci., Part A: Polym. Chem.,* **2007**, *45*, 5227-5236.

82. Lim, Y.B.; Kim, C-H.; Kim, K.; Kim S. W.; Park, J.-S.; *J. Am. Chem. Soc.,* **2000**, *122*, 6524-6525.

83. Kolishetti, N.; Dhar, S.; Valencia, P. M.; Lin, L. Q.; Karnik, R.; Lippard, S. J.; Langer R.; Farokhzad, O. C. *Proc. Natl. Acad. Sci. U. S. A.,* **2010**, *107*, 17939-17944.

84. Kihara, N.; Makabe, K.; Endo, T. *J. Polym. Sci., Part A: Polym. Chem.* **1996**, *34,* 1819

85. Kudo, H.; Nagai, A.; Ishikawa, J.; Endo, T. *Macromolecules*, **2001**, *34*, 16

86. Nagai, A.; Ishikawa, J.; Kudo, H.; Endo, T. *J. Polym. Sci., Part A: Polym. Chem.* **2004**, *42,* 1143

87. Kihara, N.; Kushida, Y.; Endo, T.; *J. Polym. Sci., Part A:Polym. Chem.* **1996**, *34*, 2173

88. Yu, J.; Lin, F.; Lin, P.; Gao, Y.; Becker, M. L. *Macromolecules*, **2014**, *47*, 121-129

89. Lin, F.; Yu, J.; Tang, W.; Zheng, J.; Xie, S.; Becker, M. L. *Macromolecules*, **2013**, *46*, 9515-9525

90. Zhou, J.; Defante, A. P.; Lin, F.; Xu, Y.; Yu, J.; Gao, Y.; Childers, E.; Dhinojwala, A.; Becker M. L. *Biomacromolecules*, **2015**, *16*, 266-274

91. Li, S.; Yu, J.; Wade, M-B.; Policastro, G. M.; Becker, M. L. *Biomacromolecules*, **2015**, *16*, 615-624

92. Policastro, G.M.; Lin, F.; Smith Callahan, L.A.; Esterle, A.; Graham, M.; Stakleff, K. S. Becker M. L. *Biomacromolecules*, **2015**, *16*, 1358-1371

93. Yu, J.; Lin, F.; Becker, M. L.; *Macromolecules*, **2015**, *48*, 2916-2924

94. Gao, Y.; Childers, E. P.; Becker, M. L. *ACS Biomater. Sci. Eng.*, **2015**, *1*, 795-804

95. Ertel, S. I.; Kohn, J.*J. Biomed. Mater. Res.* **1994**, *28*, 919-930.

96. Magno, M. H. R.; Kim, J.; Srinivasan, A.; McBride, S.; Bolikal, D.; Darr, A.; Hollinger, J. O.; Kohn, J. *J. Mater. Chem.*, **2010**, *20*, 8885-8893

97. Menz, T. L.; Chapman, T. M. *Polym Prepr* **2003**, *44*, 842-843

98. Scholl, M.; Nguyen, T. Q.; Bruchmann, B.; Klok, H-A. *J. Polym. Sci., Part A:Polym. Chem.* **2007**, *45*, 5494

99. Scholl, M.; Nguyen, T. Q.; Bruchmann, B.; Klok, H-A. *Macromolecules* **2007,** *40,* 5726-5734

100. Bao, Y-M.; Liu, X-H.; Tang, X-L.; Li, Y-S. *J. Polym. Sci., Part A: Polym. Chem.* **2010**, *48*, 5364

101. O'Reilly R. K. *Polym Int* **2010**, *59*, 568–573

102. Roy, S. G.; De, P. *J. Appl. Polym. Sci.* **2014**, Doi: 10.1002/APP.41084

103. Mori, H.; Matsuyama, M.; Sutoh, K.; Endo, T. *Macromolecules* **2006**, *39*, 4351

104. Mori, H.; Iwaya, H.; Nagai, A.; Endo, T. *Chem Commun.* **2005**, 4872.

105. Muller-Goymann, C. C. *Eur. J. Pharm. Biopharm.***2004**, *58*, 343.

106. Rothen-Weinhold, A.; Gurny, R.; Dahn, M. *Pharm. Sci. Technol. Today* **2000**, *3*, 222.

107. Kolhar, P.; Doshi, N.; Mitragotri, S. *Small* **2011**, *7,* 2094-2100.

108. Geng, Y.; Dalhaimer, P.; Cai, S.; Tsai, R.; Tewari, M.; Minko, T.; Denis, D. E. *Nat. Nanotechnol*. **2007**, *2*, 249-255

109. Zilinskas, G. J.; Soleimani, A.; Gillies, E. R. Int J Polym Sci **2012**, *2012*, 11.

110. Guo, K.; Chu, C. C. *J Biomater Sci Polym Ed* **2007**, *18*, 489-504.

111. Hindi, K. M.; Ditto, A. J.; Panzner, M. J.; Medvetz, D. A.; Han, D. S.; Hovis, C. E.; Hilliard, J. K.; Taylor, J. B.; Yun, Y. H.; Cannon, C. L.; Youngs, W. J. *Biomaterials* **2009**, *30*, 3771-3779.

112. Li, L.; Chu, C. C. *J Biomater Sci Polym Ed* **2009**, *20*, 341-361

113. Ouchi, T.; Sasakawa, M.; Arimura, H.; Toyohara, M.; Ohya, Y. *Polymer* **2004** *45*, 1583-1589.

114. Zhao, Y.; Li, J.; Yu, H.; Wang, G.; Liu, W. *Int J Pharm* **2012**, *430,* 282-291.

115. Hoyer, J.; Neundorf, I. *Acc. Chem. Res.* **2012**, *45*, 1048-1056

116. Yamanouchi, D.; Wu, J.; Lazar, A. N.; Kent, K. C.; Chu, C. C.; Liu, B. *Biomaterials* **2008**, *29*, 3269-3277.

117. Li, Z.; Huang, L.; *J Control Release* **2004**, *98*, 437-446.

118. Liu, X. Y.; Ho, W. Y.; Hung, W. J.; Shau, M. D. *Biomaterials* **2009**, *30*, 6665-6673.

119. Park, S.; Healy, K. E.; *Bioconjug Chem*, **2003**, *14*, 311-319.

120. Li, Y.; Li, Q. B.; Li, F. X.; Zhang, H. Y.; Jia, L.; Yu, J. Y.; Fang, Q.; Cao, A. M. *Biomacromolecules* **2006**, *7*, 224-231.

121. Li, Y.; Cui, L.; Li, Q. B.; Jia, L.; Xu, Y. H.; Fang, Q.; Cao, A. M. *Biomacromolecules* **2007**, *8*, 1409-1416.

122. Li, Y.; Zhu, Y. D.; Xia, K. J.; Sheng, R. L.; Jia, L.; Hou, X. D.; Xu, Y. H.; Cao, A. M. *Biomacromolecules* **2009**, *10*, 2284-2293.

123. Place, E.S.; George, J. H.; Williams, C. K.; *Chem. Soc. Rev*., **2009**, *38*, 1139-1151

124. Ohya, Y.; Matsunami, H.; Ouchi, T. *J Biomater Sci Polym Ed* **2004**, *15*, 111-123.

125. Karimi, P.; Rizkalla, A. S.; Mequanint, K. *Materials* **2010**, *3*, 2346-2368.

126. Knight, D. K. et al. *ACS Appl Mater Inter-faces* **2012**, *4*, 1303-1312.

127. Cheng, H.; Hill, P. S.; Siegwart, D. J.; Vacanti, N.; Lytton-Jean, A. K. R.; Cho, S-W.; Ye, A.; Langer, R.; Anderson, D.G. *Adv. Mater.* **2011**, *23*, H95-H100.

128. Deepa, P.; Jayakannan, M. *J. Polym. Sci. Polym. Chem.* **2008,** *46,* 2445-2458.

Chapter 2

Development of Dual Ester-Urethane Melt Condensation Approach For L-Amino acid Polymers

Chapter 2

Development of Dual Ester-Urethane Melt Condensation Approach For L-Amino acid Polymers

A new dual ester-urethane melt condensation methodology for biological monomers -amino acids was developed to synthesize new classes of thermoplastic polymers under eco-friendly and solvent free polymerization technique. Naturally abundant L-amino acids were converted into dual functional ester-urethane monomers by tailor made synthetic approach. Direct polycondensation of these amino acid monomers with commercial diols under melt condition produced high molecular weight poly(ester-urethane)s. The occurrence of the dual ester-urethane process and the structure of the new poly (ester-urethane)s were confirmed by ^{1}H and ^{13}C NMR. The new dual ester-urethane condensation approach was demonstrated for variety of amino acids: glycine, β-alanine, L-alanine, L-leucine, L-valine and L-phenylalanine. MALDI-TOF-MS end group analysis confirmed that the amino acid monomers were thermally stable under the melt polymerization condition. The mechanism of melt process and the kinetics of the polycondensation were studied by model reactions and it was found that the amino acid monomer was very special in the sense that their ester and urethane functionality could be selectively reacted by tuning reaction temperature or catalyst. The new polymers self-organized as β-sheet in aqueous or organic solvents and their thermal properties such as glass transition temperature and crystallinity could be readily varied using different L-amino acid monomers or diols in the feed. Thus, the current investigation opens up new platform of research activates for making thermally stable and renewable engineering thermoplastics from natural resource -amino acids.

2.1. Introduction

Solvent-free melt polycondensation process is one of the most widely employed synthetic approach for producing commercial engineering thermoplastics such as polyesters, polycarbonates and polyamides.[1] In this process, raw materials were melted and subjected to condensation reaction to produce high viscous resins which can be directly processed into desired objects. In 1946, Whinfield developed the first melt polymerization route trans-esterification in which a di-ester monomer was polycondensed with diols to produce polyesters (in scheme-2.1).[1] This route is adopted even today for manufacturing few million tons of polyesters every year.
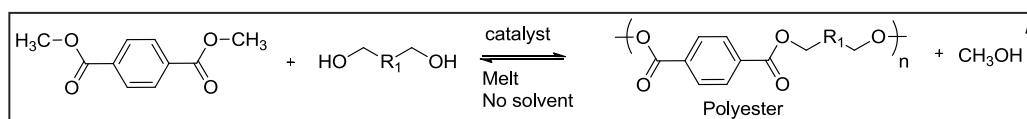
Scheme 2.1. *Polyesters synthesized using melt transesterification approach*

Ramakrishnan and coworkers had reported melt trans etherification approach for linear and hyperbranched polyether based on fully substituted benzyl ethers (in scheme-2.2).[2] Recently, this approach has been applied for various functional hyperbranched polyether synthesis including alkene, alkyne and oligoethylglycol containing polymer and their post polymerisation reactions.
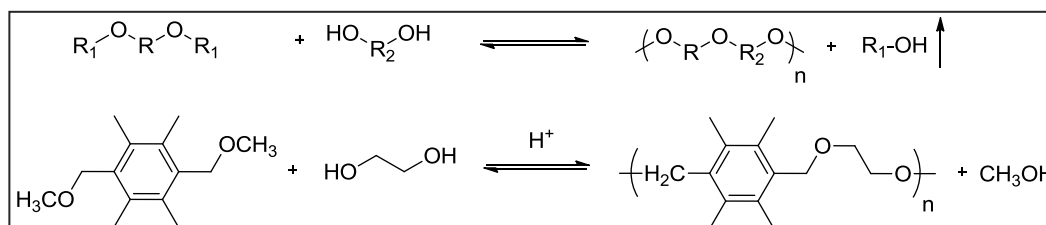
Scheme 2.2. *Synthesis of polyether by melt trans etherification approach*

From our research group Deepa et al., had reported eco-friendly melt transurethane process (in scheme-2.3) for polyurethane and the approach was aimed to replace the toxic and hazardous isocyanate synthetic pathways.[3] In this process, commercially available diamines were converted into di-urethane monomers which were polymerized with diols to make polyurethanes (in scheme 2.3).
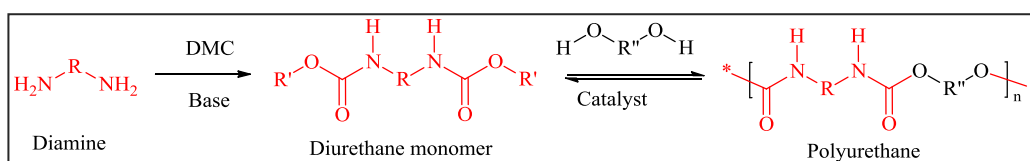
Scheme 2.3. *Non-isocyanate transurethane approach for synthesis of polyurethane*

Recently Dennis et al. prepared decahydronaphthalate dimethyl ester containing polyester using melt polycondensation approach (in scheme-2.4b).[4] In this method, decahydronaphthalate dimethyl ester was polymerised with various diols including cyclic and linear diols to deliver the polyester using solvent free melt condition in presence of Ti(OiPr)$_4$ as catalyst. This rigid polyester structure containing bicyclic derivative provided thermal stability up to 350 °C and can be processed into transparent films. Liu et al. prepared polyester based on melt polycondensation approach using dimethyl 1,4-cyclohexanedicarboxylate and triptycene diol in presence of Ti(OBu)$_4$ as catalyst (in scheme-2.4b).[5] The result revealed that triptycene diol based polyester produced high thermal stability and glass transition materials (Tg) compared to other linear diols including 1,4-butanediol, 1,6-hexanediol and oligoethyleneglycol diol. These recent literature results show the importance of melt polycondensation chemistry in polymer synthesis.
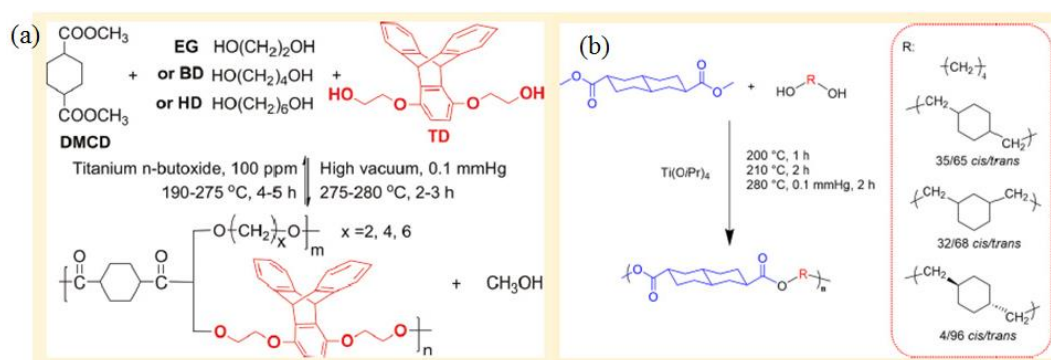
Scheme 2.4. *Melt polycondensation approach for polyester synthesis based on triptycene diol (a) and decahydronaphthalate derivative (b)(adopted from Liu et al. Macromolecules* **2011***, 44, 4049-4056(a) and Dennis et al. Macromolecules* **2015***, 48, 8733-8737(b)*

Terephthalic acid is an essential organic compound for the synthesis of commercially important poly (ethylene terephthalate) (PET) and they are obtained from petrochemical resources. Since petrochemical resources are dwindling, the monomer synthesis by renewable resources would be highly attractive for long term applications. Recently Liu et al. developed synthetic methodology for diethyl terephthalate from trans muconic acid biomass (in scheme-2.5).[6] In this process, diethyl terephthalate was synthesised in two steps; in the first step, trans muconic acid carboxylic acid was converted into ester followed by diels alder reaction using ethylene to yield the cyclo hexene dicarboxylic acid derivatives. In the second step,

dehydrogenation reaction of cyclohexene derivative produced the diethyl terephthalate. These results showed that commercially important PET monomer can be synthesised by non-petrochemical resources.
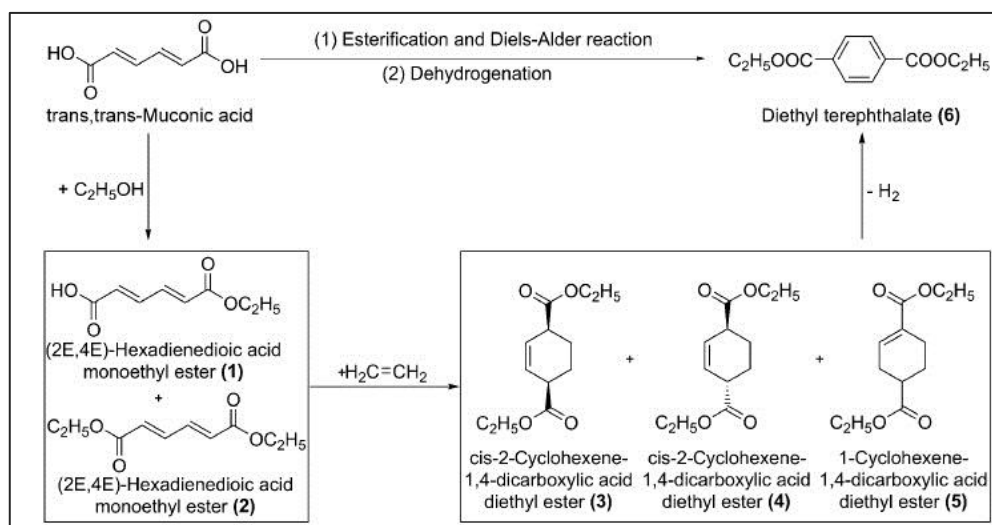
Scheme 2.5. *Diethyl terephthalate synthesised from trans, trans-Muconic acid biomass (adopted from Lu et al. Angew. Chem. Int. Ed.* **2016**, *55,* 249-253)

In recent years, the polymers obtained from renewable resources or bio-based monomers have attracted much attention in both academic and industrial research due to covern for the environment and shortage of petrochemical resources. Furan dicarboxylic acid is an important carbohydrate renewable resource based monomer for polyester synthesis.[7-8] Zhu et al. developed melt polycondensation for 2, 5- furan dicarboxylic acid (FDCA) (in scheme-2.6b). In this process FDCA was reacted with 1, 4-butanediol in presence of $Ti(OBu)_4$ as catalyst under melt condition to produce furan based polyester. These polymers showed high mechanical property and thermal property similar to that of commercialised poly (ethylene terephthalate) due to rigidity of furan aromatic ring in the polymer structure. Wu et al. fabricated melt polycondensation approach for carbohydrates based isohexide derivatives (in scheme-2.6a).[9] The results revealed that the cyclic isohexide based polyester showed high glass transition temperature and semi crystalline nature.
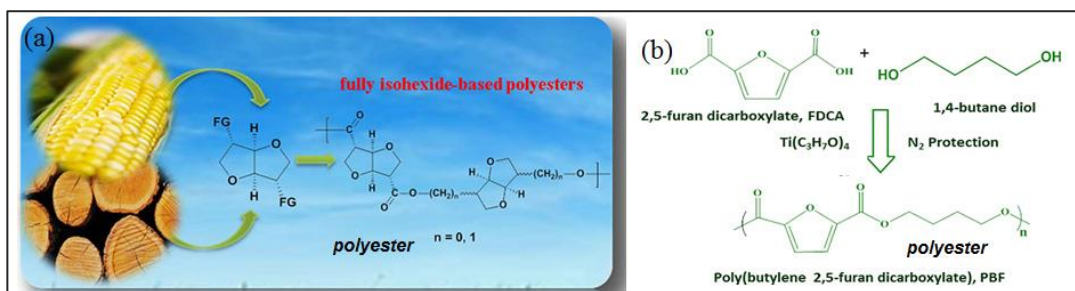
Scheme 2.6. *Carbohydrate resource based polymers synthesized from isohexide (a) and 2, 5- Furan dicarboxylic acid (b)(adopted from Wu et al. Macromolecules* **2013***, 46, 384-394(a) and Zhu et al. Macromolecules* **2013***, 46, 796-804)*

Lavilla et al. prepared mannitol based polyester using melt polycondensation approach (in scheme-2.7b).[10] In this method, the mannitol was converted into cyclic diol monomer, and they were polymerised using dimethyl succinate to yield the mannitol based polyester. These polymers were observed to be high Tg materials due to their cyclic structure it can be degraded using lipase as the enzyme. Same author reported melt polycondensation approach for galactaric acid based polyester (in scheme-2.7a).[11] In this process galactaric acid was altered into cyclic diester monomer, and then polymerised with linear aliphatic diol in presence of dibutyl tin oxide catalyst at 150 °C to deliver the galactaric acid based polyester. The results concluded that cyclic monomer based on carbohydrate produced high glass transition material and high mechanical stability similar to PET polymer. Recent literature reports show that development of naturally occurring monomer for polycondensation process is highly important because of the readily availabile of starting material in bulk scale.
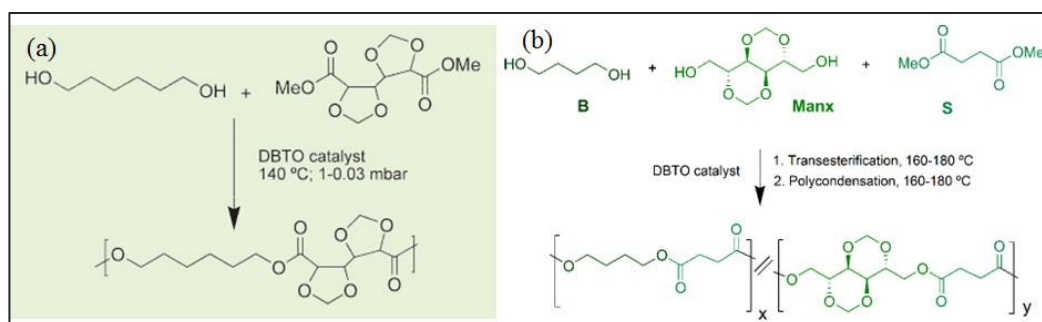
Scheme 2.7.*Synthesis of cyclic polyester obtained from galactaric acid (a) and mannitol (b) derivatives(adopted from Lavilla et al. Biomacromolecules* **2011***, 12, 2642-2652(a), Macromolecules* **2012***, 45, 8257-8266(b))*

Amino acids are biological monomers and their macromolecular peptide sequence and chain length played a crucial role on the size, function and secondary structure of proteins.[12-13] Synthetic polymers based on amino acids have been of great interest in chemistry-biology interface due to their potential application in therapeutics, cosmetics, biodegradable and biocompatible engineering thermoplastics.[14-15] Peptide linkages (amide-bonds) were routinely made by the self-condensation of amino acid using water removal agents such as DCC; however, this route was not capable of making higher molecular weight polymers having more than 8-10 repeating units.[16] In an indirect approach, amino acids were converted into di-carboxylic acid derivatives and polymerized with diols or diamines to produce poly(ester-amide) and their random copolymers.[17-19] Ring opening polymerization of amino acids via N-carboxyanhydride (NCA) intermediate was another important approach to make linear, block and star-shaped polypeptides.[20] Amino acids are naturally available bio-resources, and therefore, developing new synthetic polymerization strategies using them would open up a new direction of research activities towards amino acid polymeric materials for applications in biomedical components and thermoplastics. It is reasonable to consider amino acids as half-acids and half-amines; thus, development of solvent free melt condensation approach by combining the melt transurethane process developed in our laboratory with the whinfield one (transesterification) would open up new avenue of research opportunities for amino acids based condensation polymers.
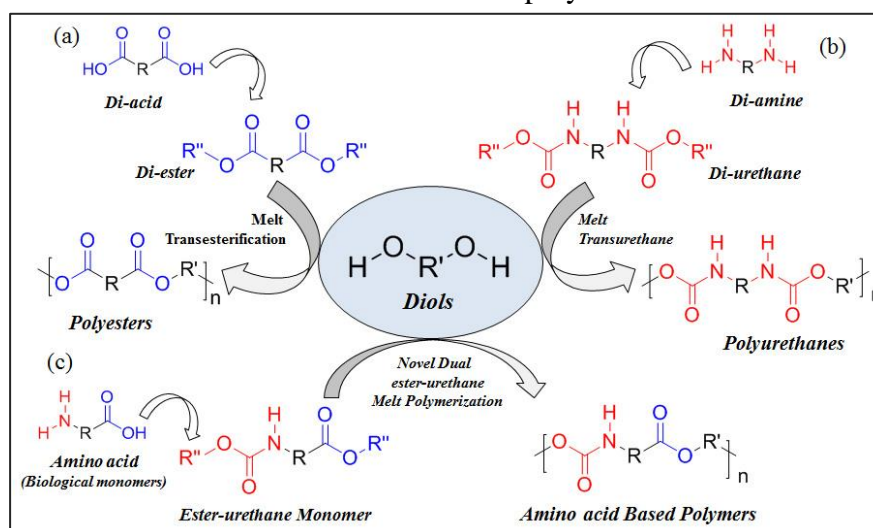
Scheme 2.8. *Schematic representation of melt trans reaction for polyester (a), polyurethane (b) and dual ester-urethane for amino acids (c).*

In this chapter, new *dual ester-urethane* melt polycondensation approach for amino acid monomers was developed (in scheme-2.8). In this new process, amino acids were converted into dual ester-urethane monomers and polycondensed with diols under melt conditions to produce high molecular weight polymers. The new synthetic process was tested for more than half-dozen of amino acids and diols. The mechanistic aspects of the process were studied by NMR and MALDI-TOF-MS and control reactions were carried out to understand the kinetics of the polymerization. The role of the catalyst, polymerization temperature and repeating unit structure on the molecular weight of the polymers and their thermal properties were also investigated. The newly synthesized amino acid polymers were found to self-organize as either β-sheet or polyproline type-II secondary structures. The present synthetic polymer approach, dual ester-urethane process is expected to pave way for new research platforms for amino acids which has huge potential in thermoplastic and bio-medical applications.

2.2. Experimental methods:

2.2.1. Materials: Glycine, L-alanine, β-alanine, L-valine, L-leucine, L-phenylalanine, 1,4-cyclohexanedimethanol (CHDM), 1,12-dodecandiol (DD), diethyleneglycol (Di-EG), triethyleneglycol (Tri-EG), tetraethylene glycol (Tetra-EG), titanium tetrabutoxide (Ti(OBu)$_4$) were purchased from Aldrich chemicals and used without further purification. Methylchloroformate, thionyl chloride and other solvents were purchased locally and purified prior to use.

2.2.2. General Procedures: ^{1}H and ^{13}C-NMR were recorded using 400-MHz JEOL NMR Spectrophotometer. All NMR spectra were recorded in CDCl$_3$ containing TMS as internal standard. High resolution mass spectra were obtained from Micro Mass ESI-TOF MS spectrometer. MALDI-TOF MS of the polymers were determined by using Applied Biosystems 4800 PLUS Analyzer. The polymer samples were dissolved in tetrahydrofuran (THF) at 10mg/mL and dihydroxybenzoic acid (DHB) was used as matrix. The matrix solution was prepared by dissolving 30 mg in 1.0 mL THF. A 1-2μL aliquot of the polymer/matrix mixture was used of the MALDI-TOF analysis. FT-IR spectra of all compounds were recorded using Bruker alphaT Fourier transform infrared spectrophotometer. Gel permeation chromatographic (GPC) analysis of the polymer samples were performed using Viscotek VE 1122 pump,

Viscotek VE 3580 RI detector and Viscotek VE 3210 UV/Vis detector in tetrahydrofuran (THF) using polystyrene as standards. Thermal analysis of the polymers were performed using TA Q20 Differential Scanning Calorimeter. The instrument was calibrated with indium standards. All the polymers were heated to melt before recording their thermo grams to remove their previous thermal history. Polymers were heated and cooled at 10 °C/min under nitrogen atmosphere and their thermograms were recorded. Thermal stability of the polymers was determined using Perkin Elmer thermal analyzer STA 6000 model at a heating rate of 10 ^{o}C/min in nitrogen atmosphere. Circular dichroism (CD) analysis of the polymer samples were done using JASCO J-815 CD spectrometer at 20 °C in THF, methanol and water depending up on their solubility.

2.2.3. Synthesis of methyl esters of amino acids: Typical procedure for carboxylic methyl esters of amino acids was described for L-phenylalanine. To a suspension of L-phenylalanine (8.67 g, 0.052 mol) in methanol (85 mL), thionylchloride (11.4 mL, 18.74 g, 0.157 mol) was added drop wise at 5 °C under nitrogen atmosphere. The reaction was refluxed for 12 h by under nitrogen. The solvent and excess of thionylchloride were removed by distillation. The residue solid washed with dry diethyl ether (120 mL) and dried to get product as white solid. Yield = 10.4 g (93%). ^{1}H-NMR (400 MHz, D$_2$O) δ ppm: 7.41-7.24 (m, 5H, Ar**H**), 4.39 (m, 1H, C**H**CH$_2$Ar), 3.79 (s, 3H, COOC**H$_3$**), 3.33-3.18 (d, 2H, C**H$_2$**Ar). FT-IR (cm^{-1}): 3926, 2852, 2618, 1742, 1581, 1491, 1443, 1232, 1145 and 1056. HR-MS (ESI+): m/z [M+H$^+$] calcd. for C$_{10}$H$_{13}$NO$_2$ [M+]: 180.1025; Found: 180.1025.

Methyl ester of other amino acids glycine, β-alanine, L-valine, L-leucine and L-alanine were prepared by similar procedure as described above and their details are provided below.

<u>Methyl ester of L-alanine:</u> L-alanine (7.75 g, 0.055 mol) in methanol (80 mL), thionylchloride (8.0 mL, 13.21 g, 0.165 mol). Yield = 10.93 g (90 %). ^{1}H NMR (400 MHz, CDCl$_3$) δ ppm: 4.17 (m, 1H, C**H**), 3.80 (s, 3H, COOC**H$_3$**), 1.51 (m, 3H, CHC**H$_3$**).   FT-IR (cm^{-1}): 3405, 2923, 2525, 1730, 1598, 1488, 1382, 1233, 1112 and 1009. HRMS (ESI+): m/z [M+H$^+$] calcd. for C$_4$H$_{10}$NO$_2$ [M$^+$]: 104.0712; found: 104.0716.

Methyl ester of β-alanine: β-alanine (5.20 g, 0.058 mol) in methanol (50 mL), thionylchloride (15 mL, 24.58 g, 0.206 mol). Yield = 7.24 g (92 %). ^{1}H NMR (400 MHz, D_2O) δ ppm: 3.67 (s, 3H, COOC**H$_3$**), 3.20 (q, 2H, C**H$_2$**COOCH$_3$), 2.73 (t, 2H, C**H$_2$**NHCOOCH$_3$). FT-IR (cm^{-1}): 3405, 2917, 1716, 1492, 1401, 1182, 1052. HRMS (ESI+): m/z [M+H$^+$] calcd. for $C_4H_9NO_2$ [M$^+$]: 105.0790; found: 104.0724.

Methyl ester of L-valine: L-valine (4.50 g, 0.038 mol) in methanol (50 mL), thionylchloride (8.4 mL, 13.60 g, 0.115 mol). Yield = 5.6 g (89 %). ^{1}H NMR (400 MHz, D_2O) δ ppm: 3.99 (m, 1H, C**H**), 3.81 (s, 3H, COOC**H$_3$**), 2.31 (m, 1H, C**H**), 0.99 (m, 6H, C**H$_3$**). FT-IR (cm-1): 2927, 2853, 1736, 1504, 1434, 1288, 1164 and 1033. HRMS (ESI+): m/z [M+H$^+$] calcd. for $C_6H_{14}NO_2$ [M$^+$]: 132.1025; found: 132.1024.

Methyl ester of L-leucine: L-leucine (3.95 g, 0.021 mol) in methanol (40 mL), thionylchloride (4.57 mL, 7.49 g, 0.063 mol). Yield = 5.07 g (93 %). ^{1}H NMR (400 MHz, D_2O) δ ppm: 4.11 (m, 1H, C**H**), 3.78 (s, 3H, COOC**H$_3$**), 1.82-1.65 (m, 3H, C**H$_2$**C**H** (CH$_3$)$_2$), 0.90 (m, 6H, C**H$_3$**). FT-IR (cm^{-1}): 2925, 2856, 2637, 1730, 1586, 1505, 1449, 1219 and 1036. MALDI TOF: m/z [M+Na$^+$] calcd. for $C_7H_{15}NNaO_2$[M$^+$]:168.1000; found:168.0811.

Methyl ester of Glycine: Glycine (10.05 g, 0.134mol), methanol (100 mL) and thionylchloride (29.2 mL, 47.8 g, 0.402 mol). Yield = 15.2 g (91 %). ^{1}H NMR (400 MHz, D_2O) δ ppm: 3.91 (m, 2H, C**H$_2$**), 3.80 (s, 3H, COOC**H$_3$**). FT-IR (cm^{-1}): 3103, 2879, 2683, 2629, 1741, 1581, 1497, 1432, 1400, 1246, 1138, 1099 and 1052.

2.2.4. Synthesis ester-urethane monomers of amino acids: Typical procedure is described for L-phenylalanine monomer. Hydrochloride salt of the above methyl ester of L-phenylalanine (7.10 g, 0.032 mol) was stirred in sodium bicarbonate solution (25 wt %, 65 mL) at 5 °C under nitrogen atmosphere. To this ice cold solution, methyl chloroformate (5.1 mL, 0.066 mol) was added drop wise and the reaction was continued for 12 h at 25 °C. The reaction mixture was extracted with dichloromethane and the organic layer was dried over anhydrous Na_2SO_4. The liquid was further purified by passing through silica gel column using ethyl acetate and pet ether (1:4 v/v) as eluent. Yield = 6.0 g (89 %). ^{1}H NMR (400 MHz, CDCl$_3$) δ ppm: 7.32-7.24 (m, 3H, Ar**H**), 7.12 (d, 2H, Ar**H**), 5.12 (b, 1H, -N**H**), 4.64 (q, 1H, C**H**CH$_2$Ar), 3.73 (s, 3H, COOC**H$_3$**), 3.67 (s, 3H, NHCOOC**H$_3$**), 3.11 (d, 2H, C**H$_2$**Ar). ^{13}C-NMR (100 MHz, CDCl$_3$) δ ppm: 172.95, 156.24, 135.69, 129.15 (2C), 128.52

(2C), 127.06, 54.69, 52.24 (2C), 38.13. FT-IR (cm^{-1}): 3338, 2954, 1705, 1518, 1444, 1355, 1253, 1210 and 1057. HR-MS (ESI+): m/z [M+Na$^+$] calcd. for C$_{12}$H$_{15}$NO$_4$ [M$^+$]: 260.0898; Found: 260.0899.

Dual ester-urethane monomers of other amino acids: glycine, β-alanine, L-valine, L-leucine, L-alanine were prepared as described above and details are provided below.

Glycine Monomer: Glycine (15.0 g, 0.120 mol), sodium bicarbonate solution (25wt %, 125 mL) and methyl chloroformate (18.5 mL, 0.234 mol). Yield =13.3 g (75 %). ^{1}H NMR (400 MHz, CDCl$_3$) δ ppm: 5.21 (b, 1H, -N**H**), 3.98 (d, 2H, **CH$_2$**), 3.76 (s, 3H, COOC**H$_3$**), 3.71 (s, 3H, NHCOOC**H$_3$**). ^{13}C-NMR (100 MHz, CDCl$_3$) δ ppm: 170.56, 156.91, 52.38, 52.25 and 42.52. FT-IR (cm^{-1}): 3443, 3057, 2956, 1719, 1523, 1440, 1372, 1287, 1212, 1056 and 1014. HRMS (ESI+): m/z [M+Na$^+$] calcd. for C$_5$H$_9$NO$_4$ [M$^+$]:170.0429; found: 170.0429.

Alanine Monomer: L-Alanine methyl ester HCl (10.01 g, 0.072 mol), methyl chloroformate (13.54 g, 11.0 mL, 0.144 mol) and sodium bicarbonate solution (25wt %, 80 mL). Yield= 10.2 g (85%). ^{1}H NMR (400 MHz, CDCl$_3$) δ ppm: 5.29 (b, 1H, -N**H**), 4.36 (m, 1H, C**H**), 3.74 (s, 3H, COOC**H$_3$**), 3.67 (s, 3H, NHCOOC**H$_3$**), 1.39 (d, 3H, CHC**H$_3$**). ^{13}C-NMR (100 MHz, CDCl$_3$) δ ppm: 173.51, 156.22, 52.25, 52.08, 49.38 and 18.33. FT-IR (cm^{-1}): 3434, 3056, 2988, 2956, 1719, 1516, 1455, 1377, 1348, 1297, 1268, 1215 and 1077. HRMS (ESI+): m/z [M+Na$^+$] calcd. for C$_6$H$_{11}$NO$_4$ [M$^+$]: 184.0585; found: 184.0587.

β-Alanine Monomer: β-Alanine methyl ester HCl (7.80 g, 0.056 mol), methyl chloroformate (10.60 g, 8.7 mL, 0.112 mol) and sodium bicarbonate solution (25wt %, 60 mL). Yield= 6.7 g (74%). ^{1}H NMR (400 MHz, CDCl$_3$) δ ppm: 5.26 (b, 1H, -N**H**), 3.68 (s, 3H, COOC**H$_3$**), 3.64 (s, 3H, NHCOOC**H$_3$**), 3.43 (q, 2H, **CH$_2$**COOCH$_3$), 2.51 (t, 2H, **CH$_2$**NHCOOCH$_3$). ^{13}C-NMR (100 MHz, CDCl$_3$) δ ppm: 172.75, 156.90, 51.98, 51.69, 36.40 and 34.12. FT-IR (cm^{-1}): 3445, 2955, 1720, 1636, 1519, 1440, 1368, 1290, 1267, 1239, 1199, 1080 and 1016. HRMS (ESI+): m/z [M+Na$^+$] calcd. for C$_6$H$_{11}$NO$_4$ [M$^+$]: 184.0585; found: 184.0586.

Valine Monomer: Valine methyl ester HCl (5.01 g, 0.029 mol), methyl chloroformate (5.63 g, 4.6 mL, 0.049 mol) and sodium bicarbonate solution (25 wt %, 40 mL).Yield=4.7 g (83%). ^{1}H NMR (400 MHz, CDCl$_3$) δ ppm: 5.18 (b, 1H, -N**H**), 4.28 (m, 1H, C**H**), 3.74 (s, 3H, COOC**H$_3$**), 3.69 (s, 3H, NHCOOC**H$_3$**), 2.15 (m, 1H,

CH), 0.96 (d, 3H, **CH₃**), 0.90 (d, 3H, **CH₃**). ¹³C-NMR (100 MHz, CDCl₃) δ ppm: 172.63, 156.84, 58.92, 52.26, 52.07, 31.13, 18.86 and 17.43. FT-IR (cm⁻¹): 3347, 2964, 1705, 1521, 1438, 1392, 1371, 1354, 1313, 1236, 1206, 1162, 1097 and 1024. HRMS (ESI+): m/z [M+Na⁺] calcd. for C₈H₁₅NO₄ [M⁺]: 212.0898; found: 212.0899.

Leucine Monomer: Leucine methyl ester HCl (5.04 g, 0.027 mol), methyl chloroformate (5.20 g, 4.3 mL, 0.055 mol) and sodium bicarbonate solution (25 wt %, 30 mL). Yield=4.2 g (75%). ¹H NMR (400 MHz, CDCl₃) δ ppm: 5.10 (b, 1H, -N**H**), 4.38 (m, 1H, C**H**), 3.74 (s, 3H, COOC**H₃**), 3.68 (s, 3H, NHCOOC**H₃**), 1.72-1.51 (m, 3H, C**H₂**C**H** (CH₃)₂), 0.95 (d, 6H, **CH₃**). ¹³C-NMR (100 MHz, CDCl₃) δ ppm: 173.73, 156.59, 52.32, 52.19, 41.59, 24.62, 22.75(2C), 21.64. FT-IR (cm⁻¹): 3341, 2957, 1703, 1520, 1440, 1352, 1257, 1223, 1205, 1169, 1122, 1056 and 1019. HRMS (ESI+): m/z [M+Na⁺] calcd. for C₉H₁₇NO₄ [M⁺]: 226.1055; found: 226.1055.

2.2.5. Dual ester-urethane melt polycondensation Process: Typical dual ester-urethane melt polymerization procedure is explained for L-phenylalanine monomer with 1,12-dodecanediol. Equimolar amounts of amino acid monomer L-phenylalanine monomer (0.76 g, 3.0 mmol) and 1,12-dodecanediol (0.65 g, 3.0 mmol) were taken in a test tube-shaped polymerization vessel and melted by placing the tube in oil bath at 100°C. The polycondensation apparatus was made oxygen and moisture free by purging with nitrogen and subsequent evacuation by vacuum under constant stirring. Titanium tetrabutoxide (11.0 mg, 0.03 mmol, 1.0 mol % equivalent to monomer) was added as catalyst and the melt polycondensation was carried out at 150 °C for 4h with constant stirring under nitrogen purge. During this stage, the methanol was removed along with the purge gas and the polymerization mixture became viscous. The viscous melt was further subjected to high vacuum (0.01 mm of Hg) at 150 °C for 2h under stirring. At the end of the polycondensation, the polymer, poly (ester-urethane), was obtained as a white mass (weight=0.98 g (82 %). It was purified by dissolving in tetrahydrofuran, filtered and precipitated into methanol to obtain fibrous product. Yield =0.72 g (59%). ¹H NMR (400 MHz, CDCl₃) δ ppm: 7.31-7.12 (m, 5H, Ar**H**), 5.13 (b, 1H, N**H**), 4.62 (m, 1H, C**H**), 4.10-4.04 (m, 4H, COOC**H₂**, NHCOOC**H₂**), 3.10 (t, 2H, C**H₂**Ar), 1.56-1.25 (m, 20H, C**H₂**). ¹³C-NMR (100 MHz, CDCl₃) δ ppm: 171.74, 155.93, 135.85, 129.25, 128.46, 126.98, 65.56, 65.29, 54.65, 38.35, 29.50,

29.16, 28.89, 28.38 and 25.76. FT-IR (cm^{-1}): 3348, 2924, 2853, 1717, 1505, 1458, 1397, 1346, 1249, 1196 and 1057. Molecular weights are given in the table -1.

All other amino acid based polymers with various diols: 1,4-cyclohexanedimethanol (CHDM), 1,12-dodecandiol, diethylene glycol (Di-EG), triethylene glycol (Tri-EG), tetraethylene glycol (Tetra-EG) are synthesized by similar procedure. The details are provided below.

Poly(Gly-DEG): Monomers used are Di-EG (0.54 g, 5.0 mmol) and Gly (0.75 g, 5.0 mmol). Titanium tetrabutoxide (17.0 mg, 0.05 mmol, 1.0 mol %). Yield = 0.68 g (68%). ^{1}H NMR (400 MHz, CDCl$_3$) δ ppm: 5.85 (b, 1H, -N**H**), 4.31 (t, 2H, COOC**H$_2$**), 4.24 (t, 2H, NHCOOC**H$_2$**), 4.00 (d, 2H, **CH$_2$**), 3.72 (t, 4H, **CH$_2$**O). ^{13}C NMR (100 MHz, CDCl$_3$) δppm: 170.12, 156.54, 72.32, 70.21, 69.29, 68.61, 64.05, 61.28 and 42.41. FT-IR (cm^{-1}): 3345, 2952, 1700, 1654, 1636, 1526, 1448, 1338, 1352, 1250, 1190, 1125 and 1049.

Poly(Gly-Tri-EG): Monomers used are Gly (1.00 g, 7.0 mmol) and Tri-EG, (1.03 g, 7.0 mmol). Titanium tetrabutoxide (23.0 mg, 0.07 mmol, 1.0 mol %). Yield = 1.06 g (66%). ^{1}H NMR (400 MHz, CDCl$_3$) δ ppm: 5.70 (b, 1H, -N**H**), 4.31 (t, 2H, COOC**H$_2$**), 4.24 (t, 2H, NHCOOC**H$_2$**), 3.99 (d, 2H, **CH$_2$**), 3.68 (m, 9H, **CH$_2$**O). ^{13}C NMR (100 MHz, CDCl$_3$) δppm: 170.20, 156.51, 72.31, 70.25, 69.22, 68.66, 64.10, 61.23, 42.44. FT-IR (cm^{-1}): 3344, 2878, 1706, 1528, 1455, 1390, 1351, 1250, 1218, 1193, 1106 and 1050.

Poly(Gly-TEG): Monomers used are Gly (1.01 g, 7.0 mmol) and Tetra-EG (1.34 g, 7.0 mmol). Titanium tetrabutoxide (23.0 mg, 0.07 mmol, 1.0mol %). Yield =1.35 g (71%). ^{1}H NMR (400 MHz, CDCl$_3$) δ ppm: 5.66 (b, 1H, -N**H**), 4.31 (t, 2H, COOC**H$_2$**), 4.24 (t, 2H, NHCOOC**H$_2$**), 3.99 (d, 2H, **CH$_2$**), 3.69 (m, 14H, **CH$_2$**O). ^{13}C NMR (100 MHz, CDCl$_3$) δppm: 170.11, 156.43, 72.39, 70.28, 69.98, 69.24, 68.65, 64.13, 61.26, 42.18. FT-IR (cm^{-1}): 3356, 2874, 1711, 1530, 1453, 1391, 1351, 1250, 1194 and 1051.

Poly(Gly-CHDM): Monomers used are Gly (0.94 g, 6.0 mmol) and CHDM (0.92 g, 6.0 mmol). Titanium tetrabutoxide (20.0 mg, 0.06 mmol, 1.0mol %). Yield =1.01 g (70%). ^{1}H NMR (400 MHz, CDCl$_3$) δ ppm: 5.23 (b, 1H, -N**H**), 4.08-3.88 (m, 6H, COOC**H$_2$**, NHCOOC**H$_2$**, **CH$_2$**), 1.79-1.40 (m, 15H, **CH$_2$, CH,** others).   FT-IR (cm^{-1}): 3357, 2915, 2853, 1696, 1519, 1451, 1397, 1360, 1260, 1104 and 1050.

Poly(Gly-DD): Monomers used are Gly (0.99 g, 7.0 mmol) and DD (1.37 g, 7.0 mmol). Titanium tetrabutoxide (23.0 mg, 0.07 mmol, 1.0 mol %). Yield =1.43 g

(73%). ^{1}H NMR (400 MHz, CDCl$_3$) δppm: 5.22 (b, 1H, -N**H**), 4.12 (t, 2H, COOC**H$_2$**), 4.05 (t, 2H, NHCOOC**H$_2$**), 3.94 (d, 2H, **CH$_2$**), 1.63-1.25 (m, 22H, **CH$_2$,** others). ^{13}C NMR (100 MHz, CDCl$_3$) δppm: 170.22, 156.59, 65.46, 65.36, 62.81, 42.57, 32.65, 29.38, 29.15, 28.83, 28.38, 25.68. FT-IR (cm^{-1}): 3324, 2917, 2849, 1744, 1685, 1530, 1470, 1446, 1409, 1372, 1247, 1210, 1097 and 1054.

Poly(β-ala-DD): Monomers used are Beta alanine (0.76 g, 5.0 mmol) and DD (0.96 g, 5.0 mmol). Titanium tetrabutoxide (17.0 mg, 0.05 mmol, 1.0 mol %). Yield =0.91 g (64%). ^{1}H NMR (400 MHz, CDCl$_3$) δ ppm: 5.20 (b, 1H, -N**H**), 4.08 (t, 2H, COOC**H$_2$**), 4.03 (t, 2H, NHCOOC**H$_2$**), 3.44 (q, 2H, **CH$_2$**), 2.51 (t, 2H, **CH$_2$**), 1.62-1.25 (m, 22H, **CH$_2$,** others). ^{13}C-NMR (100 MHz, CDCl$_3$) δ ppm: 173.44, 156.19, 65.73, 65.37, 49.66, 29.51, 28.63, 25.98, 28.91 and 19.04. FT-IR (cm^{-1}): 3356, 2915, 2848, 1691, 1531, 1470, 1439, 1422, 1395, 1366, 1326, 1298, 1248, 1181, 1144, 1067 and 1022.

Poly(β-ala-TEG): Monomers used are Beta alanine (0.75 g, 5.0 mmol) and Tetra-EG (0.91 g, 5.0 mmol). Titanium tetrabutoxide (17.0 mg, 0.05 mmol, 1.0 mol %). Yield =0.99 g (72%). ^{1}H NMR (400 MHz, CDCl$_3$) δ ppm: 5.59 (b, 1H, -N**H**), 4.26 (t, 2H, COOC**H$_2$**), 4.20 (t, 2H, NHCOOC**H$_2$**), 3.68 (m, 14H, **CH$_2$O**), 3.45 (q, 2H, **CH$_2$**), 2.53 (t, 2H, **CH$_2$**). FT-IR (cm^{-1}): 3346, 2874, 1712, 1650, 1530, 1453, 1383, 1349, 1294, 1250, 1218, 1182, 1101 and 1070.

Poly(β-ala-CHDM): Monomers used are Beta alanine (0.99 g, 6.0 mmol) and CHDM (0.89 g, 6.0 mmol). Titanium tetrabutoxide (20.0 mg, 0.06 mmol, 1.0 mol %). Yield =0.87 g (58%). ^{1}H NMR (400 MHz, CDCl$_3$) δ ppm: 5.23 (b, 1H, -N**H**), 4.01-3.86 (m, 4H, COOC**H$_2$**, NHCOOC**H$_2$**), 3.42 (q, 2H, **CH$_2$**), 2.53 (t, 2H, **CH$_2$**), 1.79-0.98 (m, 10H, **CH$_2$, CH**). FT-IR (cm^{-1}): 33577, 2924, 2855, 1695, 1516, 1450, 1394, 1357, 1322, 1241, 1177, 1139, 1071 and 1007.

Poly(Ala-DD): Monomers used are Ala (0.75 g, 5.0 mmol) and DD (0.94 g, 5.0 mmol). Titanium tetrabutoxide (17.0 mg, 0.05 mmol, 1.0 mol %). Yield =1.08 g (77%). ^{1}H NMR (400 MHz, CDCl$_3$) δ ppm: 5.24 (b, 1H, -N**H**), 4.36 (m, 1H, C**H**), 4.13 (t, 2H, COOC**H$_2$**), 4.05 (t, 2H, NHCOOC**H$_2$**), 1.40 (d, 3H, **CH$_3$**), 1.64-1.27 (m, 24H, **CH$_2$,** others). ^{13}C-NMR (100 MHz, CDCl$_3$) δ ppm: 173.41, 156.15, 65.71, 65.39, 49.68, 29.53, 28.64, 25.94, 28.91 and 19.00. FT-IR (cm^{-1}): 3322, 2916, 2849, 1737, 1722, 1686, 1530, 1469, 1455, 1353, 1298, 1258, 1211, 1181, 1127, 1075 and 1030.

Poly(Ala-TEG): Monomers used are Ala (0.73 g, 4.0 mmol) and Tetra-EG (0.88 g, 4.0 mmol). Titanium tetrabutoxide (14.0 mg, 0.04 mmol, 1.0 mol %). Yield =0.93 g (73%). ^{1}H NMR (400 MHz, CDCl$_3$) δ ppm: 5.72 (b, 1H, N**H**), 4.39-4.23 (m, 4H, COOC**H$_2$**, NHCOOC**H$_2$**), 3.71 (m, 15H, **CH$_2$**O), 1.43 (d, 3H, **CH$_3$**). FT-IR (cm^{-1}): 3330, 2874, 1712, 1650, 1530, 1453, 1383, 1349, 1294, 1250, 1218, 1182, 1101 and 1070.

Poly(Ala-CHDM): Monomers used are Ala (0.79 g, 5.0 mmol) and CHDM (0.71 g, 5.0 mmol). Titanium tetrabutoxide (17.0 mg, 0.05 mmol, 1.0 mol %). Yield =0.85 g (73%). ^{1}H NMR (400 MHz, CDCl$_3$) δ ppm: 5.28 (b, 1H, -N**H**), 4.35 (m, 1H, **CH**) 4.05-3.86 (m, 4H, COOC**H$_2$**, NHCOOC**H$_2$**), 1.79 -1.40 (m, 13H, **CH$_2$**), 1.39 (d, 2H, **CH$_3$**). FT-IR (cm^{-1}): 3329, 2929, 2825, 1699, 1524, 1451, 1398, 1376, 1335, 1330, 1247, 1206, 1176, 1115, 1068 and 1034

Poly(Val-DD): Monomers used are Val (0.75 g, 4.0 mmol) and DD (0.80 g, 4.0 mmol). Titanium tetrabutoxide (14.0 mg, 0.04 mmol, 1.0 mol %). Yield =0.95 g (68%). ^{1}H NMR (400 MHz, CDCl$_3$) δ ppm: 5.16 (b, 1H, N**H**), 4.25 (m, 1H, **CH**), 4.09 (t, 2H, **CH$_2$**), 4.01 (t, 2H, **CH$_2$**), 2.13 (m, 1H, **CH**), 1.63-1.24 (m, 20H, **CH$_2$**), 0.95 (d, 3H, **CH$_3$**), 0.86 (d, 3H, **CH$_3$**). ^{13}C-NMR (100 MHz, CDCl$_3$) δ ppm: 172.38, 156.59, 65.35, 58.82, 31.33, 29.50, 29.27, 29.16, 28.94, 28.51, 25.81, 18.95 and 17.47. FT-IR (cm^{-1}): 3346, 2924, 2853, 1719, 1511, 1467, 1392, 1348, 1308, 1220, 1162, 1095 and 1033.

Poly(Val-TEG): Monomers used are Val (0.71 g, 3.0 mmol) and Tetra-EG (0.72 g, 3.0 mmol). Titanium tetrabutoxide (10.0 mg, 0.03 mmol, 1.0mol %). Yield = 0.95 g (68%). ^{1}H NMR (400 MHz, CDCl$_3$) δ ppm: 5.44 (b, 1H, N**H**), 4.32-4.23 (m, 4H, COOC**H$_2$**, NHCOOC**H$_2$**), 3.66 (m, 16H, **CH$_2$**O), 2.18 (m, 1H, **CH**), 0.97 (d, 3H, **CH$_3$**), 0.90 (d, 3H, **CH$_3$**). FT-IR (cm^{-1}): 3351, 2961, 2874, 1716, 1530, 1457, 1392, 1373, 1349, 1241, 1220, 1095 and 1039.

Poly(Val-CHDM): Monomers used are Val (0.80 g, 4.0 mmol) and CHDM (0.61 g, 4.0 mmol). Titanium tetrabutoxide (14.0 mg, 0.04 mmol, 1.0mol %). Yield =0.72 g (59%). ^{1}H NMR (400 MHz, CDCl$_3$) δ ppm: 5.30 (b, 1H, N**H**), 4.25 (m, 1H, **CH**), 4.29-3.95 (m, 4H, COOC**H$_2$,** NHCOOC**H$_2$**), 2.15(m, 1H, **CH**) 1.82-1.42 (m, 11H, **CH$_2$**, **CH**), 0.98 (d, 3H, **CH$_3$**), 0.88 (d, 3H, **CH$_3$**). FT-IR (cm^{-1}): 3341, 2925, 2855, 1704, 1519, 1468, 1452, 1393, 1371, 1345, 1309, 1265, 1231, 1188, 1162, 1092 and 1025.

Poly(Phe-TEG): Monomers used are Phe (0.60 g, 2.0 mmol) and Tetra-EG (0.49 g, 2.0 mmol). Yield =0.65 g (70%). ^{1}H NMR (400 MHz, CDCl$_3$) δ ppm: 7.28-7.14 (m, 5H, Ar**H**), 5.41 (b, 1H, N**H**), 4.62 (m, 1H, C**H**), 4.27 (t, 2H, COOC**H$_2$**), 4.23 (t, 2H, NHCOOC**H$_2$**), 3.64 (m, 12H, **CH$_2$O**) and 3.09 (t, 2H, C**H$_2$**). FT-IR (cm^{-1}): 3330, 2949, 2874, 1711, 1650, 1529, 1453, 1384, 1349, 1250, 1218, 1126 and 1056.

Poly(Phe-CHDM): Monomers used are Phe (0.84 g, 4.0 mmol) and CHDM (0.51 g, 4.0 mmol). Titanium tetrabutoxide (14.0 mg, 0.04 mmol, 1.0mol %). Yield =0.83 g (74%). ^{1}H NMR (400 MHz, CDCl$_3$) δ ppm: 7.29-7.11 (m, 5H, Ar**H**), 5.15 (b, 1H, N**H**), 4.63 (m, 1H, C**H**), 3.80 (m, 4H, COOC**H$_2$**, NHCOOC**H$_2$**), 3.09 (t, 2H, C**H$_2$**), 1.75-0.93 (m, 10H, C**H$_2$**, C**H**). FT-IR (cm^{-1}): 3340, 2892, 2842, 1713, 1696, 1505, 1497, 1453, 1397, 1345, 1247, 1185 and 1049.

Poly(Leu-DD): Monomers used are Leu (0.71 g, 3.0 mmol) and DD (0.71 g, 3.0 mmol). Titanium tetrabutoxide (10.0 mg, 0.03 mmol, 1.0mol %). Yield =0.89 g (75%). ^{1}H NMR (400 MHz, CDCl$_3$) δ ppm: 5.08 (b, 1H, N**H**), 4.36 (m, 1H, C**H**), 4.11 (t, 2H, COOC**H$_2$**), 4.04 (t, 2H, NHCOOC**H$_2$**), 1.63-1.26 (m, 24H, C**H, CH$_2$**), 0.92 (d, 6H, C**H$_3$**). ^{13}C-NMR (100 MHz, CDCl$_3$) δ ppm: 172.63, 156.77, 64.99, 36.52, 34.56, 29.60, 29.31, 29.08, 28.63 and 25.96. FT-IR (cm^{-1}): 3332, 2924, 2854, 1718, 1517, 1467, 1387, 1367, 1333, 1255, 1220, 1198, 1170, 1121 and 1053.

Poly(Leu-TEG): Monomers used are Leu (0.60 g, 3.0 mmol) and Tetra-EG (0.58 g, 3.0 mmol). Titanium tetrabutoxide (10.0 mg, 0.03 mmol, 1.0 mol %). Yield =0.73 g (73%). ^{1}H NMR (400 MHz, CDCl$_3$) δ ppm: 5.35 (b, 1H, N**H**), 4.29 (m, 4H, COOC**H$_2$**, NHCOOC**H$_2$**), 3.66 (m, 12H, C**H$_2$O**), 1.72-1.55 (m, 3H, C**H$_2$**C**H** (CH$_3$)$_2$) and 0.95 (d, 6H, C**H$_3$**). FT-IR (cm^{-1}): 3332, 2954, 2872, 1715, 1530, 1454, 1385, 1349, 1331, 1251, 1219, 1115 and 1056.

Poly(Leu-CHDM): Monomers used are Leu (0.86 g, 4.0 mmol) and CHDM (0.61 g, 4.0 mmol). Titanium tetrabutoxide (14.0 mg, 0.04 mmol, 1.0 mol %). Yield =1.07 g (89%). ^{1}H NMR (400 MHz, CDCl$_3$) δ ppm: 5.11 (b, 1H, N**H**), 4.37 (m, 1H, C**H**), 4.05-3.90 (m, 4H, COOC**H$_2$**, NHCOOC**H$_2$**) and 1.88-0.94 (m, 27H, CH, C**H$_2$**, C**H$_3$**). FT-IR (cm^{-1}): 3341, 2925, 2856, 1697, 1520, 1469, 1451, 1388, 1368, 1333, 1261, 1220, 1197, 1121 and 1048.

2.2.6. Model Reactions for Kinetic Studies: Typical reaction is described for benzylalcohol (**Bz**) with the glycine monomer. Benzyl alcohol (2.21 g, 20.0 mol) and glycine monomer (1.50 g, 10.0 mol) were taken in a test tube shaped polymerization

apparatus and melted by placing in an oil bath at 100 $^{\circ}$C with constant stirring. After degassing as described for the polymerization, Ti(OBu)$_4$ (0.035 g, 1 mol%) was added and the condensation was carried out at 120 $^{\circ}$C under nitrogen purge for 3 h, then temperature was increased to 150 °C with nitrogen purge for 3 h. Further, controlled vacuum (1 mm of Hg) was applied at 150 °C for 2 h. During the nitrogen and vacuum stage various aliquots were taken at every half-an hour interval. At the end of the condensation reaction, the product was obtained as slight yellow viscous liquid. ^{1}H NMR (400 MHz, CDCl$_3$) δ ppm: 7.36 (m, 10H, Ar**H**), 5.18 (b, 1H, -N**H**), 5.09 (s, 2H, PhC**H$_2$**COO), 5.03 (s, 2H, PhC**H$_2$**NHCOO) and 3.91 (d, 2H, C**H$_2$**). ^{13}C-NMR (100 MHz, CDCl$_3$) δ ppm: 170.19, 156.56, 136.44, 135.39, 128.91(2C), 128.79(2C), 128.66 (2C), 128.47, 128.37, 67.45, 67.38 and 43.08. FT-IR (cm^{-1}): 3359, 2923, 1712, 1524, 1361, 1161 and 1052. MALDI-TOF MS: m/z [M+Na$^+$] calcd. for C$_{17}$H$_{17}$NO$_4$ [M$^+$]= 322.1055; Found = 322.0435.

The other model reactions: (i) stepwise in the absence of catalyst and (ii) direct at 150 °C in presence of catalyst followed the similar procedure.

2.2.7. Model Reaction for A-A + B Route (absence of Catalyst)

Benzyl alcohol (1.47 g, 14.0 mmol), glycine monomer (1.00 g, 7.0 mmol).^{1}H NMR (400 MHz, CDCl$_3$) δ ppm: 7.37-7.34 (m, 4H, Ar**H**), 5.20 (b, 1H, -N**H**), 5.17 (s, 2H, OC**H$_2$**Ar), 4.00-3.96 (d, 2H, C**H$_2$**), 3.68 (s, 3H, NHCOOC**H$_3$**). ^{13}C-NMR (100 MHz, CDCl$_3$) δ ppm: 170.19, 156.56, 136.44, 135.39, 128.91(2C), 128.79(2C), 128.66 (2C), 128.47, 128.37, 67.45, 67.38 and 43.08. FT-IR (cm^{-1}):3354, 2953, 1702, 1524, 1361, 1182, 1050. MALDI TOF: m/z [M+Na$^+$] calcd. for C$_{11}$H$_{13}$NO$_4$ [M$^+$]:246.0742; found:246.0802 .

2.2.8. Model Reaction for A-A + B Route (Direct at 150 °C)

Benzyl alcohol (2.21 g, 0.020 mol), glycine monomer (1.50 g, 0.010 mol) and 3 drops of Ti(OBu)$_4$ (0.034 g, 1mol%) catalyst, product color: yellowish liquid. ^{1}H NMR (400 MHz, CDCl$_3$) δ ppm: 7.36 (m, 10H, Ar**H**), 5.18 (b, 1H, -N**H**), 5.09 (s, 2H, PhC**H$_2$**COO), 5.03 (s, 2H, PhC**H$_2$**NHCOO) and 3.91 (d, 2H, C**H$_2$**). ^{13}C-NMR (100 MHz, CDCl$_3$) δ ppm: 170.19, 156.56, 136.44, 135.39, 128.91 (2C), 128.79 (2C), 128.66 (2C), 128.47, 128.37, 67.45, 67.38 and 43.08. FT-IR (cm^{-1}):3359, 2923, 1712, 1524, 1361, 1161 and 1052. MALDI TOF: m/z [M+Na$^+$] calcd. for C$_{17}$H$_{17}$NO$_4$ [M$^+$]:322.1055; found:322.0435.

2.3. Results and Discussion

2.3.1. Synthesis of Ester-Urethane Monomer

Ester-urethane monomers were synthesized starting from naturally available L-amino acids as shown in scheme-2.9. Amino acids were converted into carboxylic acid chlorides and subsequently reacted with methanol to yield amino acid methyl ester hydrochloride salts. The amine salt was converted into its free amine by washing with aqueous $NaHCO_3$, then reacted with methyl chloroformate to obtain dual ester-urethane monomer. Monomers of glycine, L-alanine, L-valine, L-phenylalanine, L-leucine, and β-alanine were synthesized as described above and their structures were characterized by NMR, FT-IR and Mass spectroscopic analysis. The monomers were synthesized in average yield of 75-84 %.
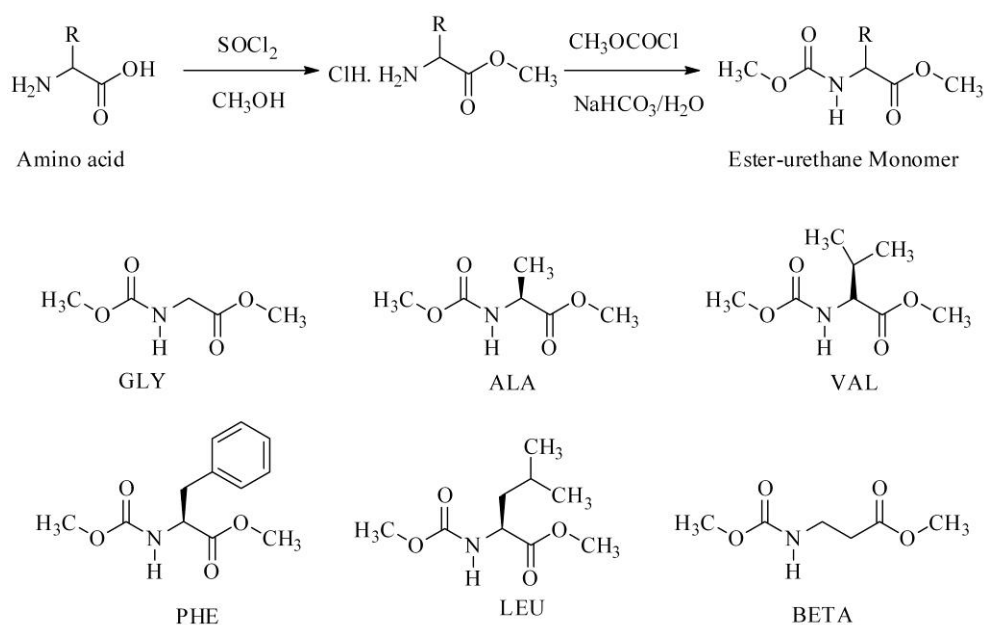
Scheme 2.9. *Synthesis of dual ester-urethane monomer from amino acids*

2.3.2. Dual ester-urethane melt polycondensation Route

Dual ester urethane melt condensation reaction was carried out in one pot two steps as shown in figure 2.1b. The reaction vessel for the polymerization process is provided in figure 2.1 a). Equimolar amounts of amino acid monomer and diols were poly condensed using $Ti(OBu)_4$ as catalyst (1 mole %) under nitrogen purge and high vaccum (0.01 mm of Hg). During this process, the viscosity of the melt increased very rapidly and the stirring stopped at the end of the polycondensation. The white polymer mass was purified by carrying out precipitation and dried in vacuum oven

(0.1 mm of Hg) prior to further analysis. In the current process, the diol reacted with both methyl ester and methyl urethane units in the amino acid monomers; as a result the new class of polymers are named as poly(ester-urethane)s. The new polycondensation process was tested for various diols of di-, tri- and tetraethylene glycols, 1,12-dodecandiol (linear aliphatic diols) and 1,4-cyclohexanedimethanol (cycloaliphatic diols) and for various amino acid monomers (in figure 2.1b).
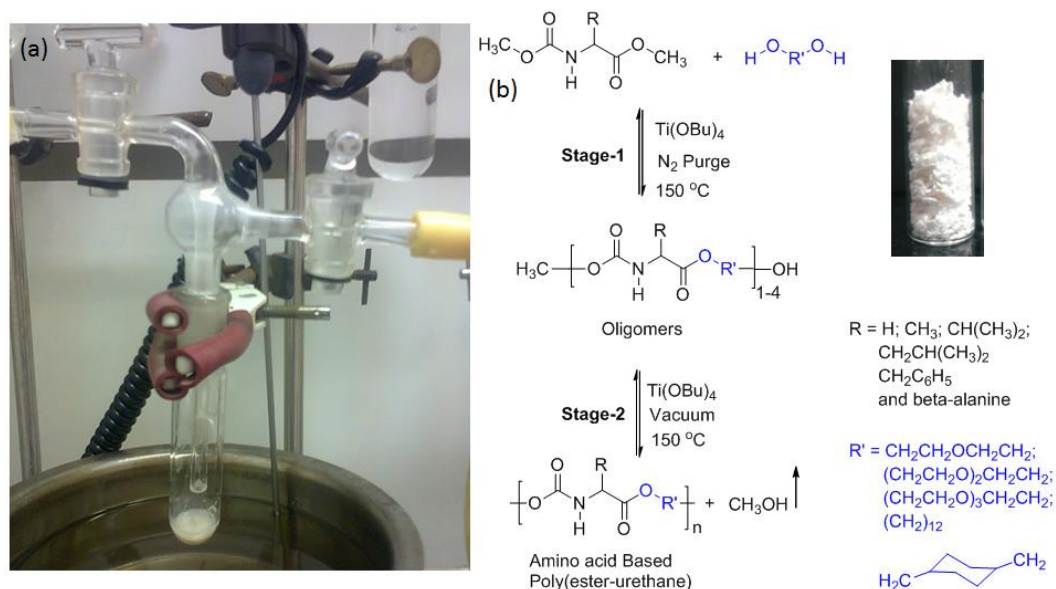
Figure 2.1. *The reaction vessel for the polymerization process (a) and* s*ynthesis of Polymers via dual ester-urethane melt polycondensation (b). The sample in the vial showed the fibrous polymer obtained using 1,12-dodecandiol with glycine monomer.*

Both diols and amino acid monomers were varied in the feed to produce wide range of polymer structures. The structures of amino acid based poly (ester-urethanes) were summarized in scheme- 2.10.
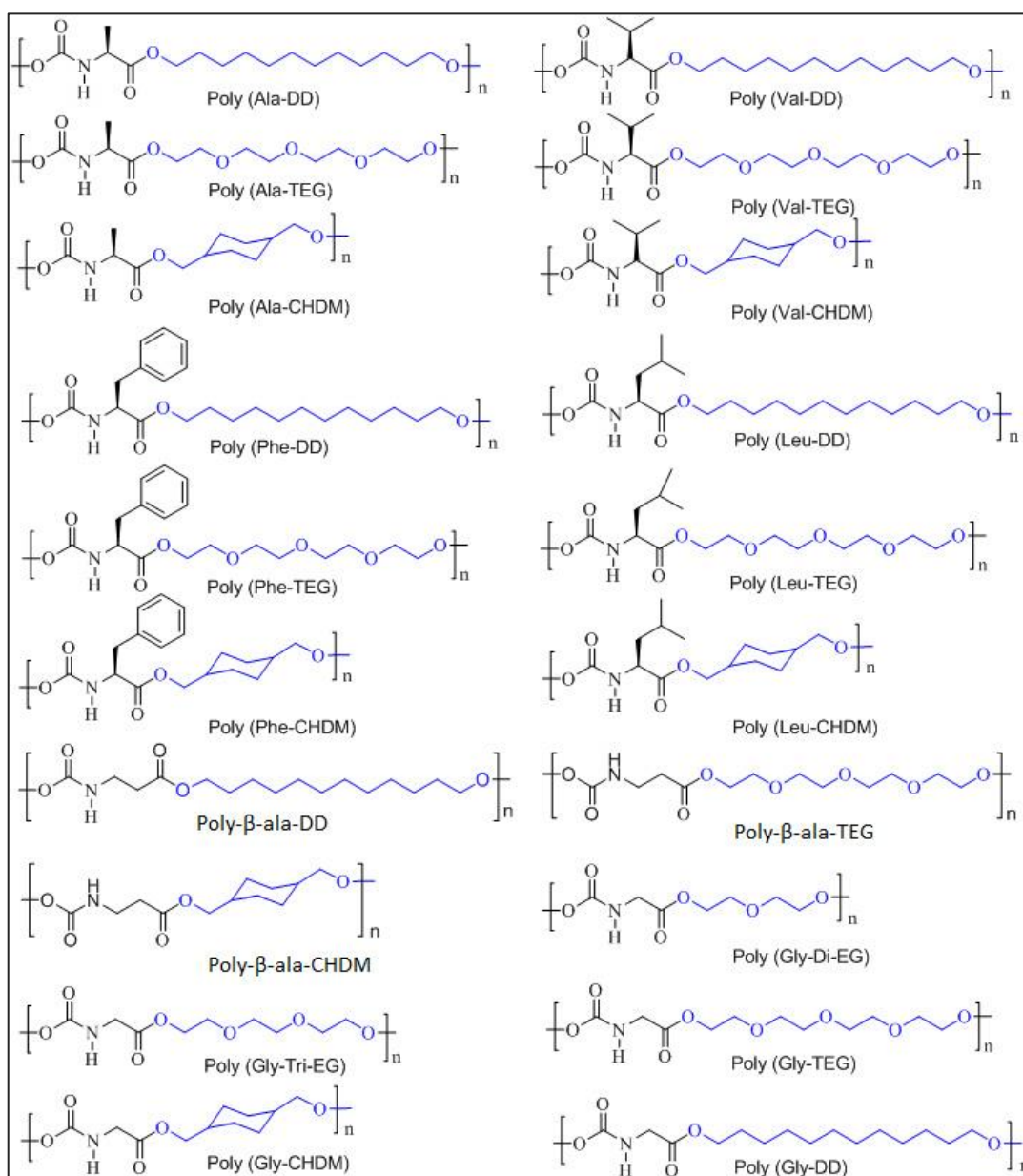
Scheme 2.10. *Structures of various amino acid polymers synthesized via the dual ester-urethane process.*

2.3.3. NMR characterization of polymer

The occurrence of dual ester-urethane process and the structure of the new poly (ester-urethane)s were confirmed by NMR spectroscopy. NMR spectra of glycine monomer and its corresponding polymer with 1, 12-dodecanol are shown in figure 2.2. The different types of the protons and carbon atoms in the monomer and polymer structure are assigned by alphabets.
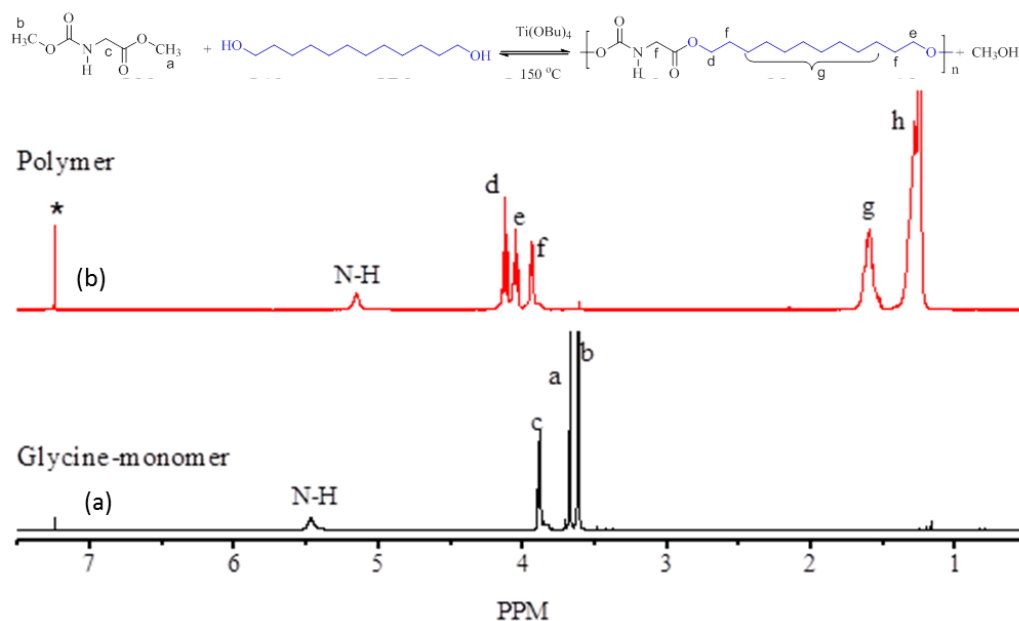
Figure 2.2. *¹H NMR stack plot of glycine monomer and their corresponding polymer with 1,12-dodecandiol*

In the ¹H-NMR spectrum, the methyl ester protons in the ester (a) and the urethane (b) appeared very closely as singlet at 3.67 and 3.62 ppm, respectively. The N-H proton and the NH-C**H**$_2$-COO (c) from the amino acid unit appeared at 5.47 ppm and 3.88 ppm, respectively. Upon polymerization, two new triplets appeared at 4.12 ppm and 4.05 ppm corresponding to -CH$_2$C**H**$_2$OOC (d) and –CH$_2$C**H**$_2$OOCNH (e) protons in the ester and urethane linkages. All other aliphatic protons in the 1, 12-dodecandiol unit appeared below 2.00 ppm. During the polycondensation process, the nucleophilic attack of –OH groups in the diols at the carbonyl of ester and urethane linkages lead to the removal of low boiling alcohol (as methanol in the present case). The fast and efficient removal of methanol from the reaction mixture drove the equilibrium towards polycondensation to produce higher molecular weight chains. The comparison of NMR spectra revealed that –OC**H$_3$** protons and carbon in the monomer had completely vanished in the polymer spectra (at 3.70- 3.64ppm) which confirmed the occurrence the dual ester-urethane process as well as formation of high molecular weight polymers. In ¹³CNMR, upon polymerization glycine monomer – OCH$_3$ carbon peak observed at 52.2 ppm, disappeared and the corresponding new peak belonging to polymer –COOCH$_2$ of ester and urethane appeared at 65.5 ppm

respectively. ^{13}C-NMR spectra of the monomer and polymers also confirmed the occurrence of the polycondensation (in figure 2.3).
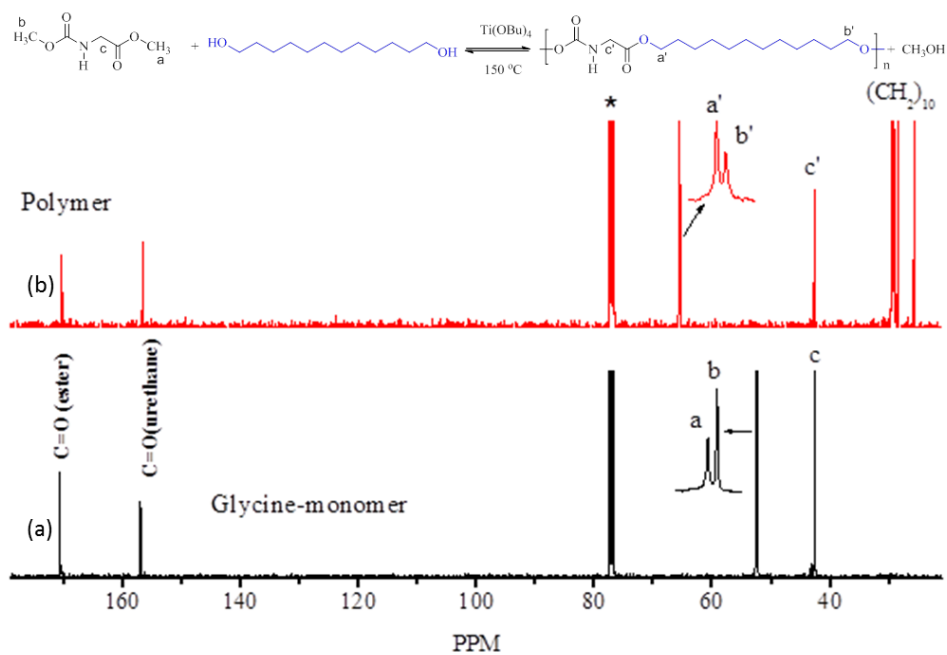
Figure 2.3. *^{13}C-NMR spectra of glycine monomer and its 1,12-dodecandiol polymer*

A similar NMR spectral analysis for various amino acid monomers in polycondensation with 1,12-dodecanediol is provided in figure 2.4.
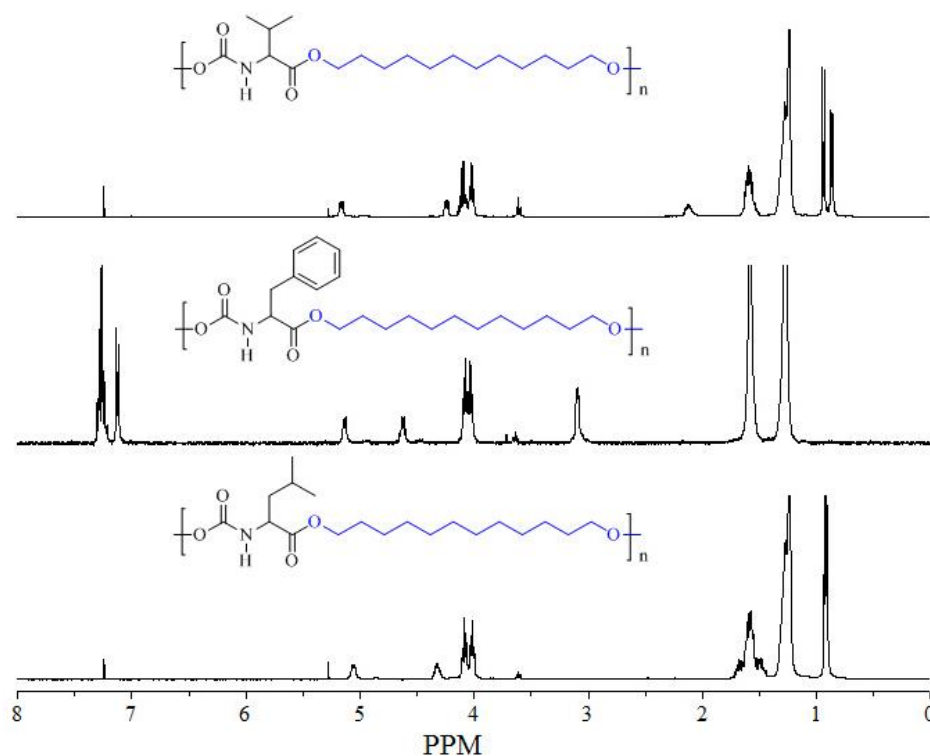
Figure 2.4. *^{1}H NMR spectra of various amino acid based polymers with 1,12-dodecandiol*

Similarly FT-IR spectra of the polymers were recorded to confirm the formation of ester and urethane linkages (in figure 2.5). The polymers showed peaks at 3317 cm^{-1} and 1526 cm^{-1} with respect to the N-H and C-N stretching frequencies, respectively. The peaks for ester and urethane linkages appeared at 1739 cm^{-1} and 1687 cm^{-1}, respectively,[14] which confirmed the formation of expected poly(ester-urethane) structure.
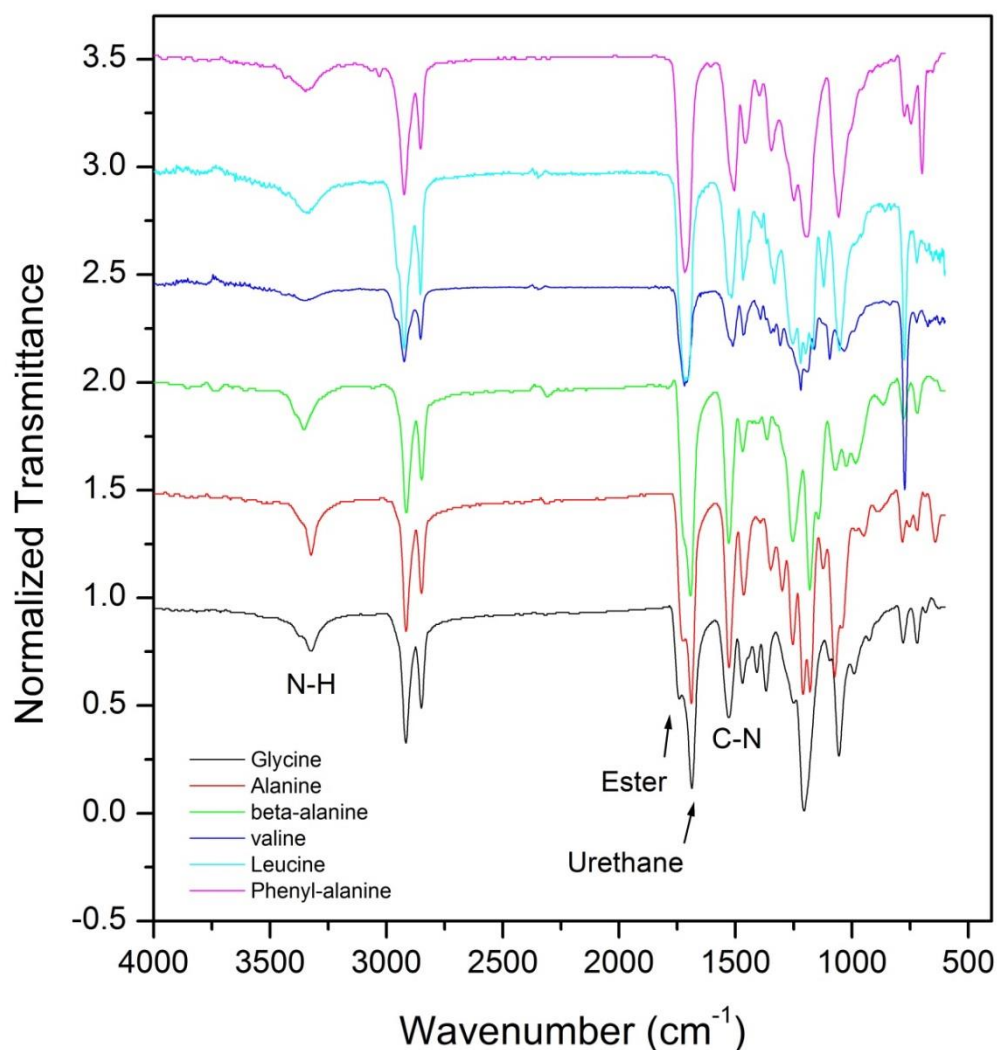
Figure 2.5. *FT-IR spectra of the polymers synthesized using 1,12-dodecandiol with various amino acid monomers.*

2.3.4. Molecular Weight of polymers

The molecular weight of the newly synthesized amino acid poly(ester-urethane)s was determined by gel permeation chromatography (GPC) in THF. The GPC chromatograms are provided in the figure 2.6. and their molecular weights are

summarized in table 1. All the polymers showed mono-modal distribution indicating the formation of uniform molecular weight chains by the melt route (in figure 2.6).
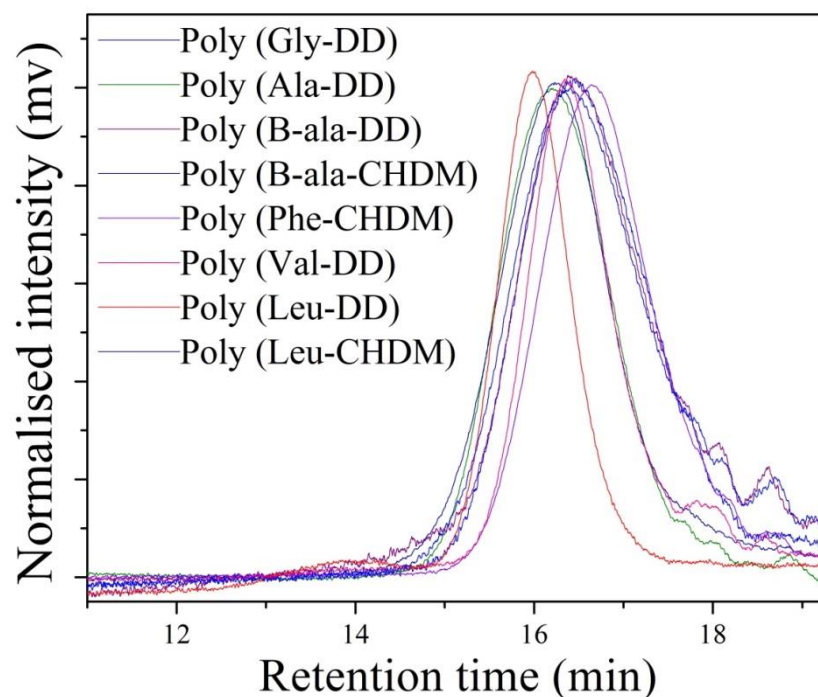
Figure 2.6. *GPC chromatograms of amino acid based poly (ester-urethane) in THF solvent*

The molecular weight of the polymers were obtained in the range of $M_n = 5.0$-19.2×10^3 and $M_w = 10.1$-32.6×10^3 g/mol with the average polydispersity in the range of 2.1. The number average degrees of polymerization (x_n) of the polymers were determined from the equation, $M_n = (M_o) \times (x_n)$, where M_o is the repeating units mass.[21] Based on the Carrothors equation,[21] $x_n = 1/(1-P)$ for the step condensation process where 'P' is the percent conversion (or extent of the reaction), both x_n and p were obtained as 20-40 units and 96-98 % of occurrence of reaction, respectively (in table 1). These values are very good for a laboratory scale (1.0-2.0 g) newly developed melt polycondensation reaction. Typically, the condensation polymerisation process follows the Carothers equation, $M_w/M_n = 1+P$, where P = extend of the polymerisation reaction. For example if the extend of reaction is 95%, and then PDI would expected to be 1.95. The condensation polymerisation is not a controlled polymerisation process, therefore the condensation polymerisation PDI is usually expected to be > 2.0.

Table 1.*Monomers, molecular weights, % conversion and thermal properties of polymers*

Monomer	Diol[a]	M_n[b] (g/mol)	M_w[b] (g/mol)	M_w/M_n	x_n[c]	P[d]	T_D[e] (°C)	T_D[f] (°C)	T_g[g] (°C)
Glycine	DEG	4600	6700	1.5	24	96	240	230	8.6
	TREG	4900	8800	1.8	21	95	240	217	-2.9
	TEG	5200	8600	1.6	18	94	250	225	-13.3
	CHDM	9300	10400	1.3	40	97	280	243	58.3
	DD	5500	14100	2.5	19	95	275	253	14.8
L-Alanine	TEG	4800	7300	1.5	16	93	250	221	-26.6
	CHDM	3400	7200	2.1	14	92	280	242	6.7
	DD	8600	14200	1.7	28	96	250	214	6.0
β-Alanine	TEG	6100	10900	1.8	20	95	250	226	-24.3
	CHDM	8600	15300	1.8	18	97	260	233	24.1
	DD	5600	11000	2.0	35	94	270	239	13.7
L-Valine	TEG	4400	6700	1.6	14	93	255	218	-29.6
	CHDM	5600	11000	2.0	20	95	260	226	43.5
	DD	8400	11000	1.3	25	96	270	239	-
L-Leucine	TEG	5900	9800	1.7	18	94	250	216	-15.7
	CHDM	5900	11900	2.0	20	95	260	223	50.4
	DD	13300	17000	1.4	39	97	300	268	-13.1
L-Phenyl -alanine	TEG	7000	14000	2.0	19	95	265	231	-0.1
	CHDM	4800	8300	1.7	15	93	300	267	64.0
	DD	17900	32700	1.9	47	98	300	265	-8.3

[a] DEG, TREG and TEG refer di, tri-and tetra ethylene glycols, respectively. CHDM, and DD refer 1,4-cyclohexanedimethanol and 1,2-dodecandiol, respectively. [b] Number (M_n) and weight average (M_w) molecular weights were determined by GPC using THF as solvent. [c] The degree of polymerization (x_n) was calculated using the formula $M_n = n\,M_o$, where M_o is repeating unit mass. [d] The percent conversion (P) was calculated using Carothers eqn. $x_n = 1/(1-P)$. [e] The decomposition temperature (T_D) of the sample was determined for 10 % weight loss using TGA under nitrogen. [f] The decomposition temperature (T_D) of the sample was determined for onset point using TGA under nitrogen. [g] The glass transition temperature (T_g) was determined by DSC at 10°/min.

The molecular weights of the polymer samples were also determined in dimethylformaamide (DMF) GPC columns and their molecular weights are listed in table-2. The comparison of the molecular weights indicated that the molecular weights obtained by DMF columns were much higher (up to $M_w = 62,000$) than those obtained by tetrahydrofuran solvent. The molecular weight of polymer in DMF was higher compared to THF due to the hydrogen bonding interaction of urethane functional group in the polymer chain. In THF solvent, the hydrogen bonding interaction can exist whereas in DMF, the hydrogen bonding was partially broken. Hence the polymer different conformation in THF solvent and DMF and their hydrodynamic volumes vary significantly. As a result, the THF column obtained low

molecular weights compared to DMF. However, some of the polymers were only partially soluble in DMF which restricted their molecular weight determination. Nevertheless, the GPC-technique confirmed that the new dual ester-urethane methodology developed in the present investigation is very robust in producing high molecular weight polymers based on amino acid monomers.The comparison of molecular weights in the table indicated that oligoethylene diols produced relatively low molecular weight polymer chains compared to that of the linear aliphatic (1,12-dodecandiol) and cycloaliphatic diols (CHDM). Among the amino acid monomers, phenylalanine produced very high molecular weight polymers with fibrous products compared to that of other counterparts.

Table 2.*Molecular weight of the polymers was characterized by GPC analysis using DMF solvent.*

Monomer	Diol	M_n (g/mol) in THF	M_w (g/mol) in THF	M_n (g/mol) in DMF	M_w (g/mol) in DMF
Glycine	DEG	4600	6700	Partially Soluble	
	TREG	4900	8800	Partially Soluble	
	TEG	5200	8600	19600	22700
	CHDM	9300	10400	Partially Soluble	
	DD	5500	14100	24300	30800
L-Alanine	TEG	4800	7300	19300	23900
	CHDM	3400	7200	20200	23700
	DD	8600	14200	25100	30900
β-Alanine	TEG	6100	10900	27100	45600
	CHDM	8600	15300	31700	44000
	DD	5600	11000	22300	27400
L-Valine	TEG	4400	6700	Partially Soluble	
	CHDM	5600	11000	24200	32400
	DD	8400	11000	13000	15400
L-Leucine	TEG	5900	9800	25200	30600
	CHDM	5900	11900	30200	37000
	DD	13300	17000	Partially Soluble	
L-Phenyl -alanine	TEG	7000	14000	28900	38600
	DD	17900	32700	45600	62000

Glycine monomer with 1, 12-dodecandiol polymerization was carried out and aliquots were collected at various intervals to check the thermal stability and chain growing ability of the developed dual ester-urethane process. The TGA profiles (in figure 2.7a) of the aliquots showed continuous enhancement of the thermal stability of the polymers with formation of higher molecular weight chains from 180 to 280 °C.

The GPC chromatograms (in figure 2.7b) of the aliquots also showed enhancement in the molecular weight and the polymer samples shifted from multi-model distribution to mono-model distribution due to the formation of high molecular weight chain length.
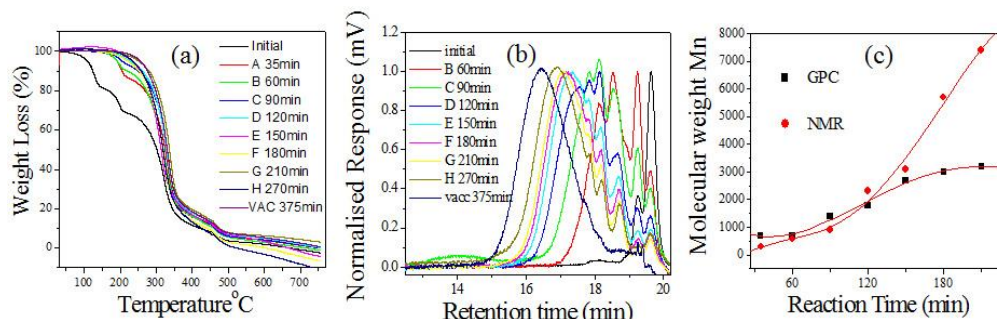
Figure 2.7. *TGA profiles (a) and GPC chromatograms (b) of glycine monomer and 1,12-dodecandiol polymerization aliquots. The M_n determined by NMR and GPC technique were plotted for aliquots at various reaction times (c).*

The number average molecular weights (M_n) of the aliquots were determined by comparing the intensities of repeating unit peaks with end groups in the ^{1}H-NMR spectra. From the expression, $M_n = x_n M_o$, where M_o is the repeating unit mass, the number average molecular weight (M_n) of polymer chains in the aliquots were estimated based on NMR. The molecular weight (M_n) obtained from GPC and NMR techniques was plotted against the reaction time and shown in figure 2.7c. The molecular weight of the polymers linearly increased with time up to $M_n = 3000$ amu and showed sudden increase at larger reaction time (especially in the NMR data). The increase in the molecular weight at higher conversion was attributed to the rapid increase in the melt viscosity of the polymerization during the condensation process. The M_n based on NMR was much higher than that obtained from GPC in the higher molecular weight range. This suggested that the polystyrene standard used for the calibration of GPC column could be under-estimating the actual molecular weights of the polymers at higher conversion. Therefore, the molecular weight of the synthesized polymers could be much higher than that summarized in the table 1 based on GPC. Thus, the above studies confirmed that the newly developed dual ester-urethane process is thermally stable and is a very efficient synthetic methodology for amino acid polymers under solvent free melt conditions.

2.3.5. End Group Analysis by MALDI-TOF-MS

MALDI-TOF MS techniques is a very powerful tool for studying the polymerization reaction via end group analysis. In a typical A-A and B-B type of melt polycondensation reaction, four different types of end groups are possible: (i) chain with AA-ends, (ii) chain with BB-ends, (iii) chain with AB ends and (iv) macrocycles having the mass of repeating units (in figure 2.8a).[22]
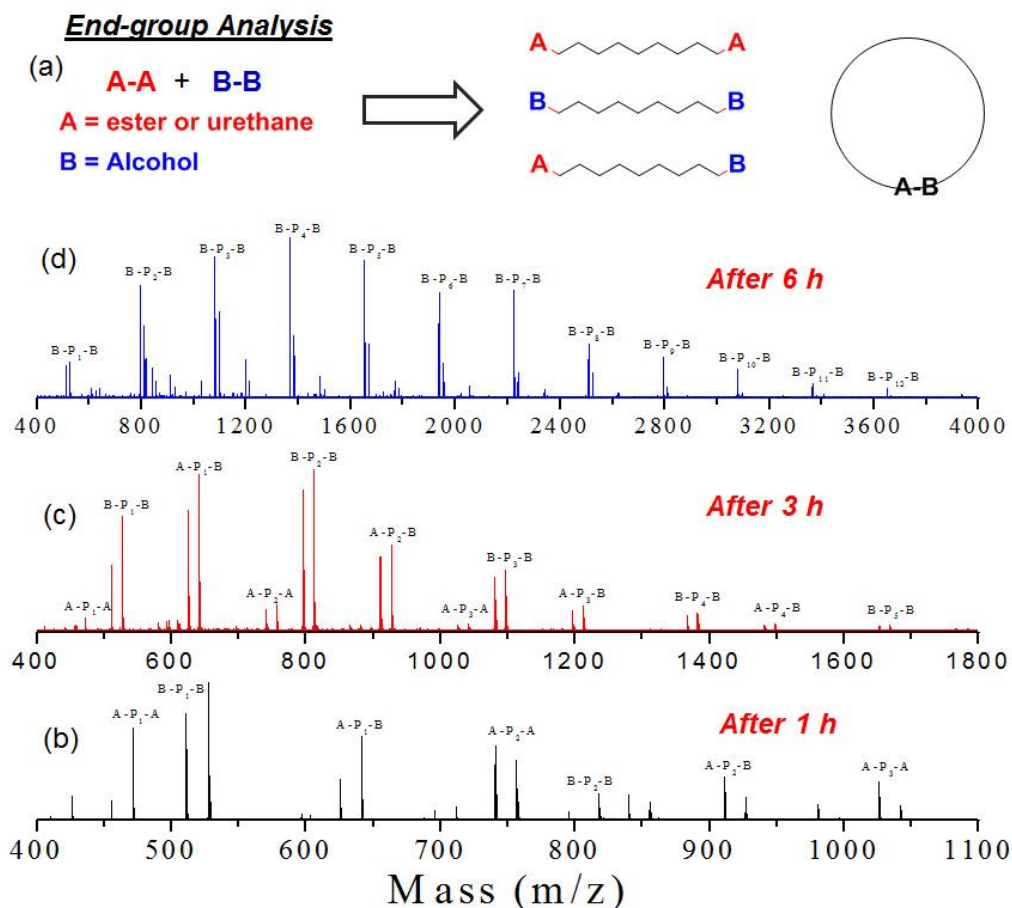
Figure 2.8. *Schematic representation of possible end group formation in A-A + B-B type condensation (a) and MALDI-TOF Mass spectra of glycine monomer and 1,12-dodecanol polymer at 1h (b), end of nitrogen purge at 4h (c) and at the vacuum stage at 6h (d).*

In order to trace the functional groups in the chain ends, aliquots were collected at various intervals in the polymerization of glycine monomer and 1, 12-dodecanediol and they were subjected to MALDI-TOF MS analysis. MALDI-TOF MS spectra of the aliquots corresponding to nitrogen purge stage (1 h and end of the N$_2$ purge stage) and vaccum stage are shown in figure 2.8b-d. Mass values corresponding to the polymer chain with end groups: A-(P)$_n$-A, B-(P)$_n$-B and A-(P)$_n$-

B and cyclic $(P)_n$ were theoretically calculated for n = 1-10 and the values are given in table-3. After 1h reaction time (in figure 2.8b), the samples showed mass peaks in the range of m/z = 300 to 1100 amu with respect to the formation of oligomer species. The peaks were assigned (Na^+ and K^+ ions) to the chain-AA, chain-BB and chain-AB end groups (for values, in table-3). At the end of the nitrogen purge stage (in figure 2.8 c), the chain length increased up to 5 repeating units. Subsequent condensation under vacuum increased the molecular weight of the polymers and chain length with repeating units up to 12 were clearly visible in figure 2.8 d.

Table 3.*The values for various types of end groups in the polymerization of glycine monomer with 1,12-dodecandiol.*

n	P_n-AA 147+(285)n	P_n-BB 202+(285)n	AA-P_n-BB 317+(285)n	P_n
1	455	510	625	308
2	740	795	910	593
3	1025	1080	1195	878
4	1310	1365	1480	1163
5	1595	1650	1765	1448
6	1880	1935	2050	1733
7	2165	2220	2335	2018
8	2450	2505	2620	2303
9	2735	2790	2905	2588
10	3020	3075	3190	2873
11	3305	3360	3475	3158
12	3590	3645	3760	3443

Few observations from the MALDI-TOF MS analysis were: (i) the ester and urethane functional groups of the amino acid monomers were stable under high temperature melt polymerization process, (ii) the molecular weight of the polymers increased with increase in the reaction time, (iii) all three possible chain ends like AA, BB and AB were involved in the condensation route and (iv) there is no macrocycle formation in the dual ester-urethane polycondensation process. The absence of macrocycle formation in the present melt condensation approach is a very crucial point. This is because polycondensation chemistry for other naturally occurring monomers like lactic acid[23] or NCA mediated route for amino acids were known to form macrocycles which hampered their high molecular weight formation. Interestingly, the amino acid monomers underwent linear chain formation rather than cyclization in the dual ester-urethane process which is very crucial for high molecular weight formation. Thus, it could be concluded that the amino acid functional groups

(urethane and ester groups) were thermally stable in the newly developed dual ester-urethane melt polymerization and produced high molecular weight polymers.

2.3.6. Temperature Dependent Reactivity and Kinetics

To study the mechanism and the role of the melt temperature on the dual ester-urethane process, model reactions were carried as shown in figure 2.9. Typically, temperature and catalyst are the two important parameters that drove the polycondensation synthetic process.
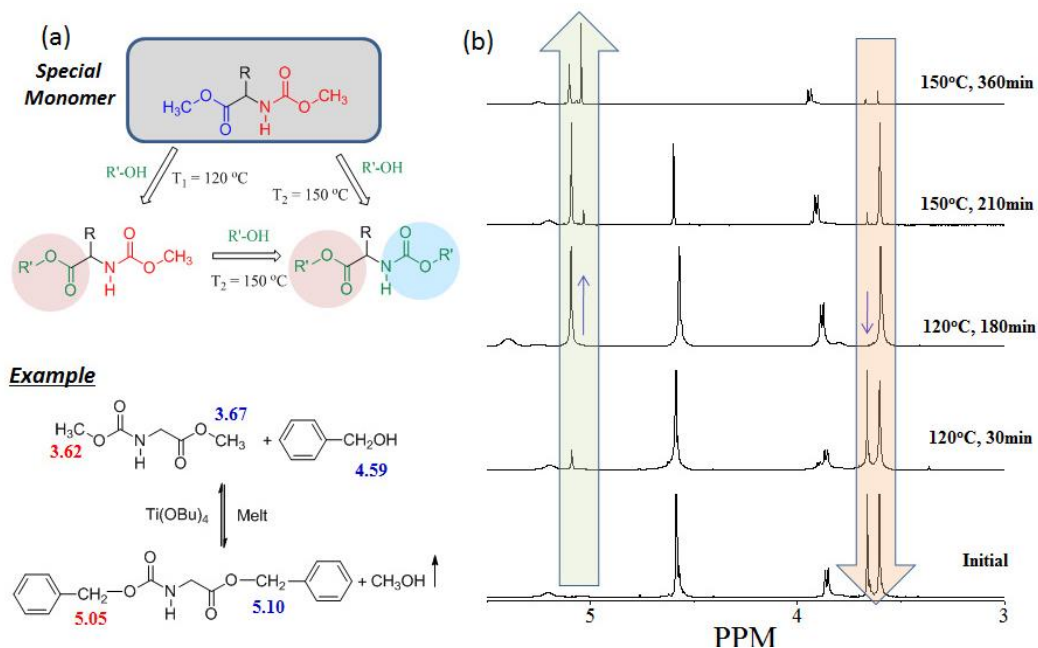
Figure 2.9. *Model Reaction of benzyl alcohol with glycine monomer at 120 and 150 °C. ¹H-NMR spectra of the aliquots are given for various time intervals.*

The thermogravimetric analysis of the amino acid monomers showed that the ester and urethane linkages were thermally stable only up to 150-180 °C depending upon their structures (in figure 2.14a). Therefore, the melt reaction was performed at 80°, 100°, 120° and 150 °C and it was found that both ester and urethane units in the amino acid monomer were only active above 120 °C. Based on these finding, two temperatures were chosen for the model reaction at 120° and 150 °C. Benzylalcohol was selected as suitable alcohol for the condensation because it provided possibility for identification and quantification of ester and urethane products in the dual ester-urethane reaction by NMR. Glycine monomer was condensed with twice the amount of benzyl alcohol and the following classification was adopted: (i) stepwise increase of the temperature at 120° and 150 °C in the presence of catalyst, (ii) stepwise increase of the temperature at 120° and 150 °C in the absence of catalyst and (iii)

direct condensation at 150 °C in the presence of catalyst. Aliquots were taken at regular interval and they were subjected to ^{1}H-NMR analysis to quantify the un-reacted monomers and products. ^{1}H-NMR spectra of the aliquots for the model reaction (i) are shown in figure 2.9 [for model reactions (ii) and (iii), in 2.10 a and 2.10 b].
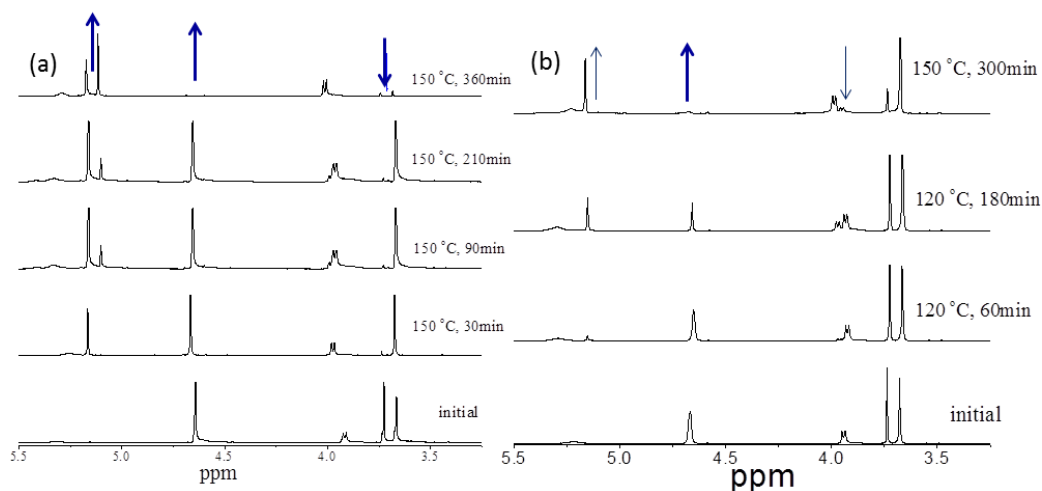
Figure 2.10. *^{1}HNMR spectra model reaction of glycine monomer with benzyl alcohol in absence of catalyst (a) and in presence of catalyst direct at 150 °C (b).*

In the initial mixture, peaks corresponding to the protons $C_6H_5CH_2OH$, gly-CH_2COOCH_3 (ester) and gly-$HNCOOCH_3$(urethane) appeared at 4.59 ppm, 3.67 ppm and 3.62 ppm, respectively (the chemical shift region above 5.5 not shown for simplicity). At 120 °C, only the carboxylic ester of the amino acid monomer underwent reaction with benzyl alcohol; as a result the protons corresponding to ester part (at 3.67 ppm) disappeared and new peak with respect to protons in the product $PhCH_2OOCCH_2$-gly appeared at 5.10 ppm. During this ester-exchange process, the urethane part in the amino acid monomer was completely inert. Upon subsequent increase in the reaction temperature to 150 °C, the urethane functionality in the monomer became active and underwent reaction with benzyl alcohol to produce new urethane linkage $PhCH_2OOCNH$-gly. The disappearance of protons at 3.62 ppm of gly-$HNCOOCH_3$ and appearance of new peak at 5.05 ppm confirmed the formation of $PhCH_2OOCNHCH_2$-gly. Thus, it is clearly evident that the ester and urethane reactivity could be easily varied by adjusting the appropriate condensation temperature in the present dual ester-urethane process. The extent of the ester or urethane exchange reaction at particular temperature (either at 120° and 150° C) over a period of reaction time was determined by comparing relative peak intensities in the

gly- monomer at 3.67 ppm or 3.62 ppm. The extent of the reaction (or percent conversion) of the monomer was plotted against the reaction time in figure 2.11. In the presence of catalyst (in figure 2.11 a), at 120 °C, the ester-exchange reaction occurred more than 98 % within 90 minutes. Upon increasing the temperature of the same vessel to 150° C (180 minutes was corresponding to the initial time for the reaction at 150° C), the urethane unit became active and gave 98 % conversion at the end of reaction. In the absence of catalyst, the ester part of the amino acid monomer underwent slow exchange with benzyl alcohol to produce 80 % of product at the end of the reaction (in figure 2.11b). However, the urethane unit was completely inert in the absence of catalyst throughout the reaction. Direct polycondensation at 150 °C (in figure 2.11c), in the presence of catalyst both ester and urethane exchange reaction occurred simultaneously. The ester exchange was very rapid (95 % within 30 minutes) compared to the urethane exchange reaction which occurred over a period of 360 minutes.
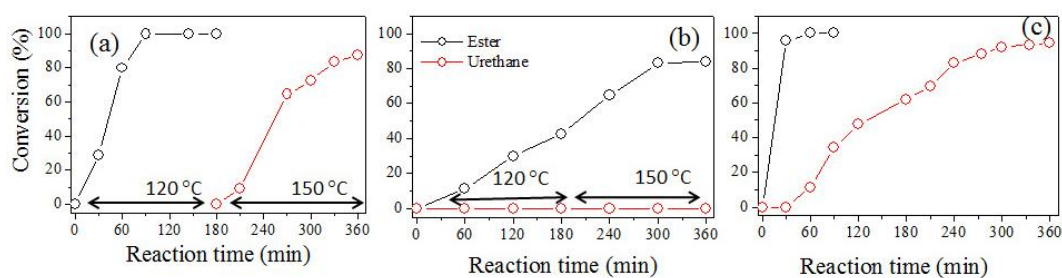
Figure 2.11.*Plots of percent conversion versus reaction time in the presence Ti -catalyst (a) and in absence of catalyst (b) at stepwise 120° to 150 °C reaction, and direct condensation at 150 °C in the presence of Ti -catalyst (c).*

These percent conversion data indirectly reflected on the composition and the amount of un-reacted monomer at any given time. Therefore, these data could be directly utilized for determination of kinetic rate constant for the condensation process. The data were fitted in the first order ester exchange reaction using the logarithmic equation: ln {[A]/[A$_o$]}=-kt, where [A] is the concentration of un-reacted monomer at time 't', [A$_o$] is the initial concentration of the monomer and 'k' is the rate constant. The plots of ln {[A]/[A$_o$]} versus 't' for all model reactions were given in figure 2.12a. The rate constant for the model reaction were obtained from the slope of the plots and the values are summarized in table 2.12b. At 120 °C, the rate constant for ester-exchange reaction was obtained as $2.7 \times 10^{-2} \text{min}^{-1}$ which is in accordance with

the values from literature.[24] In the absence of the Ti-catalyst, the ester-exchange process was one order magnitude lower. The rate constants for the urethane-exchange reaction were obtained as of 0.9 - $1.2 \times 10^{-2} min^{-1}$ which was almost half compared to its ester counterpart. The comparison of the rate constant values revealed that the ester exchange process was almost twice as fast as the urethane-exchange in the dual ester-urethane process of amino acid based monomers. The rate constant for the polymerization reaction was also determined using the aliquots data of glycine monomer with 1,12-dodecandiol at 150 °C (in figure 2.12b).

(b) Reaction Conditions	k (min^{-1})
Ester, 120°C, No catalyst	4.01×10^{-3}
Ester, 120 °C, Ti-catalyst	2.72×10^{-2}
Urethane, 150 °C, No-catalyst	No reaction
Urethane, step-150 °C, Ti-catalyst	1.24×10^{-2}
Urethane, Direct 150 °C, Ti-catalyst	9.30×10^{-3}
Polymer, Direct 150 °C, Ti-catalyst	1.43×10^{-2}
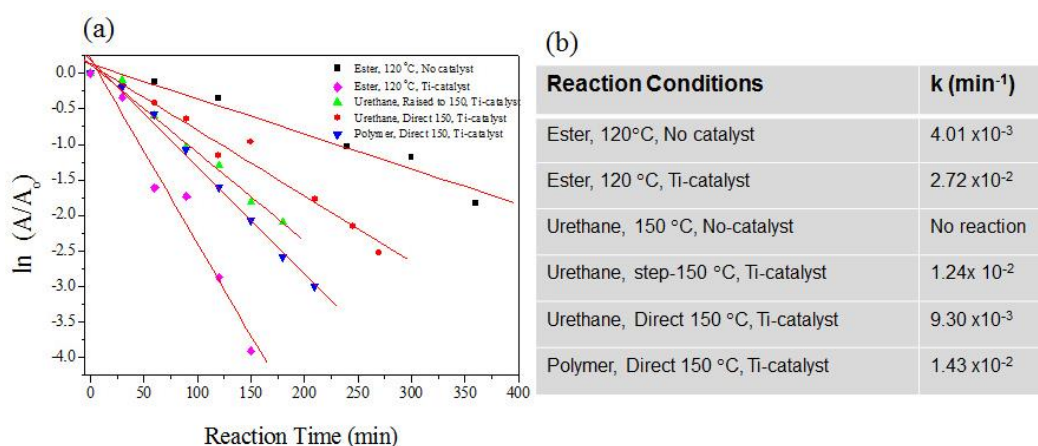
Figure 2.12. *First order kinetic plots versus reaction time (a) and the rate constant (k) were determined from the slopes of linear fitting and the values are summarized in the table (b).*

Based on the procedure explained for model reactions, the rate constant for the polycondensation was obtained as $1.4 \times 10^{-2} min^{-1}$ (in plot in figure 2.12b). The rate constants for the polymerization was almost comparable to that of model reaction, hence, it may be concluded that both model reaction and polycondensation followed similar kinetics in dual ester-urethane process. The above model reactions revealed that the amino acid monomers were very special for the condensation polymerisation. Unlike the ester units, the urethane linkage is very selective to the temperature of the reaction (at 150 °C) and also need Ti-catalyst for the exchange reaction to occur. Hence, using appropriate reaction conditions, one could easily fine tune the dual ester-exchange process for making bis- or tri-urethane small molecules as well as block copolymers based on naturally available amino acid as starting materials. Currently the dual ester-urethane synthetic methodology is continued in these directions.

2.3.7. Secondary Structures of Amino acid polymers

The newly synthesized polymers were derived from repeating units of L-amino acid monomers, and therefore, circular dichroism (CD) spectroscopic analysis was carried out for the polymers to investigate their ability to form secondary structures. Generally, CD measurements are based on the difference in the absorbance between right and left circularly polarized light of optically active molecules. In the present case, the ester-urethane chemical linkage of the chains absorbed in the far-UV region with three electronic transitions: (i) n-π^* transition at~ 220 nm polarized along the carbonyl bond, (ii) π-π^* transition at 185-200 nm polarized in the direction of the C-N bond, and (iii) π-π^* transition at 140 nm polarized approximately perpendicular to the C-N bond direction.[25] Typically, peptides show a positive band at 192 nm and two negative bands at 208 and 222 nm for α-helical conformation and the β-sheet structure exhibit a positive CD band at 195-198 nm and a negative CD band at 218 nm.[26a] Random coil structures are expected to show single negative CD band at 195 nm.[26a]
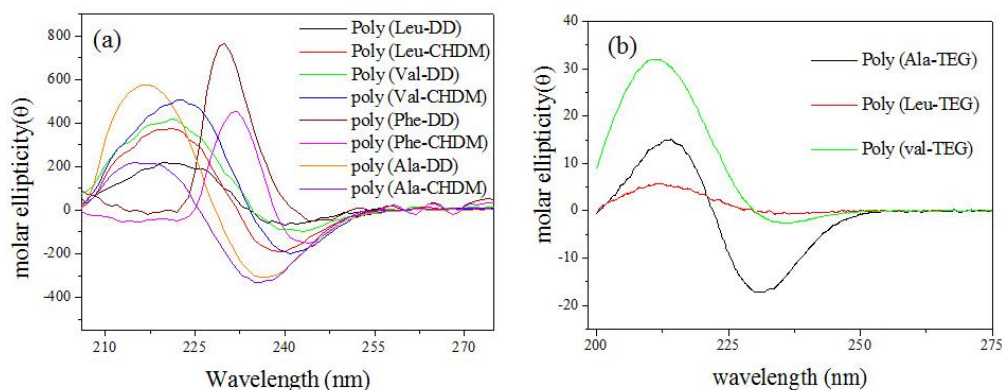
Figure 2.13. *CD spectra of polymers in tetrahydrofuran (a) and in water (b) at 25 °C.*

Among the amino acid monomers chosen for the present investigation, the monomers L-alanine, L-valine, L-leucine and L-phenylalanine are optically active, and therefore, their polymers can be expected to have tendency to form self-assembled secondary structures like those observed in peptides and proteins. Polymers belonging to these amino acid monomers were subjected to CD studies in tetrahydrofuran, water, and methanol depending upon their solubility. CD spectra of representative polymers in THF and water are shown in figure 2.13. In THF all the polymers (except phenylalanine), showed one positive CD band at 210 - 215 nm for π-π^* and a negative CD band around 230 nm for n-π^* transition corresponding to the secondary structure in β-sheet conformation.[26a] The water soluble polymers also

showed CD bands as observed in THF solvent, which confirmed that the β-sheet secondary structure was retained even in the aqueous medium. Phenylalanine based polymers showed positive CD band at 230 nm which was attributed to the aromatic side chains and their spectral features resembled the polyproline type II helical coil conformation.[26b] The above results confirmed that the newly synthesized amino acid poly(ester-urethanes) are very efficient in forming secondary structures similar to that of polypeptides. Hence, these polymers can be very useful for applications in biological systems.
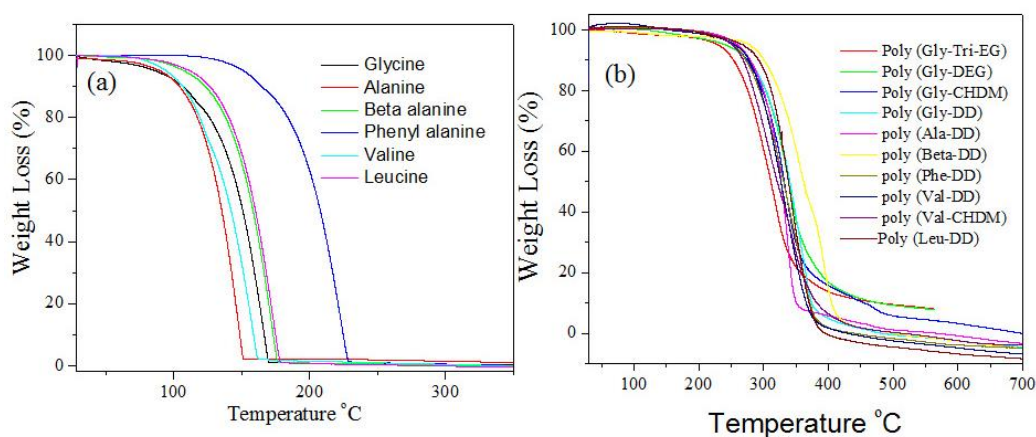
Figure 2.14. *TGA analysis of amino acid based monomer (a) and poly (ester-urethanes) at 10 ℃/min heating rates.*

2.3.8. Thermal Properties of Amino acid Polymers

TGA analysis of the polymers revealed that these newly synthesized polymers were thermally stable up to 280-300 °C (in figure 2.14b). The thermal properties of the newly synthesized polymers were analyzed by DSC and few representative thermograms are shown in figure 2.15. Most of the poly (ester-urethanes) were sluggish to crystallization and showed only glass transition temperatures (T_g) (in table-1). Interestingly, polymers of 1,12-DD with glycine, alanine and β-alanine showed clear melting and crystallization peaks under the heating/cooling cycles (in figure 2.15b). The role of the crystallinity on the polymer structure is one of the futuristic researches in the group and it will be investigated separately. The present thesis is primarily emphasized to demonstrate the new synthetic pathway for L-amino acid polymers. Their transition temperatures and enthalpy values are given in the table-4. The crystalline nature was attributed to the less steric hindrance provided by these amino acid units in the polymer backbone. The enthalpy of crystallization values for glycine, alanine and beta alanine with 1,12-dodecanediol polymers shows

the following trend gly> beta >ala; It indicated that packing of glycine based polymer chain is more compared to other two polymers. Since the enthalpy of alanine based polymer is less compared to the other two polymers, it may be attributed to misalignment of α-substitution methyl group in polymer chain packing.

Table 4. Enthalpies of melting and crystallization of poly (ester-urethanes)

Sample	T_m (^oC)	ΔH_m (kJ/mol)	T_c (^oC)	ΔH_c (kJ/mol)
Poly (Gly-DD)	90.11	17.09	70.58	18.96
Poly (Ala-DD)	76.42	15.95	10.91	7.65
Poly (β-ala-DD)	73.72	13.51	52.94	14.73
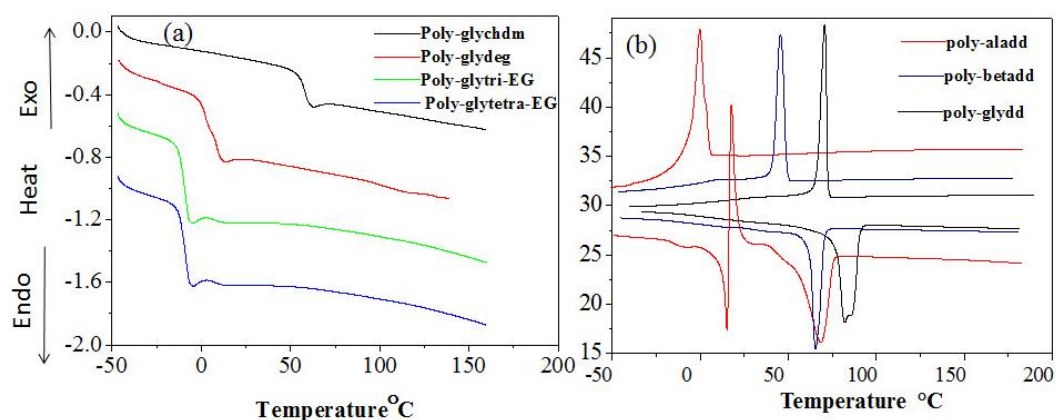
Figure 2.15. *DSC thermograms of the amorphous (a) and semi-crystalline (b) polymers at 10 °C/min heating/cooling rate.*

Glycine based polymer with PEGs showed decrease in T_g with increase in the length of the ethylene oxide units (in figure 2.15a). The polymers synthesized from phenylalanine were found to have maximum T_g values which is attributed to the high rigidity contributed by the amino acid repeating units. The thermal analysis suggested that by choosing appropriate amino acid based monomers and diols, the thermal properties of the poly (ester-urethane)s could be easily fine-tuned for various thermoplastic applications.

2.4. Conclusion

A dual ester-urethane condensation approach was successfully developed for biological monomers-amino acids to make new classes of thermoplastic polymers under solvent free polymerization methodology. L-aminoacids were converted into

their corresponding ester-urethane monomers by simple tailor made approach. These monomers were condensed with various commercial diols under melt polycondensation process in one-pot in two stages. In this process, oligomers of 1-4 repeating units were initially obtained under nitrogen purge which upon further polycondensation under reduced vacuum produced high molecular weight polymers. The occurrence of the melt dual ester-urethane process and the structure of the new poly (ester-urethane)s were confirmed by ^{1}H and ^{13}C NMR spectroscopies. The new dual ester-urethane condensation approach was demonstrated for variety of amino acids: glycine, β-alanine, L-alanine, L-leucine, L-phenylalanine and L-valine along with commercial diols: di-, tri- and tetraethylene glycols, 1,12-dodecandiol (linear aliphatic diols) and 1,4-cyclohexanedimethanol (cycloaliphatic diols). The molecular weights of the polymers were obtained in the range of moderate to high values with polydispersity ~ 2.1. The percentage conversion of the new process was found to be more than 97- 98 % with respect to degree of polymerization, X_n = 30-40 units. The end group analysis by MALDI-TOF MS revealed that the amino acid functional groups (urethane and ester groups) were thermally stable in the dual ester-urethane melt polymerization process and produced high molecular weight polymers. The mechanism of melt dual ester-urethane process and the kinetics of the polycondensation were studied by model reactions using benzyl alcohol. It was found that the amino acid monomer was very special in the sense that the selective reactivity of ester and urethane could be tuned either by the catalyst or the polymerization temperature. The presence of Ti-Catalyst and 150 °C are essential for the urethane-exchange reaction whereas the ester-exchange could occur at much lower temperatures of 120 °C. The rate constant values revealed that the ester exchange process was almost twice as fast as the urethane-exchange in the amino acid based monomers. The thermal properties of the newly synthesized polymers obtained using 1, 12-dodecandiol along with glycine, alanine and β-alanine were found to be semi-crystalline solid and showed melting and crystallization peaks. CD analysis of the synthesized polymers confirmed that these new poly(ester-urethane)s were efficient structures to produce self-organized β-sheets like polypeptides in water or organic solvents. In a nut shell, the new dual ester-urethane process is very robust in producing thermally stable, high molecular weight β-sheet structure from poly(ester-urethanes) obtained largely abundant from natural abundant biological monomer

amino acids. Further, the temperature selective reactivity of the current process could in potential be exploited for making tailor made block copolymers and oligomers in amino acid chemistry. Thus, the new melt condensation approach will open up new platform of research activates based on amino acids in synthetic polymer chemistry.

2.5. References:

1. Whinfield, J. R. *Nature* **1946**, *158*, 930.
2. (a) Jayakannan, M.; Ramakrishnan, S. *Chem. Commun.* **2000**, *19*, 1967-1968. (b) Jayakannan, M.; Ramakrishnan, S. *Macromol. Chem. Phys.* **2000**, *201*, 759-767. (c) Jayakannan, M.; Ramakrishnan, S. *Macromol. Rapid Commun.* **2001**, *22*, 1463-1473. (d) Behera, G. C.; Ramakrishnan, S. *Macromolecules* **2004**, *37*, 9814-9820. (e) Roy, R. K.; Ramakrishnan, S. *Macromolecules* **2011**, *44*, 8398-8406.
3. (a) Deepa, P.; Jayakannan, M. *USPTO* 2007/0117950 A1, **2007.** (b) Deepa, P.; Jayakannan, M. *J. Polym. Sci. Polym. Chem.* **2008,** *46,* 2445-2458. (c) Deepa, P.; Jayakannan, M. *J. Polym. Sci. Polym. Chem.* **2007,** *45,* 2351-2366.
4. Dennis, J. M.; Enokida, J. S.; Long, T. E.*Macromolecules* **2015**, *48*, 8733-8737.
5. Liu, Y.; Turner, S. R.; Wilkes, G. *Macromolecules* **2011**, *44*, 4049-4056.
6. Lu, R.; Lu, F.; Chen, J.; Yu, W.; Huang, Q.; Zhang, J.; Xu, J. *Angew. Chem. Int. Ed.* **2016**, *55*, 249-253.
7. Zhu, J.; Cai, J.; Xie, W.; Chen, P-H.; Gazzano, M.; Scandola, M.; Gross, R. A. *Macromolecules* **2013**, *46*, 796-804
8. Gubbels, E.; Jasinska-Walc, L.; Koning, C. E. *J. Polym. Sci. Polym. Chem.* **2013,** *51,* 890-898.
9. Wu, J.; Eduard, P.; Jasinska-Walc, L.; Rozanski, A.; Noordover, B. A. J. Van Es, E. S.; Koning, C. E. *Macromolecules* **2013**, *46*, 384-394.
10. Lavilla, C.; Ilarduya, M. D.; Alla, A.; Garcia-Martin, M. G.; Galbis, J. A.; Munoz-Guerra, S. *Macromolecules* **2012**, *45*, 8257-8266.
11. Lavilla, C.; Alla, A.; Ilarduya, M. D.; Benito, E.; Garcia-Martin, M. G.; Galbis, J. A.; Munoz-Guerra, S. *Biomacromolecules* **2011**, *12*, 2642-2652.
12. Deming, T. J. *Adv. Mater.* **1997**, *9*, 299 – 311.
13. Yu, M.; Nowak, A. P.; Deming, T. J. *J. Am. Chem. Soc.* **1999**, *121*, 12210 – 12211.
14. Katz, J. S.; Zhong, S.; Ricart, B. G.; Pochan, D. J.; Hammer, D. A.; Burdick, J. A. *J. Am. Chem. Soc.* **2010**, *132*, 3654-3655.
15. Uhrich, K. E.; Cannizzaro, S. M.; Langer, R. S.; Shakesheff, K. M. *Chem. Rev.* **1999**, *99*, 3181-3198.
16. Wadhvani, P.; Afonin, S.; Leronimo, M. ; Buerck, J.; Ulrich, A. S. *J. Org. Chem.* **2006,** *71,* 55-61.
17. Sun, H.; Meng, F.; Dias, A. A.; Hendriks, M.; Feijen, J.; Zhong, Z. *Biomacromolecules,* **2011**, *12*, 1937-1955.

18. (a) Guo, K.; Chu, C. C. *Biomacromolecules,* **2007**, *8*, 2851-2861. (b) Guo, K.; Chu, C. C. *J. Polym. Sci. Polym. Chem.* **2007**, *45*, 1595-1606. (c) Deng, M.; Wu, J.; Reinhart-King, C. A.; Chu, C. C. *Biomacromolecules,* **2009**, *10*, 3037-3047. (d) De Wit, M. A.; Wang, Z.; Atkins, K. M.; Mequanint, K.; Gillies, E. R. *J. Polym. Sci. Polym. Chem.* **2008**, *46*, 6376-6392.

19. (a) Paredes, N.; Rodriguez-Galan, A.; Puiggali, J. *J. Polym. Sci. Polym. Chem.* **1998**, *36*, 1271-1282. (b) Asin, L.; Armelin, E.; Montane, J.; Rodriguez-Galan, A.; Puiggali, J. *J. Polym. Sci. Polym. Chem.* **2001**, *39*, 4283-4293.

20. (a) Kricheldorf, H. R. *Angew. Chem. Int. Ed.* **2006**, *45*, 5752-5784. (b) Zhong, B.; Fischer, K.; Schmidt, M. *Macromol. Chem. Phys.* **2005**, *206,* 157-162. (c) Inoue, K.; Sakai, H.; Ochi, S.; Itaya, T.; Tanigaki, T. *J. Am. Chem. Soc.* **1994**, *116,* 10783-10784.

21. Odian, G. *Principles of Polymerization*; John Wiley & Sons. Inc.: New York, **1991**; Third Ed.,Chapter 2, p. 53.

22. Jayakannan, M.; van Dongen, J. L. J.; Janssen, R. A. J. *Macromolecules* **2001**, *34*, 5386-5393

23. Chmura, A. J.; Chuck, C. J.; Davidson, M. G.; Jones, M. D.; Lunn, M. D.; Bull, S. D.; Mahon, M. F.*Angew. Chem. Int. Ed.* **2007**, *46*, 2280-2283.

24. (a) Collins, S.; Kenwright, A. M.; Pawson, C.; Peace, S. K.; Richards, R. W.; MacDonald, W. A.; Mills, P. *Macromolecules* **2000**, *33*, 2974-2980. (b) Yang, H.; He, J.; Liang, B. *J. Polym. Sci. Polym. Phys.* **2001**, *39*, 2607-2614.

25. Violette, A.; Averlant-Petit, M. C.; Semetey, V.; Hemmerlin, C.; Casimir, R.; Graft, R.; Marraud, M. ; Braiand, J. P.; Rongnan, D. ; Guichard, G. *J. Am. Chem. Soc.* **2005**, *127,* 2156-2164.

26. (a) Greenfield, N.; Davidson, B.; Fasman, G. D. *Biochemistry* **1967**, *6*, 1630-1637. (b) Shi, Z.; Olson, C. A.; Rose, G. D.; Baldwin, R. L.; Kallenbach, N. R. *Proc. Natl. Acad. Sci. U.S.A.* **2002**, *99*, 9190.

Chapter 3

Catalysts and Temperature Selective Melt Polycondensation Reaction for Small molecule derivatives and Helical Poly(ester-urethane)

Chapter 3

Catalysts and Temperature Selective Melt Polycondensation Reaction for Small molecule derivatives and Helical Poly(ester-urethane)

Catalyst and temperature selective melt polycondensation reaction was developed for natural L-amino acid monomers to produce new classes of poly(ester-urethane)s. Wide ranges of catalysts from alkali, alkali earth metal, transition metal and lanthanides were developed for the condensation of amino acid monomers with diols to yield poly(ester-urethane)s. A-B diblock and A-B-A triblock species were obtained by carefully choosing mono- or diols in the model reactions. More than two dozens of transition metal and lanthanide catalysts were identified for the polycondensation to yield high molecular weight poly(ester-urethane)s. Theoretical studies revealed that the carbonyl carbon in ester possessed low electron density compared to the carbonyl carbon in urethane which drives the thermo-selective polymerization process. Optical purity of the L-amino acid residues in the melt polycondensation process was investigated using D- and L-isomer and the resultant products were analyzed by chiral-HPLC and CD spectroscopy. CD analysis revealed that the amino acid based polymers self-assembled as β-sheet and polyproline type II secondary structures. Electron and atomic force microscopic analysis confirmed the formation of helical nano-fibrous morphology in poly(ester-urethane)s. The newly developed melt polycondensation process is very efficient and optimized for wide range of catalysts to produce diverse polymer structures from natural L-amino acids.

3.1. Introduction

Catalyst driven polycondensation reactions are important synthetic methodologies for large scale manufacturing of thermoplastic engineering materials such as polyesters, polyamides, polycarbonates and polyurethanes for commercial applications.[1,2] Among these polymers, polyesters are particularly interesting due to their diversity in chemical structures and their excellent mechanical stability and chemical resistance.[3] The polyesters based on aromatic dicarboxylic acids (or esters) and aliphatic diols are one of the widely used commercial polymers owing to their excellent semi-crystalline properties that allow for processing them into consumer plastic products.[4] Wide range of transition metal catalysts and non-metal oxides were employed for the transesterification (or direct esterification) and polycondensation reactions[5-6] in the synthesis of polyesters such as poly(ethyleneterephthalate) (PET)[7-8] and poly (butyleneterephthalate) (PBT)[9] in few million tons/year.
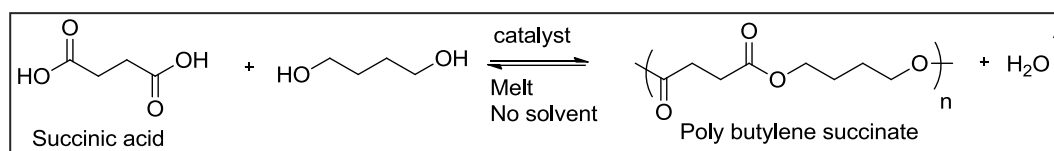
Scheme 3.1. *Poly butylene succinate synthesized from succinic acid by various metal catalysts*

Buzin et al. developed the catalyst trace for polyesters based on aliphatic diacids and 1,4-butanediol or 1,6-hexanediol (in scheme 3.1);[10] in this process, the polycondensation reactions are carried out at 80-100 °C using various triflate catalyst: sodium, bismuth, magnesium, aluminum, zinc, tin(II), scandium, and hafnium. Among the triflate catalyst bismuth delivered high molecular weight aliphatic polyester compared to other catalysts. Recently, Moyori et al. prepared aliphatic and aromatic polyester at <100 °C using bis (nonafluorobutanesulfonyl)imide as catalyst via melt polycondensation approach.[11] The benefit of this approach is that catalyst sublimes to the top of the tube once the polymerisation process is complete and the sublimed catalyst can be reused for new polymerisation reaction without any loss of catalytic reactivity. Although the polycondensation reactions can be done at low temperature (<100 °C), it requires longer time to deliver moderate molecular weight polymers.

Kricheldorf et al. prepared poly (butylene terephthalate)s using dimethyl terephalate and 1,4-butanediol under solvent free melt polycondensation conditions in presence of various catalyst: Bi_2O_3, $BiCl_3$, Bi-subsalicylate, bismuth(III) acetate, ZnO,

$ZnCl_2$, SnO, $SnCl_2$, Y_2O_3, YCl_3, La_2O_3, $LaCl_3$, Sb_2O_3/manganese (II) acetate, and $Ti(OBu)_4$.[9] Among the catalyst $Ti(OBu)_4$ produced the highest molecular weight polymer compared to other catalysts. Ignatov et al. demonstrated the catalyst trace for poly (ethylene terephthalate) using various lanthanide catalysts (scheme 3.2), the result revealed that the lanthanide catalyst showed high performance for polymerisation process compared to other catalysts.[8]
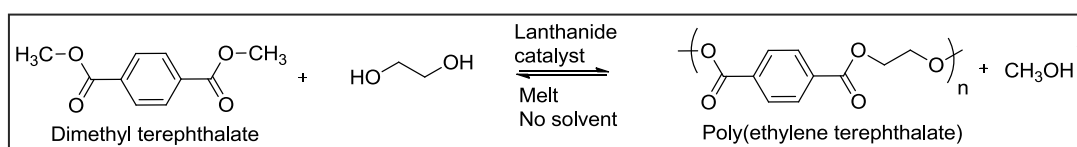
Scheme 3.2. *Poly(ethylene terephthalate) synthesised using lanthanide metal catalyst*

Park et al. synthesised the poly (ethylene 2, 6-napthalate) from dimethyl 2, 6-napthalate and ethylene glycol in presence of different metal catalysts using solvent free melt polycondensation reaction (scheme 3.3).[12] The catalytic activity of metal catalyst in polycondensation reaction are found to be in the decreasing order of Ti(IV) > mixtures of Ti(IV) and Sb(III) > Sn(II) > Sb(III) > Co(II) > Zn(II) > Pb(II) > Mn(II) > Mg(II). The above literature reports showed the importance of catalyst trace for high molecular weight aliphatic and aromatic polyester synthesis. Aliphatic polyesters are biocompatible and enzymatically biodegradable and they are largely used for biomedical applications.[13] Aliphatic polyesters from adipic acid,[14-15] succinic acid,[16-17] sebacic acid[18] and 1,4-cyclohexane dicarboxylic acid are some of the important examples.
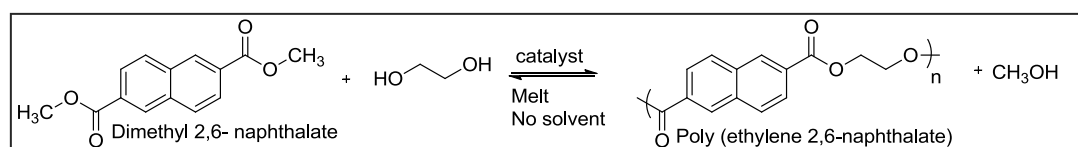
Scheme 3.3. *Poly (ethylene 2,6- naphthalate) synthesized using various metal catalyst via melt polycondensation approach*

Another important aspect of metal catalyst in polycondensation reaction is their mechanistic role in the polymerization process. Shigemoto et al. performed theoretical calculation for transesterification reaction with various metal catalysts (scheme 3.4).[19] Typically transesterification follows three different mechanistic paths 1. Lewis acid mechanism, 2. Coordination of the ester alkoxy oxygen atom

3. Coordination of the carboxyl oxygen atom. The results show that transition metal catalysts follow the four-membered cyclic transition state mechanism, whereas other metal catalysts were observed to follow the Lewis acid mechanism in the transesterification process. Although the detailed mechanistic study for transesterification is known in the literature, there is no report known for mechanism of trans urethane and novel trans (ester-urethane) reaction.
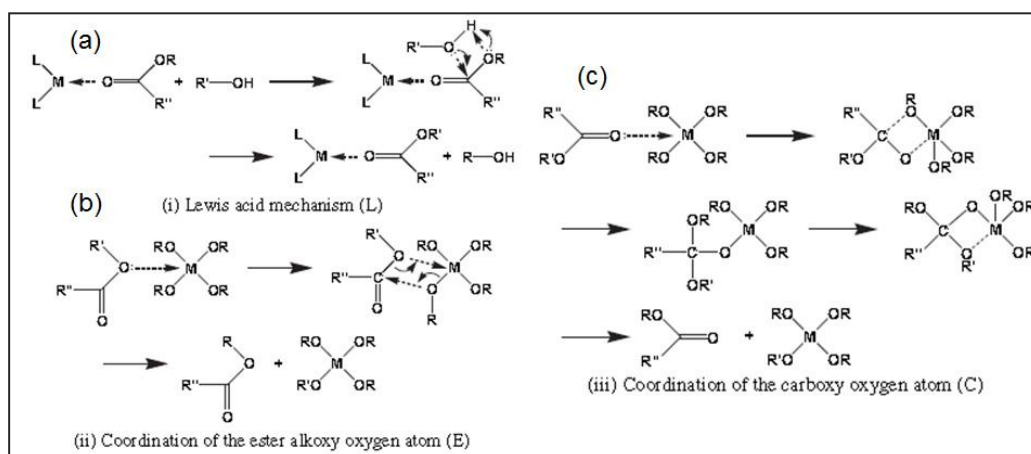
Scheme 3.4. P*roposed mechanism for polyesterification process (a) lewis acid mechanism, (b) coordination of the ester alkoxy oxygen atom and (c) coordination of the carboxy oxygen atom*

In the chapter-2 investigations were largely devoted to making new amino acid polymers by employing Ti(OBu)$_4$ as catalyst (only one catalyst was used). Unfortunately, Ti(OBu)$_4$ is moisture sensitive; thus it is necessary to put effort into exploring wide range of catalysts for the synthesis of amino acid based poly(ester-urethane)s.[20] Further, L-amino acids are important natural resources; hence, optimizing wide range of catalyst types would provide long term impact on the manufacturing of renewable resource thermoplastic materials based on L- amino acid resources under solvent free polycondensation reactions.

In this chapter investigation is emphasised to develop wide range of catalysts for the new dual ester-urethane condensation chemistry in amino acid monomers and study the role of catalysts type and polycondensation temperature in the production of poly(ester-urethane)s. Catalysts from alkali, alkali earth metal, transition metals and lanthanides having halides, nitrates, oxides, acetates and alkoxides were investigated. Model reactions were performed and the resultant products were analysed by NMR spectroscopy to trace the roles of catalysts and polymerization temperature on the

molecular weight of the polymers. The new process was investigated for more than 8 amino acid residues and mono alcohols and diols. Based on these studies, more than 20 catalysts were identified for the condensation reaction to make high molecular weight poly(ester-urethane)s.
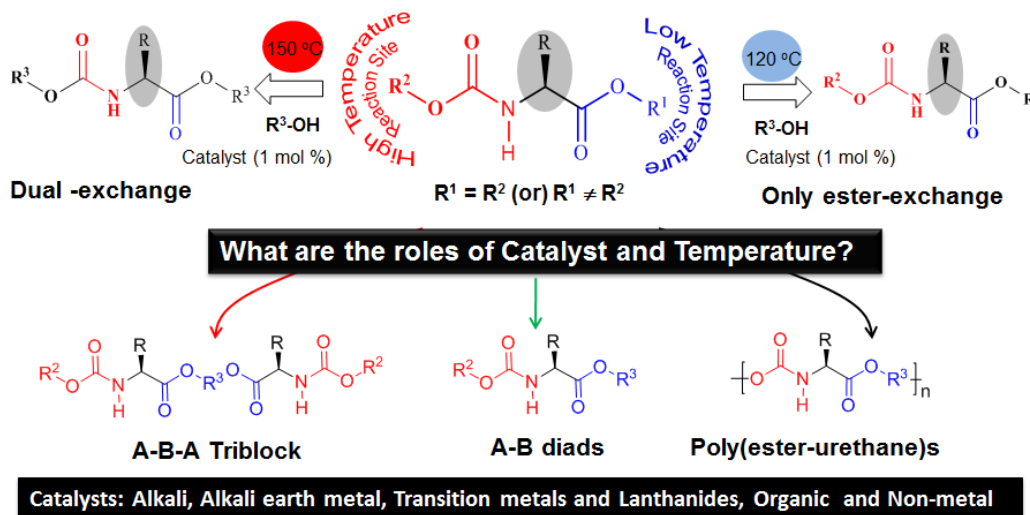
Figure 3.1. *Development of poly (ester-urethane) using various catalyst via melt polycondensation approach*

The polycondensation reaction was further investigated using D- and L-isomers of amino acids to trace the optical purity of the resultant polymers. The resultant products were analysed by chiral-HPLC and circular dichroism spectroscopy to establish their optical purity. Electron and atomic force microscopes showed the formation of highly ordered helical nano-fibrous morphology in the polymers. These helical assemblies were found to remain unaltered by the choice of the catalysts employed in the polymerization. The mechanism of the reaction in amino acid residue was established through energy minimized structures by Gaussian programme. In a nut shell, the present approach opens up new synthetic routes for helical poly (ester-urethane)s based on L-amino acids and also identified wide range of catalysts useful for the production of polymers based on L-amino acid natural resources for long term industrial applications.

3.2. Experimental methods

3.2.1. Materials: Glycine, L-alanine, β-alanine, L-valine, L-leucine, L-phenylalanine, D-alanine, D-valine, D-phenyl alanine, 1,12-dodecandiol, 1,10-decanediol, 1,5-pentanediol, 1,4-cyclohexanedimethanol, 1,4-butanediol, 1-decanol, 1-adamantanethanaol, β-citronellol, diethylene glycol (Di-EG), diethylene glycol monomethyl ether (DEG-OMe), titanium tetrabutoxide Ti(OBu)$_4$ and remaining metal catalyst were purchased from Aldrich chemicals and used without further purification. Methyl and ethyl chloroformate, thionyl chloride, ditert butyl dicarbonate and other solvents were purchased locally and purified prior to use.

3.2.2. General Procedures: ^{1}H and ^{13}C-NMR were recorded using 400-MHz JEOL NMR Spectrophotometer. All NMR spectra were recorded in CDCl$_3$ containing TMS as internal standard. High resolution mass spectra were obtained from Micro Mass ESI-TOF MS spectrometer. MALDI-TOF MS of the samples was determined by using Applied Biosystems 4800 PLUS Analyzer. FT-IR spectra of all compounds were recorded using Bruker alphaT Fourier transform infrared spectrophotometer. Gel permeation chromatographic (GPC) analysis of the polymer samples were performed using Viscotek VE 1122 pump, Viscotek VE 3580 RI detector and Viscotek VE 3210 UV/Vis detector in tetrahydrofuran (THF) using polystyrene as standards. Thermal stability of the polymers was determined using Perkin Elmer thermal analyzer STA 6000 model at a heating rate of 10 ^{o}C/min in nitrogen atmosphere. Circular dichroism (CD) analysis of the polymer samples was done using JASCO J-815 CD spectrometer at 20 °C in THF. Quantum mechanical calculations were carried out on Gaussian 03 (1) program. Density functional theory (DFT) with Becke's three-parameter hybrid exchange functional and the Lee-Yang-Parr correlation functional (B3LYP) and 6-31G (d, p) basis set for all the atoms were employed in the calculations. FE-SEM images were recorded using Zeiss Ultra Plus scanning electron microscope. For FE-SEM analysis, the samples were prepared by drop casting on silicon wafers and coated with gold. Atomic force microscope (AFM) images were recorded by drop casting the samples on freshly cleaved mica surface, using Veeco Nanoscope IV instrument. The experiment was done in tapping mode.

3.2.3. Synthesis of ester-urethane monomers of amino acids: The monomer synthesis of amino acid is described for L-phenylalanine. L-Phenylalanine (26.1 g, 0.157 mol) was taken in a 500 mL three neck RB flask and 200 mL of dry methanol

was added into it. At 0 °C thionylchloride (28.5 mL, 46.7 g, 0.239 mol) was added drop wise under nitrogen atmosphere. The reaction mixture was refluxed for 12 h under nitrogen atmosphere. The solvent and excess thionylchloride were removed by distillation. The solid product hydrochloride salt of the above methyl ester of L-phenylalanine (33.8 g, 0.157 mol) was stirred in sodium carbonate solution (33.0 g, 0.314 mol, 330 mL H_2O, 150 mL of DCM) at 5 °C in open atmosphere. At 0 °C, methyl chloroformate (24.0 mL, 0.310 mol) was added drop wise and the reaction was continued for 12 h at 25 °C. The reaction mixture was extracted with dichloromethane and the organic layer was dried over anhydrous Na_2SO_4. The liquid was further purified by passing through silica gel column using ethyl acetate and pet ether (1:4 v/v) as eluent. Yield = 35.1 g (93%). ^1H NMR (400 MHz, $CDCl_3$) δ ppm: 7.32-7.24 (m, 3H, Ar**H**), 7.12 (d, 2H, Ar**H**), 5.12 (b, 1H, -N**H**), 4.64 (q, 1H, C**H**CH$_2$Ar), 3.73 (s, 3H, COOC**H$_3$**), 3.67 (s, 3H, NHCOOC**H$_3$**), 3.11 (d, 2H, C**H$_2$**Ar). ^{13}C-NMR (100 MHz, $CDCl_3$) δ ppm: 172.95, 156.24, 135.69, 129.15 (2C), 128.52 (2C), 127.06, 54.69, 52.24 (2C), 38.13. FT-IR (cm^{-1}): 3338, 2954, 1705, 1518, 1444, 1355, 1253, 1210 and 1057. HR-MS (ESI+): m/z [M+Na$^+$] calcd. for $C_{12}H_{15}NO_4$ [M$^+$]: 260.0898; Found: 260.0899.

Dual ester-urethane monomers of other amino acids: D-valine, D-alanine and D-phenyl alanine were prepared as described above.

D-phenylalanine Monomer: (R^1=CH$_3$,R^2= CH$_3$) D-Phenyl alanine (4.01 g, 0.024 mol) in methanol (40 mL), thionylchloride (5.3 mL, 8.68 g, 0.073 mol). D-phenylalanine methyl ester HCl (5.21 g, 0.024 mol), methyl chloroformate (4.89 g, 4.0mL, 0.052 mol) and sodium carbonate solution (5.0 g, 0.004 mol, 50 mL H_2O and 25 mL DCM). Yield 5.7 g (90%). ^1H NMR (400 MHz, $CDCl_3$) δ ppm: 7.32-7.24 (m, 3H, Ar**H**), 7.12 (d, 2H, Ar**H**), 5.12 (b, 1H, -N**H**), 4.64 (q, 1H, C**H**CH$_2$Ar), 3.73 (s, 3H, COOC**H$_3$**), 3.67 (s, 3H, NHCOOC**H$_3$**), 3.11 (d, 2H, C**H$_2$**Ar). ^{13}C-NMR (100 MHz, $CDCl_3$) δ ppm: 172.15, 156.35, 135.80, 129.31 (2C), 128.70 (2C), 127.24, 54.80, 52.40 (2C) and 38.32. FT-IR (cm^{-1}): 3338, 2954, 1705, 1518, 1444, 1355, 1253, 1210 and 1057. HR-MS (ESI+): m/z [M+Na$^+$] calcd. for $C_{12}H_{15}NO_4$ [M$^+$]: 260.0898; Found: 260.0905.

D-Valine Monomer: (R^1=CH$_3$,R^2= CH$_3$) D-Valine methyl ester HCl (2.01 g, 0.011 mol), methyl chloroformate (2.44 g, 2.0 mL, 0.026 mol) and sodium carbonate solution (2.50 g, 0.024 mol, 25 mL H_2O and 10 mL DCM). Yield= 1.9 g (84 %). ^1H

NMR (400 MHz, CDCl$_3$) δ ppm: 5.15 (b, 1H, -N**H**), 4.28 (m, 1H, **CH**), 3.72 (s, 3H, COO**CH$_3$**), 3.67 (s, 3H, NHCOO**CH$_3$**), 2.14 (m, 1H, **CH**), 0.95 (d, 3H, **CH$_3$**), 0.87 (d, 3H, **CH$_3$**). ^{13}C-NMR (100 MHz, CDCl$_3$) δ ppm: 172.73, 156.95, 59.05, 52.42, 52.21, 31.31, 19.00 and 17.57. FT-IR (cm^{-1}): 3347, 2964, 1705, 1521, 1438, 1392, 1371, 1354, 1313, 1236, 1206, 1162, 1097 and 1024. HRMS (ESI+): m/z [M+Na$^+$] calcd. for C$_8$H$_{15}$NO$_4$ [M$^+$]: 212.0898; found: 212.0900.

D-Alanine Monomer: (R^1=CH$_3$,R^2= CH$_3$) D-Alanine methyl ester HCl (4.63 g, 0.033 mol), methyl chloroformate (5.14 g (4.2 mL), 0.0054 mol) and sodium carbonate solution (10 wt %, 73 mL). Yield= 3.71 g (69%). ^{1}H NMR (400 MHz, CDCl$_3$) δ ppm: 5.24 (b, 1H, -N**H**), 4.37 (m, 1H, **CH**), 3.74 (s, 3H, COO**CH$_3$**), 3.67 (s, 3H, NHCOO**CH$_3$**), 1.40 (d, 3H, CH**CH$_3$**). ^{13}C-NMR (100MHz, CDCl$_3$) δ ppm: 173.70, 156.39, 52.56, 52.38, 49.68 and 18.79. FT-IR (cm^{-1}): 3335, 2993, 2955, 1702, 1526, 1451, 1347, 1300, 1253, 1210, 1175, 1111 and 1073. HRMS (ESI+): m/z [M+Na$^+$] calcd. for C$_6$H$_{11}$NO$_4$ [M$^+$]: 184.0585; found: 184.0504.

L-Alanine Boc Monomer: (R^1= CH$_2$CH$_3$,R^2= BOC) L-Alanine ethyl ester HCl (3.02 g, 0.020 mol), (Boc)$_2$O (6.13 g, 5.0 mL, 0.023 mol) and sodium carbonate (4.47 g, 0.042 mol, 10 wt. %, 45 mL). Yield = 3.55 g (83%). ^{1}H NMR (400 MHz, CDCl$_3$) δ ppm: 5.06 (b, 1H, -N**H**), 4.28 (m, 1H, **CH**), 4.19 (q, 2H, COO**CH$_2$**), 1.44 (s, 9H, NHCOO (**CH$_3$)$_3$**), 1.38 (d, 3H, CH**CH$_3$**) and 1.28 (t, 3H, CH$_2$**CH$_3$**). ^{13}C-NMR (100 MHz, CDCl$_3$) δ ppm: 173.4, 154.9, 79.8, 61.3, 49.3, 28.4, 18.8 and 14.2. FT-IR (cm^{-1}): 3434, 3056, 2988, 2956, 1719, 1516, 1455, 1377, 1348, 1297, 1268, 1215 and 1077. HRMS (ESI+): m/z [M+Na$^+$] calcd. for C$_{10}$H$_{19}$NO$_4$ [M$^+$]: 240.1212; found: 240.1213.

3.2.4. Synthesis of Poly(ester-urethane)s via dual ester-urethane melt polycondensation: Herein we described for dual ester-urethane melt polymerization procedure for L-phenylalanine monomer with 1,12-dodecanediol. Equimolar amounts of amino acid monomer L-phenylalanine monomer (0.53 g, 0.002 mol) and 1,12-dodecanediol (0.45 g, 0.002 mol) were taken in a test tube-shaped polymerization vessel and melted by placing the tube in oil bath at 100 °C. The polycondensation apparatus was made oxygen and moisture free by purging with nitrogen and subsequent evacuation by vacuum under constant stirring. Titanium isopropoxide (6.3 mg, 0.02 mmol, 1.0 mol %) was added as catalyst and the melt polycondensation was

carried out at 150 °C for 4h with constant stirring under nitrogen purge. During this stage, the methanol was removed along with the purge gas and the polymerization mixture became viscous. The viscous melt was further subjected to high vacuum (0.01 mm of Hg) at 150 °C for 2h under stirring. At the end of the polycondensation, poly (ester-urethane), was obtained as a viscocus product. It was purified by dissolving in tetrahydrafuran, filtered and precipitated into methanol to obtain fibrous product. Yield = 0.63 g (75%). ^{1}H NMR (400 MHz, CDCl$_3$) δ ppm: 7.31-7.12 (m, 5H, Ar**H**), 5.13 (b, 1H, N**H**), 4.62 (m, 1H, C**H**), 4.10-4.04 (m, 4H, COOC**H$_2$**, NHCOOC**H$_2$**), 3.10 (t, 2H, C**H$_2$**Ar), 1.56-1.25 (m, 20H, C**H$_2$**). ^{13}C-NMR (100 MHz, CDCl$_3$) δ ppm: 171.74, 155.93, 135.85, 129.25, 128.46, 126.98, 65.56, 65.29, 54.65, 38.35, 29.50, 29.16, 28.89, 28.38 and 25.76. FT-IR (cm^{-1}): 3348, 2924, 2853, 1717, 1505, 1458, 1397, 1346, 1249, 1196 and 1057.

All other amino acid based linear poly(ester-urethane) with various amino acid monomers and catalysts were done using similar procedure.

Monomers used are D-alanine monomer (0.79 g, 5.0 mmol), 1, 10-decanediol (0.85 g, 5.0 mmol) and Titanium tetrabutoxide (17.0 mg, 0.05 mmol, 1.0 mol %) Yield = 0.49 g (73%). ^{1}H NMR (400 MHz, CDCl$_3$) δ ppm: 5.25 (b, 1H, -N**H**), 4.35 (m, 1H, C**H**), 4.13 (t, 2H, COOC**H$_2$**), 4.04 (t, 2H, NHCOOC**H$_2$**), 1.62 (d, 3H, C**H$_2$**), 1.40 (d, 3H, C**H$_3$**) and 1.28 (m, 12H, C**H$_2$**). ^{13}C-NMR (100MHz, CDCl$_3$) δ ppm: 173.41, 156.15, 65.71, 65.39, 49.68, 29.53, 28.64, 25.94, 28.91 and 19.00. FT-IR (cm^{-1}): 3897, 3865, 3743, 3677, 3646, 3617, 3565, 2916, 2851, 2360, 1736, 1689, 1650, 1521, 1460, 1425, 1396, 1341, 1263, 1209, 1177, 1124 and 1073.

Monomers used are L-alanine (0.73 g, 0.005 mol) and 1,10-decanediol (0.78 g, 0.005 mol). Titanium tetrabutoxide (0.015 g, 0.005 mmol, 1.0 mol %) Yield = 0.92 g (75%). ^{1}H NMR (400 MHz, CDCl$_3$) δ ppm: 5.22 (b, 1H, -N**H**), 4.35 (m, 1H, C**H**), 4.14 (m, 2H, COOC**H$_2$**), 4.05 (t, 2H, NHCOOC**H$_2$**), 1.65-1.57 (m, 8H, C**H$_2$**), 1.40 (d, 3H, C**H$_3$**), 1.28 (m, 17H, C**H$_2$**). FT-IR (cm^{-1}): 3859, 3742, 3677, 3615, 2912, 2852, 2359, 1917, 1836, 1737, 1693, 1648, 1522, 1463, 1266, 1178 and 1074.

Monomers used are L-valine (0.73 g, 0.004 mol) and 1,10-decanediol (0.67 g, 0.004 mol), Titanium tetrabutoxide (13.0 mg, 0.04 mmol, 1.0 mol %) Yield =1.05 g (86%). ^{1}H NMR (400 MHz, CDCl$_3$) δ ppm: 5.21 (b, 1H, N**H**), 4.26 (m, 1H, C**H**), 4.11 (t, 2H,

COOC**H₂**), 4.03 (t, 2H, NHCOOC**H₂**), 2.14 (m, 1H, C**H**), 1.61 (m, 12H, C**H₂**), 0.95 (d, 3H, C**H₃**), 0.88 (d, 3H, C**H₃**). ^{13}C-NMR (100 MHz, CDCl₃) δ ppm: 172.27, 156.56, 65.26, 58.81, 31.28, 29.32, 28.47, 25.76, 18.91 and 17.44. FT-IR (cm^{-1}): 3853, 3743, 3677, 3616, 3351, 2927, 2856, 2360, 1711, 1515, 1463, 1395, 1342, 1308, 1233, 1194, 1094 and 1032.

Monomers used are L-phenylalanine (0.76 g, 0.003 mol) and 1,10-decanediol (0.55 g, 0.003 mol). Titanium tetrabutoxide (0.01 g, 0.03 mmol, 1.0 mol %). Yield = 1.01 g (85%). ^{1}H NMR (400 MHz, CDCl₃) δ ppm: 7.27-7.12 (m, 5H, Ar**H**), 5.15 (b, 1H, N**H**), 4.63 (m, 1H, C**H**), 4.09-4.02 (m, 4H, COOC**H₂**, NHCOOC**H₂**), 3.10 (t, 2H, C**H₂**Ar), 1.59-1.28 (m, 16H, C**H₂**). FT-IR (cm^{-1}): 3348, 2924, 2853, 1717, 1505, 1458, 1397, 1346, 1249, 1196 and 1057.

Monomers used are D-valine (0.43 g, 0.002 mol) and 1,10-decanediol (0.39 g, 0.002 mol), Titanium tetrabutoxide(0.008 g, 0.02 mmol, 1.0 mol %). Yield = 0.29 g (83%). ^{1}H NMR (400 MHz, CDCl₃) δ ppm: 5.19 (b, 1H, N**H**), 4.28 (m, 1H, C**H**), 4.13 (t, 2H, COOC**H₂**), 4.05 (t, 2H, NHCOOC**H₂**), 2.15 (m, 1H, C**H**), 1.62-1.59 (m, 5H, C**H₂**), 1.28 (m, 3H, C**H₂**), 0.98 (d, 3H, C**H₃**), 0.90 (d, 3H, C**H₃**). ^{13}C-NMR (100 MHz, CDCl₃) δ ppm: 172.48, 156.76, 65.48, 59.00, 31.50, 29.57, 29.53, 28.67, 25.93, 19.12 and 17.64. FT-IR (cm^{-1}): 3853, 3743, 3677, 3647, 3616, 3353, 2926, 2856, 2360, 1709, 1516, 1463, 1395, 1341, 1309, 1265, 1233, 1194, 1094 and 1032.

Monomers used are D-Phenylalanine (0.60 g, 0.003 mol) and 1,10-decanediol (0.41 g, 0.003 mol). Titanium tetrabutoxide (0.009 g, 0.03 mmol, 1.0 mol %). Yield = 0.67 g (81%). ^{1}H NMR (400 MHz, CDCl₃) δ ppm: 7.31-7.12 (m, 5H, Ar**H**), 5.15 (b, 1H, N**H**), 4.63 (m, 1H, C**H**), 4.09-4.02 (m, 4H, COOC**H₂**, NHCOOC**H₂**), 3.10 (t, 2H, C**H₂**Ar), 1.59-1.28 (m, 16H, C**H₂**). FT-IR (cm^{-1}): 3737, 3450, 3021, 2930, 2855, 1738, 1507, 1445, 1367, 1210 and 1054

3.2.5. Model reaction for Entries 1 to 11: (Entry-2) Here the reaction is described for 1-decanol with the L-valine monomer. L-valine monomer (0.50 g, 0.003 mol) and 1-decanol (0.43 g, 0.003 mol) were taken in a test tube shaped apparatus and melted by placing in an oil bath at 100 °C with constant stirring. The condensation apparatus was made oxygen and moisture free by purging with nitrogen under constant stirring.

After degassing Titanium tetrabutoxide (0.018 g, 0.05 mmol) was added and the condensation was carried out at 120 ^{o}C under nitrogen purge for 4 h. At the end of the condensation reaction, the product was obtained as colorless liquid. Yield = 0.69 g (83%) ^{1}H NMR (400 MHz, CDCl$_3$) δ ppm: 5.21 (b, 1H, -N**H**), 4.29 (m, 1H, C**H**), 4.14 (m, 2H, COOC**H$_2$**), 3.69 (s, 3H, NHCOOC**H$_3$**), 2.15 (m, 1H, **CH**), 1.64 (d, 2H, **CH$_2$**), 1.27 (m, 14H, C**H$_2$**), 0.97 (d, 3H, C**H$_3$**) and 0.88 (m, 6H, C**H$_3$**). ^{13}C-NMR (100 MHz, CDCl$_3$) δ ppm: 172.3, 157.0, 65.5, 59.0, 52.4, 31.9, 29.6, 29.4, 28.6, 25.9, 22.8, 19.0, 17.5 and 14.2. FT-IR (cm^{-1}): 3742, 3357, 2925, 2856, 2360, 1714, 1525, 1456, 1343, 1304, 1257, 1206, 1178 and 1073. HRMS (ESI): m/z [M+H] $^+$ calcd. For C$_{17}$H$_{34}$NO$_4$: 316.2489; found: 316.2486.

Entry-1: Glycine methyl derivative (0.51 g, 0.003 mol), 1-decanol (0.55 g, 0.67 mL, 0.003 mol) and Titanium tetrabutoxide (0.011 g, 1mol %), Yield = 0.85 g (89%) Colorless oil. ^{1}H NMR (400 MHz, CDCl$_3$) δ ppm: 5.19 (b, 1H, -N**H**), 4.12 (t, 2H, COOC**H$_2$**), 3.95 (d, 2H, **CH$_2$**), 3.68 (s, 3H, NHCOOC**H$_3$**), 1.65-0.85 (19H, aliphatic **CH$_2$**, **CH$_3$**). ^{13}C-NMR (100 MHz, CDCl$_3$) δ ppm: 170.3, 157.0, 65.7, 52.5, 42.8, 31.9, 29.6, 29.4, 29.3, 28.6, 25.9, 22.7 and 14.2. FT-IR (cm^{-1}): 3359, 2923, 1712, 1525, 1365, 1189, 1052. HRMS (ESI): m/z [M+H] $^+$ calcd. for C$_{14}$H$_{28}$NO$_4$: 274.2018; found: 274.2021.

Entry-3: L-Leucine methyl derivative (0.53 g, 0.003 mol), 1-decanol (0.41 g, 0.003 mol) and Titanium tetrabutoxide (0.009 g, 0.003 mmol), Yield = 0.65 g (76%). Colorless oil ^{1}H NMR (400 MHz, CDCl$_3$) δ ppm: 5.09 (b, 1H, -N**H**), 4.37 (m, 1H, C**H**), 4.12 (t, 2H, COOC**H$_2$**), 3.68 (s, 3H, NHCOOC**H$_3$**), 1.64 (m, 5H, CH, **CH$_2$**), 1.26 (m, 14H, C**H$_3$**), 0.95 (d, 6H, C**H$_3$**) and 0.88 (t, 3H, C**H$_3$**). ^{13}C-NMR (100 MHz, CDCl$_3$) δ ppm: 173.4, 156.7, 65.6, 52.6, 52.4, 42.0, 32.9, 31.9, 29.6, 29.4, 29.3, 28.6, 25.8, 24.8, 22.7, 21.9, 21.8 and 14.2. FT-IR (cm^{-1}): 3742, 3337, 2925, 2857, 2360, 1713, 1526, 1458, 1342, 1266, 1199, 1172, 1123 and 1057. HRMS (ESI): m/z [M+H] $^+$ calcd. for C$_{18}$H$_{36}$NO$_4$: 330.2645; found: 330.2642.

Entry-4: L-Phenyl methyl derivative (0.68 g, 0.003 mol), 1-decanol (0.45 g, 0.003 mol) and Titanium tetrabutoxide (0.026 g, 0.008 mmol), Yield = 0.73 g (71%) Colorless oil. ^{1}H NMR (400 MHz, CDCl$_3$) δ ppm: 7.29-7.09 (m, 5H, Ar-H), 5.16 (b, 1H, -N**H**), 4.63 (m, 1H, C**H**), 4.07 (m, 2H, COOC**H$_2$**), 3.64 (s, 3H, NHCOOC**H$_3$**), 3.09 (m, 2H, CH$_2$-Ar) 1.56 (t, 2H, **CH$_2$**), 1.25 (m, 12H, C**H$_2$**) and 0.87 (t, 3H, C**H$_3$**).

^{13}C-NMR (100 MHz, CDCl$_3$) δ ppm: 171.2, 156.4, 135.9, 129.4, 128.6, 127.2, 65.8, 54.9, 52.4, 38.4, 32.0, 29.6, 29.4, 29.3, 25.9, 22.8 and 14.2. FT-IR (cm^{-1}): 3742, 3337, 2925, 2857, 2360, 1713, 1526, 1458, 1342, 1266, 1199, 1172, 1123 and 1057. HRMS (ESI): m/z [M+H]$^+$ calcd. for C$_{21}$H$_{34}$NO$_4$: 364.2489; found: 364.2486.

Entry-5 Alanine methyl derivative (0.51 g, 0.003 mol), 1-decanol (0.50 g, 0.003 mol) and Titanium tetrabutoxide (0.014 g, 0.004 mmol) Yield = 0.88 g (89%). ^{1}H NMR (400 MHz, CDCl$_3$) δ ppm: 5.25 (b, 1H, -N**H**), 4.34 (m, 1H, **CH**), 4.14 - 4.08 (m, 2H, COO**CH$_2$**), 3.66 (s, 3H, NHCOO**CH$_3$**), 1.61 (m, 2H, **CH$_2$**), 1.38 (d, 3H, **CH$_3$**), 1.25 (m, 15H, **CH$_2$**) and 0.86 (t, 3H, **CH$_3$**). ^{13}C-NMR (100 MHz, CDCl$_3$) δ ppm: 173.2, 156.3, 65.7, 52.3, 49.7, 31.9, 29.6, 29.4, 28.6, 25.8, 22.8 and 14.9. FT-IR (cm^{-1}): 3742, 3340, 2924, 2856, 2360, 1714, 1525, 1456, 1343, 1304, 1257, 1206, 1178 and 1073. HRMS (ESI): m/z [M+H]$^+$ calcd. for C$_{15}$H$_{30}$NO$_4$: 288.2176; found: 288.2172.

Entry-6: L-Alanine ethyl derivative (0.39 g, 0.002 mol), 1-decanol (0.38 g, 0.002 mol) and Titanium tetrabutoxide (0.010 g, 0.003 mmol) yield = 0.56 g (84%) Colorless oil ^{1}H NMR (400 MHz, CDCl$_3$) δ ppm: 5.19 (b, 1H, -N**H**), 4.36 (m, 1H, **CH**), 4.13 (m, 4H, COO**CH$_2$**), 1.64 (m, 3H, **CH$_2$**), 1.40 (d, 3H, **CH$_3$**), 1.27 (m, 19H, **CH$_2$**) and 0.88 (t, 3H, **CH$_3$**). ^{13}C-NMR (100 MHz, CDCl$_3$) δ ppm: 173.3, 155.9, 65.7, 63.2, 61.1, 49.6, 32.9, 31.9, 29.6, 29.4, 29.3, 22.7, 18.9, 14.6 and 14.2. FT-IR (cm^{-1}): 3867, 3744, 3616, 3341, 2925, 2856, 2361, 1712, 1523, 1457, 1377, 1355, 1304, 1251, 1206, 1178 and 1068. HRMS (ESI): m/z [M+H]$^+$ calcd. for C$_{16}$H$_{32}$NO$_4$ [M$^+$]: 302.2331; found: 302.2329.

Entry-7: L-Alanine phenyl derivative (0.17 g, 0.001 mol), 1-decanol (0.16 g, 0.001 mol) and Titanium tetrabutoxide (0.003 g, 0.001 mmol) yield = 77 % Colorless oil ^{1}H NMR (400 MHz, CDCl$_3$) δ ppm: 7.29 (m, 5H, Ar-H), 5.26 (b, 1H, -N**H**), 5.25, (s, 2H, **CH$_2$**Ph), 4.08 (m, 1H, **CH**), 4.07 (m, 4H, COO**CH$_2$**), 1.57 (m, 2H, **CH$_2$**) and 1.36-0.82 (m, 14H, **CH$_3$**, **CH$_2$**). FT-IR (cm^{-1}): 3864, 3742, 3614, 3330, 2951, 2359, 1705, 1523, 1451, 1340, 1299, 1257, 1172, 1108 and 1069. MALDI-TOF: m/z [M+Na$^+$] calcd. for C$_{21}$H$_{33}$NO$_4$ [M$^+$]: 386.23; found:386.14.

Entry-8: L-Alanine Boc derivative (0.31 g, 0.001 mol), 1-decanol (0.25 g, 0.001 mol) and Titanium tetrabutoxide (0.008 g, 0.002 mmol), Yield = 0.40 g (80%) Colorless oil ^{1}H NMR (400 MHz, CDCl$_3$) δ ppm: 5.04 (b, 1H, -N**H**), 4.30 (m, 1H, **CH**), 4.20 - 4.09

(m, 2H, COOC$\mathbf{H_2}$), 1.64 (m, 3H, C$\mathbf{H_2}$), 1.45 (s, 3H, NHCOO(C$\mathbf{H_3}$)$\mathbf{_3}$), 1.38 (d, 3H, C$\mathbf{H_3}$), 1.28 (m, 16H, C$\mathbf{H_2}$) and 0.88 (t, 3H, C$\mathbf{H}_3$). FT-IR (cm^{-1}): 3744, 3362, 2925, 2857, 1711, 1508, 1456, 1366, 1305, 1250, 1164 and 1060. HRMS (ESI): m/z [M+Na$^+$] calcd. for C$_{18}$H$_{35}$NO$_4$Na [M$^+$]: 352.2463; found:352.2469.

Entry-9: L-Alanine ethyl derivative (4.19 g, 0.024 mol), Diethyleneglycol monomethylether (5.76 g, 0.048 mol) and Titanium tetrabutoxide (0.063 g, 0.001 mmol), Yield = (84%), colorless oil; Eluent (35% ethyl acetate in hexane) ^{1}HNMR (400 MHz, CDCl$_3$) δ ppm: 5.23 (b, 1H, -N$\mathbf{H}$), 4.36 (m, 1H, C$\mathbf{H}$), 3.67 (t, 2H, OC$\mathbf{H_2}$), 3.59 (t, 2H, OC$\mathbf{H_2}$), 3.51 (t, 2H, OC$\mathbf{H_2}$), 3.35 (S, 3H, OC$\mathbf{H_3}$), 1.38 (d, 3H, CH$_3$) and 1.20 (t, 3H, CH$_2$C$\mathbf{H_3}$). ^{13}C-NMR (100 MHz, CDCl$_3$) δ ppm: 172.1, 154.8, 70.8, 69.4, 67.8, 63.3, 59.9, 57.9, 48.4, 17.5 and 13.4. FT-IR (cm^{-1}): 3330, 2983, 2883, 1708, 1527, 1454, 1377, 1334, 1298, 1248, 1181, 1103 and 1068. HRMS (ESI): m/z [M+Na$^+$] calcd. for C$_{11}$H$_{21}$NO$_6$ Na: 286.1266; found: 286.1262.

Entry-10: L-Alanine methyl derivative (0.42 g, 0.003 mol), Adamantine ethanol (0.46 g, 0.003 mol) and Titanium tetrabutoxide (0.020 g, 0.006 mmol), Yield = 0.68 g (88%), Colorless oil; ^{1}H NMR (400 MHz, CDCl$_3$) δ ppm: 5.25 (b, 1H, -N$\mathbf{H}$), 4.34 (m, 1H, C$\mathbf{H}$), 4.18 (m, 2H, COOC$\mathbf{H_2}$), 3.65 (s, 3H, NHCOOC$\mathbf{H_3}$), 1.94 (m, 3H, CH$_2$), 1.71 (m, 21H, C$\mathbf{H_2}$, C$\mathbf{H_3}$). ^{13}C-NMR (100 MHz, CDCl$_3$) δ ppm: 173.2, 156.3, 62.1, 52.3, 49.7, 42.8, 42.5, 42.3, 37.1, 37.0, 31.8, 28.6 and 18.9. FT-IR (cm^{-1}): 3743, 3616, 3339, 2899, 2846, 2361, 1711, 1525, 1452, 1343, 1305, 1256, 1177, and 1072. HRMS (ESI): m/z [M+H$^+$] calcd. for C$_{17}$H$_{28}$NO$_4$: 310.2019; found: 310.2013.

Entry-11: L-Alanine methyl derivative (0.39 g, 0.002 mol), β-citrullenol (0.34 g, 0.002 mol) and Titanium tetrabutoxide (0.020 g, 0.006 mmol), Yield = 0.50 g (82%), Colorless oil; ^{1}H NMR (400 MHz, CDCl$_3$) δ ppm: 5.19 (b, 1H, -N$\mathbf{H}$), 5.02 (m, 1H, =CH), 4.29 (m, 1H, C$\mathbf{H}$), 3.62 (s, 3H, C$\mathbf{H_3}$), 1.92 (d, 2H, CH$_2$), 1.62-1.13 (m, 14H, CH,CH$_2$ and CH$_3$) and 0.85 (d, 3H, C$\mathbf{H_3}$). ^{13}C-NMR (100 MHz, CDCl$_3$) δ ppm: 173.2, 131.5, 124.5, 108.3, 64.1, 52.3, 49.7, 37.0, 35.4, 29.5, 25.8, 25.4, 19.4 and 17.7. FT-IR (cm^{-1}): 3853, 3743, 3677, 3616, 3341, 2961, 2918, 2360, 1714, 1525, 1454, 1377, 1334, 1304, 1254, 1177 and 1073. HRMS (ESI): m/z [M+H $^+$] calcd. for C$_{15}$H$_{27}$NO$_4$ [M$^+$]: 286.2019; found: 286.2092.

3.2.6. Model reaction for Entries 12 to 16: (Entry 13) Herein the model reactions were carried out at 120 °C; amino acid monomer and diol were taken in the ratio of 1.0 : 0.5 equivalents. The rest of the procedure is similar to the one provided in the model reaction entries 1-11. The procedure is described for L-valine monomer (0.91 g, 0.048 mol) with 1,5-pentanediol (0.26 g, 0.024 mol) at 120 °C in presence of Ti(OBu)$_4$ catalyst (0.018 g, 0.052 mmol, 1 mole %). Yield = 0.74 g (71%). Colorless oil; eluent (30% ethyl acetate in hexane) ^{1}H NMR (400 MHz, CDCl$_3$) δ ppm: 5.31 (b, 2H, -N**H**), 4.21 (m, 1H, C**H**), 4.07 (t, 4H, COOC**H$_2$**), 3.61 (s, 6H, NHCOOC**H$_3$**), 3.61 (m, 2H, -C**H**), 1.62 (m, 4H, C**H$_2$**), 1.36 (m, 2H, C**H$_2$**) and 0.91-0.82 (d, 12H, C**H$_3$**). ^{13}C-NMR (100 MHz, CDCl$_3$) δ ppm: 172.2, 156.9, 64.9, 59.1, 52.3, 31.2, 28.1, 22.4, 19.0 and 17.5. FT-IR (cm^{-1}): 3340, 2962, 1706, 1519, 1461, 1351, 1309, 1238, 1189, 1096, and 1031. HRMS (ESI): m/z [M+H$^+$] calcd. for C$_{19}$H$_{35}$N$_2$O$_8$: 419.2394; found: 419.2393.

The other model compounds were synthesised by similar procedure. The details are provided below.

Entry-12: L-alanine methyl derivative (0.89 g, 0.006 mol), 1, 5-pentanediol (0.29 g, 0.003 mol) and Titanium tetrabutoxide (0.024 g, 0.007 mmol), Yield = 0.75 g (75%). Colorless oil; Eluent (30% ethyl acetate in hexane). ^{1}H NMR (400 MHz, CDCl$_3$) δ ppm: 5.30 (b, 2H, -N**H**), 4.32 (m, 2H, COOC**H$_2$**), 4.12 (t, 4H, COOC**H$_2$**), 3.65 (s, 6H, NHCOOC**H$_3$**), 1.65 (m, 4H, C**H$_2$**), 1.43 (m, 2H, C**H$_2$**) and 1.38 (d, 6H, C**H$_3$**). ^{13}C-NMR (100 MHz, CDCl$_3$) δ ppm: 173.2, 156.4, 65.2, 52.3, 49.7, 28.2, 22.3 and 18.8. FT-IR (cm^{-1}): 3334, 2951, 1701, 1525, 1455, 1344, 1299, 1252, 1208, 1174, 1109, 1071 and 1043. HRMS (ESI): m/z [M+H$^+$] calcd. for C$_{15}$H$_{27}$N$_2$O$_8$:363.1765; found: 363.1765.

Entry-14: L-leucine derivative (0.75 g, 0.037 mol), 1, 5-pentanediol (0.20 g, 0.019 mol) and Titanium tetrabutoxide (0.024 g, 0.007 mmol), Yield = 0.62 g (72%). Colorless oil; Eluent (25 % ethyl acetate in hexane) ^{1}H NMR (400 MHz, CDCl$_3$) δ ppm: 5.17 (b, 2H, -N**H**), 4.32 (m, 2H, NHC**H**), 4.10 (m, 4H, COOC**H$_2$**), 3.64 (s, 6H, NHCOOC**H$_3$**), 1.68-1.37 (m, 12H, C**H**, C**H$_2$**), 0.92 (d, 6H, CH (C**H$_3$**)$_2$) and 0.92 (d, 6H, CH (C**H$_3$**)$_2$). ^{13}C-NMR (100 MHz, CDCl$_3$) δ ppm: 173.4, 159.7, 65.0, 52.6, 52.4, 41.7, 28.2, 24.8, 22.9 and 21.8. FT-IR (cm^{-1}): 3336, 2956, 2872, 1704, 1526, 1459, 1342, 1260, 1196, 1170, 1122 and 1054. HRMS (ESI): m/z [M+H$^+$] calcd. for C$_{21}$H$_{39}$N$_2$O$_8$: 447.2707; found: 447.2711.

Entry-15: L-phenyl alanine derivative (0.96 g, 0.004 mol), 1,5-pentanediol (0.27 g, 0.002 mol) and Titanium tetrabutoxide (0.024 g, 0.007 mmol), Yield = 0.91 g (69%). Colorless oil; eluent (25% ethyl acetate in hexane). ^{1}H NMR (400 MHz, CDCl$_3$) δ ppm: 7.23-7.08 (m, 10H, Ar**H**), 5.44 (b, 2H, -N**H**), 4.59-4.54 (m, 2H, C**H**), 4.04 - 3.99 (s, 4H, COOC**H$_2$**), 3.58 (s, 6H, NHCOOC**H$_3$**), 3.02 (m, 4H, ArC**H$_2$**), 1.51 (m, 4H, C**H$_2$**) and 1.28 (m, 2H, C**H$_2$**). ^{13}C-NMR (100 MHz, CDCl$_3$) δ ppm: 171.9, 156.4, 136.0, 129.3, 128.6, 127.1, 65.1, 55.0, 52.4, 38.3, 28.1 and 22.2. FT-IR (cm^{-1}): 3331, 2951, 1703, 1517, 1451, 1391, 1351, 1252, 1100, and 1056. HRMS (ESI): m/z [M+H$^+$] calcd. for C$_{27}$H$_{35}$N$_2$O$_8$: 515.2394; found: 515.2401.

Entry-16: D- phenylalanine methyl deivative (0.81 g, 0.003 mol), 1,5-pentanediol (0.18 g, 0.003 mol) and Titanium tetrabutoxide (0.009 g, 0.003 mmol), Yield = 0.58 g (67%). Colorless oil; Eluent (15% ethyl acetate in hexane). ^{1}H NMR (400 MHz, CDCl$_3$) δ ppm: 7.29-7.09 (m, 10H, Ar**H**), 5.19 (b, 2H, -N**H**), 4.60-4.55 (m, 2H, C**H**), 4.08 - 3.98 (s, 4H, COOC**H$_2$**), 3.61 (s, 6H, NHCOOC**H$_3$**), 3.04 (m, 4H, ArC**H$_2$**), 1.54 (m, 4H, C**H$_2$**) and 1.22 (m, 2H, C**H$_2$**). ^{13}C-NMR (100 MHz, CDCl$_3$) δ ppm: 171.8, 156.4, 135.9, 129.3, 128.6, 127.2, 65.2, 54.9, 52.4, 38.4, 28.1 and 22.2. FT-IR (cm^{-1}): 3331, 2951, 1703, 1517, 1451, 1391, 1351, 1252, 1100, and 1056. HRMS (ESI): m/z [M+H$^+$] calcd. for C$_{27}$H$_{35}$N$_2$O$_8$: 515.2393; found: 515.2401.

3.2.7. Model reaction for Entries 17 to 19: (Entry 17) The model reaction is described for 1-decanol with the L-valine monomer at 150 °C. 1-decanol (2.01 g, 0.013 mol) and L-valine monomer (1.21 g, 0.006 mol) were taken in polymerization apparatus and melted by placing in an oil bath at 100 ^{o}C with constant stirring. After degassing, Titanium tetrabutoxide (0.023 g, 0.006 mmol) was added and the condensation was carried out at 150 ^{o}C under nitrogen purge for 4 h. Further, controlled vacuum (1 mm of Hg) was applied at 150 °C for 1 h. Yield = 2.32 g (83%). Colorless oil; Eluent (5 % ethyl acetate in hexane) ^{1}H NMR (400 MHz, CDCl$_3$) δ ppm: 5.14 (b, 1H, -N**H**), 4.25 (m, 1H, C**H**), 4.10 (t, 2H, COOC**H$_2$**), 4.03 (t, 2H, NHCOOC**H$_2$**), 2.13 (m, 1H, C**H**(CH$_3$)$_2$), 1.65-1.55 (m, 4H, C**H$_2$**), 1.24 (m, 27H, C**H$_2$**), 0.95 (d, 3H, C**H$_3$**) and 0.86 (m, 9H, C**H$_3$**). ^{13}C-NMR (100 MHz, CDCl$_3$) δ ppm: 172.4, 156.7, 65.4, 58.9, 31.9, 29.6, 29.4, 29.2, 29.0, 25.9, 22.7, 19.0, 17.5 and 14.2. FT-IR (cm^{-1}): 3437, 3370, 2924, 2855, 1723, 1509, 1463, 1343, 1308, 1230,

1194, 1094 and 1035. HRMS (ESI$^+$): m/z [M+H$^+$] calcd. for C$_{26}$H$_{51}$NO$_4$ [M$^+$]: 441.3818; found: 442.3897.

The other model reactions (at 150 °C) of amino acid monomer with monoalcohol are described below.

Entry-18: L-Valine derivative (0.26 g, 0.001 mol), β-citrullenol (0.42 g, 0.003 mol) andtitanium tetrabutoxide (0.024 g, 0.003 mmol),Yield=0.45 g (74%).Colorless oil; Eluent (5% ethyl acetate in hexane). ^{1}H NMR (400 MHz, CDCl$_3$) δ ppm:5.17 (b, 1H, -N**H**), 5.11-5.09 (m, 2H, =C**H**), 4.27 (m, 1H, C**H**), 4.18 (t, 2H, COOC**H$_2$**), 4.18 (m, 2H, NHCOOC**H$_2$**), 2.16-1.17 (m, 25H, C**H**, C**H$_2$**) and 0.98-0.89 (m, 10H, C**H$_3$**). ^{13}C-NMR (100 MHz, CDCl$_3$) δ ppm:172.4, 156.7, 131.5, 124.7, 124.5, 63.8, 58.9, 37.1, 37.0, 35.5, 31.4, 29.4, 25.8, 25.5, 19.5, 17.7 and 17.6. FT-IR (cm^{-1}):3364, 2962, 2919, 1722, 1509, 1459, 1374, 1346, 1308, 1230, 1194, 1093 and 1053. HRMS (ESI): m/z [M+Na$^+$] calcd. for C$_{26}$H$_{47}$NO$_4$ Na: 460.3402; found: 460.3603.

Entry-19 L-valine derivative (0.49 g, 0.002 mol), Adamantanethanol(0.97 g, 0.005 mol) and titanium tetrabutoxide(0.024 g, 0.003 mmol), Yield=1.03 g (82%). Colorless oil; Eluent (5% ethyl acetate in hexane). ^{1}H NMR (400 MHz, CDCl$_3$) δ ppm: 5.11 (b, 1H, -N**H**), 4.25 (m, 1H, C**H**), 4.17 (t, 2H, COOC**H$_2$**), 4.10 (t, 2H, NHCOOC**H$_2$**), 2.14 (m, 1H, C**H**), 1.92 (m, 5H, C**H**, C**H$_2$**), 1.70-1.37 (m, 26H, C**H**, C**H$_2$**), 0.95 (d, 3H, CH(C**H$_3$**)$_2$) and 0.88 (d, 3H, CH(C**H$_3$**)$_2$). ^{13}C-NMR (100 MHz, CDCl$_3$) δ ppm:172.4, 156.7, 61.8, 59.0, 42.8, 42.5, 37.0, 31.8, 28.6, 19.1 and 17.5. FT-IR (cm^{-1}): 3364, 2962, 2919, 1722, 1509, 1459, 1374, 1346, 1308, 1230, 1194, 1093 and 1053. HRMS (ESI): m/z [M+H$^+$] calcd. for C$_{30}$H$_{48}$NO$_4$ [M$^+$]: 486.3584; found: 486.3593.

3.3. Results and Discussion

3.3.1. Role of catalyst in transreactions

To study the role of the catalyst on the reactivity of functional groups (ester and urethane) of the amino acid monomer towards alcohols; model reactions were carried out for glycine monomer with 1-decanol at various temperatures (80 to 150 °C). Below 110 °C, in the absence of catalyst, both ester and urethane groups in the monomer were found to be non-reactive towards alcohol. ^{1}H-NMR spectra of the glycine monomer and its reaction products at 120 °C and 150 °C are shown in figure 3.3. The monomer showed two distinct peaks for ester -COOC**H$_3$** protons (at 3.76 ppm, proton-b, in figure 3.3a) and urethane -NHCOOC**H$_3$** protons (at 3.70 ppm,

proton-c, in figure 3.3a) in the amino acid monomer. Thus, the disappearence of these peaks in the products (spectra 3.3b to 3.3e) provides evidence for the reaction of particular functional group (ester or urethane) in the monomer towards alcohol. At 120 °C, in the absence of the catalyst, both ester and urethane functional groups did not undergo reaction with alcohol (in figure 3.3b). At 150 °C, in the absence of the catalyst, the ester group in the monomer became partially active to produce new esters (60 % conversion, in new ester peak-b' at 4.15 ppm in figure 3.3c); however, the urethane group was completely non-reactive. At 120 °C, in the presence of Ti-catalyst, only the ester functional group underwent reaction with alcohol (in figure 3.3d) and this was evident from the appearance of new ester $-COOC\textbf{H}_2(CH_2)_8CH_3$ at 4.15 ppm (peak- b') in figure 3.3d. However, the urethane group was completely non-reactive at 120 °C even in the presence of Ti-catalyst. At higher temperature (at 150 °C), in the presence of Ti-catalyst, the urethane (as well as ester) underwent reaction with alcohol to produce new urethane at 4.08 ppm (>98 %, peak-c', in figure 3.3e) and new ester product at 4.15 ppm (>98 %, peak-b', in figure 3.3e). At this reaction condition, there was no unreacted alcohol left in the reaction medium which is evident from the vanishing of $R-CH_2OH$ protons at 3.60 ppm (in figure 3.3e).These studies clearly postulated the following points: (i) in the absence of catalyst at 120 °C or lower temperature; both the ester and urethane functional groups are inert; (ii) in the presence of Ti-catalyst, at 120 °C; only the ester group became active and (iii) in the presence of Ti-catalyst, at 150 °C; both urethane and ester functional groups were active for the occurrence of the dual ester-urethane exchange reaction with alcohols.
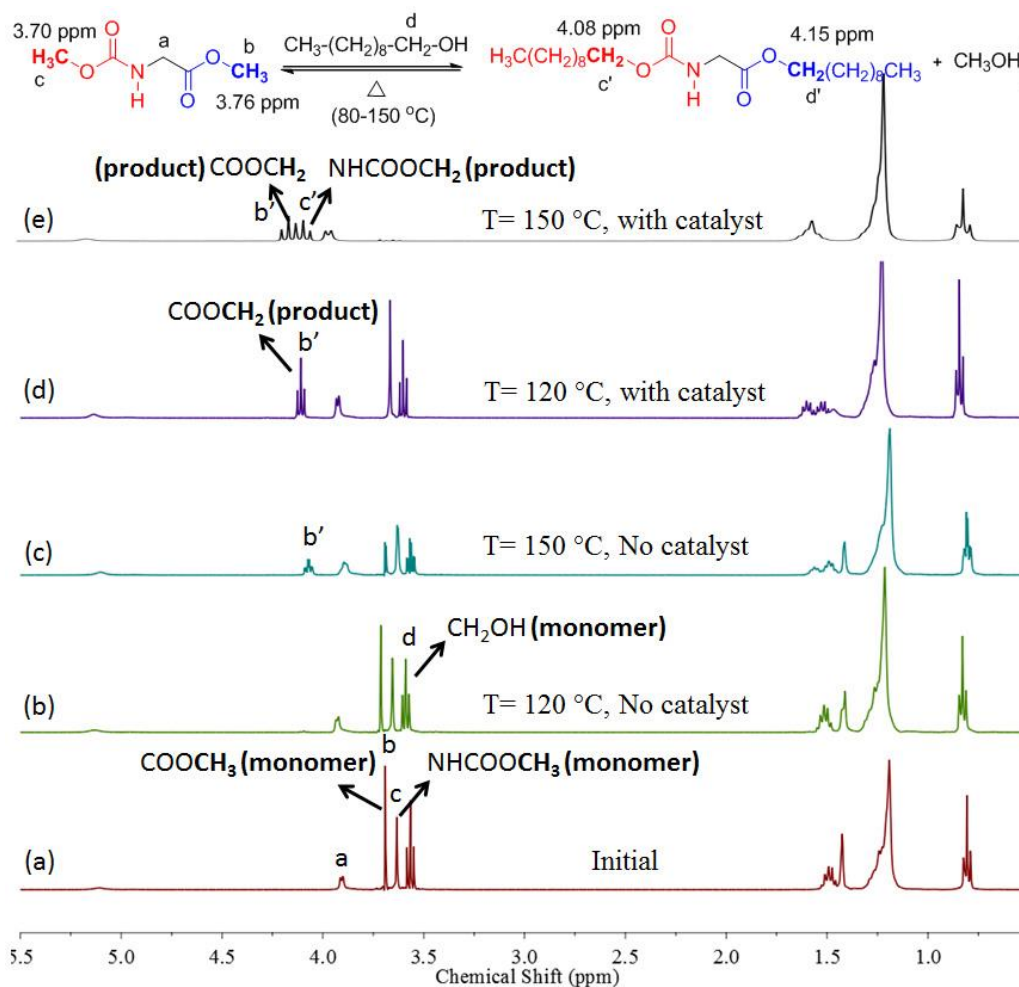
Figure 3.3. *^{1}HNMR spectra of the model reaction of Glycine monomer with1-decanol (a) in absence of catalyst initial, (b) absence of catalyst at 120 ℃, (c) absence of catalyst at 150 ℃, (d) in presence of Ti(OBu)₄ catalyst at 120 °C and (e) in presence of Ti(OBu)₄ catalyst at 150 °C. The spectra were recorded in CDCl₃ and only expanded region form 0.5 to 5.5 ppm are shown for simplicity.*

3.3.2. Catalyst trace for selective reactivity of functional group

In order to study the role of the catalyst on the monomer reactions; L-valine monomer was chosen and reacted with 1-decanol using wide range of catalysts (1 mole %). The temperature of the reaction was chosen at 120 °C since the ester and urethane functional groups showed significant reactivity difference towards alcohols at this temperature. The percentage conversion of the products were determined from their ^{1}H-NMR spectra as described in figure 3.3. The amount of new ester and urethane products obtained from the above studies are given in figure 3.4. For this reaction, the metal catalysts chosen were oxides, nitrates, chloride, acetates, acetylacetonate and alkoxides based on the alkali [Li(OAc), Na₂CO₃, Na(OAc),

K_2CO_3, K(OAc), CS_2CO_3, Cs(OAc), $Cs(CH_3)_3CCOO$, CsF,], alkali earth metal [$Mg(NO_3)_2$, $CaCl_2$, $Sr(NO_3)_2$ and $Ba(NO_3)_2$)], other metals [Al(iPrO)$_3$, Al_2O_3, Ge(Oipr)$_4$, Sn(Oct)$_2$, $SnCl_2$, SnO_2, $Bi(NO_3)_3$ and SeO_2], transition metal [$Y(NO_3)_3$, Y_2O_3, Ti(OBu)$_4$, Ti(OiPr)$_4$, TiO_2, Zr(acac)$_4$, $Cr(NO_3)_3$, CrO_3, Mn(OAc)$_2$, $MnCl_2$, MnO_2, Fe(acac)$_3$, $FeCl_3$, $Fe(NO_3)_3.9H_2O$, $RuCl_3$, $Co(NO_3)_3.6H_2O$, Co(OAc)$_2$, CoO, Ni(acac)$_2$, $Ni(NO_3)_2$, Cu(OAc)$_2$, $Cu(NO_3)_2. 3H_2O$, Zn(OAc)$_2$, $Zn(NO_3)_2$, ZnO, $CdCl_2$, Cd(OAc)$_2$, $Cd(NO_3)_2$ and CdO)] and lanthanides [$LaCl_3.9H_2O$, $La(NO_3)_3.H_2O$, $Pr(NO_3)_3.6H_2O$, Pr_2O_3, Nd_2O_3, $Nd(NO_3)_3.6H_2O$, Sm_2O_3, $Eu(NO_3)_3.5H_2O$, $Gd(NO_3)_3.6H_2O$, Gd_2O_3, Dy_2O_3, $DyCl_3$ and $Dy(NO_3)_3.H_2O$]. Metal oxide catalyzed model reactions showed < 40% conversion of ester product and they did not produce any new urethane products. Among the nitrates, Eu^{3+}, Y^{3+} and Zn^{2+} and Cd^{2+} produced more esters compared to urethanes. Interestingly, $Gd(NO_3)_3$ exclusively underwent transesterification to produce 70 % ester product. In the chloride series, Fe^{3+} and La^{3+} produced > 80 % esters (along with 10 to 25 % of urethane) compared to other metal chlorides. All the acetates were found to be efficient catalyst for producing new esters in 80 to 98 % yield along with 10 to 25 % of urethanes. Fe(acac)$_3$, Sn(Oct)$_2$, Ti(i-OPr)$_4$ were also found to produce > 98 % of esters along with 10-20 % of urethanes. Based on these studies, the following trend may be written for the transesterification of esters with alcohol in the presence of metal-catalysts: metal oxides < nitrates < chlorides < acetates. Among all the catalysts; CdO, $Gd(NO_3)_3$, CSA and Ti(OBu)$_4$ catalysts were found to be very selective towards transesterification in the amino acid monomers at 120 °C (the urethane part was completely inert). Among them, Ti(OBu)$_4$ catalyst showed very high selectivity at 120 °C for new ester formation (> 99 %) with negligible amount of urethanes reactivity (< 1 %).
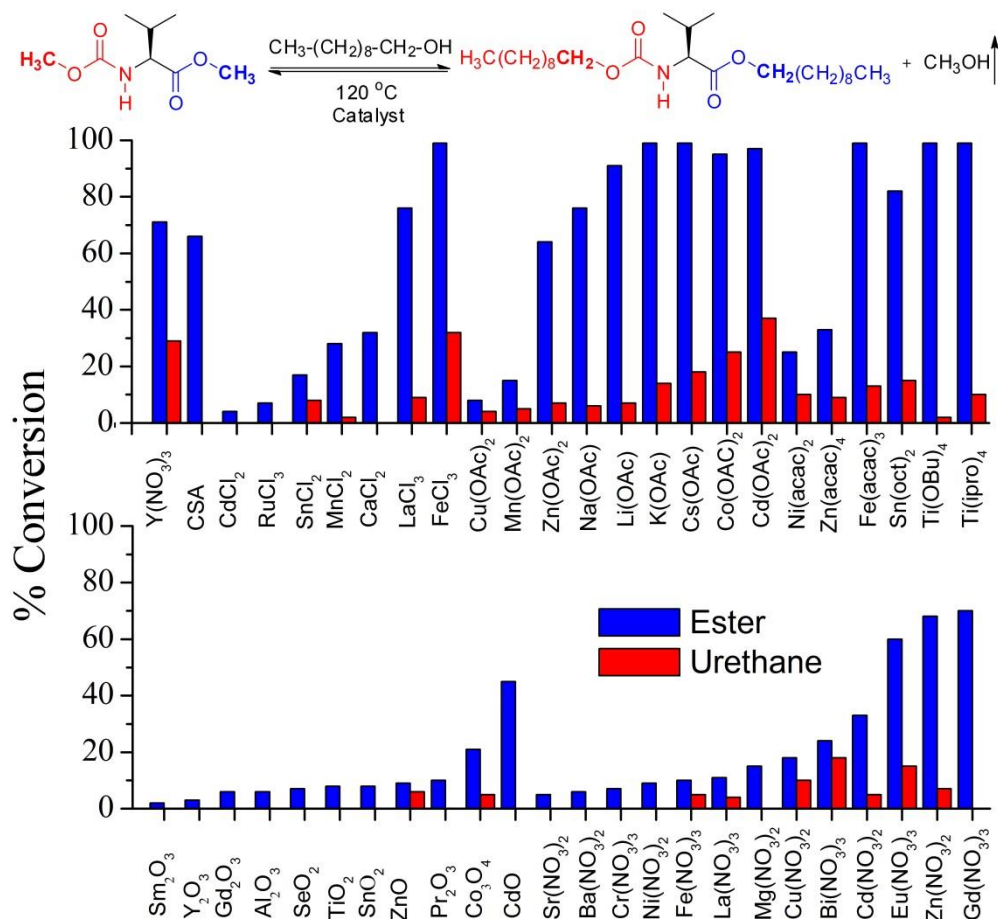
Figure 3.4. *Percentage conversion of ester and carbamate linkages for the reaction of L-valine monomer with 1-decanol at 120 °C in the presence of 1 mole % of catalysts.*

3.3.3. Synthesis of Amino acid derivatives A-B, A-B-A and A-B'

In order to investigate the effect of the α-structural differences in the amino acid monomer on the selective trans-reactions; 6 to 8 different amino acid residues were chosen. These monomers were reacted with mono-alcohol at 120 °C and their yields are given in table 1 (in table-1, entries 1-11). The steric hindrance in the monomers increased in the order of glycine < alanine < valine < phenylalanine (in entry 1 to 4). The increase in the steric hindrance at the α-position reduced the yield of the product. Further, the selective reactivity of ester functional group was also investigated by varying the nature of the substituents in alanine derivative R^2 = methyl, ethyl and t-butyl in the urethane part and carboxylic ester part as R^1 = methyl or ethyl (in entry 5 to 8). In all these cases, only carboxylic ester part underwent reaction and the urethane was completely inert at 120 °C (to produce A-B type species). The nature of monoalcohols were also varied as aliphatic, cyclic, aromatic, oligoethylene glycol and double bond containing alcohol to study their effect on

exchange reaction (in entry 9 to 11). These results revealed that the temperature selective ester-exchange was exclusively retained irrespective of the nature of the alcohols and R, R^1, R^2 in the amino acids. Further, this catalyst and thermoselective reaction was found to be same irrespective of the substituents at ester (R^1) and urethane (R^2) units $R^1=R^2$ or $R^1 \neq R^2$ as shown in Figure 3.1.

Table- 1. *Reactions of amino acid monomers with monoalcohols at 120 °C.*

Entry	R	R^1	R^2	R^3	Yield (%) (^{1}HNMR)	Yield (%) (isolated)
A-B Type						

Entry	R	R^1	R^2	R^3	Yield (%) (^{1}HNMR)	Yield (%) (isolated)
1	H	CH_3	CH_3	$CH_3(CH_2)_9$	94	89
2	$CH(CH_3)_2$	CH_3	CH_3	$CH_3(CH_2)_9$	89	83
3	$CH_2CH(CH_3)_2$	CH_3	CH_3	$CH_3(CH_2)_9$	79	76
4	CH_2Ph	CH_3	CH_3	$CH_3(CH_2)_9$	75	71
5	CH_3	CH_3	CH_3	$CH_3(CH_2)_9$	93	89
6	CH_3	CH_3	CH_2CH_3	$CH_3(CH_2)_9$	94	84
7	CH_3	CH_3	CH_2Ph	$CH_3(CH_2)_9$	85	69
8	CH_3	CH_2CH_3	$C(CH_3)_3$	CH_3-$(CH_2)_9$	84	80
9	CH_3	CH_3	CH_2CH_3	CH_3ODEG	94	84
10	CH_3	CH_3	CH_3	$ADM-CH_2$	92	88
11	CH_3	CH_3	CH_3	β-Citronellol	80	75

The melt condensation was also carried out with diols and amino acid monomers at 120 °C in presence of Ti-catalyst. For this reaction, the ratio of the amino acid monomer to diol was taken as 2:1 in the feed (in table-2, entry 12 to 16). This produced A-B-A type triblock species. At 120 °C, the ester functional group underwent exchange reaction to make diester with un-reacted urethane functional groups at the ends. At 150 °C, in presence of Ti-catalyst, both ester and urethane functional groups in the amino acid monomers underwent reaction with monoalcohol to produce both ester and urethane products (A-B' type products). This reaction was also investigated for various mono alcohols: 1-decanol, citrullenol and adamantane methanol (in entry 17-19). The dual ester-urethane exchange reaction produced in ~ 80 % yield. The catalyst and temperature selective reactivity of the amino acids are

not restricted only to few examples that are shown in tables 1-3, in principle it can be adopted to make wide range of other structures.

Table- 2. *Reactions of amino acid monomers with bis-alcohols at 120 ℃.*

Entry	R	R¹	R²	R³	Yield (%) (¹HNMR)	Yield (%) (isolated)

A-B-A Type

12	CH_3	CH_3	CH_3	$(CH_2)_3$	86	75
13	$CH(CH_3)_2$	CH_3	CH_3	$(CH_2)_3$	84	71
14	$CH_2CH(CH_3)_2$	CH_3	CH_3	$(CH_2)_3$	84	72
15	CH_2ph	CH_3	CH_3	$(CH_2)_3$	82	69
16	CH_2ph (D)	CH_3	CH_3	$(CH_2)_3$	80	67

Table- 3. *Reactions of amino acid monomers with monoalcohols at 150 ℃.*

Entry	R	R¹	R²	R³	Yield (%) (¹HNMR)	Yield (%) (isolated)

A-B' Type

17	$CH(CH_3)_2$	CH_3	CH_3	$CH_3(CH_2)_9$	95	89
18	$CH(CH_3)_2$	CH_3	CH_3	β-Citronellol	80	74
19	$CH(CH_3)_2$	CH_3	CH_3	$ADM-CH_2$	86	82

3.3.4. Proposed mechanism for poly (ester-urethane)s

The mechanism for high temperature selective condensation was elucidated in figure 3.5. In the case of metal salt catalysts assisted condensation reaction, the metal centre polarize the carbonyl oxygen (C=O) and makes the carbon atom as an active nucleophilic centre for the attack of R-O-H species (in figure 3.5a). Among the two carbonyl centres, the ester carbon is more nucleophilic compared to urethane. The relatively less nucleophilicity of the urethane carbonyl carbon is associated with the loan pair of electrons donated from the nitrogen atom N-H bond to the C=O. In the case of transition metal catalyzed condensation reactions such as $Ti(OBu)_4$; the reaction of catalyst $Ti(OBu)_4$ with R-OH produces the active species Ti-O-R. The Ti-O-R species attacks the carbonyl carbon to produce an active four membered

transition state. These experimental results (entries 1 to 19) clearly suggested that the attack of ester carbon is more favourable at 120 °C which produced exclusively ester-exchange product (in figure 3.5b).
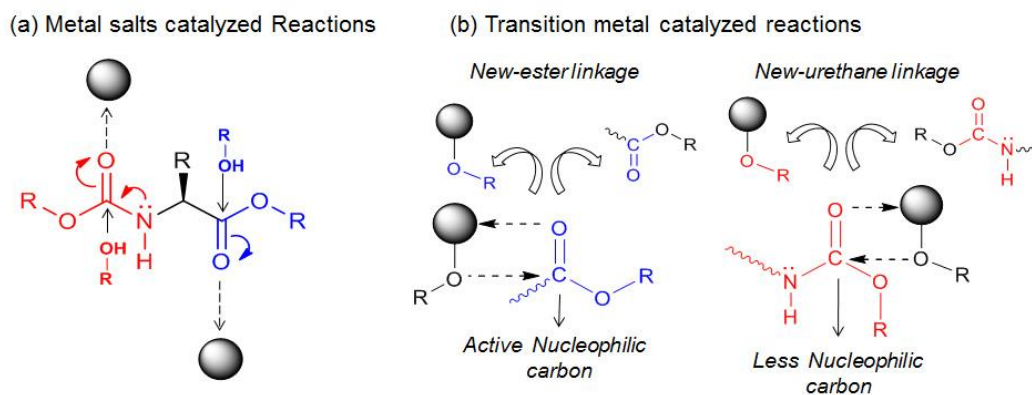

Figure 3.5. *Proposed mechanism for m*elt polyconsation reaction catalyzed by metal salts (a) and transition metal through cyclic transition states (b).*

To understand the difference in the nucleophilicity of these two carbonyl carbon atoms, single crystal structure for aspartic acid monomer was resolved and is shown in figure 3.6a (other monomers are liquid). The crystal structure of the aspartic acid monomer showed that N-C=O bond existed in the same plane. This facilitated the overlap of the nitrogen lone pair with the p-orbitals on the carbon and oxygen atom. Recently, Deetz et al.[21] had reported theoretical calculation for the effect of electron releasing to electron withdrawing functionality on carbamate groups. It was found that the electron withdrawing group decreased the C-N bond rotation which made the carbon atom in carbamate units less nucleophilic. Zhao et al.[22] studied the influence of extended double bond of C-N bond by alkyl substitution and concluded that the loan pair electron in the nitrogen donated to carbonyl carbon through conjugation. Shigemoto et al.[19] had done detailed theoretical calculation for binding of ester unit at the Ti-O-R centre through RO-C=O...Ti; O=C-O(R)...Ti and Lewis acid in the transesterification reaction. They found that the RO-C=O...Ti was the most viable in the Ti-catalyst transesterification of esters with alcohol.
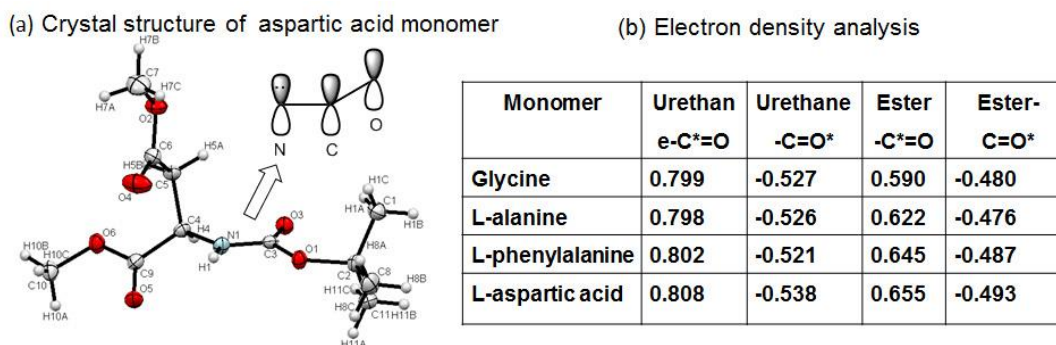
(a) Crystal structure of aspartic acid monomer

(b) Electron density analysis

Monomer	Urethane-C*=O	Urethane -C=O*	Ester -C*=O	Ester-C=O*
Glycine	0.799	-0.527	0.590	-0.480
L-alanine	0.798	-0.526	0.622	-0.476
L-phenylalanine	0.802	-0.521	0.645	-0.487
L-aspartic acid	0.808	-0.538	0.655	-0.493

Figure 3.6. *Single crystal strcuture of the aspartic acid monomer (a). Table exhibiting the electron density at the carbonyl carbon and oxygen calculated using Guassion 03 programme (b).*

In the present investigation, efforts have been taken to calculate the electron density of carbonyl carbons at ester and carbamate units using Gaussian programmer 03 (in figure 3.6b). From the theoretical studies we observed that; (i) the electron density of ester carbon was less compared to urethane carbon, (ii) the carbonyl oxygen electron density was more in case of urethane than ester. The above results clearly indicate that the urethane –NH group is in conjugation with the carbonyl oxygen which account for the difference in electron density between ester and urethane. Hence the electron density of carbonyl carbon ester was less compared to urethane which drives the ester functional group to undergo nucleophilic substitution at 120 °C whereas the urethane group is completely inert (at 120 °C). Both single crystal structure and DFT calculation, confirmed that the electron rich urethane carbonyl carbon was less susceptible for attack by Ti-O-R at 120 °C. As expected, at higher temperatures, the N-C bond in the urethane became more rotationally active; as a result the overlap between the nitrogen lone pair and C=O vanishes. This enhanced the nucleophilicity of the urethane carbonyl carbon atom for the attack by Ti-O-R at 150 °C. This difference in the carbonyl carbon nucleophilicity enabled us to make a wide variety of structures such as A-B diads and A-B-A triblocks using amino acids (in table 1-3).

3.3.5. Role of catalyst in linear poly(ester-urethane)

The amino acid monomers B-B' designed in the present work has ester (B) and urethane functionality (B'). Both B and B' functional groups are reactive towards alcohol in the presence of catalyst; however, their kinetics are controlled by the temperature of the melt condensation reaction. For example, at 120 °C, only the ester functional group (B) is reactive to produce new ester and under this condition the urethane (B') is completely inert. At higher temperature (at 150 °C), both ester (B) and urethane (B') became equally reactive to produce new ester and urethane linkages. This was demonstrated in the table 1, in entries 17 to 19. Earlier studies revealed that the polymerization kinetic rate constants for ester (B) and urethane (B') towards alcohol are 2.72 $\times 10^{-2}$ and 1.43x10^{-2}, respectively. These rate constants were comparable for both ester and urethane reaction towards alcohols. Thus, at 150 °C, the dual ester urethane amino acid monomer equally reacts with diols to produce poly(ester-urethane)s. Hence, during the polycondensation reaction, the B-B' monomer actually behaved as B-B type monomer for reaction towards diols (A-A) to produce poly(ester-urethane)s. Based on the model reactions (in figure-3.4), more than 24 different catalysts of carbonate, acetate, alkoxide, halide and nitrate were chosen for the polycondensation of amino acid monomer with diol at 150 °C to produce poly(ester-urethane)s. These catalysts were chosen based on the criteria that they showed more than > 70% conversion for new ester and more than 20 % for new urethane in the model reactions at 120 °C (in figure 3.4). This selection was done based on the evidence that at 150 °C both ester and urethane groups in the amino acid monomer reacted equally with diols to produced A-B' diads (in entries 17 to 19, in table 3). Further, this also allowed us to investigate the thermoselectivity of the polymerization on the L-amino acid monomers.

Melt polycondensation process for polyester is known for past 50 years; however, melt polycondensation for polyurethane or poly(ester-urethane)s were developed in the past 5 years by our research group. Thus, it was necessary to optimize various types of catalysts for this new melt process to make poly(ester-urethane)s based on the natural L-amino acids. However, no effort has been taken to optimize the catalyst type for the high temperature melt polymerization (at 150 °C) to produce poly(ester-urethanes). It is very crucial to trace wide range of catalysts for

poly(ester-urethane)s for their futuristic large scale commercial applications. L-phenylalanine monomer was chosen and the polymerization reaction was carried out with 1,12-dodecane diol in the presence of 1 mole % catalyst (in figure 3.7). L-phenylalanine monomer -COOC**H**$_3$ and -NHCOOC**H**$_3$ protons (b and c) were appeared at 3.71 and 3.65 ppm, respectively (in figure 3.7a). In the Cd(OAc)$_2$ catalyzed polymerisation, the peaks at 3.71 ppm and 3.65 ppm (b and c) disappeared and new peak belonging to –COOC**H**$_2$ and –NHCOOC**H**$_2$ appeared at 4.08 ppm and 4.04 ppm (b' and c') respectively (in figure 3.7b). On the other hand, ^{1}H-NMR spectra of K$_2$CO$_3$ catalyzed polymer showed that the monomer -COOC**H**$_3$ and -NHCOOC**H**$_3$ protons (b and c) did not vanish completly with due to low reaction conversion (in figure 3.7c)
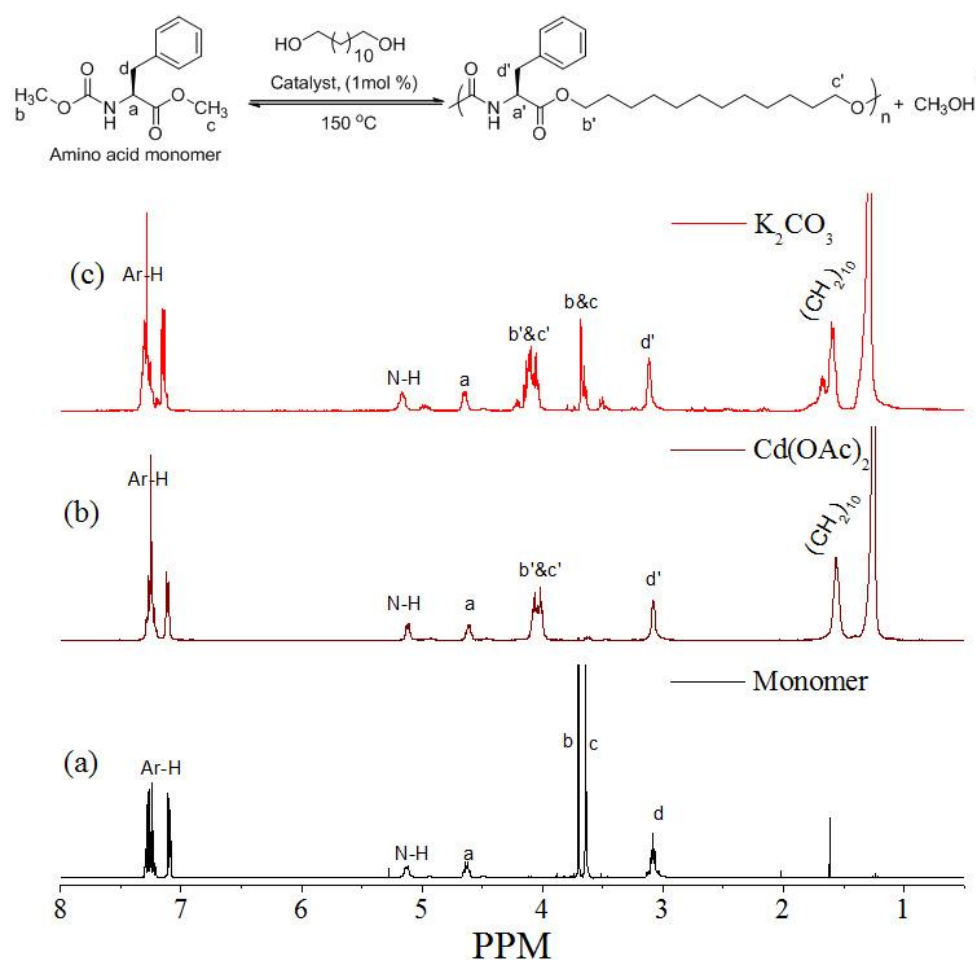

Figure 3.7. *^{1}H-NMR spectra of phenylalanine monomer (a) and its poly(ester-urethane)s produced using Cd(OAc)$_2$ (b) and K$_2$CO$_3$ (c).*

The molecular weight of the poly(ester-urethane)s produced by various catalysts were determined by GPC and their M_n and M_w are plotted and shown in figures 3.8a and 3.8b. The metal carbonate such as K_2CO_3 and Cs_2CO_3 did not facilitate the polycondensation reaction and the polymers showed higher retention time with respect to low molecular weight polymer formation. Among the metal halides in poly(ester-urethane) synthesis, $LaCl_3$ produced higher molecular weight polymers. Among the metal acetate catalysts, $Co(OAc)_2$, $Zn(OAc)_2$ and $Cd(OAc)_2$ afforded high molecular weight polymers compared to other metal acetates. Among metal nitrate, $Eu(NO_3)_3$ produced higher molecular weight polymers whereas other metal nitrate $Zn(NO_3)_2$, $Y(NO_3)_3$ and $Gd(NO_3)_3$ produced moderate molecular weight polymers (in figure-3.9). The molecular weight of functional polymers produced by $K(OAc)$, Cs_2CO_3, $FeCl_3$ and K_2CO_3 catalysts were found to be very low. Though, $K(OAc)$, Cs_2CO_3, $FeCl_3$ and K_2CO_3 catalyzed model reaction (in figure 3.4) showed the ester product formation from 70 to 90 % (in figure 3.4) they failed to produce higher molecular weight poly(ester-urethane)s. As per Carrothers equation for step-growth polymerization approach, $X_n = 1/(1-p)$, where p = extent of the reaction[1]; the catalyst should be able to facilitate more than 98% conversion of ester functional group for producing at least 50-mers on laboratory scale. Among all these catalyst, $Ti(OBu)_4$, $Ti(iOpr)_4$, $Fe(acac)_3$, $LaCl_3$, $Eu(NO_3)_3$, $Cd(OAc)$ and DBTDL model compound afforded more than 99 % of the ester conversion; hence it also facilitated the formation of higher molecular weight polymers.
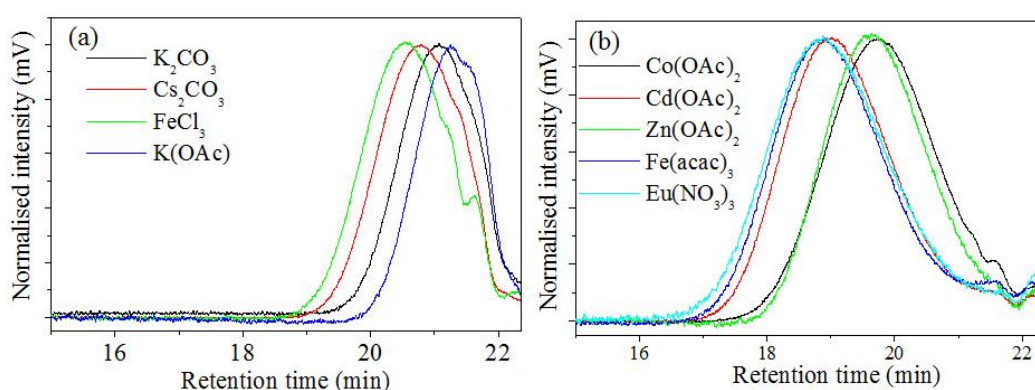

Figure 3.8. *Representative GPC chromotograms of polymers produced by diverse catalysts corresponding to low (a) and high molecular weights (b).*
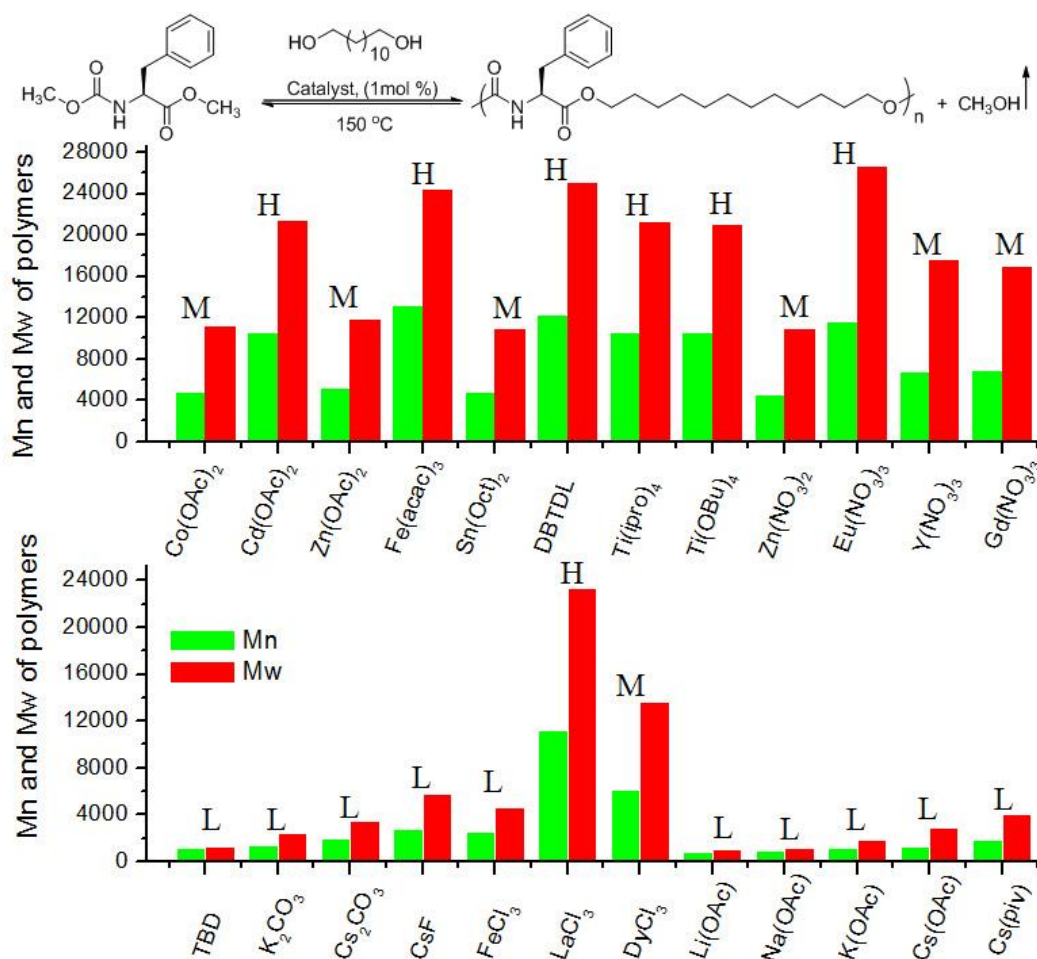
Figure 3.9. *Molecular weights (M_n and M_w) of linear poly(ester-urethane)s made by various catalysts at 150 °C. The molecular weights of the polymers were classified into L-low ($< M_n = 3000$ g/mol), M-moderate ($M_n = 3000$ to 9000 g/mol) and H-high ($M_n > 9000$ g/mol) for comparison purpose.*

The molecular weights of the poly(ester-urethane)s produced by more than 20 catalysts are plotted and shown in figure 3.9. Among the tin catalysts, $Sn(Oct)_2$ catalyst afforded moderate molecular weight whereas DBTDL gave higher molecular weight polymer. Titanium based catalysts $Ti(OBu)_4$ and $Ti(iOpr)_4$ catalysts were found to be producing high molecular weight poly(ester-urethane)s. Based on the molecular weight of the polymers (in figure 3.9), the catalysts were divided into three different categories: (i) low molecular weight catalyst [$\leq M_n = 3000$, Li(OAc), Na(OAc), K(OAc), Cs(OAc), Cs(OiPv), K_2CO_3, Cs_2CO_3, CsF, $FeCl_3$ and TBD], (ii) moderate molecular weight catalyst [$\leq M_n = 9000$, Co(OAc), Zn(OAc), $Zn(NO_3)_2$, $Y(NO_3)_3$, $Gd(NO_3)_3$, Sn (Oct)$_2$ and $DyCl_3$] and (iii) high molecular weight catalyst ($M_n > 9000$, $Ti(OBu)_4$, $Ti(iOpr)_4$, $Fe(acac)_3$, $LaCl_3$, $Eu(NO_3)_3$, Cd(OAc) and DBTDL]. Though, the above catalyst screening was done in detail for amino acid based on L-phenylalanine it

could in principle be used for other amino acid resources under solvent free melt polycondensation approach to make poly(ester-urethane)s.
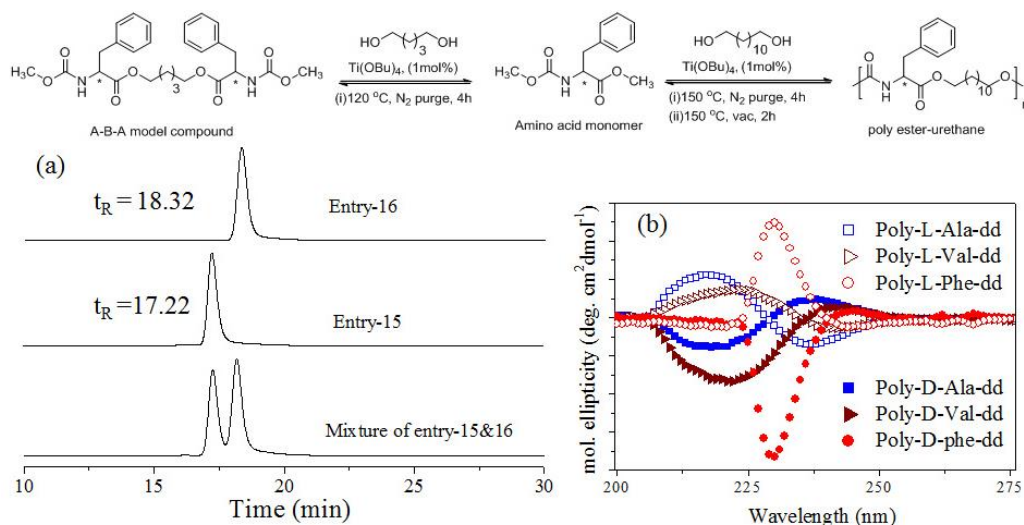

Figure 3.10. *(a) HPLC profiles for D and L- phenyl alanine model reactions at 120 °C. (b) CD spectra of few representative linear poly(ester-urethane)s made by D and L- amino acid monomers at 150 °C.*

3.3.6. Self-assembly of poly (ester-urethane)

The new condensation reaction was investigated for L- and D- phenylalanine and their details are given in table 2, entries 15-16. The phenyl alanine reaction products (entries 15 and 16) were subjected to chiral HPLC analysis. The solvent was chosen was 50:50 v/v ratios of isopropanol and hexane as the eluent and the HPLC profiles were recorded with 0.5 mL/min flow rate. HPLC traces are given in figure 3.10a.[23] The analysis of L-phenyl alanine product (entry 15) showed single peak at retention time t_R = 17.22 minutes. Similarly, the D-phenyl alanine derivative (entry 16) showed a peak at t_R 18.32 minutes. To further confirm these t_R with respect to the particular isomers, the product of D- and L- (entries 15 and 16) were mixed in equal amounts and subjected to HPLC analysis. It showed two signals at t_R = 17.22 and 18.32 minutes for L- and D- enantiomers, respectively. Thus, the HPLC traces confirmed that the high temperature chemoselective reaction is also stereospecific and retained the L and D enantiomers with more than > 99 % purity in analog to the amino acid source. Further, the poly(ester-urethane) were subjected to circular dichroism (CD) analysis to confirm their optical purity (chiral HPLC analysis are not possible for high molecular weight polymers). The L-alanine and L-valine based poly(ester-urethane) showed a positive CD band at 217 nm and a negative band at 237 nm (in Figure 3.10b). On the other hand, D-alanine and D-valine based poly (ester-

urethane) showed a negative CD band at 217 nm and a positive CD band at 237 nm (in figure 3.10b). The CD signals were attributed to the right and left handed β-sheet conformation.[24-25] A similar trend was also observed in L- and D-phenyl alanine based products at 230 nm with respect to right and left-handed polyproline type-II secondary structures (in figure- 3.10b).[26] Interestingly L and D isomer of amino acid polymers perfectly retained their optical activity at high temperature reaction condition. This confirmed that the high temperature condensation chemistry is also very good for making exclusively right or left handed helical polymers.
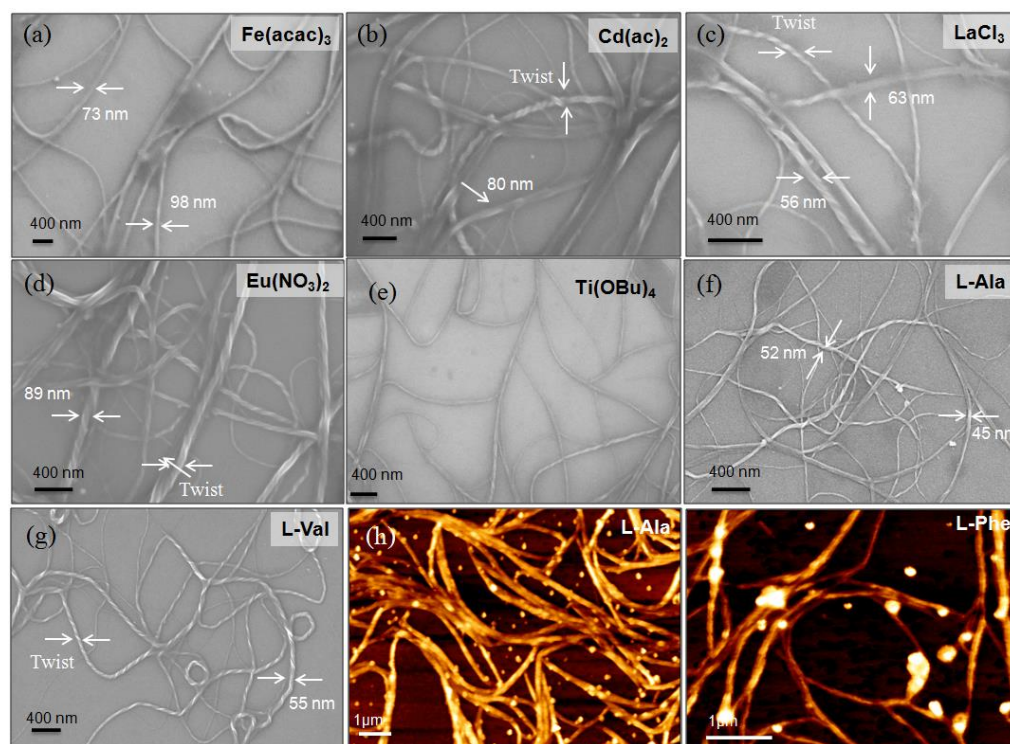

Figure 3.11. *Field emission scanning electron microscopy (FE-SEM) images of phenylalanine based linear poly(ester-urethane)s synthesized by various catalysts (a to e). FE-SEM images of poly(ester-urethane)s from L-alanine (f) and L-valine monomers (g). Atomic force microscopy images of poly(ester-urethane)s from L-alanine (h) and L- phenylalanine(i). All these images were recorded for drop cast film of polymer solution (in THF, 0.1 mg/mL) at 25 ℃.*

To study the self-assembly of amino acid based poly(ester-urethane)s the polymers were subjected to electron and atomic microscopy analysis. Field emission scanning electron microscope (FE-SEM) images for the polymer were recorded for the drop cast films (from tetrahydrofuran solution) and the images are shown in figure 3.11. To study the role of catalysts on the morphology of poly(ester-urethane), the phenylalanine polymers synthesized by various catalysts were analyzed by FE-SEM (in figure 3.11a-e). The FE-SEM images of the linear polymers produced by these

catalysts showed helical nanofibrous morphology. The thickness of fibers was obtained as 59 ± 8 nm and the length of the fibers varied up to few micrometers. The poly(ester-urethane)s produced by various amino acid resources were also analyzed by FE-SEM. For example, the polymers produced by the L-alanine and L-valine also showed helical nano-fibrous morphologies (in figure 3.11f-g). Further to confirm the morphology of poly(ester-urethane), they were subjected to imaging by atomic force microscopy. AFM images of the linear poly(ester-urethane)s showed the existence of thick helical nanofibrous morphology (in figure 3.11h-i). The thickness of the polymers was in the range of 65 ± 6 nm and the length of the fibers varied upto few micrometer. These studies revealed that the polymers exhibited nanofiber morphology which was retained irrespective of the catalysts or amino acids employed for the melt condensation polymerizations.
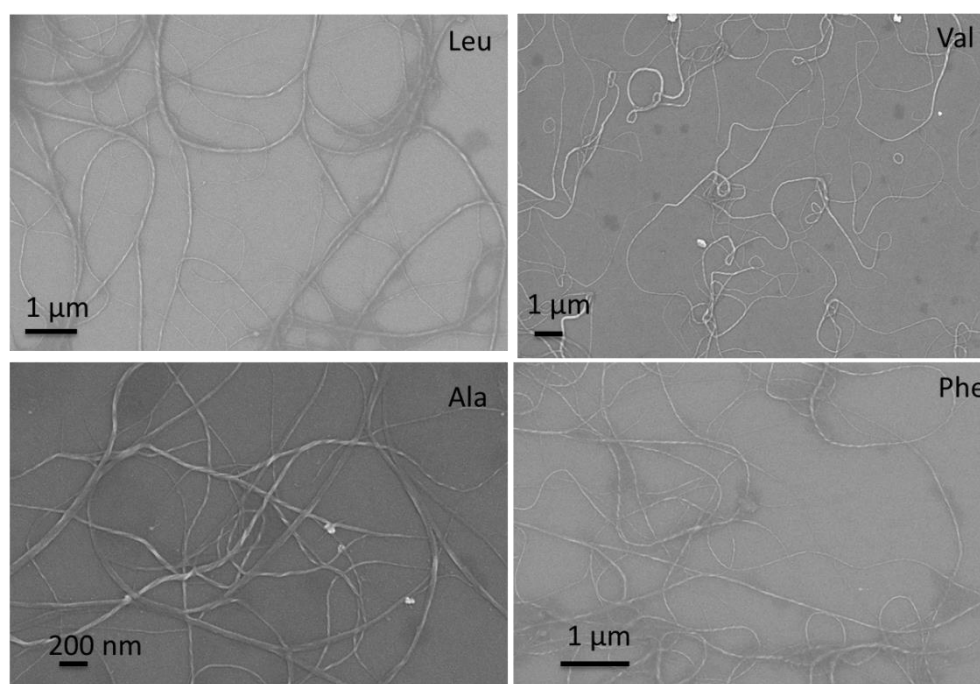
Figure 3.12. *FE-SEM images for various amino acid based poly (ester-urethane)s with same catalyst*

The plausible mechanism for the polymer self-assembly of the poly (ester-urethane)s is attributed to urethane functional polyester chain backbone that contains hydrogen bonded urethane linkages. In solvents like, THF in the present case, the inter-chain interactions in the polymer matrix displayed strong hydrogen bonding network among the chains. FT-IR spectra of the poly(ester-urethane)s showed strong N-H stretching vibration at 3350 cm^{-1} and C=O stretching vibration at 1720 cm^{-1} in corresponds to the existence of hydrogen bonded assemblies. These hydrogen boned

chains undergo subsequent self-assembly to produce long helical nano-fibers. These helical assemblies were observed as nano-fibrous in the FE-SEM and AFM images (in figure 3.11). The formation of helical assemblies was further affirmed by CD analysis. CD spectra of the polymers showed the existence β-sheet structures, primarily driven by the hydrogen bonding interactions (in figure 3.10b).

Nevertheless, the present investigation provided complete insight into the development of chemoselective polymerization approaches for amino acid based resources under solvent free melt reaction. The concept was very well demonstrated by carefully choosing appropriate model reactions (more than 80 reactions) with wide range of catalysts in the entire periodic table. The concept was successfully translated to the polymer synthesis for making poly(ester-urethane)s. Wide ranges of catalysts were identified for dual ester-urethane polycondensation which are very useful for large scale production of amino acid based polymers for thermoplastic applications. The synthetic approach was also found to be retaining the optical purity of the polymers; moreover helical nano-fibrous morphology of the amino acid polymers could also be employed as template or scaffold for biomedical applications.

3.4. Conclusion:

In conclusion, wide range of catalysts were developed for the melt polymerization of amino acid monomers to produce high molecular weight poly (ester-urethane)s under solvent free melt process. Both the temperature and catalysts were found to be main driving factors in the condensation process. The ester part showed exclusive reactivity towards alcohols at 120 °C in the presence of appropriate catalysts while keeping the urethane part non-reactive. Wide range of catalysts from alkali, alkali earth metal, transition metal and lanthanides were traced for this process. Based on the control reactions; new types of A-B and A-B-A species were produced. At 150 °C, the monomers underwent dual ester-urethane condensation to produce poly(ester-urethane)s. The molecular weights of these polymers were found to be highly selective with respect to the types of the catalysts. More than 20 efficient catalysts were identified for poly(ester-urethane)s to yield moderate to high molecular weight polymers. The process was investigated using D and L- amino acid monomers. Chiral HPLC analysis clearly supported that the optical isomers were retained in the same conformation (D or L) of their starting materials and the process also turned to

be effective in retaining their optical purity. CD spectra of D and L- amino acid poly(ester-urethane)s retained their optical purity and showed opposite signals. FE-SEM and AFM analysis confirmed that these polymers were found to exhibit helical nano-fibrous morphology. The nano-fibrous morphology was retained irrespective of the catalysts or amino acid resources, confirming that the newly developed polymerization process is very efficient in making self-assembled polymers. Though, the new approach has been demonstrated here only to amino acid based monomers; in principle, this approach can be expanded to any bi-functional monomers having ester and urethane functionalities.

3.5. Reference

1. Odian, G. *Principles of Polymerization*; John Wiley & Sons. Inc.: New York, **1991**; Third Ed.,

2. Kricheldrof, H. R.; Nuyken, O.; Swift, G. *Handbook of Polymer Synthesis: Second Edition (Plastics Engineering).* **2004***,* CRC Press; Second Ed.,

3. Pang, K.; Kotek, R.; Tonelli, A. Prog. Polym. Sci., **2006**, *31*, 1009–1037.

4. Vilela, C.; Sousa, A. F.; Fonseca, A. C.; Serra, A. C.; Coelho, J. F. J.; Freire, C. S. R.; Silvestre, A. J. D. *Polym. Chem.* **2014**, *5*, 3119-3141.

5. Jacquel, N.; Freyermouth, F.; Fenouillot, F.; Rousseau, A.; Pascault, J. P.; Fuertes, P.; Saint-Loup, R. *J. Polym. Sci. Polym. Chem.* **2011,** *49,* 5301-5312.

6. Serio, M. D.; Tesser, R.; Trulli, F.; Santacesaria, E. *J. Appl. Polym. Sci.,* **1996**, *62*, 409-415.

7. Zahedi, P.; Arefazar, A. *J. Appl. Polym. Sci.,* **2008**, *107*, 2917-2922.

8. Ignatov, V. N.; Pilati, F.; Berti, C.; Tartari, V.; Carraro, C.; Nadali, G.; Fiorini, M.; Toselli, M. *J. Appl. Polym. Sci.,***1995**, *58*, 771-777.

9. Kricheldorf, H. R.; Masri, M. A.; Lomadze, N.; Schwarz. G. M*acromolecules* **2005**, *38*, 9085-9090.

10. Buzin, P.; Lahcini, M.; Schwarz, G.; Kricheldorf, H. R. *Macromolecules* **2008**, *41*, 8491-8495.

11. Moyori, T.; Tang, T.; Takasu. *Biomacromolecules* **2012**, *13*, 1240-1243.

12. Park, S. S.; Im, S. S.; Kimz, D.K. *J. Polym. Sci. Polym. Chem.* **1994,** *32, 2873-*2881.

13. Vert. M. *Biomacromolecules* **2005**, *6*, 538-546.

14. Moyori, T.; Tang, T.; Takasu. *Biomacromolecules* **2012**, *13*, 1240-1243.

15. Takasu, A.; Makino, T.; Yamada, S. M*acromolecules* **2010**, *43*, 144-149.

16. Takasu, A.; Oishi, Y.; Iio Y.; Inai, Y.; Hirabayashi, T. M*acromolecules* **2003**, *36*, 1772-1774.

17. Ishi, M.; Okazaki, M.; Shibasaki, Y.; Ueda, M. *Biomacromolecules* **2001**, *2*, 1267-1270.

18. Guo, B.; Chen, Y.; Lei, Y.; Zhang, L.; Zhou, W. Y.; Rabie, A. B. M.; Zhao, J. *Biomacromolecules* **2011**, *12*, 1312-1321.

19. Shigemoto, I.; Kawakami, T.; Taiko, H.; Okumura, M. *Polymer* **2011**, *52*, 3443-3450.

20. Anantharaj, S.; Jayakannan, M. *Biomacromolecules* **2012**, *13*, 2446-2455.

21. Deetz, M. J.; Forbes, C. C.; Jonas, M.; Malerich, J. P.; Smith, B. D.; Wiest, O. *J. Org. Chem.* **2002***, 67,* 3949-3952.

22. Ziao, N.; Laurence, C.; Questel, J. Y. L. *Cryst Eng Comm*, **2002**, *4*, 326-335.

23. Mali, S. M.; Bandyopadhyay, A.; Jadhav, S. V.; Kumar, M. G.; Gopi, H. N.; *Org, Biomol. Chem.* **2011**, *9*, 6566-6574.

24. Violette, A.; Averlant-Petit, M. C.; Semetey, V.; Hemmerlin, C.; Casimir, R.; Graft, R.; Marraud, M.; Braiand, J. P.; Rongnan, D.; Guichard, G. *J. Am. Chem. Soc.* **2005**, *127,* 2156-2164.

25. Sinaga, A.; Hatton, T. A.; Tam, K. C. *Biomacromolecules* **2007**, *8*, 2801-2808.

26. Shi, Z.; Olson, C. A.; Rose, G. D.; Baldwin, R. L.; Kallenbach, N. R. *Proc. Natl. Acad. Sci. U.S.A.* **2002***, 99*, 9190.

Chapter 4

Amyloid-like Hierarchical Helical Fibrils and Conformational Reversibility in Functional Polyesters Based on L-Amino acids

Chapter 4

Amyloid-like Hierarchical Helical Fibrils and Conformational Reversibility in Functional Polyesters Based on L-Amino acids

The present investigation reports synthetic polymers capable of undergoing reversible conformation transformation that self-assembled to give hierarchical helical amyloid-like fibrils. A new temperature selective melt polycondensation reaction was developed for amino acid monomers of L-aspartic acid and L-glutamic acid to produce high molecular weight linear functional polyesters.These new polyesters have hydrogen bonded urethane (or carbamate) units in each repeating unit.The polymer chains adopted expanded chain conformation through β-sheet hydrogen bonding interactions and produced twisted ribbon-like assemblies.These twisted ribbons have subsequently underwent inter-chain folding for making double helical structures. The double helical fibrils aligned together to produce amyloid-like fibrils of few micrometer in length. Upon chemical de-protection of the pendent urethane units; the resultant cationic functional polyester adopted coil-like conformation and formed spherical charged nano-particles of 200 ± 20 nm in size. Dynamic light scattering and Zeta potential measurements revealed that both the charge and size of the spherical structures could be varied by altering the diol segment length in the polymer backbone.The coil-like chains in the charged spherical particles could be reversibly expanded into amyloid-like fibrils via fluorophore chemical substitution using dansyl chloride.The dansyl substituted polymer formed helical fibrils and showed strong fluorescence.Thus the L-amino acid based polyesters exhibited reversible conformation changes from hierarchical helical amyloid-like fibrils to charged nano particles and vice versa in a single polymer system.These L-amino acid based non-peptide polyester analogues, their amyloid fibrils, cationic polymer spherical assemblies and fluorescent fibrils are new in the literature L-amino acid which may be useful for biomedical applications.

4.1. Introduction

Helical self-assemblies of synthetic polymers into secondary structures of proteins, DNA or RNA are important for the development of new functional biomaterials for therapeutics as well as fundamental understanding of reversible self-assembly in macromolecular system.[1-3] Self-assembly of oligo-peptides into amyloid-like fibril networks are of immense importance since their occurrence is directly associated with a range of neurodegenerative diseases like Alzeimer's, Parkinsons' and Prion, etc.[4-5] Amyloid fibrils are thermodynamically stable species and their disassembly process does not occur spontaneously which is one of the major challenging tasks in curing these diseases.[6] Amyloid fibrils are formed by parallel (or anti-parallel) alignment of β-sheet structures that are separated by a distance of 10-15 Å.[7] These β-sheets are held together by non-covalent interactions such as hydrogen bonding, hydrophilic/hydrophobic or columbic forces that facilitates the formation of long fibril netwroks (in figure 4.1).[8-9] A large number of structurally different proteins (or peptides) are found to produce amyloid-fibrils and the formation of these fibrils does not seem to be specific to any particular peptide sequence or vitro and in vivo conditions.[10-11]
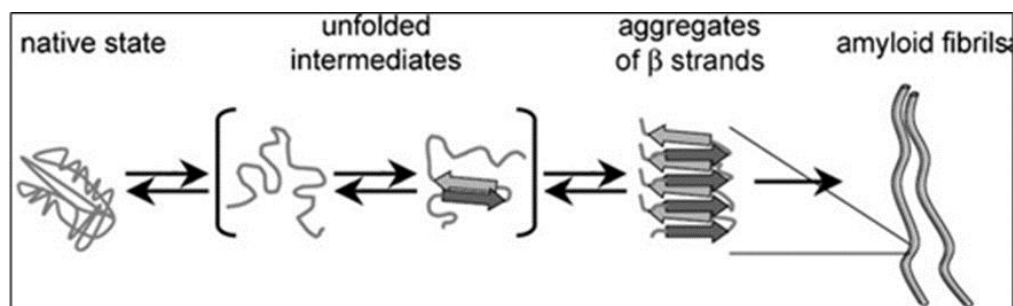

Figure 4.1. *Schematic representation of amyloid fibril formation (adopted from Cherny et al. Angew. Chem. Int. Ed. 2008, 47, 4062 -4069)*

Diverse chemical structures such as elastin-like synthetic peptides,[12] amphiphilic oligopeptides,[13] cross β-sheet oligo peptides,[8] peptide-dendron hybrids,[14] and amino acid (or oligopeptide) anchored polymers[15-18] were reported to exhibit amyloid-like fibrils. Yamada et al. fabricated amyloid like fibril formation from amphiphilic tripeptide structure,[8] which showed strong anti-parallel β-sheet secondary structure conformation. Shao et al. developed peptide-dendron hybrid structure for reversible morphology between fibrillar and nanotube aggregates depending upon the pH value or salt concentration (in figure 4.2). At pH 7.4, the peptide-dendron

structure showed nanofiber morphology, whereas decreasing pH to 5.5 converted nanofiber to nanotube structure (in figure 4.2b).[14] The pH dependent changes in the self-assembly of the structure was applied for loading and delivering of hydrophobic Nile red dye (in figure 4.2a); in this process at high pH (7.4) it could load the Nile red hydrophobic dye, whereas at low pH (5.5) it released the dye completely.
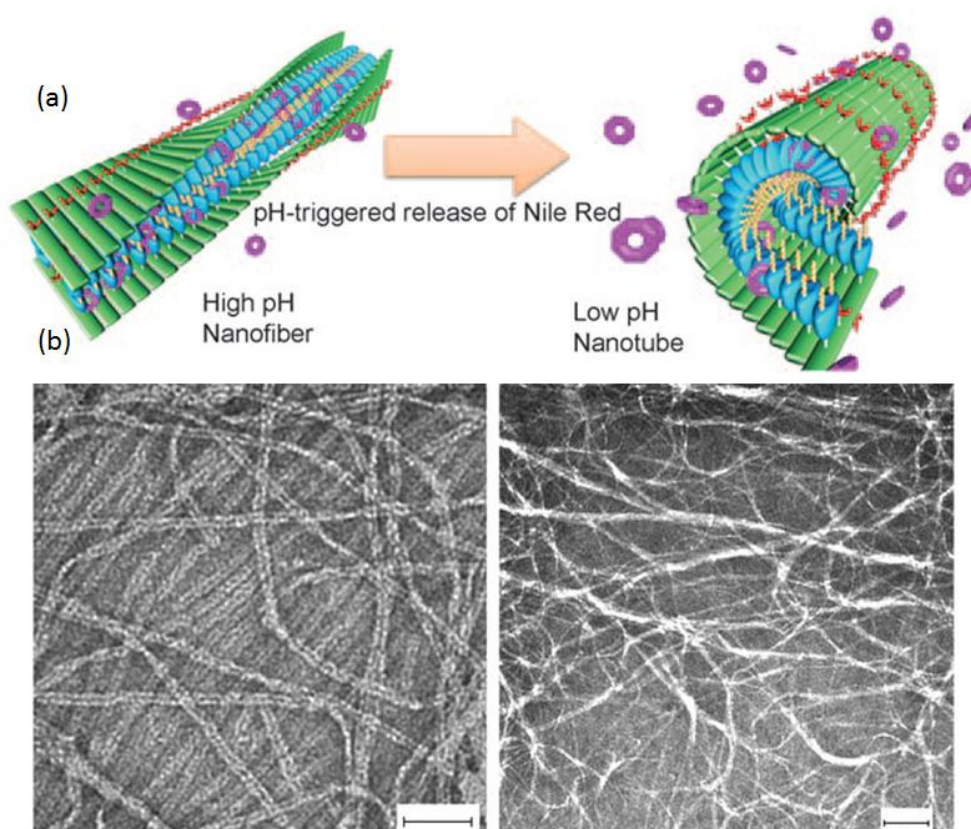

Figure 4.2. *pH dependent release of Nile red dye (a) and morphology changes from nanotube (pH=1) to nanofiber (pH=7.4) (b) (adopted from Shao et al. Angew. Chem. Int. Ed.* **2009***, 48, 2525-2528)*

Dzwolak et al. developed amyloid like fibril morphology based on poly L-lysine and poly D-lysine polymer chains interaction CD signal was observed be change from α-helix to β-sheet secondary structure by varying the temperature (in figure 4.3a-4.3b).[9] Dehn et al. demonstrated the control of β-sheet (amyloid like fibril) formation by attaching the β-sheet forming peptide chain with polymer; these polymer tend to disturb the self-assembly of peptide chain (in figure 4.3c).[18] Theoretical models,[19] X-ray diffraction,[20] near-field IR spectroscopy[21] and fluorophore encapsulation studies[22-23] were utilized to trace the physiological conditions or environments that are required for the formation of these fibrils. These studies

emphasised the importance of the amyloid fibril formation in proteins and oligo-peptides; however, more insight is required in terms of new structural designs to achieve reversible amyloid-like fibrils self-assembly and to elucidate the mechanism of fibril formation and the associated diseases.
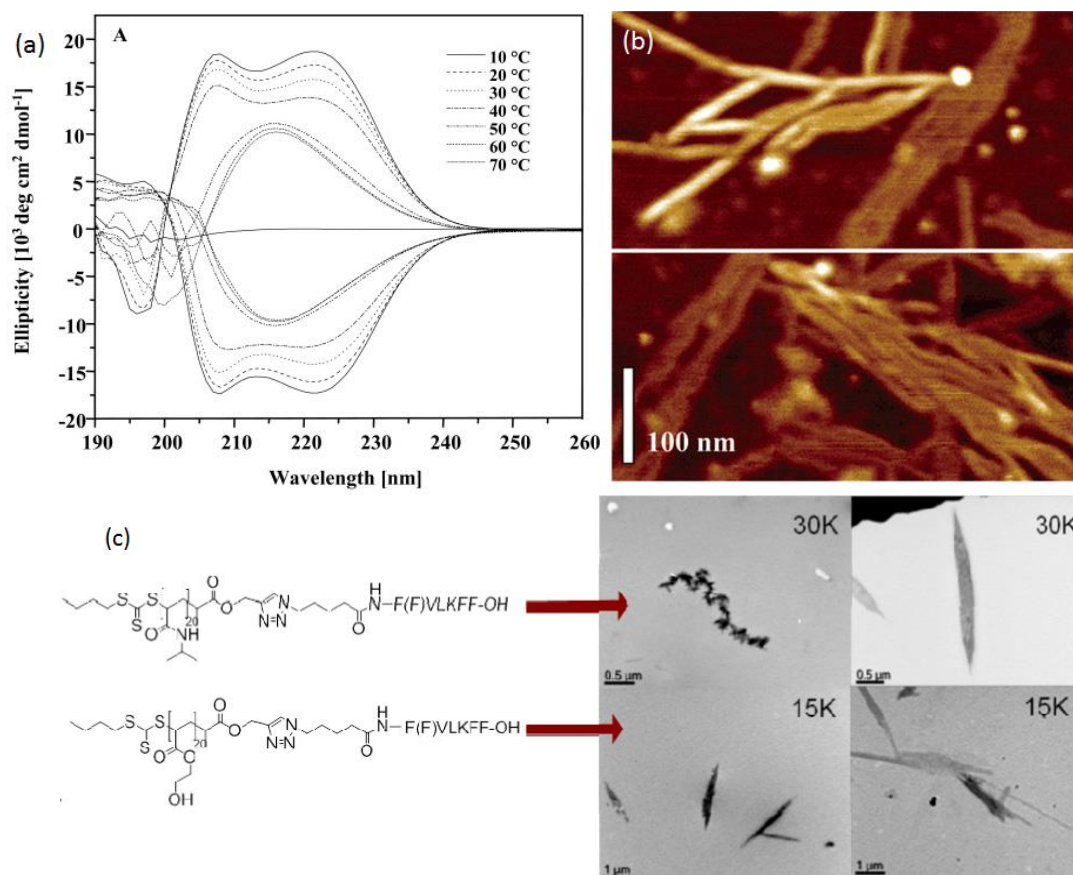

Figure 4.3. *The temperature depend CD spectra of Poly lysine (a) and their AFM image (b) control of self-assembly via attaching the polymer chain with peptides (c)(adopted from Dzwolak et al. J. Am. Chem. Soc.* **2004**, *126, 3762-3768 (a-b) and Dehn et al. Biomacromolecules* **2012**, *13, 2739-2747 (c)*

The development of new synthetic polymers that are capable of resembling biological materials such as amyloid-fibrils would be very useful artificial-peptide mimics for wide range of biomedical application in tissue engineering and scaffolds for drug delivery, etc.[24] L-Amino acids are natural building blocks in peptides and proteins; their sequence, appropriate charge and hydrophobicity control the protein secondary structures and enzymatic function in biological systems. High molecular weight polypeptides are typically produced by ring opening polymerization (ROP) of N-carboxyanhydride (NCA) intermediates of L-amino acids.[25-28] Cationic or anionic charged polypeptdies like poly(L-lysine)s, ε-poly-L-lysine, poly(L-glutamic acid) and

poly(L-aspartic acid)s were also produced by ROP route.[27] Recently Fandrich et al.[4,28] reported amyloid-like fibrils in these charge polypeptides.
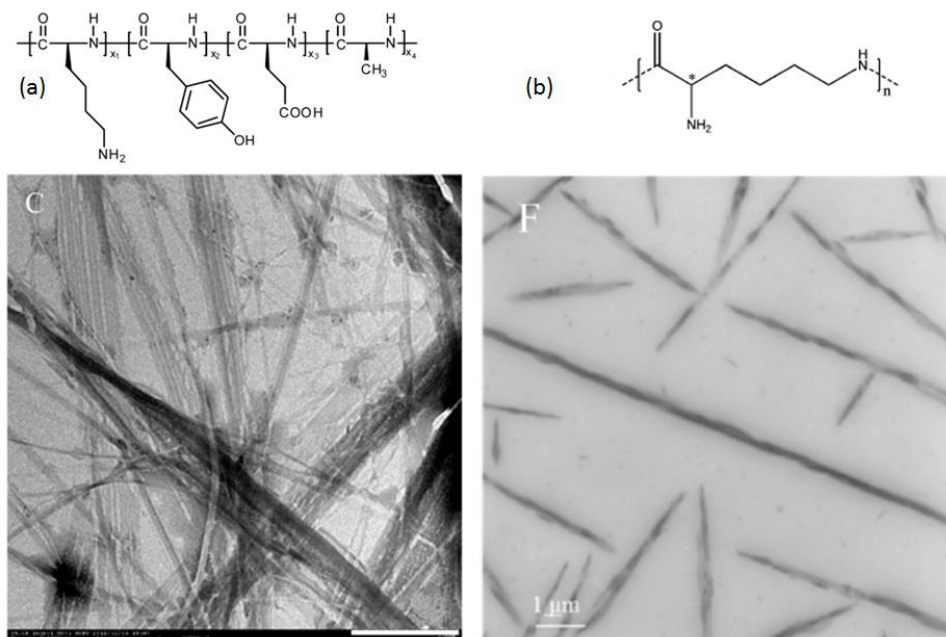

Figure 4.4. *Amyloid-like fibril formation from random copolymer based on polypeptides (a) and poly L-lysine (b) (adopted from Lai et al. Langmuir* **2014***, 30, 7221−7226 (a) Biomacromolecules* **2013***, 14, 4515-4519(b))*

Lai et al. demonstrated the formation of amyloid fibril aggregates based on random copolymers of four different amino acids containing polypeptides (in figure 4.4a). Same author reported the amyloid-like fibrils formation by poly L-lysine containing polypeptides (in figure 4.4b). It was a rather surprise to notice that there was no specific requirement for side chain interactions or sequence to produce amyloid-fibrils. Unlike in the case of protein self-assembly which was precisely driven by the side chain sequences and spherical folding, these charged polypeptides produced amyloid fibrils primarily through main chain interaction.[28] Unfortunately, these peptides (or oligo-peptides) have restricted chain mobility to undergo reversible conformation transformation due to the presence of strong hydrogen bonded amide-linkage (peptide bond) in the polymer chain backbone. Hence, new classes of non-polypetide polymers based on L-amino acids are required to mimic conformational reversibility in amyloid-like fibril formation in synthetic polymers.
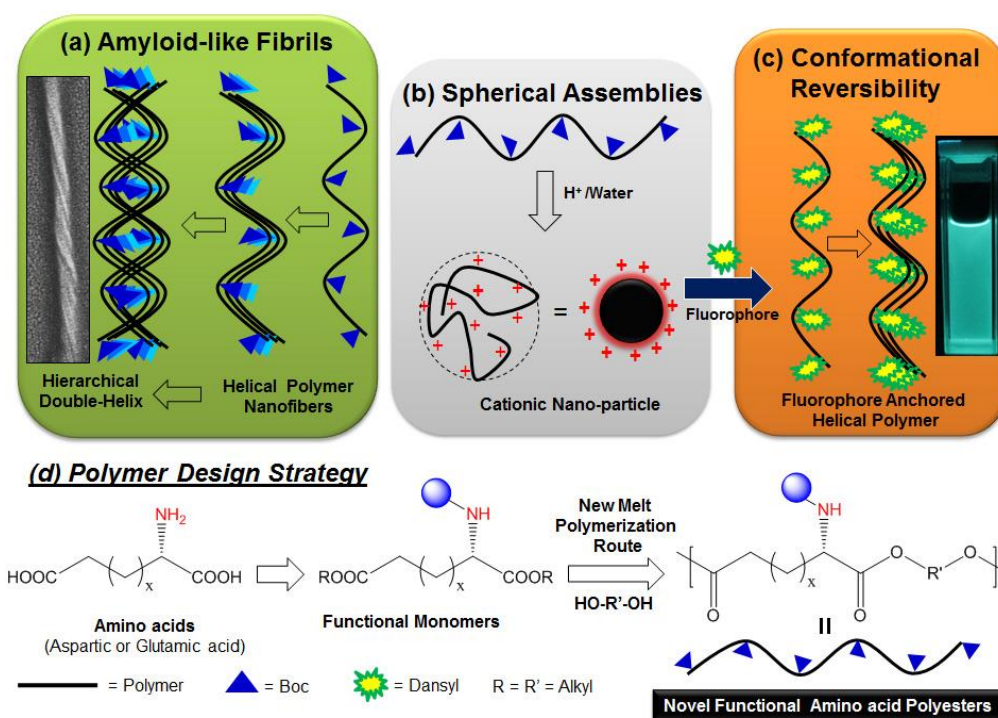
Figure 4.5. *(a) Self-organization of polymer into amyloid-like fibrils. (b) Helical nano-fibril Transformation into cationic coil-like spherical assembly. (c) Reversible conformational expansion via fluorophore (dansyl) substitution. (d) L-Amino acid based polymer design and new synthetic approach.*

In chapter-4 the development of new non-peptide functional polyesters based on natural L-amino acids that underwent reversible self-organization from amyloid-like fibrils to collapsed coil-like spherical structures are reported (in figure 4.5). The newly designed synthetic polyester self-assembled through β-sheet hydrogen bonding interactions to produce amyloid-like fibrils consisting of hierarchical double helical structures. Upon de-protection, the amyloid fibrils underwent coil-like conformational change to produce cationic spherical nano-particles in aqueous medium. Reversible conformational change from the spherical species to expanded fibril structures was achieved via fluorophore substitution. To achieve the above goal, new functional polyesters was synthesized by suitably modifying our recently developed *novel dual trans ester-urethane* melt condensation approach to poly(ester-urethane)s. In the present investigation, our earlier melt process was converted into *temperature selective transesterification polycondensation* by appropriately choosing the polymerization protocols for multi-functional L-amino acid monomers. Two multi-

functional amino acids: L-glutamic and L-aspartic acids were chosen for the above purpose and polymerized with diols under melt conditions to produce high molecular weight functional polyesters (in figure 4.5). The size and shape of the amyloid fibrils and spherical assemblies were studied by dynamic light scattering, water contact angle measurements, Zeta potential, electron and atomic force microscopes, etc. The newly developed amino acid based polymers and their self-assembled amyloid-fibrils, spherical charge nano-particles and fluorescent amyloid-fibrils.

4.2. Experimental methods

4.2.1. Materials: L-Aspartic acid, L-glutamic acid, 1,12-dodecandiol, 1,10-decanediol, 1,8-octanediol, 1,6-hexanediol, 1,4-butanediol, dansyl chloride, titanium tetrabutoxide Ti(OBu)$_4$ were purchased from Aldrich chemicals and used without further purification. methylchloroformate, thionyl chloride, Boc anhydride and other solvents were purchased locally and purified prior to use.

4.2.2. General Procedures: ^{1}H and ^{13}C-NMR were recorded using 400-MHz JEOL NMR Spectrophotometer. All NMR spectra were recorded in CDCl$_3$ containing TMS as internal standard. FT-IR spectra of all compounds were recorded using Bruker alphaT Fourier transform infrared spectrophotometer. The mass of the monomers were analysed using a HRMS-ESI-Q-time-of-flight LCMS (SynaptG2, Waters). Gel permeation chromatographic (GPC) analysis which was performed using Viscotek VE 1122 pump, Viscotek colum T6000M General mixed org 300 x 8.0 mm (THF), Viscotek colum D6000M General mixed org 300 x 8.0 mm (DMF), Viscotek VE 3580 RI detector and Viscotek VE 3210 UV/Vis detector in tetrahydrofuran (THF) and dimethyl formamide (DMF) using polystyrene as standards at 25 °C. Thermal stability of the polymers was determined using Perkin Elmer thermal analyzer STA 6000 model at a heating rate of 10 ^{o}C/min in nitrogen atmosphere. Thermal analysis of all polymers was performed using TA Q20 Differential Scanning Calorimeter. The instrument was calibrated with Indium standards. All the polymers were heated to melt before recording their thermograms to remove their previous thermal history. Polymers were heated and cooled at 10 °C/min under nitrogen atmosphere and their thermo grams were recorded. Circular dichroism (CD) analysis of the polymer samples was done using JASCO J-815 CD spectrometer at 20 °C in THF and water. Water contact angle measurements of the functional polymers were done on a GBX

model (DIGIDROP contact angle instrument) using Windrop software. To avoid the evaporation effects in the sessile contact angle measurements, measurements were monitored contact angle values within one minute. All contact angle measurements were carried out at room temperature (27 °C) under constant humidity (40−50%). The size of the amine functional polymers were carried out by dynamic light scattering (DLS) using a Nano ZS-90 apparatus by 633 nm red laser (at 90° angle) from Malvern Instruments. FE-SEM images were recorded using Zeiss Ultra Plus scanning electron microscope. For FE-SEM analysis, the samples were prepared by drop casting on silicon wafers and coated with gold. TEM images were recorded using a Technai-200 instrument by drop casting the sample on Formvar-coated copper grid. Atomic force microscope (AFM) images were recorded by drop casting the samples on freshly cleaved mica surface, using Veeco Nanoscope IV instrument. The experiment was done in tapping mode. The absorption spectra were recorded using Perkin-Elmer Lambda 45 UV−vis spectrophotometer. The emission studies were done using SPEX Fluorolog HORIBA JOBIN VYON fluorescence spectrophotometer with a double-grating 0.22 m Spex1680 monochromator and a 450 W Xe lamp as the excitation source at room temperature.

4.2.3. Synthesis of dimethyl 2-((tert-butoxycarbonyl) amino) pentanedioate (monomer 1a): L-Glutamic acid (20.0 g, 0.136 mol) in dry methanol (200 mL) was taken in three neck RB flask (500 mL capacity). Thionylchloride (42.0 mL, 68.9 g, 0.579 mol) was added drop wise under nitrogen atmosphere at 0 °C. The above reaction mixture was allowed to warm to room temperature and it was refluxed for 12 h by under nitrogen atmosphere. The methanol and excess of thionylchloride were removed under reduced pressure. The solid mass was stirred in a mixture of $NaHCO_3$ solution (57.1 g, 0.680 mol, 250 mL of H_2O) and tetrahydrofuran (250 mL) at 0 °C. To the reaction mixture, Boc anhydride (32.0 mL, 0.147 mol) was added drop wise at 0 °C. It was allowed to warm and the stirring continued for 12 h at 25 °C. The organic solvent was removed and the reaction mixture was extracted using dichloromethane. The organic layer was dried over anhydrous Na_2SO_4 and the solvent was removed to obtain clear liquid as product. It was further purified by passing through silica gel column using ethyl acetate and pet ether (1:4 v/v) as eluent. Yield = 33.2 g (89 %). ^{1}H NMR (400 MHz, $CDCl_3$) δ ppm: 5.11 (b, 1H, -N**H**), 4.33 (m, 1H,

C**H**), 3.74 (s, 3H, CHCOOC**H₃**), 3.68 (s, 3H, CH₂COOC**H₃**), 2.40 (m, 2H, C**H₂**COOCH₃), 2.17 (m, 1H, CH₂C**H₂**CH), 1.95 (m, 1H, CH₂C**H₂**CH) and 1.43 (s, 9H, -NHCOO (C**H₃**)**₃**). ¹³C-NMR (100 MHz, CDCl₃) δ ppm: 173.31, 172.80, 155.46, 80.17, 52.97, 52.57, 51.94, 30.18, 28.42 and 27.93. FT-IR (cm⁻¹): 3837, 3743, 3617, 3366, 2976, 2360, 1706, 1513, 1442, 1364, 1250, 1209, 1158 and 1051. HRMS (ESI⁺): m/z [M+Na⁺] calcd. for $C_{12}H_{21}NO_6Na$ [M⁺]: 298.1266; found: 298.1273.

L-Aspartic monomer **1b** and L-glutamic methyl monomer were prepared following the above procedures and the details are provided below.

L-Glutamicacid Methyl Monomer: L-Glutamicacid methyl ester HCl (14.7 g, 0.070 mol), methylchloroformate (14.7 g, 12.0 mL, 0.155 mol) and sodium carbonate (16.3 g, 0.155 mol) were used following the procedure of **1a**. Yield=10.1 g (81%). ¹H NMR (400 MHz, CDCl₃) δ ppm: 5.10 (b, 1H, -N**H**), 4.39 (m, 1H, C**H**), 3.75 (s, 3H, COOC**H₃**), 3.68 (s, 6H, -CH₂COOC**H₃,** -NHCOOC**H₃**), 2.42 (m, 2H, C**H₂**COOCH₃), 2.19 (m, 1H, -C**H₂**) and 1.99 (m, 1H, -C**H₂**). ¹³C-NMR (100 MHz, CDCl₃) δ ppm: 173.29, 172.48, 156.70, 53.41, 52.69, 51.91, 30.07 and 27.74. FT-IR (cm⁻¹): 3615, 3348, 2956, 1708, 1526, 1441, 1354, 1258, 1204 and 1061. HRMS (ESI+): m/z [M+Na⁺] calcd. for $C_9H_{15}NO_6$ Na[M⁺]: 256.0796; found: 256.0795.

L-Asparticacid BOC Monomer: L-Aspartic acid (25.1 g, 0.188 mol), methanol (500 mL) and trimethylsilyl chloride (105 mL, 90.2 g, 0.83 mol). L-Aspartic acid methyl ester HCl (37.0 g, 0.188 mol), Boc anhydride (45 mL, 0.206 mol) and triethylamine (170 mL) were used following the procedure of **1a**. Yield=52.6 g (78%). ¹H NMR (400 MHz, CDCl₃) δ ppm: 5.49 (b, 1H, -N**H**), 4.58 (m, 1H, C**H**), 3.76 (s, 3H, COOC**H₃**), 3.69 (s, 3H, -CH₂COOC**H₃**), 3.03-2.79 (m, 2H, C**H₂**COOCH₃), 1.45 (s, 9H, -NHCOO (C**H₃**)**₃**). ¹³C-NMR (100 MHz, CDCl₃) δ ppm: 171.66, 171.56, 155.49, 80.29, 52.85, 52.14, 50.03, 36.78 and 28.40. FT-IR (cm⁻¹): 3854, 3743, 3677, 3647, 3617, 3566, 2360, 1738, 1698, 1650, 1541, 1507, 1343, 1269, 1215, 1154 and 1029. HRMS (ESI+): m/z [M+Na⁺] calcd. for $C_{11}H_{19}NO_6$ Na[M⁺]: 284.1109; found: 284.1118.

4.2.4. Polycondensation Process: L-Glutamic monomer **1a** (2.14 g, 0.008 mol) and 1, 10-decanediol (1.35 g, 0.008 mol, for polymer **PG-10**) were taken in a test tube-shaped polymerization vessel and melted by placing the tube in oil bath at 100 °C. The polycondensation apparatus was made oxygen and moisture free by purging with

nitrogen and consequent evacuation by vacuum under constant stirring. Titanium tetrabutoxide (0.026 g, 0.08 mmol, 1.0 mol%). was added as catalyst and the melt polycondensation was carried out at 120 ^{o}C for 4h with constant stirring under nitrogen purge. During this stage, the methanol was removed along with the purge gas and the polymerization mixture became viscous. The viscous melt was further subjected to high vacuum (0.01 mm of Hg) at 120 ^{o}C for 2 h under stirring. At the end of the polycondensation, the polymer was obtained as transparent resin. It was purified by dissolving in tetrahydrofuran, filtered and precipitated into methanol to obtain fibrous product. Yield = 2.18 g (81%). ^{1}H NMR (400 MHz, CDCl$_3$) δ ppm: 5.13 (b, 1H, N**H**), 4.30 (m, 1H, C**H**), 4.12 (t, 2H, CH$_2$COOC**H$_2$**), 4.06 (t, 2H, CHCOOC**H$_2$**), 2.43-2.36 (m, 2H, C**H$_2$**COOCH$_2$), 2.18 (m, 1H, CHC**H$_2$**), 1.94 (m, 1H, CHC**H$_2$**), 1.62 (m, 4H, C**H$_2$**), 1.44 (s, 9H, -NHCOO (C**H$_3$**)$_3$) and 1.29-1.25 (m, 12H, C**H$_2$**). ^{13}C-NMR (100 MHz, CDCl$_3$) δ ppm: 172.97, 172.44, 155.60, 80.03, 65.76, 64.96, 53.10, 30.47, 29.53, 28.44, and 25.90. FT-IR (cm^{-1}): 3743, 3617, 3364, 2927, 2856, 2360, 1712, 1510, 1456, 1363, 1252, 1160 and 1051.

Similarly L-glutamic acid monomer **1a** was polymerized with 1,4-butanediol, 1,6-hexanediol 1,8-octanediol and 1,12-dodecanediol to produce PG-X, where X= 4, 6, 8 and 12, respectively. Similarly L-aspartic acid monomer (**1b**) was polymerized with 1,4-butanediol, 1,6-hexanediol 1,8-octanediol, 1,10-decanediol and 1,12-dodecandiol to produce PA-X, where X= 4, 6, 8, 10 and 12, respectively. Their structural details of these polymers are provided below.

Entry-PG-4: Monomers used are L-Glutamic acid Boc monomer (1.70 g, 0.006 mol) and 1,4-butanediol (0.61 g, 0.007 mol), Titanium tetrabutoxide (0.02 g, 0.006 mmol, 1 mol %) were used. Yield =1.54 g (81%). ^{1}H NMR (400 MHz, CDCl$_3$) δ ppm: 5.15 (b, 1H, N**H**), 4.28 (m, 1H, C**H**), 4.15 (t, 2H, CH$_2$COOC**H$_2$**), 4.07 (t, 2H, CHCOOC**H$_2$**), 2.44-2.34 (m, 2H, C**H$_2$**COOCH$_2$), 2.18-2.13 (m, 1H, CHC**H$_2$**), 1.95-1.87 (m, 1H, CHC**H$_2$**), 1.71-1.67 (m, 4H, C**H$_2$**) and 1.41 (s, 9H, -NHCOO(C**H$_3$**)$_3$). ^{13}C-NMR (100 MHz, CDCl$_3$) δ ppm: 172.82, 172.36, 155.54, 80.09, 65.01, 64.23, 64.13, 53.04, 30.35, 28.41, 27.76, 25.30 and 25.20. FT-IR (cm^{-1}): 3364, 2970, 1735, 1511, 1447, 1366, 1210, 1156 and 1049.

Entry-PG-6: Monomers used are L-Glutamic acid Boc monomer (2.61 g, 0.009 mol) and 1,6-hexanediol (1.12 g, 0.009 mol), Titanium tetrabutoxide (0.016 g, 0.05 mmol,

0.5 mol %) were used. Yield =1.70 g (78%). ^{1}H NMR (400 MHz, CDCl$_3$) δ ppm: 5.15 (b, 1H, N**H**), 4.30 (m, 1H, C**H**), 4.13 (t, 2H, C**H**$_2$COOC**H**$_2$), 4.06 (t, 2H, CHCOOC**H**$_2$), 2.43-2.37 (m, 2H, C**H**$_2$COOCH$_2$), 2.18 (m, 1H, CHC**H**$_2$), 1.94 (m, 1H, CHC**H**$_2$), 1.62 (m, 5H, C**H**$_2$), 1.43 (s, 9H, -NHCOO (C**H**$_3$)$_3$) and 1.37 (m, 4H, C**H**$_2$). ^{13}C-NMR (100 MHz, CDCl$_3$) δ ppm: 172.93, 172.43, 155.53, 80.06, 65.51, 64.73, 53.10, 30.45, 28.57, 28.52, 28.43, 27.89, 25.66 and 25.59. FT-IR (cm^{-1}): 3743, 3616, 3364, 2938, 2865, 2360, 1708, 1512, 1454, 1363, 1251, 1158 and 1052.

Entry-PG-8: Monomers used are L-Glutamic acid Boc monomer (1.00 g, 0.004 mol) and 1,8-octanediol (0.53 g, 0.004 mol), Titanium tetrabutoxide (0.013 g, 0.04 mmol, 1 mol %) were used. Yield = 0.82 g (77%). ^{1}H NMR (400 MHz, CDCl$_3$) δ ppm: 5.11 (b, 1H, N**H**), 4.25 (m, 1H, C**H**), 4.07 (t, 2H, C**H**$_2$COOC**H**$_2$), 4.01 (t, 2H, CHCOOC**H**$_2$), 2.35-2.32 (m, 2H, C**H**$_2$COOCH$_2$), 2.11 (m, 1H, CHC**H**$_2$), 1.89 (m, 1H, CHC**H**$_2$), 1.57 (m, 4H, C**H**$_2$), 1.38 (s, 9H, -NHCOO (C**H**$_3$)$_3$) and 1.27 (m, 8H, C**H**$_2$). ^{13}C-NMR (100 MHz, CDCl$_3$) δ ppm: 173.28, 172.77, 80.36, 66.01, 65.22, 53.42, 30.79, 29.52, 28.97, 28.92, 28.74, 28.25, 26.26 and 26.15. FT-IR (cm^{-1}): 3365, 2933, 2859,1734, 1510, 1449, 1365, 1209, 1158 and 1052.

Entry-PG-12: Monomers used are L-Glutamic Boc monomer (2.27 g, 0.008 mol) and 1,12-dodecanediol (1.67 g, 0.008 mol), Titanium tetrabutoxide (0.018 g, 0.06 mmol, 1 mol%) were used. Yield = 1.60 g (84%). ^{1}H NMR (400 MHz, CDCl$_3$) δ ppm: 5.13 (b, 1H, N**H**), 4.31 (m, 1H, C**H**), 4.12 (t, 2H, C**H**$_2$COOC**H**$_2$), 4.06 (t, 2H, CHCOOC**H**$_2$), 2.43-2.38 (m, 2H, C**H**$_2$COOCH$_2$), 1.63-1.94 (m, 2H, CHC**H**$_2$), 1.65-1.59 (m, 5H, CHC**H**$_2$), 1.44 (s, 9H, -NHCOO (C**H**$_3$)$_3$) and 1.28-1.24 (m, 16H, C**H**$_2$). ^{13}C-NMR (100 MHz, CDCl$_3$) δ ppm: 172.91, 172.38, 155.44, 79.96, 65.73, 64.93, 53.05, 30.42, 29.61, 28.36, 25.96 and 25.85. FT-IR (cm^{-1}): 3853, 3743, 3677, 3647, 3616, 2925, 2855, 2360, 1713, 1650, 1510, 1457, 1363, 1253, 1161 and 1052.

Entry-PG-Me-12: Monomers used are L-Glutamic acid methyl monomer (0.90 g, 0.004 mol) and 1,12-dodecanediol (0.78 g, 0.004 mol), Titanium tetrabutoxide (0.014 g, 0.04 mmol, 1.0mol%) were used. Yield = 0.66 g (86%). ^{1}H NMR (400 MHz, CDCl$_3$) δ ppm: 5.38 (b, 1H, N**H**), 4.36 (m, 1H, C**H**), 4.12 (t, 2H, CH$_2$COOC**H**$_2$), 3.66 (S, 3H, NHCOOC**H**$_3$), 2.44-2.35 (m, 2H, C**H**$_2$COOCH$_2$), 2.19 (m, 1H, CHC**H**$_2$), 1.96 (m, 1H, CHC**H**$_2$), 1.61 (M, 4H, C**H**$_2$) and 1.29-1.25 (m, 16H, C**H**$_2$). ^{13}C-NMR (100 MHz, CDCl$_3$) δ ppm: 173.00, 172.18, 156.75, 65.94, 65.07, 53.57, 52.52, 30.41,

29.65, 28.62, 27.85 and 25.91. FT-IR (cm^{-1}): 3853, 3743, 3677, 3616, 3351, 2925, 2854, 2360, 1720, 1524, 1455, 1344, 1259, 1177 and 1062.

Entry-PA-4: Monomers used are L-Aspartic acid Boc monomer (0.98 g, 0.004 mol) and 1,4-butanediol (0.34 g, 0.004 mol), Titanium tetrabutoxide (0.013 g, 0.04 mmol, 0.7 mol %) were used. Yield =0.78 g (82%). ^{1}H NMR (400 MHz, CDCl$_3$) δ ppm: 5.49 (b, 1H, N**H**), 4.55 (m, 1H, C**H**), 4.17 (t, 2H, CH$_2$COOC**H$_2$**), 4.10 (t, 2H, CHCOOC**H$_2$**), 2.95-2.79 (m, 2H, CHC**H$_2$**), 1.70 (m, 4H, C**H$_2$**) and 1.44 (s, 9H, -NHCOO (C**H$_3$)$_3$**). ^{13}C-NMR (100 MHz, CDCl$_3$) δ ppm: 171.54, 171.16, 155.50, 80.24, 65.14, 64.49, 50.10, 36.72, 28.40, 25.20 and 25.11. FT-IR (cm^{-1}): 3743, 3616, 3368, 2972, 1709, 1504, 1454, 1361, 1283, 1154 and 1029.

Entry-PA-6: Monomers used are L-Aspartic acid Boc monomer (0.89 g, 0.003 mol) and 1,6-hexanediol (0.40 g, 0.003 mol), Titanium tetrabutoxide (0.010 g, 0.03 mmol, 1.0 mol%) were used. Yield = 0.76 g (83%). ^{1}H NMR (400 MHz, CDCl$_3$) δ ppm: 5.49 (b, 1H, N**H**), 4.55 (m, 1H, C**H**), 4.13 (t, 2H, CH$_2$COOC**H$_2$**), 4.07 (t, 2H, CHCOOC**H$_2$**), 3.00-2.77 (m, 2H, CHC**H$_2$**), 1.63 (m, 4H, C**H$_2$**), 1.44 (s, 9H, -NHCOO (C**H$_3$)$_3$**) and 1.35 (m, 4H, C**H$_2$**). ^{13}C-NMR (100 MHz, CDCl$_3$) δ ppm: 171.58, 155.84, 80.46, 66.01, 65.34, 50.46, 37.17, 28.73 and 25.91. FT-IR (cm^{-1}): 3837, 3742, 3676, 3616, 3365, 2940, 2864, 2318, 1713, 1506, 1361, 1283, 1156 and 1051.

Entry-PA-8: Monomers used are L-Aspartic acid Boc monomer (0.81 g, 0.003 mol) and 1,8-octanediol (0.45 g, 0.003 mol), Titanium tetrabutoxide (0.010 g, 0.03 mmol, 1mol %) were used. Yield =0.85 g (85%). ^{1}H NMR (400 MHz, CDCl$_3$) δ ppm: 5.52 (b, 1H, N**H**), 4.58 (m, 1H, C**H**), 4.16 (t, 2H, CH$_2$COOC**H$_2$**), 4.10 (t, 2H, CHCOOC**H$_2$**), 2.96-2.75 (m, 2H, C**H$_2$**COOCH$_2$), 1.61 (m, 4H, C**H$_2$**), 1.45 (s, 9H, -NHCOO (C**H$_3$)$_3$**) and 1.32 (m, 10H, C**H$_2$**). ^{13}C-NMR (100 MHz, CDCl$_3$) δ ppm: 170.95, 170.83, 155.20, 79.78, 65.56, 64.88, 49.81, 36.56, 28.89, 28.86, 28.26, 28.22, 28.09, 25.58 and 25.50. FT-IR (cm^{-1}): 3836, 3743, 3617, 3366, 2931, 2859, 1714, 1503, 1393, 1360, 1283, 1158, 1052 and 1024.

Entry-PA-10: Monomers used are L-Aspartic Boc monomer (0.87 g, 0.003 mol) and 1,10-decanediol (0.59 g, 0.003 mol), Titanium tetrabutoxide (0.012 g, 0.03 mmol, 1.0 mol %) were used. Yield = 1.02 g (85 %). ^{1}H NMR (400 MHz, CDCl$_3$) δ ppm: 5.46 (b, 1H, **NH**), 4.54 (m, 1H, C**H**), 4.12 (t, 2H, CH$_2$COOC**H$_2$**), 4.03 (t, 2H,

CHCOOC**H₂**), 2.98-2.75 (m, 2H, CH₂COOC**H₂**), 1.62 (m, 4H, **CH₂**), 1.42 (s, 9H, -NHCOO(**CH₃)₃**) and 1.26 (m, 12H, **CH₂**). ^{13}C-NMR (100 MHz, CDCl₃) δ ppm: 170.94, 170.83, 155.21, 79.77, 65.63, 64.94, 49.82, 36.58, 29.22, 29.00, 28.98, 28.29, 28.25, 28.09, 25.64 and 25.56. FT-IR (cm^{-1}):3448, 3005, 2968, 2930, 2856, 1738, 1499, 1447, 1366, 1220, 1158 and 1051.

Entry-PA-12: Monomers used are L-Aspartic acid Boc monomer (0.80 g, 0.003 mol) and 1,12-dodecanediol (0.63 g, 0.003 mol), Titanium tetrabutoxide (0.01 g, 0.03 mmol, 1.0 mol %) were used. Yield = 1.03 g (84%). ^{1}H NMR (400 MHz, CDCl₃) δ ppm: 5.51 (b, 1H, N**H**), 4.55 (m, 1H, **CH**), 4.13 (t, 2H, CH₂COOC**H₂**), 4.07 (t, 2H, CHCOOC**H₂**), 3.02-2.78 (m, 2H, CH₂COOC**H₂**), 1.61 (m, 4H, **CH₂**), 1.45 (s, 9H, -NHCOO(**CH₃)₃**) and 1.26 (m, 16H, **CH₂**). ^{13}C-NMR (100 MHz, CDCl₃) δ ppm: 172.23, 171.12, 155.50, 80.06, 65.95, 65.25, 63.10, 50.10, 36.87, 32.87, 29.64, 29.60, 29.31, 28.59, 28.55, 28.38, 25.94 and 25.87. FT-IR (cm^{-1}): 3913, 3820, 3747, 3356, 2925, 2854, 1719, 1499, 1462, 1392, 1361, 1284, 1159, 1051 and 1024.

4.2.5. De-protection of functional polyester: PG-10 polymer (0.40 g, 0.001 mol) was dissolved in dry dichloromethane (2.0 mL). Trifluoroacetic acid (0.012 mol, 0.9 mL) was added drop wise into the polymer solution at 0 °C. The mixture was allowed to stir at 25 °C for 2 h. The polymer solution was concentrated and then precipitated into diethyl ether to yield amine functionalized polymer PGA-10. Yield = 0.38 g, (91%) ^{1}H NMR (400 MHz, CD₃OD) δ ppm: 4.18 (m, 2H, CH₂COOC**H₂**), 4.05 (t, 3H, **CH** and CH₂COOC**H₂**), 2.51 (m, 2H, **CH₂**COOCH₂), 2.13 (m, 2H, CHC**H₂**), 1.65-1.59 (m, 4H, **CH₂**), and 1.28-1.24 (m, 12H, **CH₂**). ^{13}C NMR (100 MHz, CD₃OD) δ ppm: 176.26, 172.87, 70.36, 68.75, 65.59, 52.04, 33.24, 33.04, 32.98, 32.34, 32.15, 29.65, 29.52 and 29.27. FT-IR (cm^{-1}): 3582, 3744, 3367, 2927, 2856, 1730, 1673, 1539, 1460, 1422, 1188, 1136 and 1048.

All other polymers PG-X were de-protected as described above to provide PGA-X and the details are provided below.

Entry-PGA-6:PG-6 (0.60 g, 0.002 mol), Trifuluoro aceticacid (2.8 g, 2.0 mL, 0.024 mol) and DCM (5.0 mL) were used. Yield = 0.52 g (84%). ^{1}H NMR (400 MHz, CDCl₃) δ ppm: 4.23 (t, 2H, CH₂COOC**H₂**), 4.09 (m, 3H, **CH** & CHCOOC**H₂**), 2.57 (m, 2H, **CH₂**COOCH₂), 2.17 (m, 2H, CHC**H₂**), 1.66 (m, 4H, **CH₂**) and 1.34 (m, 4H,

CH_2). ^{13}C-NMR (100 MHz, CD_3OD) δ ppm: 176.30, 172.85, 70.22, 68.59, 55.85, 32.99, 32.18, 32.00 and 29.25. FT-IR (cm^{-1}): 2937, 2865, 1670, 1530, 1416, 1185, 1133 and 1054.

Entry-PGA-8: PG-8 (0.60 g, 0.002 mol), Trifuluoro acetic acid (2.8 g, 2.0 mL, 0.024 mol) and DCM (5.0 mL) were used. Yield = (0.54 g, 87%). ^{1}H NMR (400 MHz, CD_3OD) δ ppm: 4.22 (t, 2H, CH_2COOCH_2), 4.08 (m, 3H, CH, CHCOOCH_2), 2.55 (m, 2H, CH_2COOCH_2), 2.16 (m, 2H, CHCH_2), 1.66 (m, 4H, CH_2) and 1.34 (m, 8H, CH_2). ^{13}C-NMR (100 MHz, CD_3OD) δ ppm:176.28, 172.87, 70.34, 68.73, 55.84, 32.99, 32.89, 32.30, 32.11, 29.57, 29.43 and 29.27. FT-IR (cm^{-1}): 2930, 2858,1728, 1671, 1526, 1418, 1186,1134 and 1051.

Entry-PGA-12: PG-12 (0.90 g, 0.002 mol), Trifuluoro acetic acid (2.66 g, 2.0 mL, 0.023 mol) and DCM (5.0 mL) were used. Yield=0.78 g (85%). ^{1}H NMR (400 MHz, CD_3OD) δ ppm: 4.21 (t, 2H, CH_2COOCH_2), 4.08 (m, 3H, CH, CHCOOCH_2), 2.54 (m, 2H, CH_2COOCH_2), 2.15 (m, 2H, CHCH_2), 1.66 (m, 4H, CH_2) and 1.34 (m, 16H, CH_2). ^{13}C-NMR (100 MHz, CD_3OD) δ ppm: 172.88, 70.37, 68.75, 65.60, 36.27, 33.37, 32.98, 32.36, 32.17, 29.68, 29.55 and 29.27. FT-IR (cm^{-1}): 2923, 2853,1731, 1675, 1521, 1460, 1413, 1366, 1186,1137 and 1053.

4.2.6. Post-functionalization of amine functionalized polymer with Dansyl chloride:

PGA-10 amine functionalized polymer (0.08 g, 0.0002 mol) was dissolved in dry dichloromethane (5.0 mL). Triethylamine (0.06 g, 0.0006 mol, 0.09 mL) was added into the polymer solution. Dansyl chloride (0.05 g, 0.0002) was added and the reaction was stirred at 25 °C for 12 h. The polymer solution was concentrated and then precipitated into diethyl ether. The polymer was filtered and dried. Yield = 0.07 g (78 %). ^{1}H NMR (400 MHz, $CDCl_3$) δ ppm: 8.66 (d, 1H, Ar-H), 8.38 (d, 1H, Ar-H), 8.21 (d, 1H, Ar-H), 7.44 (m, 2H, Ar-H), 7.13 (d, 1H, Ar-H), 4.16-4.03 (m, 5H, CH, COOCH_2), 2.86 (s, 6H, CH_3), 2.51-2.13 (m, 4H, CH_2) and 1.38-1.21 (m, 16H, CH_2). FT-IR (cm^{-1}): 3852, 3743, 3389, 2988, 2690, 2501, 1681, 1575, 1466, 1397, 1307, 1187, 1073 and 1027.

4.3. Results and Discussion

4.3.1. Synthesis of Functional Linear Polyesters

The amino acid based functional monomers were synthesized from natural L-aspartic acid and L-glutamic acid. These multifunctional amino acids contain two carboxylic acid and one amine functional groups. The carboxylic acids were converted into corresponding methyl esters and the amine group was converted into urethane (or carbamate) functional group using Boc anhydride (in scheme 4.1). Our earlier chapter work revealed that the amino acid monomer ester part underwent with alcohol occurred at 120 °C in the presence of Ti(OBu)$_4$ (1 mole %, as catalyst). Under this condition, the Boc-urethane part in the monomer was completely inert. The melt trans-urethane reaction of aliphatic urethane (or carbamates) became only active at 150 °C (in the presence of Ti(OBu)$_4$, 1 mole %) to produce new urethane linkages. The ester and urethane functional group selection towards the alcohol development of new temperature selective polymerization for multifunctional amino acid monomers.
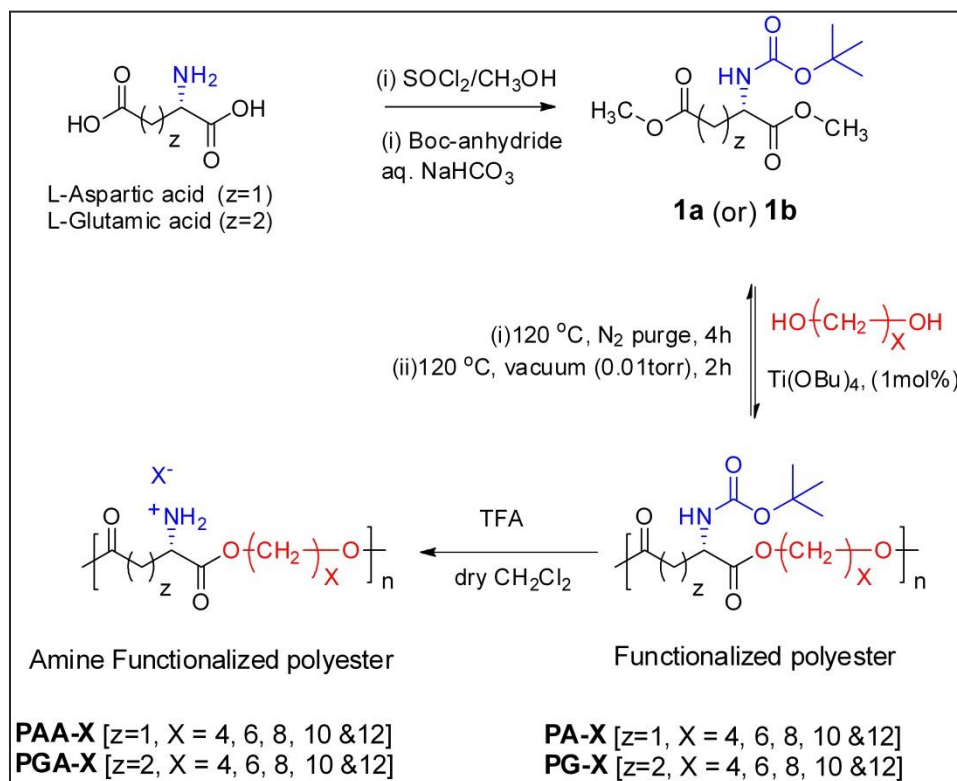
Scheme 4.1. *Synthesis of L-aspartic and L-glutamic acid monomers and their functional polyesters*

In this process, the monomer underwent reaction with diols to produce linear polyesters without disturbing the urethane (or Boc) group in each repeating units (in scheme 4.1). Monomers (**1a** or **1b**) and aliphatic diols were taken as 1: 1 mole ratio and subjected to melt condensation in presence of $Ti(OBu)_4$ (1 mole %) as a catalyst at 120 °C with continuous nitrogen purging for 4 h. The viscous mass was further polymerized under vaccum (0.01 bar) for 2 h to afford the transparent polymer. The polymers were purified dissolving in THF and precipitating into methanol. L-glutamic or L-aspartic monomers were polymerized with various diols such as 1,4-butanediol, 1,6-hexanediol, 1,8-octanediol, 1,10-decanediol and 1,12-dodecanediol to produce linear functional polyesters (in scheme 4.1). The polymers are referred as PG-X and PA-X for glutamic (G) and aspartic (A) acid series, respectively, where X-represents the number of $(CH_2)_x$ in the diols.
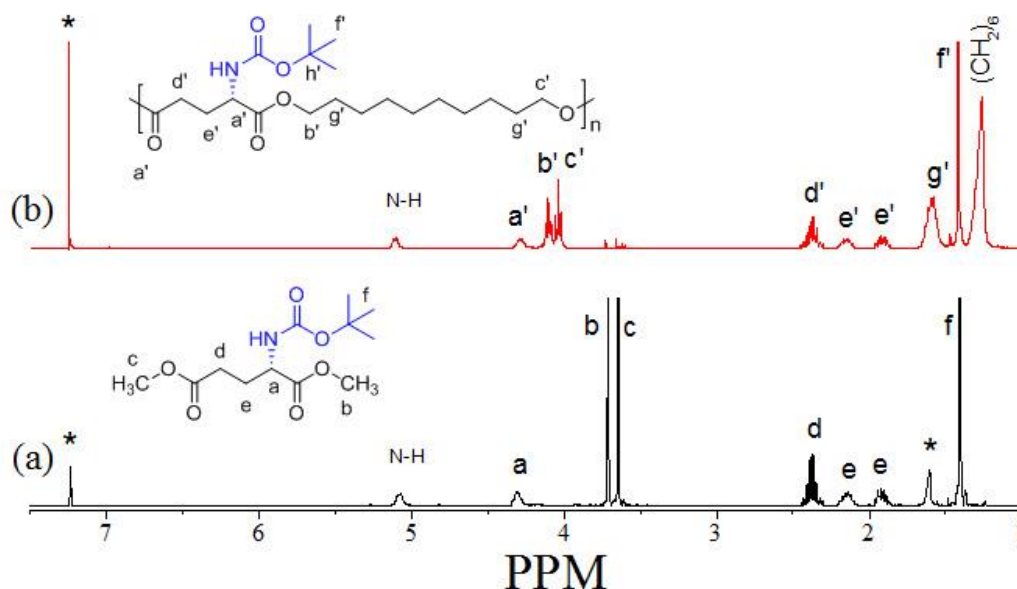

Figure 4.6. *^1H NMR spectra of L-glutamic monomer (a) and polymer PG-10 (b). The peaks for the solvent are shown by asterisk (*).*

The melt polymerization process was confirmed by NMR spectroscopy as shown in figure 4.6. The peaks in the monomer corresponding to the $COOCH_3$ protons appeared at 3.75 and 3.66 ppm (protons b and c) (in figure 4.6a). Upon polymerization, these protons disappeared and new ester peak for the polymer corresponding to $COOCH_2CH_2$ linkages (protons b' and c') appeared at 4.13 and 4.07 ppm (in figure 4.6b). The urethane Boc group $-NHCOOC(CH_3)_3$ was not disturbed by the condensation reaction and it was found to be completely inert in the presence of

Ti(OBu)$_4$ catalyst at 120 °C. The comparison of intensities of the Boc protons (peaks f') with other protons in the polymer structure (protons a', b' or c' in figure 4.6b) was confirmed by the formation of expected polyester structure. This was further confirmed by ^{13}C-NMR spectroscopy (in figure 4.7a and 4.7b). The carbon atoms in the OCH$_3$ ester groups (at 52.97 and 51.94 ppm in figure 4.7a) disappeared and a new peak belonging to ester carbon atoms –COOCH$_2$CH$_2$ was seen at 65.76 and 64.96 ppm. The Boc urethane carbon atom HNCOOC(CH$_3$)$_3$ (in h') remained unchanged at 80.03 ppm in the monomer as well as in the polymer. Thus, both ^{1}H and ^{13}C NMR spectroscopy confirmed the selective melt transesterification of multifunctional amino acid monomers for the formation of new class of functional linear polyesters. Furthermore, the temperature selective trans-reactions of carboxylic esters towards diols was investigated by varying the substitution in the carbamate. L-glutamic methyl carbamate monomer was chosen instead of Boc and the polymerization was carried out with 1,12-dodecane diol at 120 °C. This control polymerization revealed that the temperature selective condensation of carboxylic esters with the diol was not altered by the variation in the urethane functional group of the monomer (Boc to methyl).
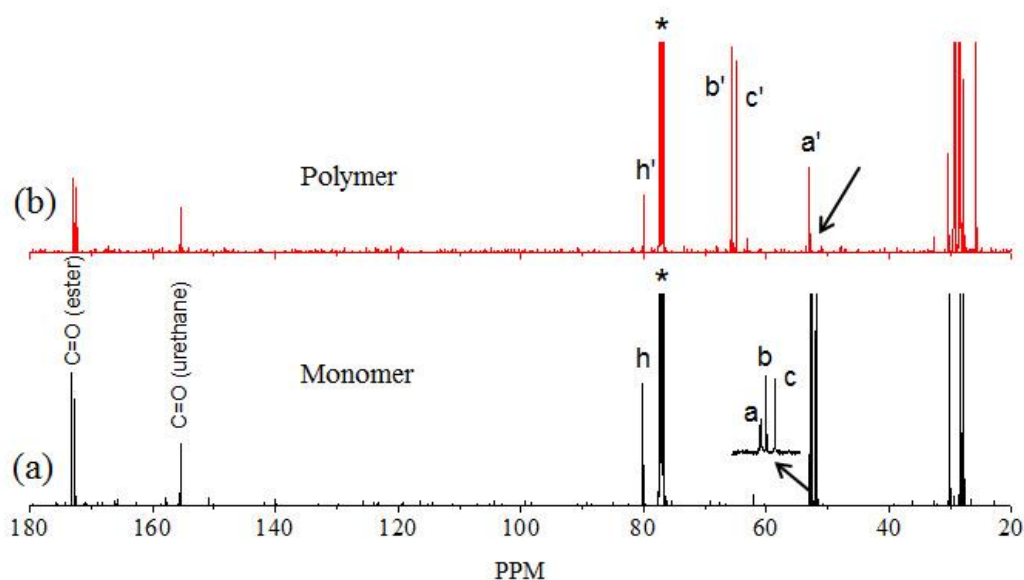

Figure 4.7. *^{13}C-NMR of L-glutamic monomer (a) and PG-10 (b). The peaks for the solvent are shown by asterisk (*).*

Table 1. Molecular weights and thermal properties of polymers

Polymer	Diol	M_n^a (g/mol)	M_w^a (g/mol)	M_n^b (g/mol)	M_w^b (g/mol)	T_D^c (° C)	T_g^d (° C)
PG-4	$HO(CH_2)_4OH$	3700	9200	40400	50000	277	16.5
PG-6	$HO(CH_2)_6OH$	5300	7400	52400	72300	283	3.2
PG-8	$HO(CH_2)_8OH$	7100	16000	46300	63200	295	-5.1
PG-10	$HO(CH_2)_{10}OH$	8600	19500	65400	112100	297	-9.5
PG-12	$HO(CH_2)_{12}OH$	11700	33300	82100	121600	295	-13.1
PA-4	$HO(CH_2)_4OH$	1700	2500	25700	28800	307	6.5
PA-6	$HO(CH_2)_6OH$	5200	14200	48400	83500	315	10.6
PA-8	$HO(CH_2)_8OH$	8100	22600	62300	99700	313	1.7
PA-10	$HO(CH_2)_{10}OH$	10400	31600	73400	103200	317	-7.7
PA-12	$HO(CH_2)_{12}OH$	9600	19300	57200	77100	323	-12.5

a) Molecular weights are determined by GPC in tetrahydrofuran and (b) DMF at 25°C using polystyrene standards. c) Determined by TGA under nitrogen and the values are taken for 10 % weight loss. d) Determined by DSC at 10 °/min heating cycle under nitrogen.
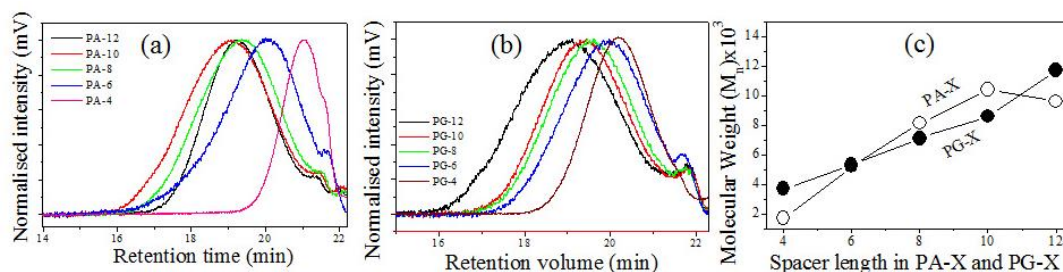

Figure 4.8. *(a) Gel permeation chromatograms of PA-X (a) and PG-X (b) polymers in THF. (c) Plot of Mn versus the number of (CH₂)x units in the diol spacer for PG-X and PA-X series.*

4.3.2. GPC molecular weight of polymers

The molecular weights of the polyesters were determined by gel permeation chromatography (GPC) in THF solvent as eluent (in table 1). The GPC chromatograms of the PA-X and PG-X polyesters are showed in figure 4.8a-4.8b. All the polymers showed mono-model distribution with high molecular weights. The molecular weights of the polymers were obtained as M_n = 2.0 to 12.0 x10^3 and M_w= 3.0 to 34 x10^3 g/mol with polydispersity index of ~ 2.0. The plots of the number of carbon atoms in the diol spacer HO-$(CH_2)_x$-OH (where x=4, 6, 8, 10 and 12) versus the M_n was plotted and is shown in figure 4.8c. These plots revealed that the molecular weight of the polymers increased with increase in the spacer length and the trend was found to be same for both L-aspartic and L-glutamic series. The increase in the molecular weight with increase in the spacer length was attributed to the reduction in the steric effect in the chain backbone by the bulky Boc functional groups. Since

the polymers have hydrogen bonded urethane linkages, the molecular weights of the polymers were also estimated by GPC using N,N-dimethylformaide (DMF) column. The molecular weight details are given in table 1. The molecular weights are obtained in the range of $M_n=2.5x10^4$ - $8.2x10^4$ and M_w $3.0x10^4$ - $1.1x10^5$. In DMF, the hydrogen bonding interaction in the polymer chains are disturbed by the solvent molecules (unlike in the case of THF); thus, the polymer chains adopted different hydrodynamic volume in DMF that yielded higher molecular weights of the polymers than the actual weight.
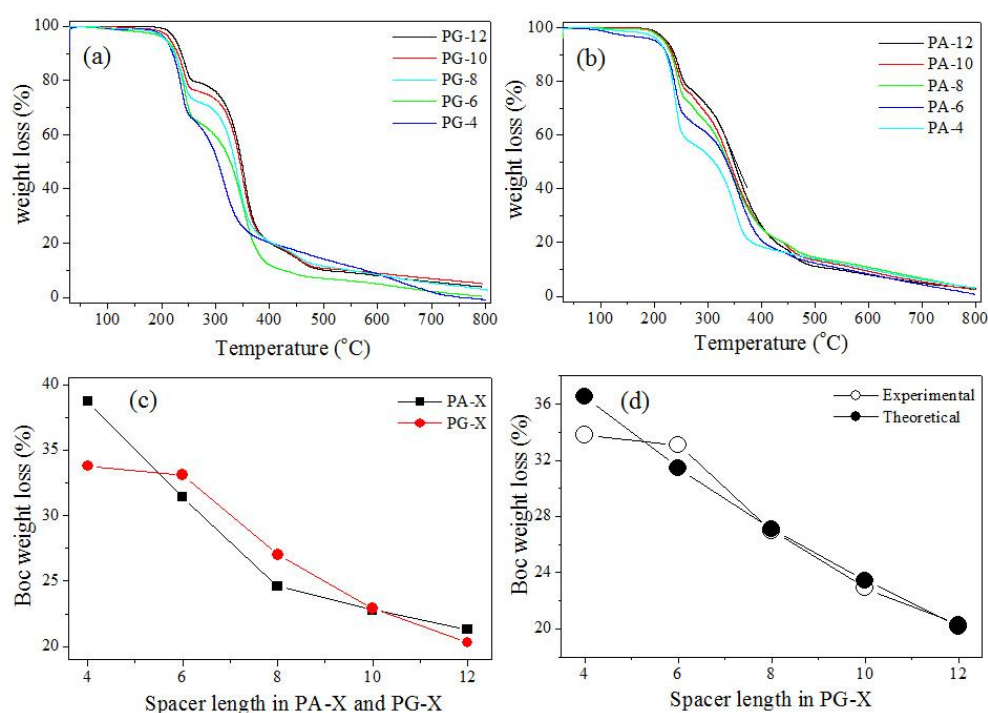

Figure 4.9. *TGA plots for PG-X (a) and PA-X (b) polymers at 10 °C/min and the thermal deprotection of Boc group of PA-X and PG-X from TGA analysis (c) and the plots for % weight loss for Boc units in both theoretical calculation and experimental values (d).*

4.3.3. Thermal analysis of functional polyester

These functional polymers were subjected to thermogravimetric analysis (TGA) with the heating rate of 10 °C/min. The functional polyesters could undergo thermal decomposition at two positions: (i) cleavage at the ester chain backbone and (ii) cleavage of pendent Boc urethane linkage. The TGA plots of PG-X and PA-X polyesters (in figure 4.9a-4.9b) showed two distinct decomposition regions: first step at 220 to 240 °C and the second step above 300 °C. The first peak was assigned to the cleavage of urethane linkages and the higher temperature decomposition region for

ester backbone as observed in earlier examples.[29-30] The percentage of Boc unit loss was determined both theoretically and experimentally (based on TGA plots) and plotted against the spacer length in diols (in figure 4.9d and for more details in table 2). The repeating unit of the Boc polymer was divided by the repeating unit of the amine polymer to calculate the theroritcal % weight loss of Boc group. The value obtained from theoritcal calculation was in good accordance with the experimental value obtained from TGA profile. This correlation with the TGA data confirmed the formation of the expected chemical structure. This process can be very useful for future applications in thermoset resins in which the active amine functional groups could be employed for cross-linking reactions with wide range of other functional groups (not part of the present study).

Table 2. Thermal deprotection of Boc group by TGA analysis

Polymer	Boc polymer R. U mass	Amine polymer R. U Mass	Deprotection % (theoretical)	Deprotection % (experimental)
PG-4	301	201	33.2	33.8
PG-6	329	229	30.4	33.1
PG-8	357	257	28.0	27.0
PG-10	385	285	26.0	22.9
PG-12	413	313	24.2	20.3
PA-4	287	187	34.8	38.7
PA-6	315	215	31.7	31.4
PA-8	343	243	29.1	24.6
PA-10	371	271	26.9	22.8
PA-12	399	299	25.1	21.3

$$\% \text{ deprotection of Boc (theoretical)} = \frac{\text{Amine repeating unit mass of polymer}}{\text{Boc repeating unit mass of polymer}} \times 100$$

The functional polymers were further subjected to differential scanning calorimetry (DSC). DSC profiles revealed that all the polymers were amorphous in nature (in figure 4.10a). The glass transition temperature (T_g) of the polymers decreased with increase in the spacer length and were tunable in the range of 16 to -13 °C with respect to spacer length (in figure 4.10 b). The viscosity of the polymers in

the melt condensation process is not possible to rule out on the molecular weight build-up. It was observed that the longer diol polymers showed more melt flow for easy stirring compared to that of made with shorted diols. The differences in melt viscosities are very difficult to measure in 1.0 g laboratory scale in melt polymerization process. This trend was indirectly supported by the glass transition temperature of the polymers (in figure 4.10b and table 1). The longer diol polymers possessed lower T_g compared to that of shorted ones. For example, the T_g of the 1,12-dodecanediol polymer has T_g = -13 °C whereas the polymer from 1,4-butanediol has T_g = 13 °C (29 deg differences). Though, the T_g values provide indirect evidence for the more flexibility for the longer diol polymers, the role of viscosity on the molecular weights of the polymers need to be addressed.
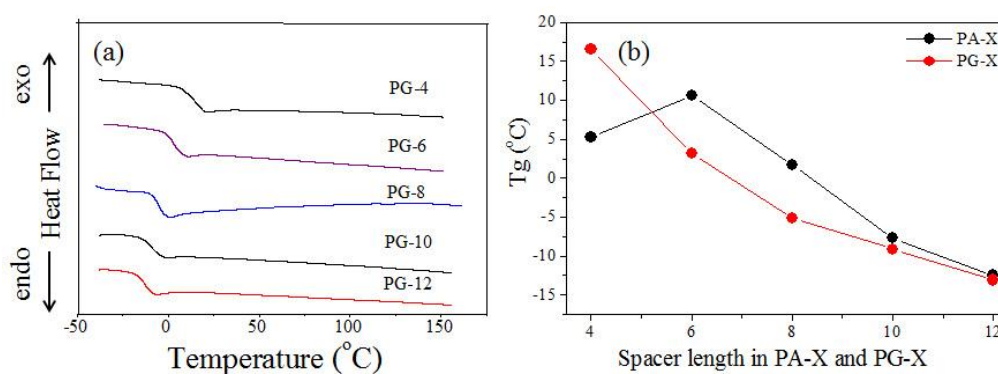

Figure 4.10. *DSC thermograms of PG-X polymers at 10 °/min heating rate (a) and the plot of Tg vs spacer length of diol in PA-X and PG-X*

4.3.4. Hierarchical Helical Self-assemblies

The functional polyesters are made from optically active L-amino acid monomers; these polymers were subjected to circular dichroism (CD) analysis to test their ability to form secondary structures. CD spectra of the PG-X and PA-X in tetrahydrofuran are shown in figure 4.11a and 4.11b. Typically, polypeptides exhibit three different types of secondary structures such as α-helix, β-sheet and random coil conformation. In the present case, the PG-X polyesters showed positive and negative CD band at 220 and 240 nm,[31] respectively. The positive CD band observed at 220 nm and the negative CD band at 240 nm were assigned to π-π* transition and n-π* transitions, respectively.[32-33] The β-sheet conformations were typically observed as a negative band first followed by positive band at lower wavelength regions. Thus, the CD spectra of the PA-X and PG-X polyesters showed CD pattern similar to that of the β-sheet conformation. Further to understand the CD signals of the polymers, the

absorption spectra of all the polymers were recorded in THF solvent. The polymers showed absorption peaks at 215 nm and 244 nm in the same range where their CD peaks were observed (at 220 and 240 nm) with respect to the β-sheet structures. The slight shift in the CD signal toward the higher wavelength region for beta-sheets in the present polyesters are indeed contributed by the non-peptide backbones (ester moieties) compared to that of the amide backbones reported in polypeptides (showed beta-sheets in the range of 196 and 220 nm).
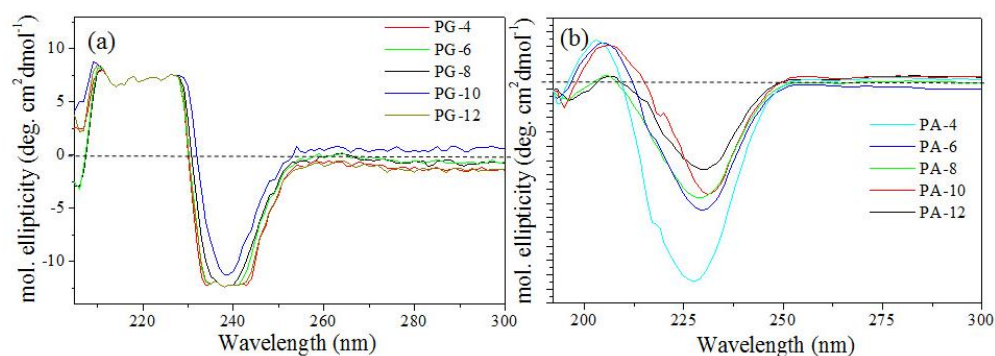

Figure 4.11. *(a) CD spectra of PG-X (a) and PA-X (b) polymers in THF as solvent*

To visualize the secondary structures of the new polyesters, the polymer samples were subjected to electron and atomic force microscopic analysis. Field emission scanning electron microscope images of the PG-X polyesters are shown in figures 4.12a to 4.12e. All functional polyesters produced amyloid-like helical fibril morphology. The individual polymer fibrils were about 45 nm in thickness and they were twisted together to produce thicker fibrils. The twisting points among the fibrils are indicated by arrows in the FE-SEM images. In PG-10 (in figure 4.12e), it is very clear that the individual nano-fibril threaded and twisted together to produce thicker long nanofibers of 119 nm. In PG-12 polymer, the twist is evident from morphological features. In the case of the aspartic acid polymers PA-12 (in figure 4.12f), almost all the individual ribbon fibrils were twisted to form cyclic ring type morphology rather than straight ones as observed in PG-X series. The polymer PA-10 also showed the formation of helically twisted polymer fibers. Similar amyloid-like fibrils were also observed in PA-6 (in figure 4.12 i).
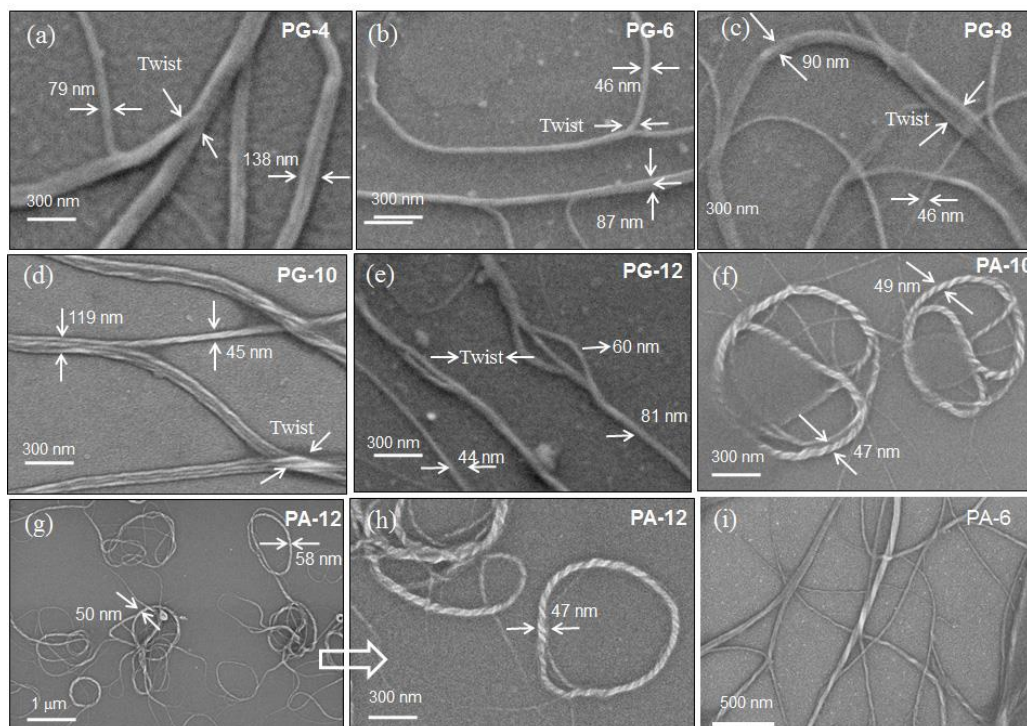
Figure 4.12. *FE-SEM images of PG-X polymers(a to e), PA-12 (f and g), PA-10 (h) and PA-6 (i).*

To further trace the inner features of the helical fibril morphology, PG-10 polyester was subjected to high resolution transmission electron microscopy (HR-TEM) and atomic force microscopy (AFM) and their respective images are shown in figure 4.13. HR-TEM images of PG-10 showed the formation of double helical fibril morphology (in figure 4.13a). The thickness of each individual fibers were obtained as 34 ± 2.2 nm and the thickness of the double helix were obtained as 50 ± 1.2 nm. The pitch length of the each twist was obtained as 220 ± 4.2 nm. The fibers were also found to be left-handed twist which was matching with that of the negative Cotton effect in the CD signals of polymers in figure 4.11a-4.11b. AFM images of the PG-10 confirmed the formation of nano-fibril morphology (in figure 4.13b). The individual fibers of thickness 63 ± 2.4 nm twisted together to produce thicker twisted fibrils of 157 ± 3.1 nm (in site A in figure 4.13b). All three independent microscopic techniques provided direct evidentce for the formation of double helix or multiple threaded nano-fibril morphologies in the newly designed functional polyesters based on L-amino acids.
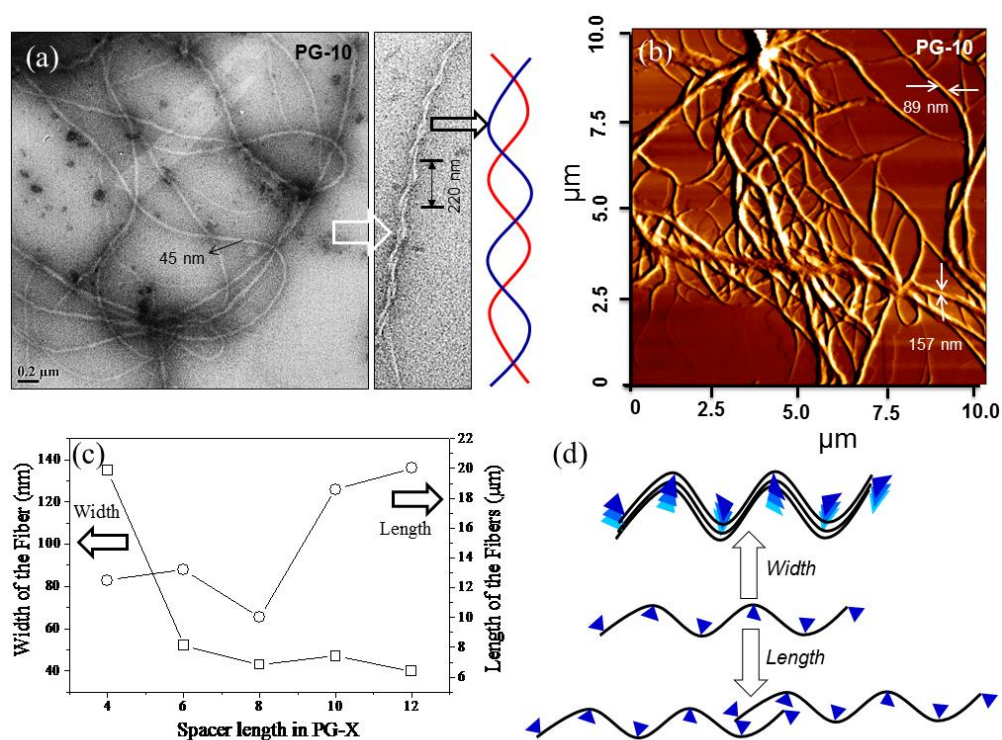
Figure 4.13. *HR-TEM (a) and AFM image (b) of PG-10. (c) Plot of width and length of the nanofibers against the (CH₂)x units in the PG-X polymers. (d) Proposed model for the polymer chain interaction in lateral and longitudinal chain packing in the formation of twisted and lengthy nano-fibrils.*

The average width and length of the amyloid-like fibrils were calculated for more than 10-15 individual fibrils and the data are plotted against the number of (CH_2) units in the polymer backbone (in figure 4.13c). The width of the **PG-4** nano-fibrils were obtained as 138 ± 15 nm and their length varied up to 12.3 ± 1.5 μm (aspect ratio ~ 90). The **PG-6** polyester showed the formation of much thinner nano-fibrils of with 52.3 ± 6.1 nm width lengths up to 13.2 ± 2.1 μm. The other longer spacer polyesters PG-8, PG-10 and PG-12 showed nano-fibrils of almost same width and lengths (in figure 4.13c). This trend indicated that the thickness of the nano-fibrils produced by the functional polyesters became thinner with increase in the alkyl spacer lengths between two adjacent repeating units. Thus, it may be summarized that the increases in the alkyl spacer length between the two adjacent repeating units make thin nano-fibrils. This trend is attributed to the decreases in the steric hindrance induced by the bulky Boc groups among the adjacent units in the chain backbone. Based on the above morphological evidence, a model has been proposed for the

144

formation of helically twisted nanofibril formation in figure 4.13d. The polymers produced individual twisted ribbons that underwent polymer chain-chain interaction both along the width and length to produce thicker and longer amyloid-like fibrils.
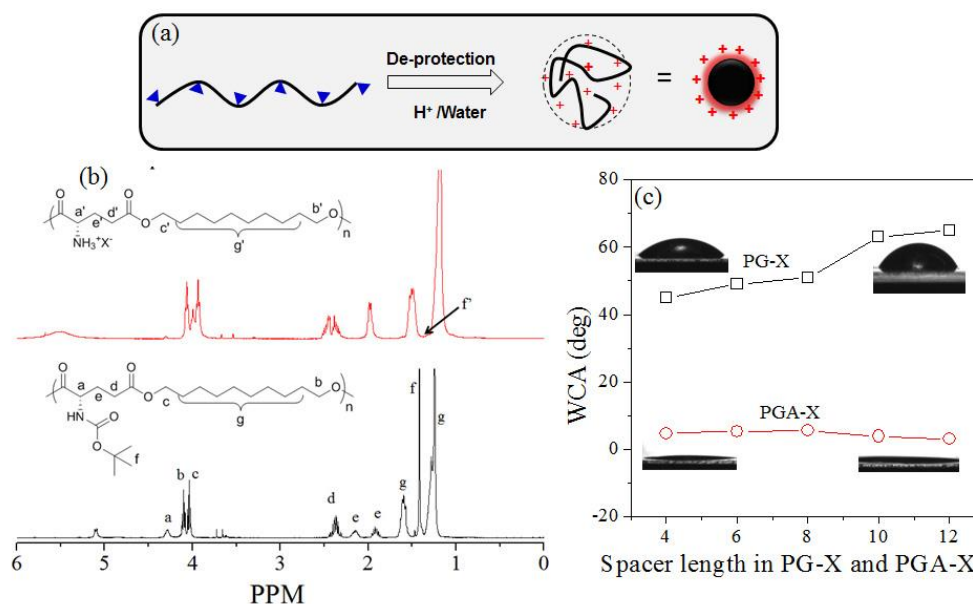

Figure 4.14. *Schematic representation of polyester deprotection into cationic nanoparticles (a), ^{1}HNMR stack plot of PG-12 and PGA-12 (b) Water contact angles of PG-X and its deprotected polymer PGA-X (c).*

4.3.5. Spherical Cationic Nano-particles

The functional polyesters were designed with Boc group as the pendant unit in the backbone. The selective deprotection of the NHCOO-C(CH$_3$)$_3$ in the pendent unit without disturbing the polyester backbone produced cationic amine functionalized polyesters. The functional PG-X polymers were deprotected using trifluoroacetic acid (TFA) in dichloromethane to yield the amine functionalized polyester PGA-X (A-represents amine functionality) (in figure 4.14a). Upon deprotection, the polymers became soluble in water. The deprotection of polymer was confirmed by ^{1}HNMR spectroscopy and the details are shown in figure 4.14b. The protons of corresponding to NHCOO-(OCH$_3$)$_3$ groups in the polymer completely disappeared after deprotection. This analysis clearly indicated that the Boc group was selectively de-protected to produce amine functional polyester. Water contact angle (WCA) experiments provide direct information on the hydrophobicity of the functional polyesters.[34] The functional polyesters before and after deprotection were subjected to WCA analysis by sessile drop method (in figure 4.14c). WCA of PG-X functional polyesters showed slight increase in the WCA values with increase in the aliphatic

chain length in the polymer back bone from 45 to 60°. This showed the hydrophobic nature of the nascent functional polyester. After deprotection of Boc group, the amine functional polyesters showed WCA ~ 5° owing to, its hydrophilic nature. Thus, the WCA experiment clearly indicated that the amine functionalized polyesters were hydrophilic whereas its nascent Boc functional polyesters were hydrophobic.
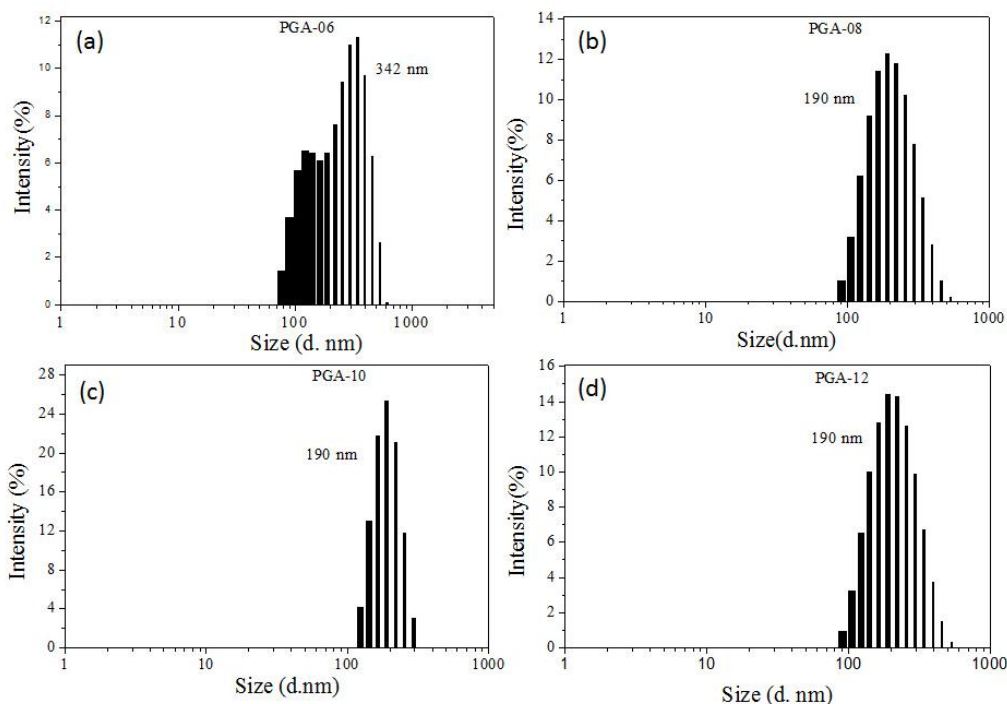

Figure 4.15. *DLS histograms of PGA-6, 8, 10 and 12 (a-d) in water*

These amine functionalized polyesters were subjected to dynamic light scattering (DLS) measurement in water. DLS histograms of deprotected PG-4 and PG-10 amine polyesters are shown in figure 4.15 (a-d). PGA-6 showed bimodal distribution with average diameter of 342 ± 64 nm. On the other hand, PGA-10 and PGA-12 deprotected polymer showed mono-model distribution with hydrodynamic size of 212 ± 25 nm. The plot of the average hydrodynamic diameter of the polymer assemblies with spacer length in the backbone is shown in figure 4.16a. The size of the aggregates decreased with increase in the aliphatic chain length. This trend was attributed to the reduction in the repulsion between the $NH_3^+X^-$ units among the adjacent repeating units in the backbone with increase in the alkyl spacer length.
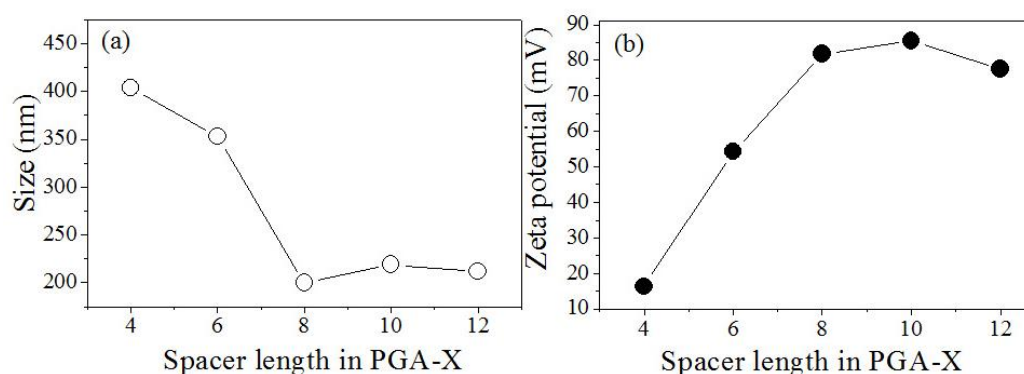
Figure 4.16. *Plots of DLS size of the polymer aggregates (a) and Zeta potential (b) versus the number of $(CH_2)x$ in the spacer length.*

Zeta potential is an important tool to study the solution dynamics of charged polymer nano-aggregates in solution. The deprotected functional polyesters contain cationic $NH_3^+X^-$ units, and therefore, they were subjected to zeta potential analysis. The zeta potential values for PG amine functional polymers are plotted and shown along with their sizes in figure 4.16b. The Zeta potentials were observed in the range of +15 to + 85 mV as expected to typical cationic function polymers. The zeta potential values increased with increasing in the aliphatic chain length in the backbone. The comparison of the size and zeta potential revealed that the smaller particles possessed higher zeta potential values and they followed the expression: is ζ = q/4πεa, where q-carrying charge, a-the electrical potential at the surface of the sphere of radius, ζ and ε are zeta potential and permittivity of the medium in which they are immersed.[35] Thus, the longer aliphatic chain length in the backbone provides stable self-assembled structure due to the reduction in the charge-charge repulsion among the adjacent repeating units.

The deprotected polymers were subjected to CD analysis both in water and in tetrahydrofuran (in figures 4.17a and 4.17b). CD spectra of the polymers showed broad positive band at 220 nm with respective to the coil-like structures observed in solutions.[33] The comparison of CD spectra of the polymers in the nascent Boc form (in figure 4.11a-4.11b) and amine cationic form (in figures 4.17a and 4.17b) suggested that the deprotection induced self-organization changes the polyesters. The deprotected polymers showed identical CD signal both in THF and water; thus, the loss of the helical structures observed in the nascent polymer structures was not due to solubility differences and it occurred primarily due to the structural changes. FE-SEM

images of the cationic polyester PG-X are recorded from both aqueous and THF solutions and they are shown in figures 4.18a-4.18c and 4.18d, respectively. The morphologies of the deprotected polymers were found to be spherical nanoparticles. The average sizes of these particles were obtained as 210 ± 25 nm which was matching with that of their DLS histograms (in figure 4.15).
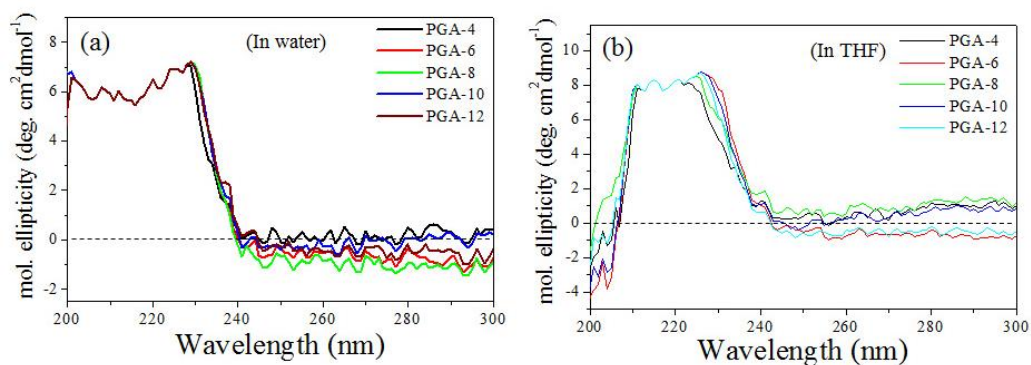

Figure 4.17. *CD spectra of deprotected polymer PGA-X in water (a) and tetrahydrofuran (b)*

HR-TEM and AFM images of the deprotected polymer sample confirmed the spherical nanoparticle morphology with average sizes of 182 ± 18 nm and 199 ± 20 nm, respectively. FE-SEM images of other deprotected polymer samples PGA-X were also found to be spherical in nature (in figure 4.18). All independent techniques such as WCA, DLS, Zeta potential, CD and FE-SEM, HR-TEM and AFM confirmed that the de-protected cationic form of the polyester exhibited spherical morphology. Based on the above discussion it could be summarized that the Boc protected functional polymers self-assembled to produce long amyloid-like fibril self-assemblies (in figure 4.12-4.13). Upon deprotecting, these amine salt polyesters adopted random coil confirmation to produce spherical nano-particle morphology. The amyloid-like fibrils to coil-like changes are typically observed in proteins; thus, the newly designed synthetic polyesters also behaved like proteins and showed conformational transformations in the same polymer chains.
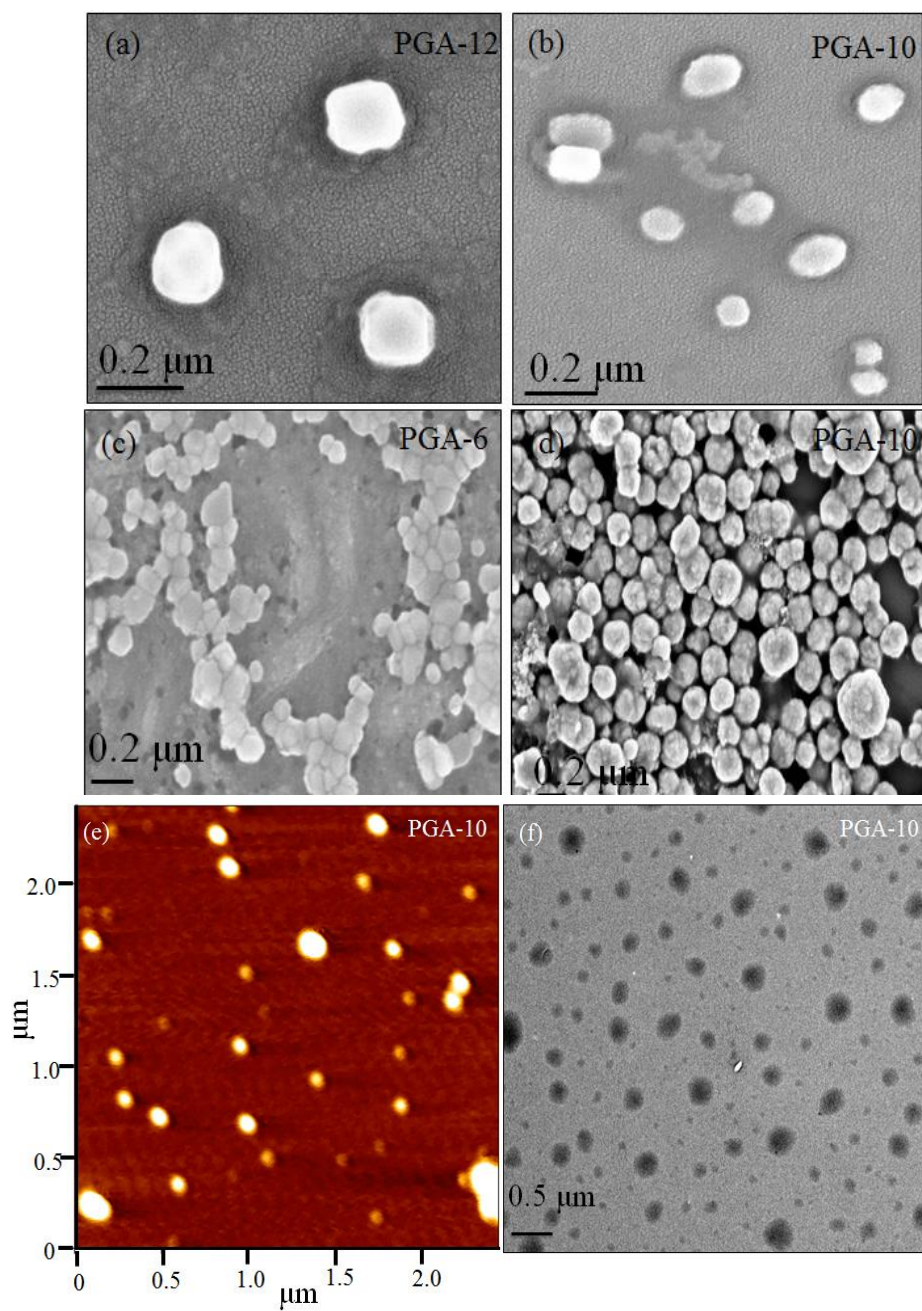
Figure 4.18. *FE-SEM images of the polymer PGA-12, 10 and 6 sample in water (a-c) and PGA-10 in tetrahydrofuran (d).* HR-TEM (e) and AFM image (f) of PGA-10 in water. The concentration of polymer solutions was retained as 1×10^{-4} M for all the analysis.
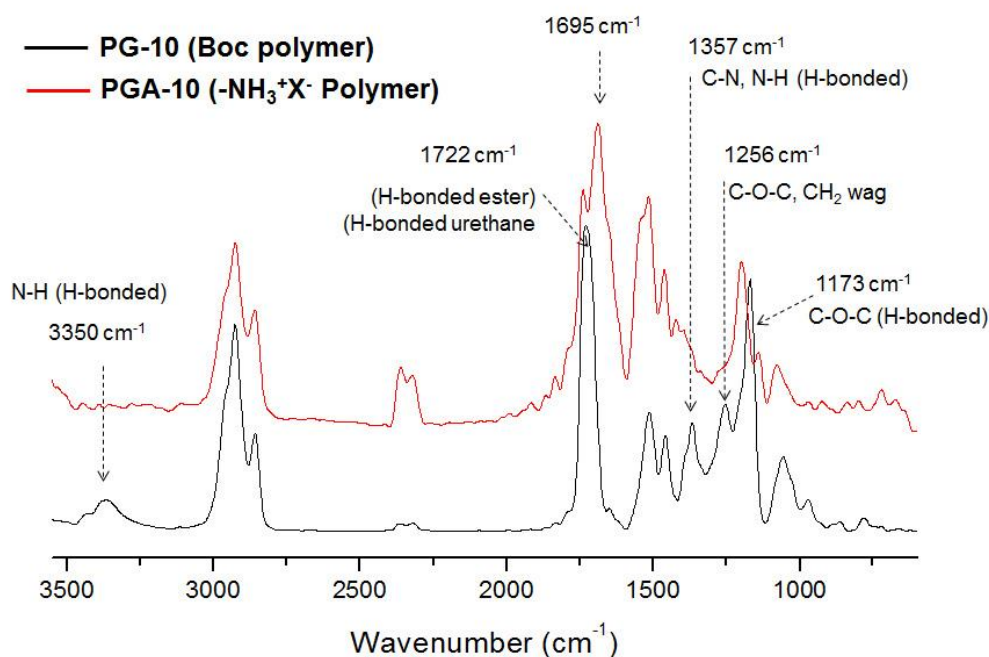
Figure 4.19. *FT-IR spectra of PG-10 and its de-protected polymer PGA-10 in the absorption mode*

FT-IR is yet other important tool to analyse the weak non-covalent interaction like hydrogen bonding in the polymer chains. In the present case, the PG-X polymers produced helical amyloid fibril self-assembly whereas its deprotected polymer PGA-X transformed into spherical nanoparticles. To confirm the morphological changes, the samples were subjected to FT-IR analysis and their spectra are shown in figure 4.19. PG-10 polymer showed N-H stretching vibrational band at $v = 3350$ cm^{-1} with respect to strong hydrogen bonding interactions. The polymer showed strong peak at $v = 1722$ cm^{-1} with respect to C=O stretching frequency that involved in hydrogen bonding interactions.[36-37] On the other hand, the de-protected polymer PGA-10 did not show any peak above 3000 cm^{-1} that indicated the absence of hydrogen bonded N-H vibrations. The deprotection of Boc group (HNCOOC(CH$_3$)$_3$ produced NH$_3^+$X$^-$ species that are expected to show no vibration peaks above 3000 cm^{-1} as reported in the literature for amino acid salts.[38-39] The carbonyl peaks at 1750 to 1600 cm^{-1} also showed multiple peaks with respect to the above structural change. Further the hydrogen bonding in PG-10 polymer was supported by the observation of peaks at $v = 1357$ cm^{-1}, 1256 cm^{-1} and 1173 cm^{-1} with respect to C-N, N-H (H-bonded); C-O-C, CH$_2$ (wag) and C-O-C (H-bonding), respectively. FT-IR analyses of all other

polymers were also showed similar observation. Based on the above analysis, it can be concluded that the amyloid-like fibril formation in the nascent Boc-polymer was driven by strong hydrogen bonding interaction between the Boc N-H groups in the polymer chain at the periphery. The de-protection of Boc made the polymer chains into cationic species that lacks the self-organization and collapses into spherical structures.
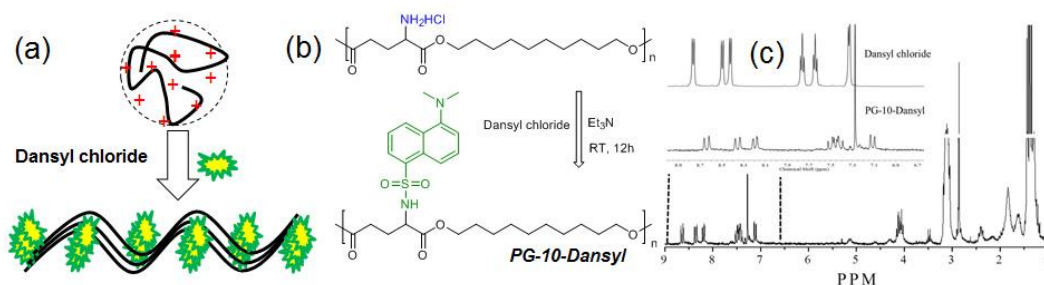

Figure 4.20. *(a) Schematic representation of reversible expansion of the polymer chains through fluorophore substitution. (b) Synthetic scheme for PG-10-Dansyl and ¹HNMR spectra of PG-10-Danysl (c).*

4.3.6. Reversible Self-assembly via Fluorophore Functionalization

To validate the reversibility of the self-assembly in the new polyester system and also unlock the polymer chains from the spherical aggregate to expanded helical confirmations; the PGA-10 deprotected polymer was subjected to post polymerization functionalization using fluorophore (in figure 4.20a-4.20b). Dansyl chloride was chosen for the above purpose. The polymer underwent 100 % substitution in the backbone to produce PG-10-Dansyl. The post polymerisation fucntionalization was confirmed by ¹HNMR spectroscopy (in figure 4.20c) and GPC analysis (in figure 4.21a). The PG-10 dansyl coupled polymer was subjected to CD analysis. It showed negative broad CD band at 200-350 nm[35] (in figure 4.21b) with respect to left handed helical conformation. FE-SEM images of the dansyl attached polyesters PG-10 (in 4.21d) showed the existence of helical amyloid-like fibril morphology with very high aspect ratio. The width of the nanofibrils were obtained as 50 ± 5.2 nm. HR-TEM images of PG-10-dansyl confirmed the formation of helical fibril morphology (in figure 4.21e) as noticed in FE-SEM images. The thickness of the double helix fibrils were obtained as 54 ± 5.4 nm. The fibrils were also found to be left-handed helix which was matching with that of the negative Cotton effect in the CD signals of polymers in figure 4.21b. CD signal for the dansyl substituted polymer is also repeated for various polymer concentration and their CD spectra are given infigure

151

4.21c. With increase in the polymer concentration, the CD signals increased to yield strong signals for β-sheet structures. Partial quenching of CD signal intensity could have arisen by the aggregation of chromophore through hydrogen bonding interaction in the helical fibers. AFM images of the PG-10-dansyl also confirmed the formation of nanofibrous morphology (in figure 4.21.f). The individual fibers of thickness 62 ± 2.4 nm twisted together to produce thicker fibers (in figure 4.21f). Additionally, bundles of nanofibers of thickness 146 ± 5.2 nm were also visible. The above analysis revealed that the dansyl subtitution in the PGA-10 cationic polymer transformed the molecular self-assembly from cationic nano-partcle to expanded amyloid-like fibrils having dansyl substitution.
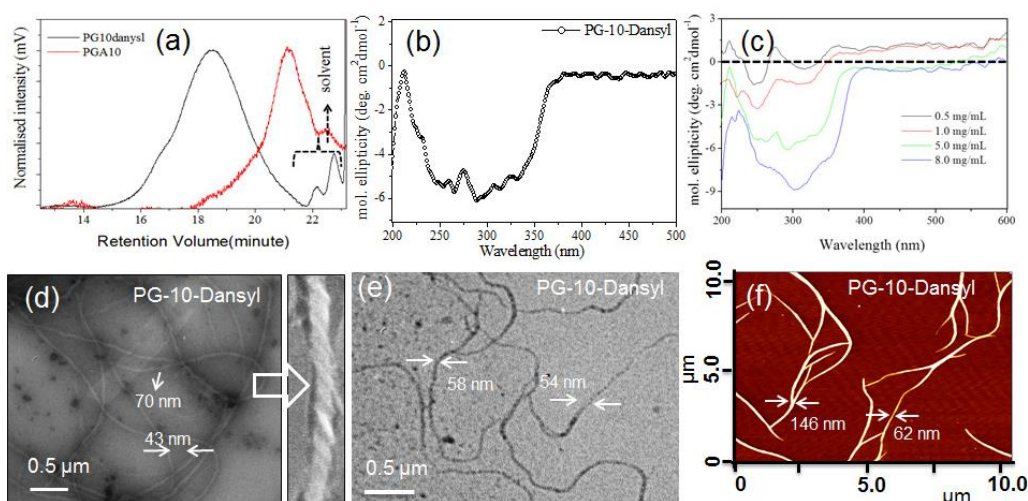

Figure 4.21. *GPC analysis of PGA-10 and PG-Dansyl polymer (a), CD spectra of PG-Dansyl polymer (b) and their concentration depent analysis in THF solution (10^{-4} M) (c). FE-SEM (d), HR-TEM (e) and AFM images (f) of PG-10-Dansyl.*

The dansyl fluorophore attached polymer was subjected to absorption and emission studies and the details are given in figures 4.22c and 4.22d, respectively. The absorption maxima of dansyl unit blue-shifted by 40 nm from 370 nm to 330 nm folowed by the formation of sulfonamide linkage at the polymer backbone.[40] Both the unsubstituted polymer PG-10 and dansyl chloride did not show any emission characteristics upon photoexcitation. Interestingly, dansyl susbtituted helical polymer showed strong emission maxima at 460 nm (in figure 4.22d). This observation was further supported by photographs of vials taken for the above samples by UV-light exposure in figure 4.22b. The photophysical studies and morphological analysis confirmed the formation of helical fluorescent amyloid-like fibril followed by the

reversible expansion of coil-like cationic polymer upon dansyl substituion. Further structural optimization is required for complete understanding of the CD signals and helical assemblies of the dansyl substituted polymer.
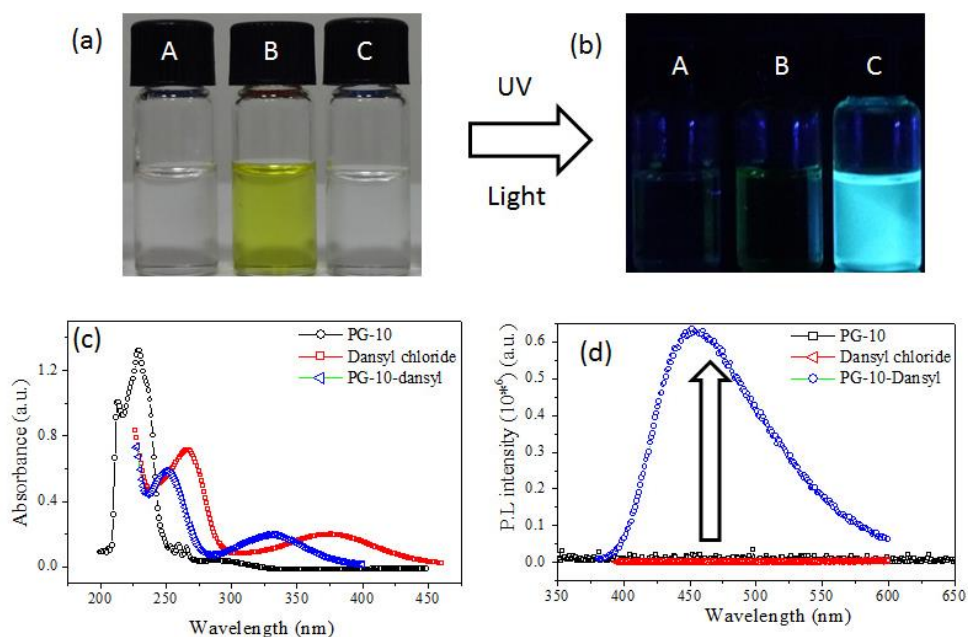

Figure 4.22. *The vials in the photographs are respective sample in normal light (a) and upon exposure to UV-light (b). Absorbance (c) and emission spectra (d) of PG-10 dansyl chloride and PG-10-dansyl polymer.*

Based on the above anlysis, the following points may be summarized: (i) the nascent polymer chains underwent molecular self-organization to produce long and thin helical amyloid-like fibrils. The thickness and length of the nano-fibres could be fine-tuned by varying the length of the diol segment in the chain backbone. (ii) Upon deprotection, the polymer chains became hydrophilic with cationic charges in each repeating units. The charge repulsion and hydrophobic nature of the polyester backbone folded (or aggregated) these chains into spherical nano-particles. The size and charge of these nanoparticles (Zeta potential) could be easily altered by the spacer length in the polymer backbone. (iii) Post polymerization susbtitution with dansyl units (fluorophore) unleach the collopsed polymer chain conformation and reversibly expand the polymer chains to adopt its original helical conformation. Thus, the entire cycle of expanded to coil-like to expanded conformations in the polyester backbone was accomplished in a single system. Thus, the newly designed amino acid functional polyester showed complete reversibility in the chain folding phenomena much like proteins in the biological system.

4.4. Conclusion

In conclusion, a new melt polymerization synthetic methodology was developed to make functional polyesters based on L-amino acids that underwent reversible conformational changes and produced amyloid-like fibrils. New classes of linear polyesters with urethane-pendants in each repeating unit was synthesized by temperature selective transesterification process of multi-functional amino acids based on L-glutamic and L-aspartic acids. These functional polyesters underwent hierarchical helical self-assembly to produce amyloid-like fibrils. The distance between the adjacent hydrogen bonding urethane units was controlled by the selection of appropriate diol segment to the polymerization process. This allowed us to control the length and width of the amyloid-like fibrils of 100 nm width and few micrometers in length. The polymers produced individual twisted ribbons that underwent polymer chain-chain interaction to assemble into DNA-like double helical configuration. These double helical threats subsequently assembled into amyloid-like fibrils. The functional polyesters turned into cationic species upon de-production. The cationic species adopted coil-like structure to produce spherical nanoparticles in water. The size and charge of the cationic spherical species were controlled by the alkyl chains length in the polymer structure. Dansyl chloride was employed as fluorophore to reversibly expand the coil-like cationic polymers into expanded helical fibrils of fluorescent nature. The emission properties of the dansyl substituted amyloid-like fibrils were characterized by photophysical techniques. The present investigation reports one of the first example for complete reversibility in molecular self-assembly like natural proteins in L-amino acid based synthetic polyesters. The developed amyloid-like fibrils, cationic nanoparticles and dansylanchored fluorescent helical fibrils are new classes of polymeric materials based on amino acids in the literature. Moreover, the newly developed temperature selective polycondensation approach is also very useful for making wide range of other macromolecular architectures such as block, graft and hyperbranched polymers. Currently, the research work is focused on using these newly developed functional polymers for polymer based drug delivery and other biomedical applications.

4.5. Reference:

1. Woolfson, D. N.; Mahmoud, Z. N. *Chem. Soc. Rev.*, **2010**, *39*, 3464-3479.

2. Vanden Akker, C. C.; Engel, M. F. M.; Velikov, K. P.; Bonn, M.; Koenderink, G. H. *J. Am. Chem. Soc.* **2011**, *133*, 18030-18033.

3. Ridgley, D. M.; Barone, J. R. *ACS Nano* **2013**, *7*, 1006-1015.

4. Fandrich, M.; Fletcher, M. A.; Dobson, C. M. *Nature* **2001**, 410, 165-166.

5. Cheng, P-N.; Liu, C.; Zhao, M.; Eisenberg, D.; Nowick, J. S. *Nature Chem.* **2012**, *4*, 927-933.

6. Etienne, M. A.; Aucoin, J. P.; Fu, Y.; McCarley, R. L.; Hammer, R. P. *J. Am. Chem. Soc.* **2006**, *128*, 3522-3523.

7. Wadai, H.; Yamaguchi, K-I.; Takahashi, S.; Kanno, T.; Kawai, T.; Naiki, H.; Goto, Y. *Biochemistry* **2005**, 44, 157-164.

8. Bowerman, C. J.; Liyanage, W.; Federation, A. J.; Nilsson, B. L. *Biomacromolecules* **2011**, *12*, 2735-2745.

9. Dzwolak, W.; Ravindra, R.; Nicolini, C.; Jansen, R.; Winter, R. *J. Am. Chem. Soc.* **2004**, *126*, 3762-3768.

10. Rubin, N.; Perugia, E.; Goldschmidt, M.; Fridkin, M.; Addadi, L. *J. Am. Chem. Soc.* **2008**, *130*, 4602-4603.

11. Rubin, N.; Perugia, E.; Wolf, S. G.; Klein, E.; Fridkin, M.; Addadi, L. *J. Am. Chem. Soc.* **2010**, *132*, 4242-4248.

12. Del Mercato, L. L.; Maruccio, G.; Pompa, P. P.; Bochicchio, B.; Tamburro, A. M.; Cingolani, R.; Rinaldi, R. *Biomacromolecules* **2008**, *9*, 796-803.

13. Yamada, N.; Ariga, K.; Naito, M.; Matsubara, K.; Koyama, E. *J. Am. Chem. Soc.* **1998**, *120*, 12192-12199.

14. Shao, H.; Parquette, J. R. *Angew. Chem. Int. Ed.* **2009**, *48*, 2525-2528.

15. Shahi, P.; Sharma, R.; Sanger, S.; Kumar, I.; Jolly, R. S. *Biochemistry* **2007**, *46*, 7365-7373.

16. Lai, J.; Fu, W.; Zhu, L.; Guo, R.; Liang, D.; Li, Z.; Huang, Y. *Langmuir*, **2014**, *30*, 7221-7226.

17. Koga, T.; Higuchi, M.; Kinoshita, T.; Higashi, N. *Chem. Eur. J.* **2006**, *12*, 1360-1367.

18. Dehn, S.; Castelletto, V.; Hamley, I. W.; Perrier, S. *Biomacromolecules* **2012**, *13*, 2739-2747.

19. Aggeli, A.; Nyrkova, I. A.; Bell, M.; Harding, R.; Carrick, L.; McLeish, T. C. B.; Semenov, A. N.; Boden, *N. Proc. Natl. Acad. Sci USA* **2001**, *98*, 11857-11862.

20. Soto, P.; Cladera, J.; Mark, A. E.; Daura, X. *Angew. Chem. Int. Ed.* **2005**, *44*, 1065-1067.

21. Paulite, M.; Fakhraai, Z.; Li, I. T. S.; Gunari, N.; Tanur, A. E.; Walker, G. C. *J. Am. Chem. Soc.* **2011**, *133*, 7376-7383.

22. Irwin, J. A.; Wong, H. E.; kwon, I. *Biomacromolecules* **2013**, *14*, 264-274.

23. Sinha, S.; Lopes, D. H. J.; Du, Z.; Pang, E. S.; Shanmugam, A.; Lomakin, A.; Talbiersky, P.; Tennstaedt, A.; McDaniel, K.; Bakshi, R.; Kuo, P-Y.; Ehrmann, M.; Benedek, G. B.; Loo, J. A.; Klarner, F-G.; Schrader, T.; Wang, C.; Bitan, G. *J. Am. Chem. Soc.* **2011**, *133*, 16958-16969.

24. Bradford, V. J.; Iverson, B. L. *J. Am. Chem. Soc.* **2008**, *130*, 1517-1524.

25. Deming, T. J. *J. Am. Chem. Soc.,* **1998**, *120*, 4240 – 4241.

26. Deming, T. J. *Nature* **1997**, *390*, 386 – 389.

27. Deming, T. J. *Adv. Mater.* **1997**, *9*, 299 – 311.

28. Fandrich, M.; Dobson, C. M. *EMBO J.* **2002**, *21*, 5682-5690.

29. Horie, M.; Yamaguchi, I.; Yamamoto, T. *Macromolecules* **2006**, *39*, 7493-7501.

30. Leonard, J. K.; Wei, Y.; Wagener, K. B. *Macromolecules* **2012**, *45*, 671-680.

31. Violette, A.; Averlant-Petit, M. C.; Semetey, V.; Hemmerlin, C.; Casimir, R.; Graft, R.; Marraud, M.; Braiand, J. P.; Rongnan, D.; Guichard, G. *J. Am. Chem. Soc.* **2005**, *127,* 2156-2164.

32. Sinaga, A.; Hatton, T. A.; Tam, K. C. *Biomacromolecules* **2007**, *8*, 2801-2808.

33. Greenfield, N.; Davidson, B.; Fasman, G. D. *Biochemistry* **1967**, *6*, 1630-1637.

34. Surnar, B.; Jayakannan, M. *Biomacromolecules* **2013**, *14*, 4377-4387.

35. Jinish Antony, M.; Jayakannan, M. *Langmuir*, **2011**, *27*, 6268-6278.

36. Mattia, J.; Painter, P. M*acromolecules* **2007**, *40*, 1546-1554.

37. Wang, H.; Aubuchon, S. R.; Thompson, D. G.; Osborn, J. C.; Marsh, A. L.; Nichols, W. R.; Schoonover, J.R.; Palmer, R. A. M*acromolecules* **2002**, *35*, 8794-8801.

38. Llusar, M.; Monros, G.; Roux, C.; Pozzo, J. L.; Sanchez, C. *J. Mater. Chem.* **2003**, *13*, 2505-2514.

39. Feldman, K. E.; Kade, M. J.; Meijer, E. W.; Hawker, C. J.; Kramer, E. J. *Macromolecules* **2009**, *42*, 9072-9081.

40. Gros, C.; Labouesse, B. *European J. Biochem.* **1969**, *7*, 463-470.

Chapter 5

Melt polycondensation approach for Disulfide Containing Functional polyester and their Hierarchical Helical Self-assemblies

Chapter 5

Melt polycondensation approach for disulfide Containing functional polyester and their Hierarchical Helical Self-assemblies

A stimuli responsive disulfide functional polyester was developed based on L-cystine amino acid for various material and thermoplastic applications. L-cystine amino acid was converted into ester-urethane functional monomer. At 120 °C, the two ester functional groups of L-cystine monomer were selectively reacted with diol in the presence of Ti(OBu)$_4$ as catalyst to yield disulfide functional polyester under solvent free melt conditions. The formation of disulfide polyester was confirmed by ^1H and ^{13}C NMR spectroscopy. The polymerisation process was further demonstrated for the same L-cystine monomer with various commercial aliphatic diols namely, 1,12-dodecanediol, 1,10-decanediol and 1,8-octanediol. Gel permeation chromatography (GPC) of these polymers showed monomodal distribution with moderate to high molecular weights. Further thermal analysis of these polymers indicated that the polymers were thermally stable up to 250 °C and they were amorphous in nature. Self-assembly of these disulfide functional polyester can be tuned from amyloid like fibres to spherical particle morphology depending upon protection and deprotection of the amine functionality present as the side chain of the polymer. The changes in the self-assembly of polymers were thoroughly characterised by DLS and CD in addition to microscopic techniques. The degradation study on these stmuli responsive polymers were performed by using DTT as a redox reagent. Upon treatment with DTT, the high molecular weight polymer was degraded into small molecular weight structures. Moreover, the degradation of these disulfide polymers were affirmed by ^1H-NMR and GPC analysis. The cytotoxicity studies of amine functional disulfide polymers (cationic polymers) were performed in MCF-7 cells and the result indicated that these polymers are nontoxic to cells and are also biocompatabile in nature.

5.1. Introduction

Macromolecular architectures with disulfide chemical linkages are in high demand for diverse applications in material and biomedical industry due to their excellent responsiveness to light, heat, pH, redox reagents and enzymes, etc.[1-3] The disulfide linkages in the polymer chains can be introduced via ring-opening polymerization of cyclic oligo-disulfides.[4-9] Hay and coworkers prepared a set of poly (thioarylene)s from cyclic disulfide oligomers and dibromo or diiodo aromatic compounds in diphenyl ether as solvent at 270 °C. The poly (thioarylene)s showed high thermal stability and melting point due to the rigid aromatic structure in the polymer backbone. Similarly Song et al. synthesized poly (arylene disulfide) using ring opening polymerization of cyclic (4, 4'-oxybis (benzene) disulfide) oligomer. The polymerizations of cyclic oligomers were carried out in hot-press under atmosphere and nitrogen atmosphere to yield poly (arylene disulfide) (scheme 5.1a). Rosenthal et al. and Lee et al. developed oxidative polymerization of thiol end-capped oligo-ethylene glycols (or PEGs) (scheme 5.1b).[10-11]
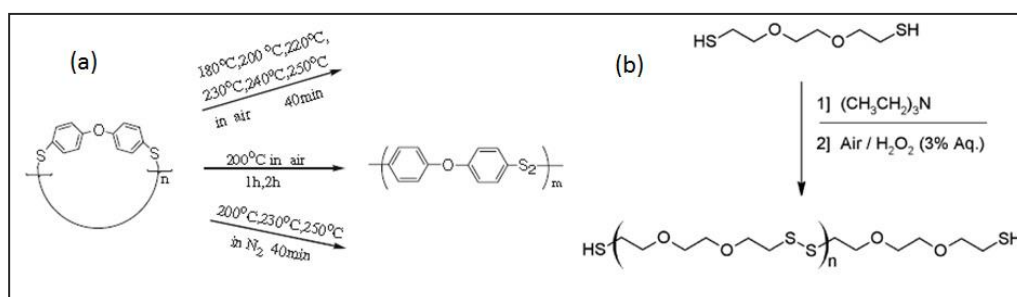

Scheme 5.1. *Disulfide containing polymers synthesis via rop of cyclic disulfide oligomers (a) and di thiol oxidative polymerization approach (b) (adopted from J Mater Sci* **2007***, 42,* 1156-1161*(a) and Rosenthal et al. Biomacromolecules,* **2012***, 13,* 154-164*(b))*

Recently, photo-induced disulfide metathesis polymerization was developed to make hybrid polymers and photo-mendable polymeric materials (in scheme 5.2a).[12-13] Ghosh and coworkers prepared telechelic poly (disulfide)s by carefully controlling the stoichiometric balance between di-thiols and 2, 2'-dithiopyridines (scheme 5.2b).[14-15] In these methodologies, the in-situ generation of sulphur radicals by light[12], heat or acid propagate the polymerization to produce high molecular weight poly(disulfides).
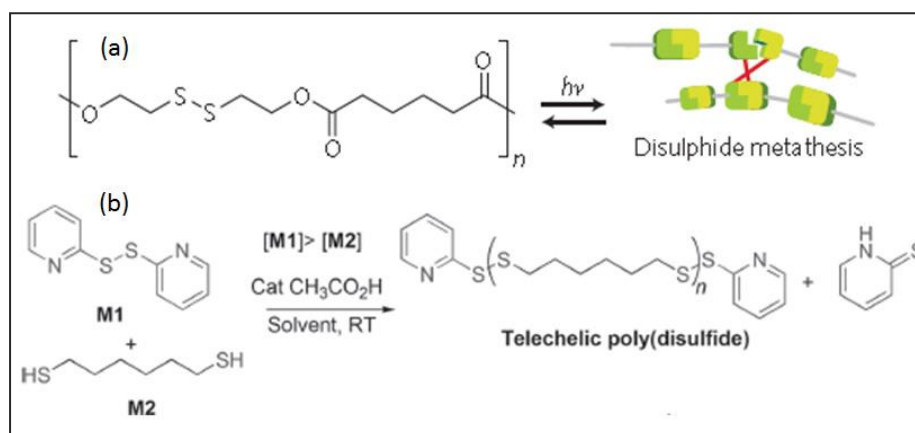
Scheme 5.2. *Disulfide metathesis reaction under photochemical condition (a) and disulfide polymers synthesis using dithio pyridines (b) (adopted from Otsuka et al.* Chem. Commun. **2010**, *46,* 1150-1152 (a) and Basak et al. *Macromol. Rapid Commun.***2014**, *35*, 1340-1344 (b))

Non-sulphur mediated or indirect methodologies were also adopted for making disulfide containing macromolecular architectures. For example, disulfide containing TEMPO initiator for polystyrene,[16] four-arm RAFT initiators for star copolymers[17] and ATRP for branched poly(t-butyl acrylate)s[18-19] are some of the important examples. Michael addition diamines or diacrylates having in-built disulfide linkages were found to produce poly(disulfide amine)s or poly(disulfide amide)s (in scheme 5.3a).[20-21] Ring opening polymerization of disulfide cyclic glycidol derivatives were found to yield redox degradable hyperbranched polyglycerols[22] and self-healing polymers (in scheme 5.3b).[23-24] Click polymerization was also utilized to make biodegradable and redox-responsive poly(aminoacid)s.[25]
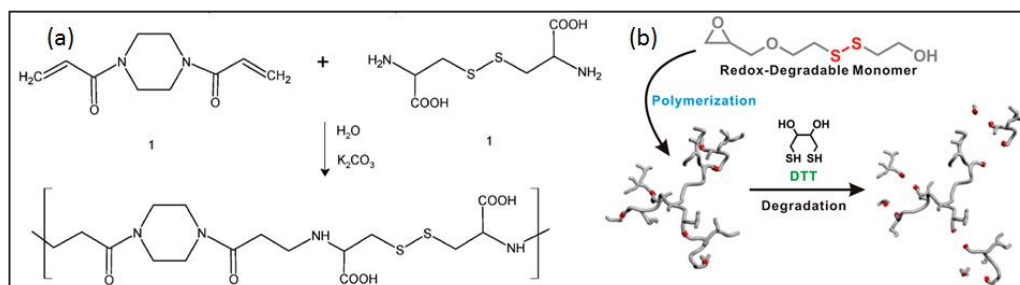
Scheme 5.3. *Michael addition approach for disulfide polymer synthesis (a) and hyper branched disulfide polymer synthesis via rop approach of epoxide(adopted from Ou al. Bioconjugate Chem.* **2008***, 19,* 626-633*(a)and Son et al.* Macromolecules **2015***, 48,* 600-609*(b))*

Recently, p-nitrophenol mediated solution polymerization was developed for redox cleavable L-phenylalanine based poly(ester-amide)s (in figure 5.1).[26] Among the natural L-amino acid resources; L-cysteine is the only residue that has thiol (-SH) functionality. L-Cysteine residues are not stable and are readily oxidized into stable disulfide dimer L-cystine. N-Carboxyl anhydrides of L-cystine[27-29] monomers were subjected to ring opening polymerization to make star shaped polymers and functional polypeptides, respectively.
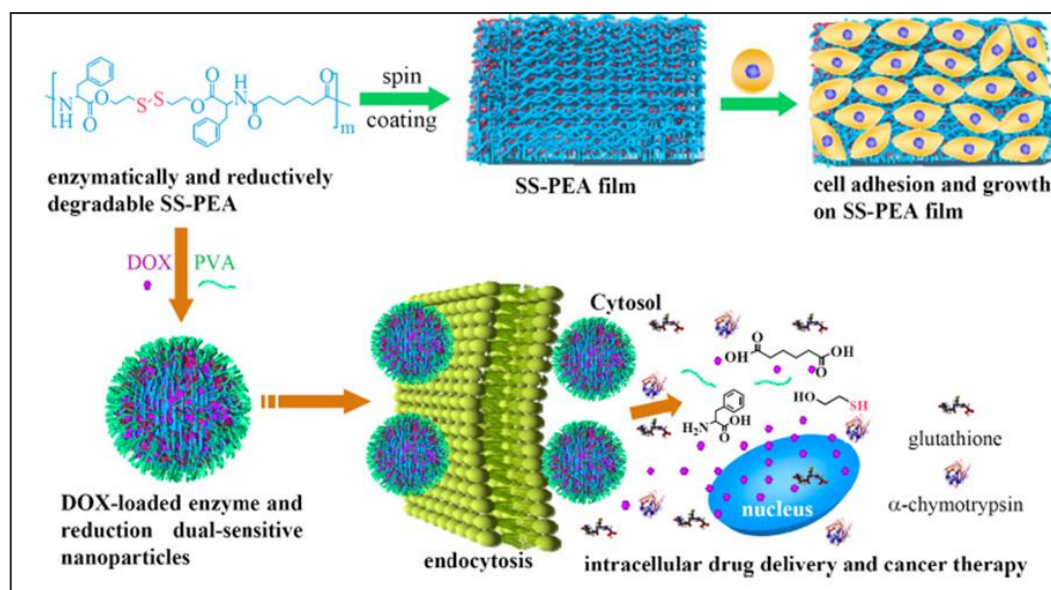

Figure 5.1. *Phenylalanine based disulfide polymer synthesis using solution polycondensation approach for drug delivery application (adopted from Sun Biomacromolecules,* **2015***, 16,* 597-605*)*

Very recently, L-cystine diamine was polymerized with fatty dicarboxylic acids in solution polycondensation route to make poly(disulfide amide) nanoparticles for docetaxel delivery (in figure 5.2).[31] These poly(disulfide)s were employed as nano-scaffolds for delivering anticancer drugs[32-37] and genes.[38] The above examples clearly envisage the importance of the disulfide polymers and their macromolecular architectures for redox degradation and biomedical applications.
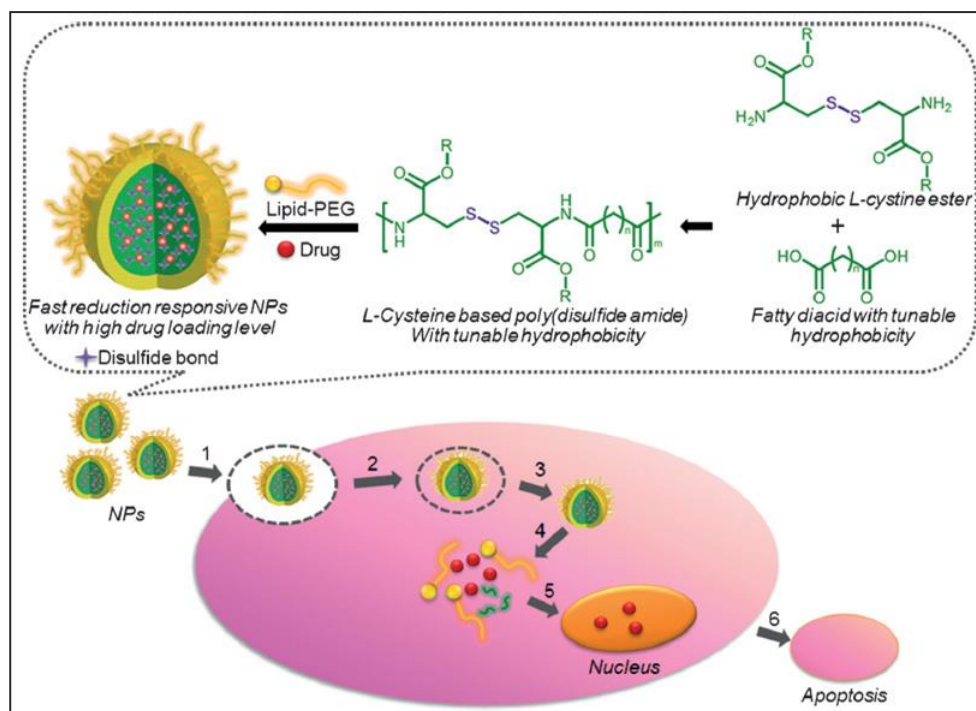
Figure 5.2. *Synthesis of poly (ester-amide) based on cystine amino acid by solution polycondensation approach and their drug delivery application (adopted from Wu et al. Angew. Chem. Int. Ed.* **2015***, 54, 9218-9223)*

Melt polycondensation is another important synthetic methodology that largely employed for the manufacture of thermoplastic engineering polymers such as polyesters, polyamides and polycarbonates in few million tons/year. Unfortunately, there are no reports for disulfide linkage polymers based on this eco-friendly melt polycondensation chemistry in the literature. The development of solvent free melt process for disulfide linkage polymer is very important since it would provide new opportunity for redox degradable polymeric materials. To accomplish this goal, the present investigation is aimed at development of disulfide linkage polyesters based on natural L-amino acid resources. By combining the melt polycondensation (green process) and natural L-amino acid (bio-resources), the approach becomes very unique to yield novel polymeric materials with redox degradability, biocompatibility and with the ability to give diverse supramolecular secondary structures (originates from L-amino acid residues) in a single system. This concept is shown in figure 5.3.
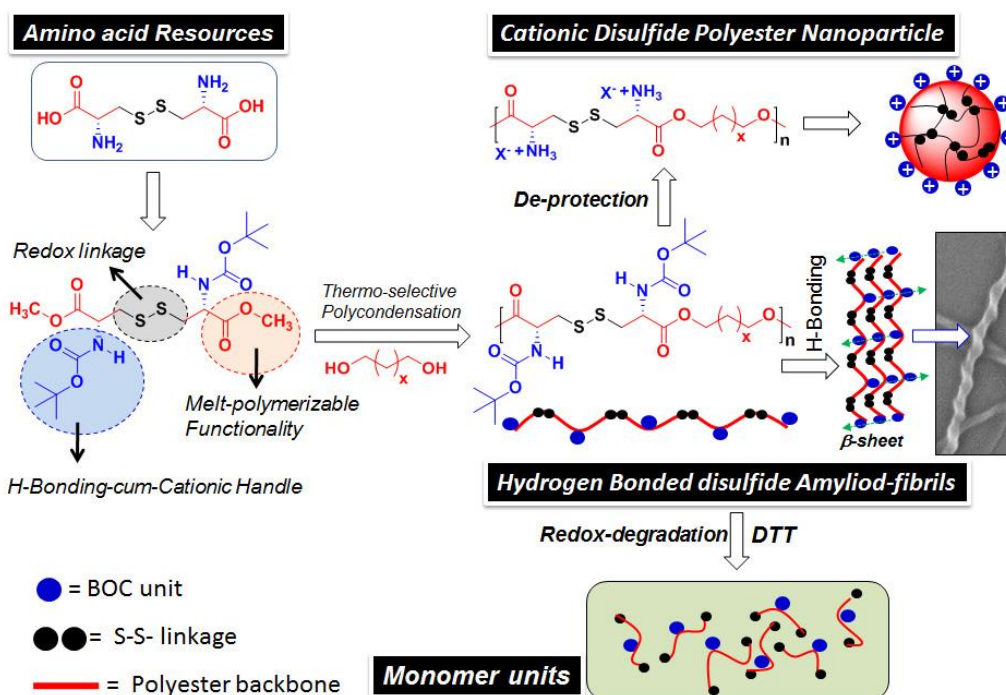
Figure 5.3. *Approaches for the development of redox-degradable amyloid-like disulfide polyesters and cationic polyester nanoparticles based on L-cystine*

For this purpose, L-cystine was chosen and it was suitably converted into multi-purpose monomer with following features: (i) amine functionality was converted into Boc urethane which act as β-sheet hydrogen bonding vector for seeding amyloid-fibril and also as cationic resources upon de-protection into -NH$_3^+$X$^-$ polymeric salts, (ii) the dicarboxylic acids were converted into methyl esters which have capabilities to undergo thermo-selective melt polymerization (developed from our laboratory) to produce disulfide linkage containing linear polyesters, and (iii) the disulfide linkages in the polyester backbone is redox degradable; thus, the polymers can be degraded into their monomer species (in figure 5.3). From earlier chapter, the development of dual ester-urethane condensation and thermo-selective melt transesterification for the preparation of L-amino acid based linear poly(ester-urethane)s and functional polyesters have been clearly understood. In this chapter, we design new multi-purpose L-cystine monomer and subject it to thermo-selective melt polycondensation to yield new disulfide containing polymers (in figure 5.3). The nascent polymer (in neutral form) was capable of self-assembling into β-sheet secondary structure in solution (confirmed by CD spectroscopy) which subsequently seeded for the amyloid-fibrils formation. Upon Boc de-protection; the disulfide

polyester turned into water dispersible cationic polyester and it was found to self-assemble as stable nanoparticles. The redox degradation behaviors of nascent disulfide polyester were studied using DTT and the process was monitored by ^{1}H-NMR and GPC techniques. It was found that the disulfide chemical linkages were completely degraded by redox reagent. The cytotoxicity studies in MCF-7 cell lines revealed that these cationic disulfide polymers are highly biocompatible and non-toxic to cells up to 50 μg/mL. The overall finding revealed that the L-cystine based cationic disulfide polyester are biocompatible materials, they show diverse supramolecular assemblies, and they are completely degradable by redox reagents. The newly developed L-cystine polymers may be very useful for future biomedical applications.

5.2. Experimental methods

5.2.1. Materials: L-cystine, 1, 12-dodecandiol, 1, 10-decanediol, 1, 8-octanediol, dithiothreitol (DTT), 1-decanol and titanium tetrabutoxide (Ti(OBu)$_4$, tetrazolium salt: 3-4,5 dimethylthiazol-2,5diphenyltetrazolium bromide (MTT), DMSO, hoechst and 4% paraformaldehyde purchased from Aldrich chemicals and used without further purification. Methyl chloroformate, Ditertbutyl dicarbonate, thionyl chloride and other solvents were purchased locally and purified prior to use.

5.2.2. General Procedures: ^{1}H and ^{13}C-NMR were recorded using 400-MHz JEOL NMR spectrophotometer. All NMR spectra were recorded in CDCl$_3$ containing TMS as internal standard. FT-IR spectra of all compounds were recorded using Bruker alphaT Fourier transform infrared spectrophotometer. The mass of the monomers were analysed using a HRMS-ESI-Q-time-of-flight LCMS (SynaptG2, Waters). Gel permeation chromatographic (GPC) analysis which was performed using Viscotek VE 1122 pump, Viscotek colum T6000M General mixed org 300 x 8.0 mm (THF), Viscotek VE 3580 RI detector and Viscotek VE 3210 UV/Vis detector in tetrahydrofuran (THF) using polystyrene as standards at 25 °C. Thermal stability of the polymers was determined using Perkin Elmer thermal analyzer STA 6000 model at a heating rate of 10 °C/min in nitrogen atmosphere. Thermal analysis of all polymers were performed using TA Q20 Differential Scanning Calorimeter. The instrument was calibrated with Indium standards. All the polymers were heated to melt before recording their thermograms to remove their previous thermal history.

Polymers were heated and cooled at 10 °C/min under nitrogen atmosphere and their thermo grams were recorded. Circular dichroism (CD) analysis of the polymer samples were done using JASCO J-815 CD spectrometer at 20 °C in THF and water. FE-SEM images were recorded using Zeiss Ultra Plus scanning electron microscope. For FE-SEM analysis, the samples were prepared by drop casting on silicon wafers and coated with gold. Atomic force microscope (AFM) images were recorded by drop casting the samples on freshly cleaved mica surface, using Veeco Nanoscope IV instrument. The experiment was done in tapping mode.

5.2.3. Synthesis of dimethyl 3, 3'-disulfanediylbis (2- ((tert-butoxycarbonyl) amino) propanoate) (monomer 1): To a suspension of L-cystine (19.8 g, 0.082 mol) in methanol (200 mL), thionylchloride (20.4 mL, 33.4 g, 0.283 mol) was added drop wise at 0 °C under nitrogen atmosphere.The above reaction mixture was brought to room temperature and refluxed for 12 h under nitrogen. Methanol and the unreacted thionylchloride were removed by distillation following which the solid mass was dissolved in triethylamine (46 mL, 33.7 g, 0.333 mol) and dichloromethane (200 mL) mixture at 0 °C. To the reaction mixture, Boc anhydride (41.0 mL, 41.1 g, 0.191 mol) was added drop wise at 0 °C. It was brought to 25 °C and stirring was continued for 12h. The reaction mixture was poured into water and then extracted with dichloromethane. The organic layer was dried over anhydrous Na_2SO_4 and the solvent was removed to obtain white solid as product. It was further purified by passing through silica gel column using ethyl acetate and pet ether (1:4 v/v) as eluent. Yield = 25.1 g (65 %). ^{1}H-NMR (400 MHz, CDCl$_3$) δ ppm: 5.41 (b, 2H, -N**H**), 4.60 (m, 2H, **CH**), 3.77 (s, 6H, CHCOOC**H₃**), 3.17 (m, 4H, C**H₂**S) and 1.45 (s, 18H, -NHCOO (C**H₃**)**₃**). ^{13}C-NMR (100 MHz, CDCl$_3$) δ ppm: 171.15, 155.04, 80.30, 52.82, 52.69, 52.62, 41.33, 41.26 and 28.30. FT-IR (cm^{-1}): 3743, 3364, 2938, 1749, 1682, 1509, 1363, 1216, 1163, 1057 and 1017. HRMS (ESI+): m/z [M+Na$^+$] calcd. for $C_{18}H_{32}N_2O_8S_2Na$ [M$^+$]: 491.1498; found: 491.1577.

5.2.4. Melt polycondensation Process: L-cystine monomer **1**(0.67 g, 0.001 mol), 1, 12-dodecanediol (0.29 g, 0.001 mol, for polymer **P-12**) and benzoquinone (catalytic amount, 2.0 mg) were taken in a test tube-shaped polymerization vessel and melted in oil bath at 100 °C. The polycondensation apparatus was made oxygen and moisture

free by purging with nitrogen and consequent evacuation by vacuum under constant stirring. Titanium tetrabutoxide (0.005 g, 0.01 mmol, 1.0 mol %) was added as catalyst and the melt polycondensation was carried out at 120 °C for 4h with constant stirring under nitrogen purge. During this stage, the methanol was removed along with the purge gas and the polymerization mixture became viscous. The viscous melt was further subjected to high vacuum (0.01 mm of Hg) at 120 °C for 2 h under stirring. At the end of the polycondensation, the polymer was obtained as transparent resin. Yield =0.67 g (82 %).^{1}H-NMR (400 MHz, CDCl$_3$) δ ppm: 5.43 (b, 2H, N**H**), 4.60 (m, 2H, C**H**), 4.17 (t, 4H, CH$_2$COOC**H$_2$**), 3.15 (m, 4H, **CH$_2$**S), 1.70 (m, 4H, **CH$_2$**), 1.47 (s, 18H, -NHCOO (C**H$_3$**)$_3$) and 1.30 (m, 16H, **CH$_2$**). ^{13}C-NMR (100 MHz, CDCl$_3$) δ ppm: 170.72, 155.06, 80.19, 65.97, 53.08, 41.47, 29.43, 29.19, 28.49, 28.33 and 25.82. FT-IR (cm^{-1}): 3743, 3377, 2925, 2859, 1709, 1503, 1363, 1163 and 1057.

Similarly L-cystine monomer **1** was polymerized with 1, 8-octanediol and 1, 10-decanediol to produce **P-8** and **P-10**, respectively. NMR data and their details for these polymers are provided below.

Entry P-10: Monomers used are L-cystine Boc monomer (0.621 g, 0.001 mol) and 1, 10-decanediol (0.24 g, 0.001 mol),Titanium tetrabutoxide (0.004 g, 0.001 mmol, 1 mol %) were used. Yield =0.66 g (86%). ^{1}H-NMR (400 MHz, CDCl$_3$) δ ppm: 5.44 (b, 2H, N**H**), 4.60 (m, 2H, C**H**), 4.17 (t, 4H, CH$_2$COOC**H$_2$**), 3.18 (m, 4H, **CH$_2$**S), 1.69 (m, 4H, **CH$_2$**), 1.47 (s, 18H, -NHCOO (C**H$_3$**)$_3$) and 1.30 (m, 12H, **CH$_2$**). ^{13}C-NMR (100 MHz, CDCl$_3$) δ ppm: 170.71, 155.05, 80.17, 66.00, 53.07, 41.49, 29.56, 29.51, 29.23, 28.49, 28.33 and 25.84. FT-IR (cm^{-1}): 3372, 2937, 2864, 1718, 1508, 1363, 1152 and 1056.

Entry P-08: Monomers used are L-cystine Boc monomer (0.721 g, 0.002 mol) and 1, 8-octanediol (0.23 g, 0.001 mol),Titanium tetrabutoxide (0.005 g, 0.002 mmol, 1 mol %) were used. Yield =0.65 g (77%).^{1}H-NMR (400 MHz, CDCl$_3$) δ ppm: 5.44 (b, 2H, N**H**), 4.60 (m, 2H, C**H**), 4.17 (t, 4H, CH$_2$COOC**H$_2$**), 3.18 (m, 4H, **CH$_2$**S), 1.70 (m, 4H, **CH$_2$**), 1.47 (s, 18H, -NHCOO (C**H$_3$**)$_3$) and 1.30 (m, 8H, **CH$_2$**). ^{13}C-NMR (100 MHz, CDCl$_3$) δ ppm: 170.72, 155.06, 80.19, 65.90, 53.07, 52.61, 41.44, 29.06, 28.45, 28.33 and 25.75. FT-IR (cm^{-1}): 3736, 2925, 1702, 1516, 1363, 1150 and 1050.

5.2.5. Model Reactions Studies: 1-decanol (0.35 g, 0.002 mol) and L-cystine monomer (0.33 g, 0.001 mol) were taken in a test tube shaped polymerization apparatus and melted by placing in an oil bath at 100 °C with constant stirring. After

degassing, Ti(OBu)$_4$ (0.003 g, 1 mol%) was added and the condensation was carried out at 120 $^{\circ}$C under nitrogen purge for 4 h. At the end of the condensation reaction, the product was obtained as viscous liquid. ^{1}H-NMR (400MHz, CDCl$_3$) δ ppm: 5.43 (b, 2H, -N**H**), 4.61 (m, 2H, C**H**), 4.17 (m, 4H, COOC**H$_2$**), 3.18 (d, 2H, C**H$_2$**), 1.68 (m, 4H, CH$_2$), 1.47 (s, 18H, -NHCOO (C**H$_3$)$_3$**), 1.28 (m, 28H, CH$_2$) and 0.88 (t, 6H, CH$_3$). ^{13}C-NMR (100 MHz, CDCl$_3$) δ ppm: 170.71, 155.05, 80.19, 53.07, 41.53, 31.88, 29.53, 29.49, 29.29, 29.21, 28.48, 28.33, 25.85, 22.67 and 14.09.FT-IR (cm^{-1}): 3324, 2928, 2856, 1709, 1515, 1459, 1451, 1193 and 1047. MALDI-TOF MS: m/z [M+Na$^+$] calcd. for C$_{36}$H$_{68}$N$_2$O$_8$S$_2$Na[M$^+$]= 743.4315; Found = 743.5544.

5.2.6. Deprotection of Boc polymer (PA-X): The disulfide polymer P-12 (0.81 g, 0.001 mol) was taken in a 50 mL single neck RB flask and then 5 mL of dry DCM was added into it. At 0 °C TFA (1.33 g, 1.1 mL, 0.012 mol) was added dropwise, the content was brought to 25 °C and the stirring was continued for 1 h. The solvent and TFA was removed by rotavapor and the product was purified by precipitation in cold diethyl ether. Yield= 0.59 g (89 %). ^{1}H-NMR (400 MHz, CD$_3$OD) δ ppm: 4.38 (m, 2H, C**H**), 4.19 (m, 4H, COOC**H$_2$**), 3.26 (d, 4H, C**H$_2$**), 1.63 (m, 4H, C**H$_2$**) and 1.28 (m, 16H, C**H$_2$**).^{13}C-NMR (100 MHz, CDCl$_3$) δ ppm:168.43, 66.58, 61.20, 51.52, 40.22, 32.81, 29.41, 29.11, 28.24, 27.91, 27.75, 27.62, 25.86, 25.65 and 25.23. FT-IR (cm^{-1}): 2927, 2856, 1750, 1661, 1532 and 1137.

Entry PA-10: P-10 (0.64 g, 0.001 mol), Trifuluoro acetic acid (1.2 g, 0.8 mL, 0.012 mol) and DCM (5.0 mL) were used. Yield=0.66 g (86%). ^{1}H-NMR (400 MHz, CD$_3$OD) δ ppm: 4.45 (m, 2H, C**H**), 4.34 (m, 4H, COOC**H$_2$**), 3.33 (d, 4H, C**H$_2$**), 1.77 (m, 4H, C**H$_2$**) and 1.37 (m, 12H, C**H$_2$**).^{13}C-NMR (100 MHz, CDCl$_3$) δ ppm: 167.61, 66.78, 51.53, 36.65, 32.23, 29.24, 28.94, 28.10, 27.78, 25.48 and 25.22. FT-IR (cm^{-1}): 2928, 2864, 1742, 1677, 1524 and 1138.

Entry PA-08: P-8 (0.51 g, 0.001 mol), Trifuluoro acetic acid (1.1 g, 1.5 mL, 0.013 mol) and DCM (5.0 mL) were used. Yield=0.50 g (81%). ^{1}H-NMR (400 MHz, CD$_3$OD) δ ppm: 4.48 (m, 2H, C**H**), 4.40 (m, 4H, COOC**H$_2$**), 3.42 (d, 4H, C**H$_2$**), 1.75 (m, 4H, C**H$_2$**) and 1.41 (m, 8H, C**H$_2$**). FT-IR (cm^{-1}): 2937, 2864, 1742, 1661, 1515 and 1137.

5.2.7. Degradation study: The disulfide polymer (P-12) (0.10 g, 0.0002 mol) and DTT (0.25 g, 0.001 mol) were taken in dry tetrahydrofuran (10 mL) in 50 mL two neck round bottom flask. The polymer solution was refluxed at 70 °C and aliquots were taken periodically. The aliquots were analyzed by GPC and ^{1}H-NMR to estimate extent of the degradation.

5.2.8. Cell Viability Assay (MTT Assay):

Tetrazolium salt 3-(4,5 dimethylthiazol)-2,5-diphenyl tetrazolium bromide (MTT) was used in an assay to determine the cytotoxic effects of the polymer **PA-8 and PA-10** in MCF-7 cell lines. 1×10^3 cells were seeded in each well of a 96- well plate (Corning, U.S.A.) having 100 µL of DMEM with 10 % FBS (fetal bovine serum) and the cells were incubated at 37ºC under CO_2 environment for 16h. Media was aspirated from each well and various concentrations of polymer **PA-8 and PA-10** were prepared in 100 µL of DMEM with FBS and were given to the cells. Along with polymer samples blank control of media alone was maintained in triplicates. The cells were further incubated for 72h without changing the media. A fresh sample of MTT in sterile PBS (5 mg/mL) was prepared and diluted to 50 µg/mL in 100 µL of DMEM with FBS and this was added to each well. Cells were then incubated with MTT for 4 h at 37 °C. The media was aspirated and purple formazan crystals were obtained. These crystals were generated as a result of reduction of MTT by mitochondrial dehydrogenase enzyme from live cells. These were dissolved in 100 µL DMSO. The 96-well plate was shook for 2 minutes and the absorbance from formazan crystals (dissolved in DMSO) was measured using microplate reader at 570 nm (Varioskan Flash). The absorbance obtained from each well was representative of the number of cells viable per well. The mean of absorbance values were calculated for the corresponding polymer and control and that of blank control samples was subtracted from the average of treated samples. The values obtained from the control samples were taken as 100% and relative percentage values for the samples were calculated accordingly. These were plotted against the concentrations of the polymer and have been shown in figure 5.15.

5.3. Results and Discussion

5.3.1. **Synthesis of functional monomer and polymer**

The L-cystine amino acid contains two carboxylic acid and an amine functional group with the disulfide bond. L-cystine amino acid carboxylic acid functional groups were converted into L-cystine methyl ester amine salt using thionyl chloride in methanol under nitrogen atmosphere. Further the amine salt was reacted with Boc anhydride to yield the L-cystine ester-urethane monomer **1** (in Figure 5.4a). The thermal gravimetric analysis (TGA) of L-cystine monomer 1 confirmed that it was thermally stable up to 190 °C and could be employed for solvent free melt polycondensation (in scheme 5.4b). Based on our earlier knowledge of polymerisation of L-amino acid polymers, the polycondensation temperature was chosen as 120 °C and Ti(OBu)$_4$ (1 mole %) was employed as catalyst. Under these conditions, the ester functional group in the custom designed monomer **1** was expected to undergo thermo-selective polymerization with diol to produce linear polyester with urethane pendant in each repeating unit (the urethane functional group was completely inert towards alcohol at 120 °C).
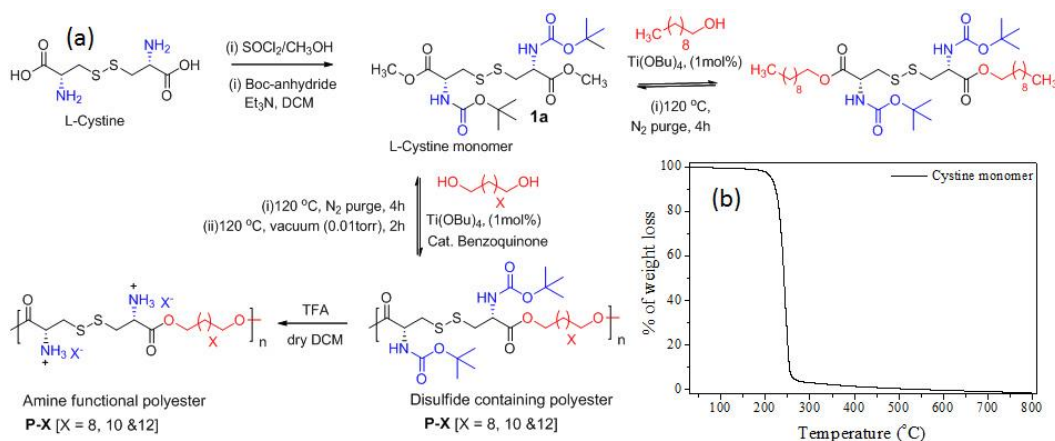

Figure 5.4. *Synthesis of disulfide functional monomer* **1**, *model compound and polymers P-X (a)and TGA analysis of monomer at 10 °C/min (b)*

In order to test the thermo-selective polymerization of monomer 1 towards alcohol; a model reaction was performed with 1-decanol at 120 °C using Ti-catalyst. One equivalent of L-cystine monomer 1 and two mole equivalents of 1-decanol were subjected to melt polycondensation reaction under nitrogen purge for 4h. A pinch of hydroquinone was added in the polymerization mixture as radical quencher to avoid

the radical cleavage of disulfide linkages in the melt condensation. ^{1}H-NMR and ^{13}C-NMR spectra of the monomer 1, polymer and model compound are shown in figure 5.5 and 5.6 and the protons in the chemical structures are assigned by alphabets.
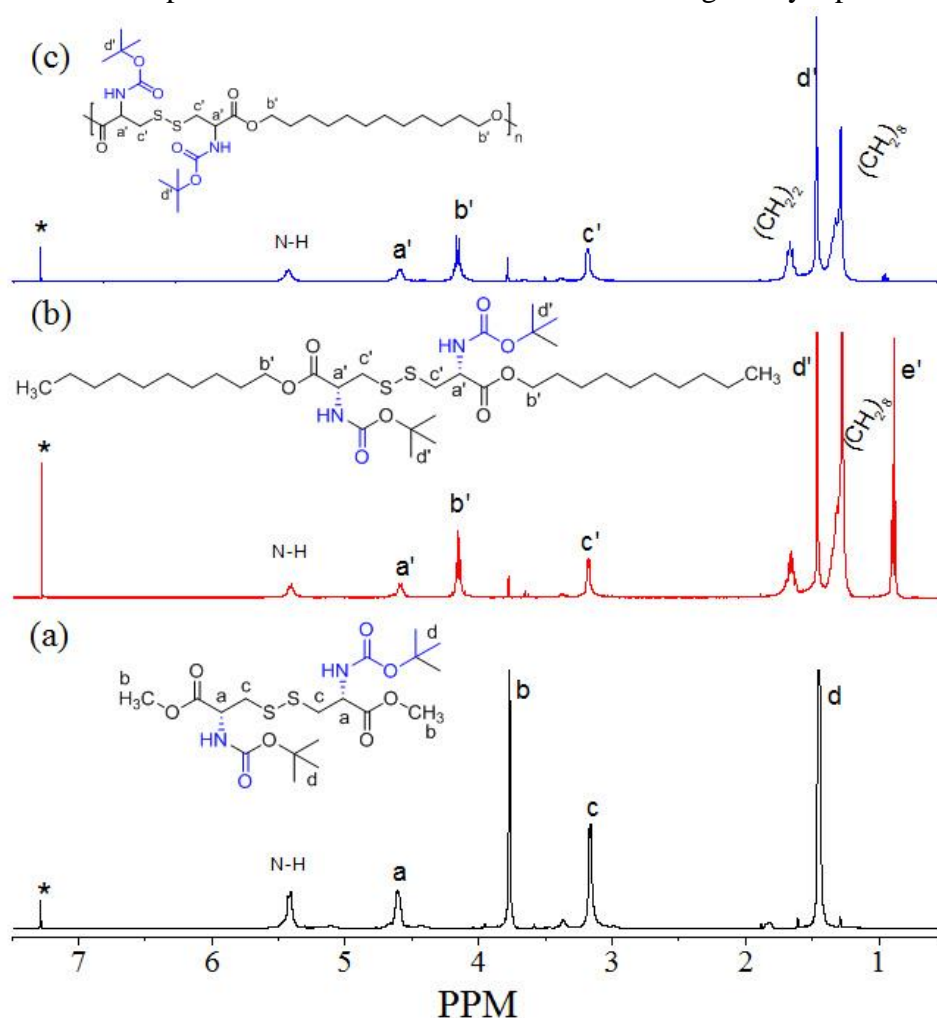

Figure 5.5. *^{1}H NMR spectra of L-cystine monomer 1 (a), model compound (b) and polymer P-1 2 (c) in CDCl$_3$*

5.3.2. Characterisation of disulfide functional polymer

The L-cystine monomer **COOCH$_3$** ester peak that normally appears at 3.65 ppm (proton b, in figure 5.5a) was seen to disappear in the model reaction (in figure 5.5b). However a new ester peak belongs to R-**COOCH$_2$CH$_2$** appeared at 4.14 ppm (proton b', in figure 5.5b) in the spectrum. Under this reaction condition, the peak corresponding to Boc proton **NHCOOC-(CH$_3$)$_3$** were retained at 1.41 ppm (proton d) in the model reaction. Similarly, ^{13}C-NMR showed that the peak corresponding to ester carbon atom –O**C**H$_3$ at 53.45 ppm (in figure 5.6a) disappeared in the model reaction and a new peak belonging to R-COO**C**H$_2$CH$_2$- appeared at 65.01 ppm (in

figure-5.6b). The peak with respect to carbon atom in Boc group NHCOO**C** (**C**H$_3$)$_3$ at 80.04 ppm was retained in the model compound (in figure 5.6c). The model compound was further subjected to MALDI-TOF analysis and its spectra showed the formation of peak at m/z =743.5 (Na+) as expected for the formation of bis-ester product with Boc urethane substitutions (in figure 5.7). This confirmed that the Boc urethane was completely inert in the polymerisation process at 120 °C towards alcohol functional groups and only the carboxylic esters underwent transesterification to produce new ester linkages.
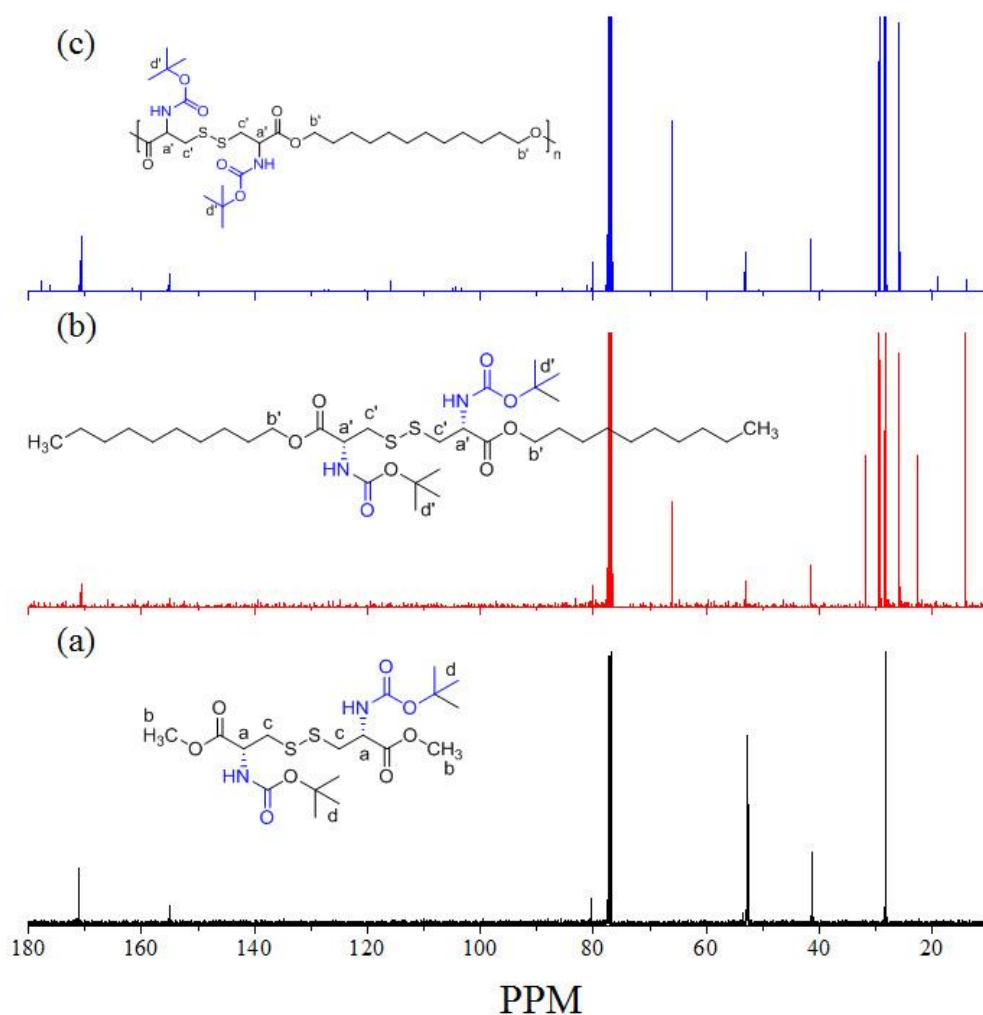

Figure 5.6. *^{13}C NMR spectra of L-cystine monomer 1 (a), model compound (b) and polymer P-1 2 (c) in CDCl$_3$.*

The polymerization was carried out for equimolar amounts of monomer **1** with diol in presence of Ti-catalyst at 120 °C. For this purpose, three commercial diols 1,8-octanediol, 1, 10-decanediol and 1, 12-dodecanediol were chosen. The initial polymerization under nitrogen purge for 4 h produced viscous mass which was further subjected to vacuum (0.01torr) to afford high molecular weight polymers. The L-

cystine based polymers were referred to as P-X, where X represents the number of aliphatic carbon present in the diol (in figure 5.4). The structures of the polymers were confirmed by ^{1}H and ^{13}C-NMR as shown in figure 5.5 to 5.6. The polymers showed the formation of new ester peaks in their respective NMR spectra. Further, the Boc peaks were retained in the polymers; thus, the thermo-selective polymerization of esters is very good in producing functional model compound and polymers having Boc urethane as pendants.
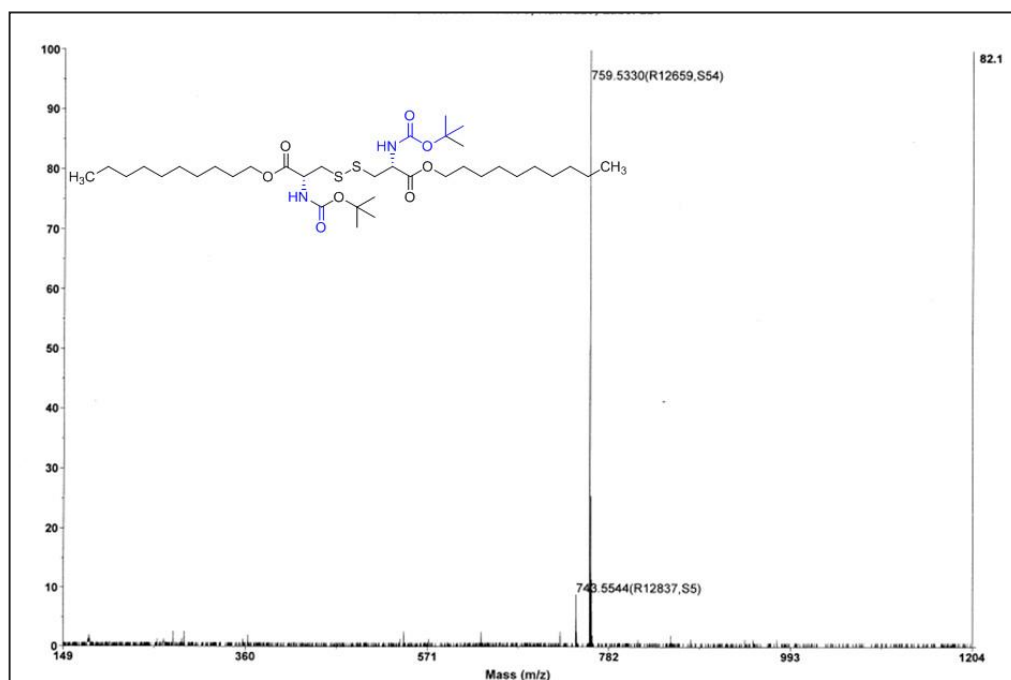

Figure 5.7. *MALDI-TOF mass spectra of L-cystine amino acid monomer with 1-decanol at 120 °C*

The molecular weight of disulfide functional polyesters were analysed by gel permeation chromatography (GPC) in tetrahydrofuran (THF) as solvent. The GPC chromatograms of the disulfide functional polymers showed monomodal distribution (in figure-5.8b). The molecular weight of disulfide functional polyesters were obtained in the range of M_n=4.0 -10.0x10^3 and M_w=8.0-31.0x10^3 with polydispersity of ~2.5. The molecular weights of the polymers synthesized using longer diols were found to be much higher than shorter ones (table in figure 5.8a). This trend was attributed to the steric effect introduced by the Boc group in the polymer backbone. For example, the polymers made from shorter diols are bound to have bulky Boc urethane groups at closer vicinity that is known to induce more steric hindrance in the backbone. Thermal gravimetric analyses (TGA) of the disulfide functional polyesters were carried out at 10 °C/min heating rate. TGA plots in figure 5.8c showed two

distinct decomposition temperatures. First step is attributed to the decomposition of side chain Boc functional group at 220-240 °C (ref) and the second step above 300 °C with respect to the polymer backbones (in figure-5.8c). Differential scanning calorimetry (DSC) studies showed that all the disulfide polyesters were amorphous in nature (in figure 5.8d). The glass transition temperature (T_g) of the polymers were increased with decrease in the spacer length of diol. Thus, the newly designed L-cystine monomer is very good in producing disulfide containing polyester with diols under thermo-selective melt polymerization process.

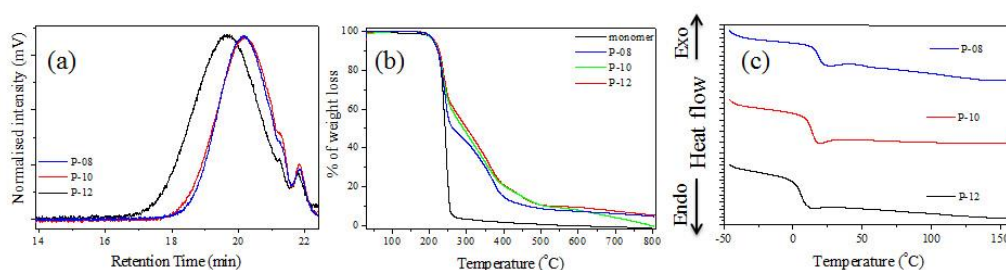| (a) Sample	M_n	M_w	M_w / M_n	T_g	T_D
P-8	4100	8400	2.1	18.6	260
P-10	6500	16300	2.5	14.1	262
P-12	10400	31500	3.0	6.2	268

Figure 5.8. *(a) Table containing GPC molecular weights, glass transition temperature (Tg) and decomposition temperature (T_D) of the polymers P-X. (b) GPC chromatogram of P-X polymers in THF using polystyrene as standard. (c) TGA plots of the P-X polymers recorded at 10 °C/min heating rate. The decomposition temperatures were determined for 10 % weight loss. (d) DSC thermograms of P-X at 10 °/min heating rate.*

The side chain Boc group of the polymers were selectively de-protected without disturbing the polyester backbone using trifluoroacetic acid (TFA). This produced new cation functionalized disulfide polyester as shown in figure 5.9. The de-protection of Boc group was confirmed by ^{1}H-NMR and FT-IR spectroscopy as shown in figures 5.9a-5.9b. The peak belongs to –NH(COO(**CH₃)₃**) proton at 1.41 ppm completely disappeared upon de-protection without affecting other protons in the polymer structure (in figure 5.9 a). The FT-IR spectra of P-12 showed –NH stretching vibration band at ν =3350 cm^{-1} with respected to –NH bond involved in the hydrogen bonding interaction, Similarly, the –C=O stretching vibration band at ν =1722 cm^{-1} was observed for hydrogen bonding interaction (in figure 5.9b). The de-

protected cationic functional polyester (amine salt $NH_3^+X^-$) did not show peak above 3000 cm^{-1} due to the lack of NH- hydrogen bonding interactions.
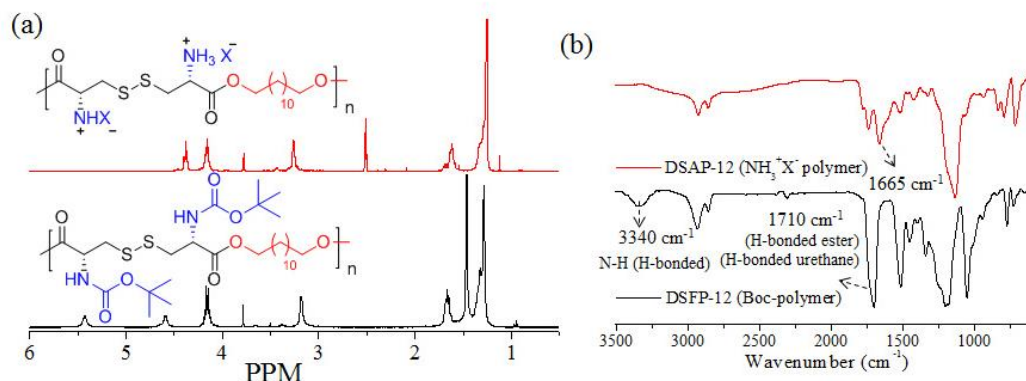

Figure 5.9. *^{1}H-NMR (a) and FT-IR (b) spectra of P-12 and its de-protected cationic polymer.*

Based on the above studies, it can be concluded that the new synthetic approach is very efficient for making disulfide containing urethane pendent functional polyester as well as cationic functionalized polyester based on L-cystine amino acid resources.

5.3.3. Self-assembly of Neutral and Cationic Polyesters

The custom designed L-cystine functional polyesters were subjected to self-assembly studies in organic solvents and water. The Boc pendant polyester was found to be insoluble in water; thus, their self-assembly studies were carried out in tetrahydrofuran (THF). On the other hand, the de-protected cationic polymer was found to be partially soluble in water. The cationic polymer was dissolved in DMSO + water mixture (1 : 1 v/v) and the solution was transferred to semi-permeable membrane. It was dialyzed against large amount of water for 24 h with constant replenishing of fresh water at regular interval. The dialyzed polymer solution was found to stable for more than a month. The disulfide functional polyester are made up of optically active L-cystine amino acid as the starting material; hence both the neutral polymer (having Boc pendent) and cationic polymer were subjected to circular dichroism (CD) analysis to determine their secondary structures (in figure 5.10). CD spectra showed broad negative CD band at 260 nm and positive CD band at 220 nm with respect to β-sheet conformation (in figure 5.10 a). The CD spectra showed broad signal form 250 nm to 280 nm due to the absorption of disulfide bond. The observation of broad spectra is attributed to the merging of β-sheet signals (at 220 nm)

with disulfide absorption (at 260 nm). The cationic polymer was subjected for CD analysis in both water and THF (in figure-4b and 4c). CD spectra of the cationic polymer showed positive CD around 220 nm in both THF and water with respect to random coil conformation. (in figure 5.10b-5.10c). The disappearance of the β-sheet conformation in the cationic polymer was attributed to the lack of the hydrogen bonding in their $NH_3^+X^-$ amine salt. This was further confirmed by the FT-IR analysis (in figure 3b) that the neutral polymer exhibited strong β-sheet hydrogen bonding with respect to Boc group whereas the cationic polymer lack hydrogen bonding in their $NH_3^+X^-$ amine salt.
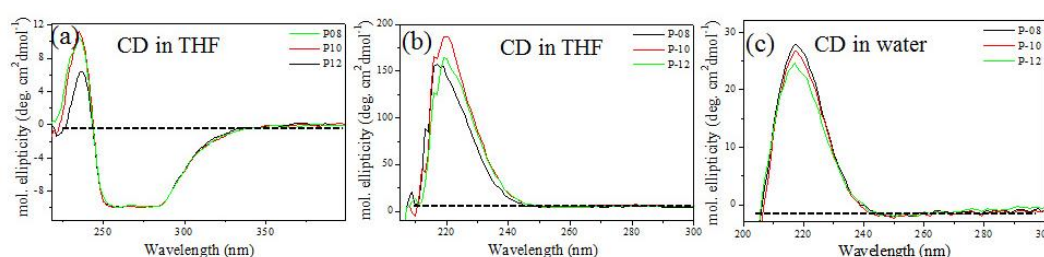

Figure 5.10. (a) CD Spectra of Boc pendant *neutral polymer P-X in THF*. CD Spectra of cationic *polymer P-X in THF (b) and aqueous dialyzed polymer sample P-X (c). The concentration of the polymer was retained as 1 mg/mL for CD measurements.*

The aqueous dialyzed cationic polyester samples were subjected to dynamic light scattering (DLS) as well as zeta potential analysis. DLS histograms of the polymers in figure 5.11 (a-c) showed mono-modal distribution with hydrodynamic diameter of 220 nm ± 20 nm. The DLS studies revealed that the disulfide cationic polyesters self-assembled as stable nano-particles in water. Zetapotential of the cationic polyesters (in figure 5.11d) showed a positive voltage of 5 mV corresponding to the positive charges at the periphery of the nano-particles. To visualize the morphology of the cationic polymer, dialyzed P-12 sample was subjected to FE-SEM and AFM analysis. FE-SEM images showed the formation of spherical nanoparticle of 200 ± 25 nm in diameter (in figure 5.11e). Further, AFM analysis also showed the spherical nanoparticle morphology with diameters of 200 ± 20 nm (in figure 5.11f). The sizes of the nanoparticles from SEM and AFM are in well matching with these solution aggregates of DLS size indicating that these cationic polymers indeed existed as spherical nanoparticle in water.
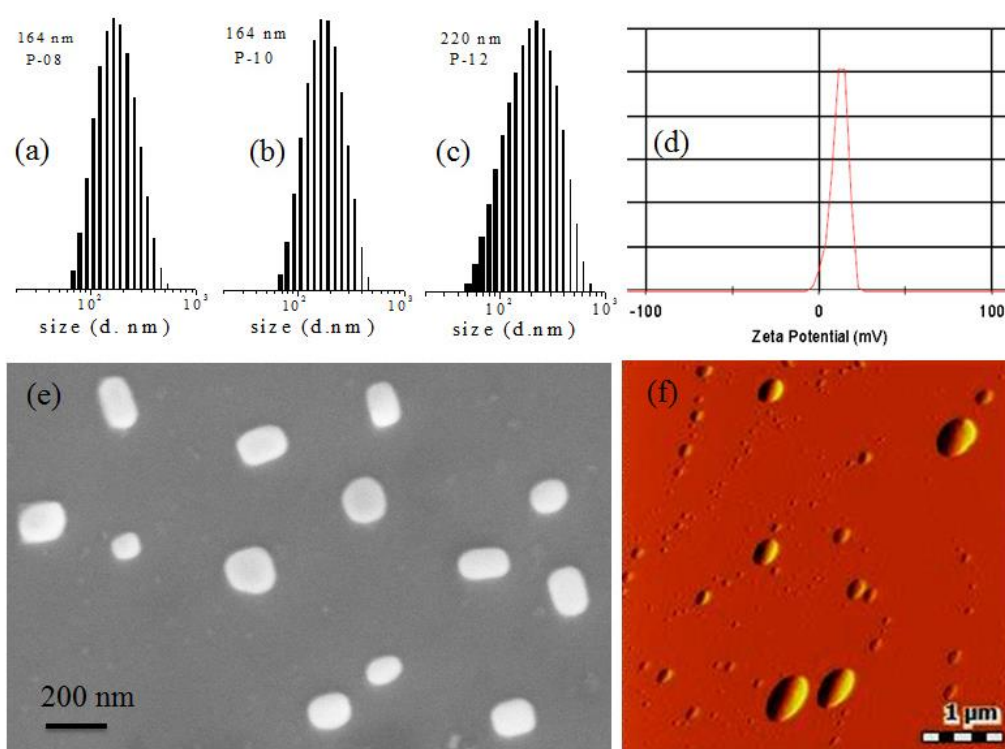
Figure 5.11.*DLS histograms (a-c) and zeta potential (d) of aqueous dialyzed polymer sample P-X. FE-SEM (e) and AFM images of the aqueous solution of cationic P-12 polymer (f). The concentration of the polymer was retained as 0.1 mg/mL for DLS measurements.*

Since the disulfide neutral polyester showed β-sheet signals in the CD spectra (in THF); they were subjected to FE-SEM and AFM microscopic analysis. The FE-SEM images of the drop cast films are shown in figure (5.12a-5.12c). The disulfide neutral polyester P-8, P-10 and P-12 exhibited amyloid-like nanofibril morphologies. The thickness of the nanofibrils was obtained as 75 ± 13 nm and the length of the fiber varied up to few micrometres. Further, the fibrils were found to contain left-handed twists with respect to their β-sheet signal in CD spectra (negative cotton effect). AFM images of disulfide neutral polyesters are shown in the following figures (5.12d-5.12f). AFM analysis showed the formation of nanofibrous morphology, as observed in the FE-SEM analysis. The thickness of the nanofibrils was found to be in the range of 89 ± 18 nm with length up to few micrometres. Thus FE-SEM and AFM analysis confirmed the nanofibrous morphology of the disulfide neutral polyesters (P-X).
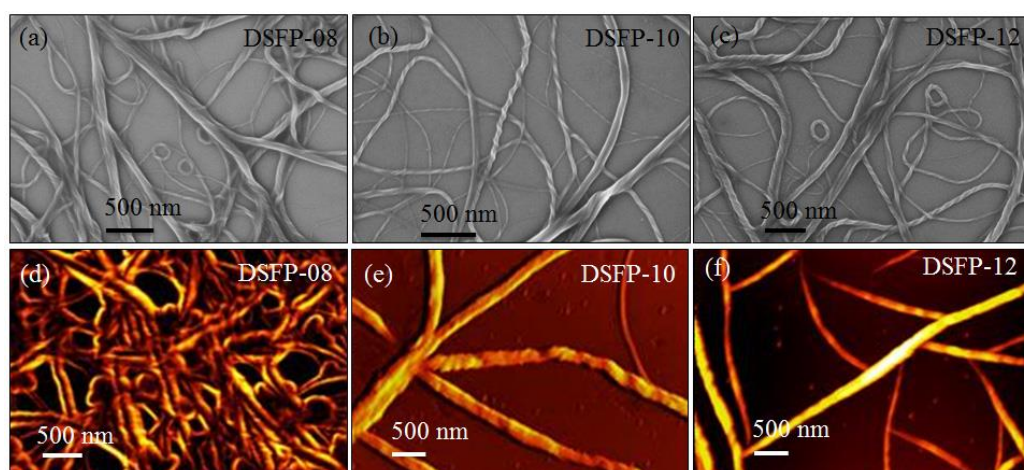
Figure 5.12.*The disulfide functional polyesters (P-X) SEM images (a-c) and AFM images of P-X (d-f), the concentration of polymer for microscopic analysis (0.1mg/mL).*

Based on the FE-SEM, AFM and CD analysis one can arrive at the following conclusions: (i) the disulfide containing Boc pendent neutral polymer adopted expanded chain confirmation in organic solvent and produced helical amyliod-fibrils morphology, (ii) the de-protection of Boc group resulted in the formation new disulfide linkage containing cationic polyester and (iii) the cationic polyester adopted random-coil conformation and self-assembled as spherically charged nanoparticles in water.

5.3.4. Redox Degradation of Functional Polyesters

To study the redox cleavages of the disulfide bond in polyester backbone, the polymer P-12 was subjected to degradation using dithiothreitol (DTT) as redox agent. The degradation of disulfide functional polyester was carried out in anhydrous tetrahydrofuran at 70 °C. The degradation of disulfide backbone by DTT is schematically shown in figure 5.13a. The degradation of disulfide polymers was studied by collecting aliquots at various time intervals and subjects them for ^{1}H-NMR and GPC studies. ^{1}H-NMR spectra of DTT, P-12, and aliquots taken from the degradation at 30 h are shown in figures 5.13b to 5.13d, respectively. The polymer showed that the -**CH₂**-S-S-**CH₂-** proton at 3.18 ppm (in figure 5.13c) completely disappeared in the aliquot (in figure 5.13d). Further, new peaks corresponding to

CH$_2$-SH appeared at 2.99 ppm in the aliquot sample (in figure 5.13d). NMR data have provided direct evidence for the disulfide linkage cleavage in the polymers by redox agent such as DTT.
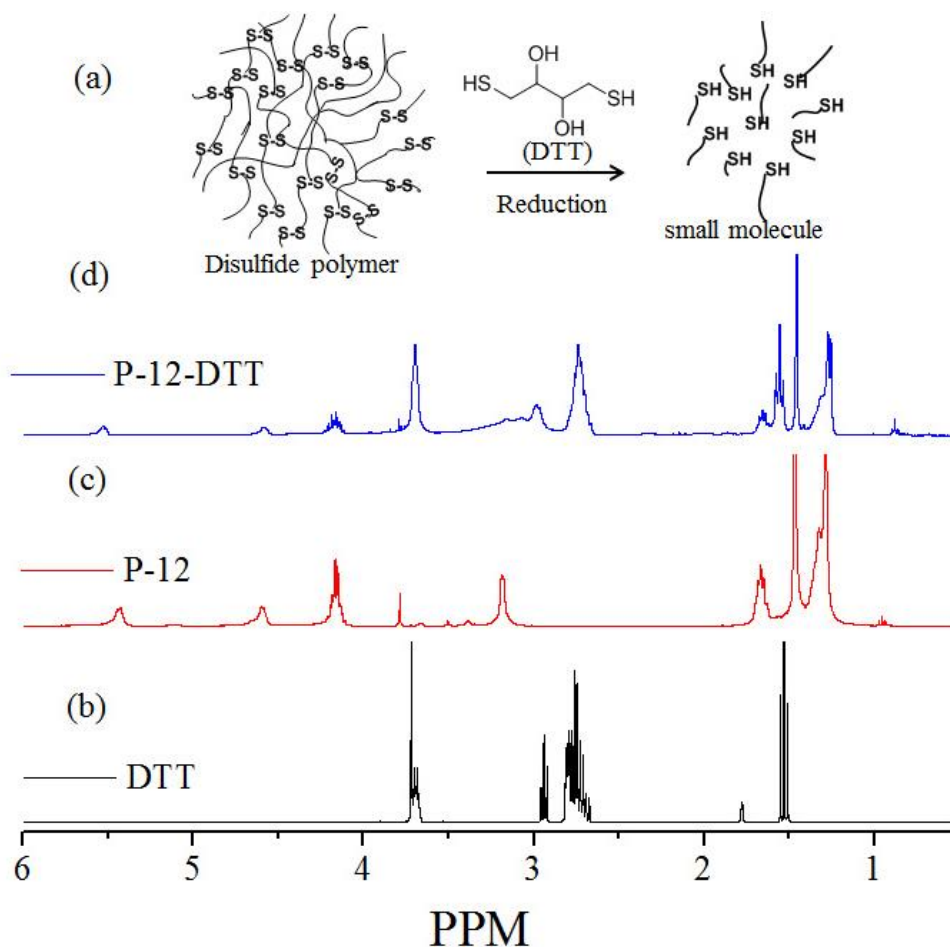

Figure 5.13. *Degradation of disulfide polymer by DTT (a).^{1}HNMR stack plot for DTT (b), disulfide polymer (P-12) (c) and DTT degraded disulfide polymer (d).*

The GPC chromatograms of degradation product aliquots are showed in figure 5.14a. At the beginning, the disulfide polymers showed peak maxima at 18 minutes. Up on degradation, the GPC chromatogram shifted towards the higher retention time with respect to the low molecular eight chains. These studies clearly indicated that the high molecular weight disulfide polymers were degraded in presence of DTT into lower molecular weight oligomers. The plot of M_n vs reaction time for all the aliquots is shown in figure 5.14b. The number average molecular weight (M_n) showed a drastic decrease from 10.0×10^3 g/mol to 500 g/mol (monomer or dimer species). This study confirmed that the custom designed disulfide containing polyesters are readily susceptible to redox cleavage. Hence, these neutral polyester materials could be useful for wide range of applications in thermo-plastic industry.

Further, the aqueous nano-assemblies of the cationic polymer samples could be employed for biomedical applications such in drug delivery and so on.
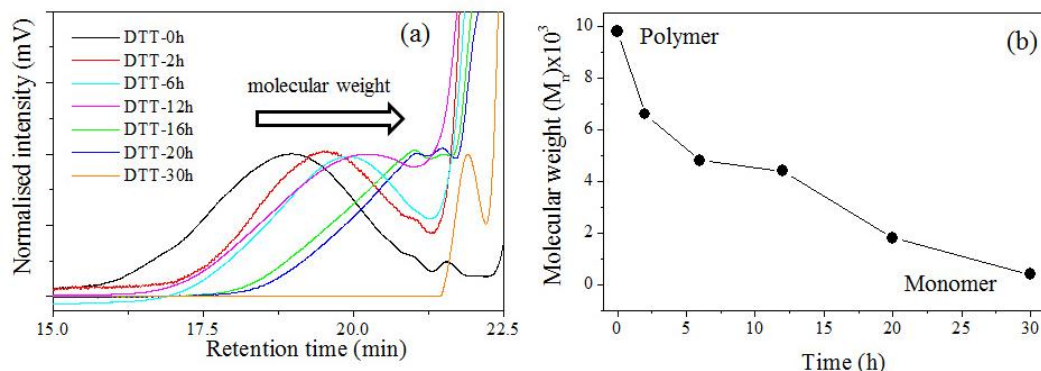

Figure 5.14.*GPC chromatogram of degradation product aliquots (a) and plot of M_n versus degradation reaction time (b)*

5.3.5.Cytotoxicity studies

The cytotoxicity of the cationic disulfide amine polyesters were investigated in breast cancer (MCF-7cells) cell lines using MTT assay method. The concentration of the polymers (P-8 and P-10) was varied from 1 μg/mL to 50.0 μg/mL. The cytotoxicity of the polymer (in figure 5.15) showed that the amino acid based cationic disulfide amine polymers were found to be non-toxic to cancer cells up to 50.0 μg/mL concentration with > 95% of cell viability. These results revealed that these polymers are highly biocompatible in nature; hence it can be used for biomaterial and biomedical applications.

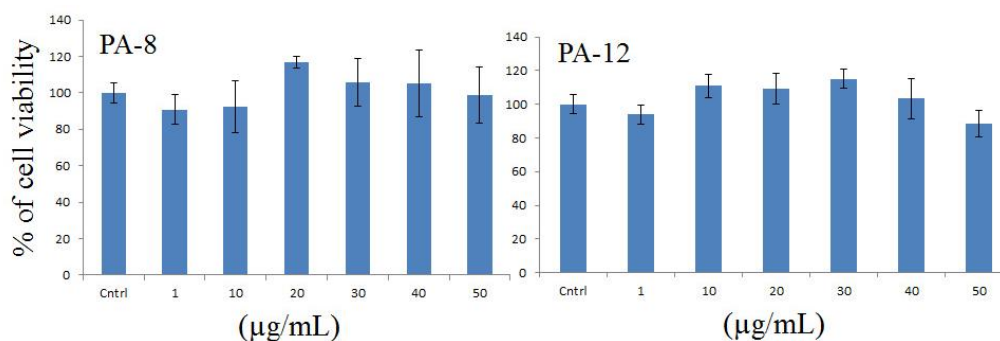**Figure 5.15**. *The cytotoxicity studies for cationic polymer (PA-8 AND PA-12) in MCF cells*

Our preliminary effort to load and stabilize the fluorescent dye molecules or anticancer drugs in these aqueous nano-particles seems to be difficult. This is partially associated with the lack of the appropriate hydrophilic substitution such as PEG-lated chains for enchaining the loading content of anticancer drugs. Currently, the research

work is focussed in these directions to explore new biomaterials based on L-cystine based cationic or neutral polyesters and their cytopalstic cleavage by GSH to delivery drugs to cancer cells.

The present investigation summarised the solvent free melt polycondensation approach developed for L-cystine amino acid based stimuli responsive disulfide polymer. L-cystine amino acid disulfide polyesters were thoroughly characterised by various techniques. The disulfide based functional polyesters were self-assembled to yield amyloid like fibrous polymer. Upon deprotection of Boc group into amine functional polyester, the self-assembly of the polymer can be tuned from amyloid like fibrous polymer into spherical particle morphology. The disulfide polymers degraded into small molecule using DTT as redox reagent. A new synthesis of disulfide functional polymers based on melt polycondensation method can open up new frontiers for multiple applications.

5.4. Conclusion

In conclusion solvent free melt polycondensation method was developed for redox degradable disulfide functional polyester based on L-cystine amino acid. The ester-urethane monomer was prepared from L-cystine amino acid, and then the thermal stability of the monomer, for melt condensation reaction was studied by TGA analysis and by carrying out a few model reactions. The ester group of the L-cystine monomer reacted with various aliphatic diols such as 1, 8 octanediol, 1, 10 decanediol and 1,12 dodecanediol in the presence of Ti(OBu)$_4$ as catalyst to yield disulfide functional polyester under solvent free melt condition. In this method ester functional group selectively reacted with diol whereas the urethane group remained absolutely inert. The formation of disulfide functional polyesters were confirmed by NMR spectroscopy, where the peak corresponding to monomer end group vanished and a new peak belonging to the polymer was seen. GPC analyses of these functional polyesters showed moderate to high molecular weight of the polymers. TGA analysis of disulfide functional polyesters indicated that these polymers are thermally stable up to 250 °C. DSC analysis of the boc protected disulfide functional polyesters further showed that the polymers are amorphous in nature possibly due to steric effect of Boc group that hampers the packing of the polymer chain. CD analysis of neutral amine protected (Boc) disulfide functional (P-X) polyester showed the formation of β-sheet

secondary structure, whereas in the case of protonated amine (cationic) disulfide functional polyester random coil secondary structure was observed. Microscopic analysis confirmed that neutral disulfide functional polyester (Boc) produced amyloid-like fibrous polymer but the cationic amine functional disulfide polyester afforded spherical particle morphology. The above results indicated that the structural differences between Boc-protected and free amine in the polymer side chain can be used to tune the self-assembly of the polymers from amyloid fibres to particles. The reason attributed to this observation is that the Boc group in the side chain of the polyester is involved in hydrogen bonding to yield fibrous polymer, whereas the absence of hydrogen bonding interaction in the cationic amine functional polyester yields spherical particle. The cell viability of cationic amine functional polymers in MCF cells showed upto 50 μg/mL of polymer are viable (non-toxic) and these polymers are biocompatible in nature. The neutral (Boc) disulfide functional polyesters upon degradation using DTT as the redox reagent converts a high molecular weight polymer into small molecular weight fragments, stressing the importance of these stimuli responsive polymers in materials application.

5.5. Reference

1. Wojtecki, R. J.; Meador, M. A.; Rowan, S. J. *Nat. Mater.* **2011**, *10*, 14-27.

2. Fiore, G. L.; Rowan, S. J.; Weder, C. *Chem. Soc. Rev*. **2013**, *42*, 7278-7288.

3. Bang, E-K; Lista, M.; Sforazzini, G.; Sakai, N.; Matile, S. *Chem. Sci.* **2012**, *3*, 1752-1763.

4. Ding, Y.; Hay, A. S. *Macromolecules,* **1996**, *29*, 6386-6392.

5. Ding, Y.; Hay, A. S. *Macromolecules*, **1997**, *30*, 2527-2531.

6. Liang, Z. A.; Meng, Y. Z.; Li, L.; Du X. S.; Hay, A. S. *Macromolecules*, **2004**, *37*, 5837-5840.

7. Meng, Y. Z.; Liang, Z. A.; Lu Y. X.; Hay, A. S. *Polymer*, **2005**, *46*, 11117-11124.

8. Song, L. N.; Xiao, M.; Shu, D.; Wang S. J.; Meng, Y. Z. *J. Mater. Sci*., **2007**, *42*, 1156-1161.

9. Rosenthal, E. Q.; Puskas J. E.; Wesdemiotis, C. *Biomacromolecules*, **2012**, *13*, 154-164.

10. Lee, Y.; Koo, H.; Jin, G.; Mo, H.; Cho, M. Y.; Park, J.-Y.; Choi J. S.; Park, J. S. *Biomacromolecules*, **2005**, *6*, 24-26.

11. Tsarevsky, N. V.; Matyjaszewski, K. *Macromolecules*, **2002**, *35*, 9009-9014.

12. Otsuka, H.; Nagano, S.; Kobashi, Y.; Maeda, T.; Takahara. A. *Chem. Comm.* **2010**, *46*, 1150-1152.

13. Fairbanks, B. D., Singh, S. P.; Bowman, C. N.; Anseth, K. S. *Macromolecules*, **2011**, *44*, 2444-2450.

14. Dan, K.; Ghosh, S. *Angew. Chem. Int. Ed.***2013**, *52*, 7300-7305.

15. Basak, D.; Kumar, R.; Ghosh, S. *Macromol. Rapid Commun*. **2014**, *35*, 1340-1344.

16. Nicolay, R.; Marx, L.; Hemery, P.; Matyjaszewski, K. *Macromolecules*, **2007**, *40*, 9217–9223.

17. Rosselgong, J.; Williams, E. G. L.; Le, T. P.; Grusche, F.; Hinton, T. M.; Tizard, M.; Gunatillake, P.; Thang, S. H. *Macromolecules*, **2013**, *46*, 9181-9188.

18. Li, Y.; Armes, S. P. *Macromolecules*, **2005**, *38*, 8155-8162.

19. Zhao, T.; Zheng, Y.; Poly, J.; Wang, W. *Nat. Commun*. **2013**, 4, 1-8.

20. Ou, M.; Wang, X-L.; Xu, R. Chang, C-W.; Bull, D. A.; Kim, S. W. *Bioconjugate Chem.***2008**, *19*, 626-633.

21. Weder, C. *Nature*, **2009**, *459*, 45-46.

22. Son, S.; Shin, E.; Kim, B-S. *Macromolecules*, **2015**, *48*, 600-609.

23. Canadell, J.; Goossens, H.; Klumperman, B. *Macromolecules*, **2011**, *44*, 2536-2541.

24. Pepels, M.; Filot, I.; Klumperman, B.; Goossens, *Polym. Chem*. **2013**, *4*, 4955-4965.

25. Wu, Y.; Kuang, H.; Xie, Z.; Chen, X.; Jing, X.; Huang, Y. *Polym. Chem*. **2014**, *5*, 4488-4498.

26. Sun, H.; Cheng, R.; Deng, C.; Meng, F.; Dias, A. A.; Hendriks, M.; Feijen, J.; Zhong, Z. *Biomacromolecules*, **2015**, *16*, 597-605.

27. Sulistio, A.; Blencowe, A.; Widjaya, A.; Zhang, X.; Qiao, G. *Polym. Chem*. **2012**, *3*, 224-234.

28. Sulistio, A.; Widjaya, A.; Blencowe, A.; Zhang, X.; Qiao, G. *Chem. Comm*. **2011**, *47*, 1151-1153.

29. Sulistio, A.; Lowenthal, J.; Blencowe, A.; Bongiovanni, M. N.; Ong, L.; Gras, S. L.; Zhang, X.; Qiao, G. G. *Biomacromolecules*, **2011**, *12*, 3469-3477.

30. Kramer, J. R.; Deming, T. J. *Chem. Comm*. **2013**, *49*, 5144-5146.

31. Wu, J.; Zhao, L.; Xu, X.; Bertrand, N.; Choi, W.; Yameen, B.; Shi, J.; Shah, V.; Mulvale, M.; MacLean, J. L.; Farokhzad, O. C. *Angew. Chem. Int. Ed.***2015**, *54*, 9218-9223.

32. Ko, N. R.; Oh, J. K. M*acromolecules*, **2014**, *15*, 3180-3189.

33. Yang, P.; Li D.; Jin, S.; Ding, J.; Guo, J.; Shi, W.; Wang, C. *Biomaterials*, **2014**, *35*, 2079-2088.

34. Jia, L.; Cui, D.; Bignon, J.; Cicco, A. D.; Wdzieczak-Bakala, J.; Liu, J.; Li, M-H. *Biomacromolecules*, **2014**, *15*, 2206-2217.

35. Song, N.; Ding, M.; Pan, Z.; Li, J.; Zhou, L.; Tan, H.; Fu, Q. *Biomacromolecules*, **2013**, *14*, 4407-4419.

36. Wang, Y.; Nie, J.; Chang, B.; Sun, Y.; Yang, W. *Biomacromolecules*, **2013**, *14*, 3034-3046.

37. Lu, W.; Wang, X.; Cheng, R.; Deng, C.; Meng, F.; Zhong, Z. *Polym. Chem.***2015**, *6*, 6001-6010.

38. Feng, F.; Li, R.; Zhang, Q.; Wang, Y.; Yang, X.; Duan, H.; Yang, X. *Polymer*, **2014**, *55*, 110-118.

Summary and Future directions

The thesis entitled "***Development of Melt Polymerization Route for Amino acid Based Functional Polymers and their Self-assembled Nanostructures***" deals with importance of amino acid polymer synthesis and their material application. The thesis is focused to develop new eco-friendly melt polycondensation approach for L-amino acid resources under solvent-free conditions. The naturally available amino acids were utilized for the development of dual ester-urethane melt polycondensation approach, in addition wide range of catalysts were developed to produce high molecular weight poly (ester-urethane)s. Based on the reactivity difference between the functional groups, *temperature selective transesterification polycondensation* was investigated for L-glutamic and L-aspartic acids amino acid monomers for synthesis of linear functional polyesters and their reversible self-assembly studies. Efforts were also put to develop a new method based on disulfide functional polyester for redox degradable polymer.

A new dual ester-urethane melt condensation methodology for biological monomers amino acids was developed to synthesize new classes of thermoplastic polymers under eco-friendly and solvent free polymerization technique. In this new process, amino acids were converted into dual ester-urethane monomers and polycondensed with diols under melt conditions to produce high molecular weight polymers. The occurrence of the melt dual ester-urethane process and the structure of the new poly (ester-urethane)s were confirmed by ^{1}H and ^{13}C NMR analysis. The new dual ester-urethane condensation approach was demonstrated for variety of amino acids: glycine, β-alanine, L-alanine, L-leucine, L-phenylalanine and L-valine along with commercial diols: di-, tri- and tetraethylene glycols, 1,12-dodecandiol (linear aliphatic diols) and 1,4-cyclohexanedimethanol (cycloaliphatic diols). The molecular weights of the polymers were obtained in the range of moderate to high values with polydispersity ~ 2.1. The mechanism of melt process and the kinetics of the polycondensation were studied by model reactions and it was found that the amino acid monomer was very special in the sense that their ester and urethane functionality could be selectively reacted by tuning reaction temperature or catalyst. CD analysis of the synthesized polymers confirmed that these new poly (ester-urethane)s were efficient structures to produce self-organized β-sheets like polypeptides in water or organic solvents. The thermal properties such as glass transition temperature and

crystallinity could be readily varied using different L-amino acid monomers or diols in the polymerization method.

To identify the role of catalyst in trans reaction wide range of catalysts were developed for the melt polymerization of amino acid monomers to produce high molecular weight poly (ester-urethane)s under solvent free melt process. Model reactions were performed and the resultant products were analysed by NMR spectroscopy to trace the roles of catalysts and polymerization temperature on the molecular weight of the polymers. The molecular weights of these polymers were found to be highly selective with respect to the types of the catalysts. More than two dozens of transition metal and lanthanide catalysts were identified for the polycondensation to yield high molecular weight poly(ester-urethane)s. Theoretical studies revealed that the carbonyl carbon in ester possessed low electron density compared to the carbonyl carbon in urethane which driven the thermo-selective polymerization process. The polycondensation reaction was further investigated using D- and L-isomers of amino acids to trace the optical purity of the resultant polymers. Electron and atomic force microscopes revealed the formation of highly ordered helical nano-fibrous morphology in the polymers. These helical assemblies were found to be not altered by the choice of the catalysts employed in the polymerization.

Based on the selective reactivity of the functional group was achieved by temperature and catalyst from the earlier chapter, a new melt polymerization synthetic methodology was developed to make functional polyesters based on L-amino acids that underwent reversible conformational changes and produced amyloid-like fibrils. The linear polyesters with urethane pendants in each repeating unit were synthesized by temperature selective transesterification process of multi-functional amino acids based on L-glutamic and L-aspartic acids. These new polyesters have hydrogen bonded urethane (or carbamate) units that are in-built in each repeating unit, which tends to produce amyloid-like fibrils consisting of hierarchical double helical structures. Upon de-production, the amyloid fibrils underwent coil-like conformational change to produce cationic spherical nano-particles in aqueous medium. The size and charge of the cationic spherical species were controlled by the alkly chains length in the polymer structure. Dansyl chloride was employed as fluorophore to reversibly expand the coil-like cationic polymers into expanded helical fibrils of fluorescent in nature.

Redox degradable disulfide functional polyester was developed based on L-cystine amino acid under solvent free melt polycondensation method. L-cystine amino acid was first converted into ester-urethane functional monomer. At 120 °C the two ester functional groups of L-cystine monomer was selectively reacted with diol in the presence of Ti(OBu)$_4$ as catalyst to yield disulfide functional polyester under solvent free melt conditions. The formation of disulfide functional polyesters was confirmed by NMR and GPC analysis. Further thermal analysis of these polymers indicated that polymers were thermally stable up to 250 °C and were amorphous in nature. The nascent polymer (in neutral form) was capable of self-assembling into β-sheet secondary structure in solution (confirmed by CD spectroscopy) which subsequently seeded for the amyloid-fibrils formation. Upon Boc de-protection; the disulfide polyester turned into water dispersible cationic polyester and it was found to self-assemble as stable nanoparticles. The cytotoxicity studies of amine functional disulfide polymers (cationic polymers) was performed in MCF-7 cells and the result indicated these polymers are nontoxic to cells and are also biocompatabile in nature. The degradation study on these stmuli responsive polymers was performed by using DTT as a redox reagent. Upon treatment with DTT, the high molecular weight polymer were degradaded into small molecular weight structures and the process was monitored by ^{1}H-NMR and GPC techniques.

Future direction

In short, the thesis work is focused on the synthesis of amino acid containing polyester and poly (ester-urethane)s using solvent free melt polycondensation method. Aliphatic polyesters are widely used for various applications, since these polymers are completely biodegradable in nature. In this thesis work synthetic methodology was developed for amino acid polymers containing ester linkages, therefore these polymers can also be used for various applications. Recently amphiphilic polymers are attracted much attention in both in industry and academic research because of their self-assembly in aqueous medium for drug delivery, gene delivery etc. Our synthetic methodology based on amino acid polymers can further expandable for preparation of amphiphilic polymers containing multiple functional groups: hydroxyl, amine and carboxylic acid depending upon side chain of the amino acids. These polymers can be useful for loading and delivering the anticancer drug molecule.
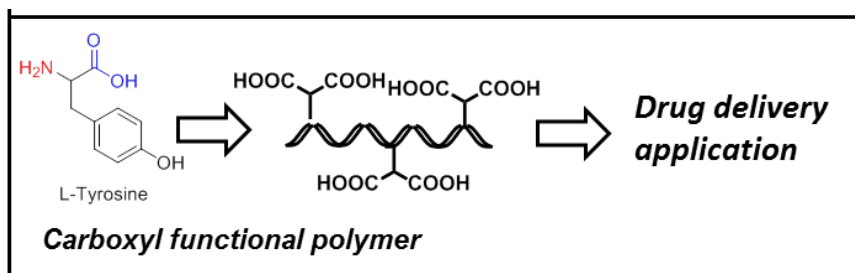
Figure 6.1. *The carboxylic functional polymers based on L-tyrosine amino acid for drug delivery application*

Therefore ongoing projects concentrated on the synthesis of carboxylic acid functional polymer based on tyrosine based amino acid for loading and delivering anti-cancer drug molecule. These polymers can be used as stimuli responsive because of carboxylic functional group.

List of Publications

List of Publications from Thesis work

1. Anantharaj, S.; Jayakannan, M. Polymers from Amino acids: Development of Dual Ester-Urethane Melt Condensation Approach and Mechanistic Aspects *Biomacromolecules* **2012**, *13*, 2446-2455.

2. Anantharaj, S.; Jayakannan, M. Amyloid-like Hierarchical Helical Fibrils and Conformational Reversibility in Functional Polyesters Based on L-Amino acids *Biomacromolecules* **2015**, *16*, 1009-1020.

3. Anantharaj, S.; Jayakannan, M.Catalysts and Temperature Driven Melt Polycondensation Reaction for Helical Poly(ester-urethane)s Based on Natural L-Amino acids *J. Polym. Sci., Polym. Chem.* **2016**, DOI: 10.1002/pola.27970

4. Anantharaj, S.; Jayakannan, M. Melt polycondensation approach for disulfide based functional polyester and their Hierarchical Helical Self-assemblies" *Manuscript Submitted for publication.*

5. Anantharaj, S.; Jayakannan, M. Hydroxyl functional polymer based on amino acids and their self-assemblies (*Manuscript under preparation).*

Publications in International Conference Proceedings:

1. Polymer Based on Amino Acids Plastic Materials from Bio-resources. Anantharaj, S.; Jayakannan, M. MACRO-2013. IISC-Bangalore, May 15-18, 2013.

2. Development of New Ester-urethane Melt Polycondensation Approach for Amino acids. Anantharaj, S.; Jayakannan, M. Inter IISER Meeting-2011, IISER, Trivandrum, May 14-16, 2011.

3. Development of Dual Ester-Urethane Melt Ester-urethane condensation Approach for small molecules and linear polymer based on Amino acids. Anantharaj, S.; Jayakannan, M. Polytech-2012. Pune, December 15-17, 2012.